

INVESTIGATING THE RELATIONSHIP BETWEEN USP50 AND WRN IN DNA REPLICATION

By KATHERINE ELLIS

A thesis submitted to the University of Birmingham for the degree

DOCTOR OF PHILOSOPHY



Institute of Cancer and Genomic Sciences

College of Medical and Dental Sciences

University of Birmingham

December 2023

UNIVERSITY OF
BIRMINGHAM

University of Birmingham Research Archive

e-theses repository

This unpublished thesis/dissertation is copyright of the author and/or third parties. The intellectual property rights of the author or third parties in respect of this work are as defined by The Copyright Designs and Patents Act 1988 or as modified by any successor legislation.

Any use made of information contained in this thesis/dissertation must be in accordance with that legislation and must be properly acknowledged. Further distribution or reproduction in any format is prohibited without the permission of the copyright holder.

Abstract

USP50 is a poorly understood deubiquitinase with emerging roles in replication. Previous work in the laboratory revealed an epistatic relationship between USP50 and the RECQ helicase WRN in preventing replication-associated DNA double-strand breaks. In this thesis we probed the relationship between USP50 and WRN further and examined their shared and independent roles in replication fork progression and restart, DNA double-strand break formation, and response to replication stress. We found that USP50 and WRN co-operate to support fork progression in replicating cells, with USP50 promoting WRN localisation to stalled forks. We found that RECQL4 and RECQL5 rescue DNA replication in cells depleted of USP50 and WRN. We saw that USP50 promotes formation of DNA double-strand breaks near transcription start sites, indicating a novel role in promoting transcription. Investigation of the roles of USP50 and WRN in microsatellite unstable colorectal cancer cells revealed that USP50 is not a synthetic lethal target in these cells, unlike WRN. WRN loss in microsatellite unstable cells leads to loss of DNA damage repair proteins and cell death. Together the data presented in this thesis deepens our understanding of the USP50-WRN relationship in microsatellite stable and unstable cancer cells, and reveals the surprising ability of RECQ helicases to compensate for each other in DNA replication.

Acknowledgements

I would like to sincerely thank my supervisor Jo Morris for her input, advice and support over the last four years. Thanks also goes to my APR examiners Marco Saponaro and Tanja Stankovic for their guidance and encouragement, with special thanks to Marco for the bioinformatics help. I would also like to thank Cancer Research UK for funding my PhD studentship- I consider it a badge of honour to be funded by CRUK. Thanks also to Hannah for providing much of the background to the project and for sticking with USP50 through thick and thin.

I would like to thank everyone in the Morris group, especially Alexa, Lanz, Libby and Yara. Alexa has provided over four years of love, support, and high kicks to the face, and has never allowed me to stop using my lambie brain. Lanz has been there for my whole PhD journey, from my interview, to my first day in the lab, and to my final day in the office. He has provided constant friendship and humour, and is never too busy to have a nerdy discussion about experiments. Libby and Yara are my fellow slug queens, and they have always been there for me in good times and bad. I would also like to shout out all my Young Masters: Rosie, Nicole, Ciara, Lucy and Lauren. You all made the tough times better and the good times amazing.

Outside of the department, I would like to thank my brother Philip, and my wonderful Dad for his love and support. He may not quite understand what USP50 and WRN are, but he has always rooted for me, and has provided a relaxing and recuperating environment in which to unwind during holidays. I would also like to thank my extended family, especially Juan and Diane, for always lending an ear to listen and a shoulder to cry on. Marta is almost family, having been my best friend since we were eleven, and her endless positivity has always helped cure my self-doubt. Rhiannon has been a solid and faithful friend for over 10 years, and knows

all too well the trials and tribulations of doing a Biology PhD. I would also like to thank Amy, Dong and Oktawia. Though we may not live in the same city or work together anymore, these ladies provide much-needed friendship and love.

Lastly, I would like to thank my ~~boyfriend fiancé~~ husband Richard and our cat baby. Noodles has provided more cuddles, comfort and joy than I could ever count, and offers the most welcome distraction imaginable from work. Richard has provided endless healing cups of tea and hugs during my PhD, and has always been interested to hear about the lab and my experiments. I would not want to have done it without his love and support.

Table of contents

Abstract	i
Acknowledgements	ii
Table of contents	iv
List of abbreviations	xii
1. Introduction	1
1.1 Eukaryotic DNA replication.....	1
1.1.1 Replication initiation.....	2
1.1.2 Replication progression.....	5
1.1.3 Replication termination and completion.....	8
1.2 Replication stress and cancer.....	13
1.2.1 Endogenous and exogenous inducers of replication stress.....	13
1.2.2 Oncogene-induced replication stress and genomic instability.....	16
1.2.3 Replication stress response.....	18
1.3 Mechanisms of replication fork recovery.....	21
1.3.1 Lesion bypass.....	21
1.3.2 Replication fork reversal.....	25
1.3.3 Replication fork protection.....	26

1.3.4 Replication fork recovery/ restart.....	28
1.3.5 Replication fork recombination repair.....	28
1.3.6 Conclusion.....	29
1.4 RECQ helicase family.....	30
1.4.1 WRN helicase/ exonuclease.....	30
1.4.2 Werner syndrome.....	32
1.4.3 Werner syndrome cells.....	33
1.4.4 WRN post-translational modifications.....	34
1.4.5 WRN interactors and partners.....	36
1.4.6 WRN in DNA replication and replication stress.....	37
1.4.7 RECQ helicase-associated diseases.....	39
1.4.8 RECQ helicases in replication.....	41
1.4.9 WRN in DNA repair.....	42
1.4.10 Targeting WRN for cancer therapy.....	43
1.5 Mismatch repair pathway and Lynch syndrome.....	44
1.5.1 Microsatellite instability and cancer.....	46
1.5.2 WRN synthetic lethality with mismatch repair deficiency.....	48
1.5.3 Current treatments for microsatellite unstable cancers.....	53

1.6 USP50 in replication.....	54
1.6.1 Thesis aims.....	59
2. Materials and methods.....	60
2.1 Molecular biology.....	60
2.1.1 Bacterial transformation.....	60
2.1.2 Plasmid DNA purification.....	60
2.1.3 DNA quantification.....	60
2.1.4 Guide RNA (gRNA) design.....	61
2.1.5 Double stranded homology directed repair (HDR) template design.....	61
2.1.6 Genomic DNA (gDNA) extraction.....	62
2.1.7 gDNA screening.....	62
2.1.8 Gel electrophoresis.....	63
2.1.8 Gel extraction.....	64
2.1.8 DNA sequencing.....	64
2.2 Protein biology.....	64
2.2.1 SDS-PAGE.....	64
2.2.2 Western blotting.....	65
2.3 Cell biology.....	66

2.3.1 Tissue culture.....	66
2.3.2 siRNA transfection.....	66
2.3.3 CRISPR cell line generation.....	67
2.3.4 Stable cell line generation.....	67
2.3.5 Plasmid transfection.....	68
2.3.6 Inducible shRNA expression.....	68
2.3.7 Immunofluorescence staining.....	69
2.3.8 DNA fibre labelling.....	69
2.3.9 Fibre immunostaining.....	70
2.3.10 Fibre scoring and analysis.....	71
2.3.11 Clonogenic survival assay.....	71
2.3.12 Cell viability assay.....	71
2.3.13 Broken String Biosciences double strand break site mapping.....	72
2.4 Microscopy.....	72
2.5 Chromatin fractionation.....	73
2.6 Buffers.....	73
2.7 Primer sequences.....	74
2.8 siRNA sequences.....	75

2.9 gRNA sequences.....	75
2.10 Antibodies.....	75
2.11 Chemicals.....	77
2.12 Statistical methods.....	78
3. USP50 regulates WRN at ongoing and stalled forks.....	79
3.1 Introduction.....	79
3.2 3xFLAG-tagged USP50 HeLa cells engineered using homology-directed CRISPR.....	81
3.3 USP50-deficient cells are not hypersensitive to UV treatment.....	86
3.4 USP50 acts to prevent fork stalling before MUS81 cleavage of stalled replication forks.....	88
3.5 WRN depletion/ inhibition rescues fork stalling in USP50-depleted cells.....	91
3.6 Both enzymatic activities of WRN are needed to rescue fork stalling in USP50- depleted cells.....	96
3.7 Targeting USP50 and WRN together rescues formation of DSBs in replicating cells.....	102
3.8 Co-depletion of USP50 and WRN does not rescue cell survival in HeLa cells	106
3.9 USP50 regulates WRN localisation to chromatin after hydroxyurea treatment.....	108

3.10 WRN and USP50 operate in the same pathway to restart stalled forks after hydroxyurea treatment.....	112
3.11 Replication fork progression during hydroxyurea treatment is promoted by USP50 and WRN.....	116
3.12 RECQL4 and RECQL5 can compensate for loss of WRN and USP50 to rescue stalled replication forks.....	120
3.13 Discussion.....	124
3.14 Experimental limitations.....	134
3.15 Future experiments.....	137
4. USP50 and WRN in replication in MSS vs MSI cells.....	141
4.1 Introduction.....	141
4.2 Optimisation of siRNA transfection in a panel of colorectal cancer cell lines with and without WRN dependency.....	143
4.3 WRN-dependent MSI cells are not hypersensitive to USP50 depletion compared to MSS cells.....	146
4.4 Co-depletion of USP50 and WRN does not rescue fork stalling in MSI cells.....	150
4.5 Depletion of USP50 combined with WRN helicase inhibition does not rescue fork stalling in MSI cells.....	153
4.6 WRN depletion inhibits fork restart more severely in MSI vs MSS cells.....	155

4.7 Co-depletion of USP50 and WRN affects fork progression during HU treatment differently in MSS vs MSI cells.....	157
4.8 MSI cells are sensitive to USP50 overexpression.....	160
4.9 MSI cells are not hypersensitive to WRN helicase inhibition compared to MSS cells.....	164
4.10 WRN depletion, but not inhibition, leads to loss of DNA repair proteins in MSI cells.....	167
4.11 DNA damage response inhibition does not sensitise MSI cells to WRN helicase inhibition compared to MSS cells.....	180
4.12 Discussion.....	183
4.13 Future experiments.....	191
5. USP50 suppresses or promotes DSB formation depending on genomic location.....	194
5.1 Introduction.....	194
5.2 USP50 depletion leads to an overall increase in INDUCE-seq reads.....	196
5.3 Recurrent INDUCE-seq reads are enriched or lost upon USP50 depletion in a locus-dependent manner.....	200
5.4 USP50 loss has mixed effects on numbers of breaks at common fragile sites.....	204
5.5 USP50 loss has mixed effects on numbers of breaks at very large genes.....	206
5.6 USP50 affects proximity of breaks to transcription start sites.....	208

5.7 Discussion.....	210
5.8 Future experiments.....	213
6. General discussion.....	216
7. References.....	221

Abbreviations

Ac- acetylation

ALT- alternative lengthening of telomeres

Alt-NHEJ- alternative NHEJ

ARSE- autonomously replicating sequence

BGS- Baller-Gerold syndrome

BIR- break-induced replication

BS- Bloom syndrome

BTR- BLM-TOPIII α -RMI1-RMI2

CFS- common fragile site

CIN- chromosomal instability

CMG- CDC45-MCM-GINS

cNHEJ- classical NHEJ

DDR- DNA damage response

DDT- DNA damage tolerance

dNTP- deoxyribonucleotide triphosphate

DSB- double-strand break

dsDNA- double-stranded DNA

FA- Fanconi anaemia

G1- growth phase 1

G2- growth phase 2

gDNA- genomic DNA

GIN- genomic instability

gRNA- guide RNA

H3- histone 3

H4- histone 4

HDR- homology directed repair

HJ- Holliday junction

HR- homologous recombination

HRDC- helicase-and-ribonuclease D/C-terminal

HU- hydroxyurea

ICI- immune checkpoint inhibitor

ICL- inter-strand crosslink

Indel- insertion/ deletion

IF- immunofluorescence

IR- ionising radiation

K- lysine

LAD- lamina-associated domain

M- mitosis

MCM- mini chromosome maintenance

Me- methylation

MiDAS- mitotic DNA synthesis

MMR- mismatch repair

MMS- methyl methane sulphonate

MRN- MRE11-RAD50-NBS1

MSI- microsatellite instability/ unstable

MSS- microsatellite stability/ stable

NER- nucleotide excision repair

NHEJ- non-homologous end joining

NLS- nuclear localisation signal

NTC- non-targeting control

OIRS- oncogene-induced replication stress

ORC- origin recognition complex

PAM- protospacer adjacent motifs

PARP- poly(ADP-ribose) polymerase

PCNA- proliferating cell nuclear antigen

PCR- polymerase chain reaction

PML- promyelocytic leukaemia

Pol- polymerase

Pre-RC- pre-recognition complex

RFC- replication factor C

RNR- ribonucleotide reductase

ROS- reactive oxygen species

RQC- RecQ-conserved

RS- replication stress

RTS- Rothmund-Thomson syndrome

S- serine

S phase- synthesis phase

SD- standard deviation

SDM- site-directed mutagenesis

SEM- standard error of mean

SSA- single-stranded annealing

SSB- single-strand break

ssDNA- single-stranded DNA

T- threonine

TAD- topological associated domain

TLS- translesion synthesis

TRC- transcription-replication conflict

TS- template switching

TSS- transcription start site

UV- ultraviolet

VLG- very large gene

WRNi- WRN inhibitor

WS- Werner syndrome

1 Introduction

1.1 Eukaryotic DNA replication

DNA replication is the duplication of the genome from a parent cell to create two genetically identical daughter cells. It is essential that DNA replication is highly accurate to avoid the accumulation of potentially harmful mutations in DNA, and to ensure that genetic material is maintained (Ekundayo & Bleichert, 2019; Fragkos *et al.*, 2015; Negrini *et al.*, 2010; Prioleau & MacAlpine, 2016). DNA replication is therefore tightly controlled and monitored during the synthesis phase (S phase) of the cell cycle. S phase is preceded by growth (G) 1 phase, and followed by G2 and mitosis (M) phase. DNA replication is highly conserved between the different domains of life (Burgers & Kunkel, 2017; Ekundayo & Bleichert, 2019; Masai *et al.*, 2010; Parker *et al.*, 2017). DNA replication is a semi-conservative process whereby each daughter cell ends up with one strand of genetic material from the parent cell, and one newly synthesised strand (Meselson & Stahl, 1958). Synthesis of new DNA occurs at the replication fork, where DNA is unwound to present a single strand of DNA, which is then copied by replicative polymerases to create a new and accurate copy of DNA complementary to the sequence of the original strand (Burgers & Kunkel, 2017; Masai *et al.*, 2010; Stillman, 2008). Problems in DNA replication can lead to alteration of the genetic code, for example through point mutations in single DNA bases, to larger losses or gains of genes or chromosome regions, or chromosome fusions (Deshmukh *et al.*, 2016; Kunkel & Erie, 2015; Loeb & Monnat, 2008; Negrini *et al.*, 2010). These changes to the genetic code can lead to disease, ageing, and cancerous transformation (Clarke & Mostoslavsky, 2022; Marian, 2013; Mazouzi *et al.*, 2014; Stead & Bjedov, 2021).

1.1.1 Replication initiation

DNA synthesis is initiated at origins of replication, where the replicative machinery is assembled and activated (Ekundayo & Bleichert, 2019; Fragkos *et al.*, 2015; Prioleau & MacAlpine, 2016). In human cells, replication origins are distributed unevenly across the genome, and are activated at different times during S phase (Costa & Diffley, 2022; Masai *et al.*, 2010; Parker *et al.*, 2017; Reuswig & Pfander, 2019). Replication origins tend to fire at similar times to other proximal origins and are localised in foci known as “replication factories” (Berezney *et al.*, 2000; Boos & Ferreira, 2019; Fragkos *et al.*, 2015; Kitamura *et al.*, 2006). Areas with a higher density of origins tend to be replicated earlier in S phase (Fragkos *et al.*, 2015; Masai *et al.*, 2010). Not all replication origins end up being used during replication: only a small subset of origins (10-30%) will be activated and engage in DNA synthesis, with the rest remaining dormant unless needed to rescue stalled replication (Ekundayo & Bleichert, 2019; Evrin *et al.*, 2009; Fragkos *et al.*, 2015; Ge *et al.*, 2007; Masai *et al.*, 2010; Méchali, 2010).

The bacterial chromosome generally contains a single origin of replication which is defined by a consensus sequence, as well as a highly AT-rich downstream region (Trojanowski *et al.*, 2018). The genome of budding yeast contains the autonomously replicating sequence (ARS), which has a highly conserved sequence and is capable of binding to replicative proteins and initiating origin firing. In fission yeast, replication origins are not defined by a specific sequence, but are generally AT-rich (Prioleau & MacAlpine, 2016). Human and other metazoan replication origins are not defined by a consensus nucleotide sequence. Certain genetic elements have been found to be enriched at replication origins, however none identified are sufficient for replication (Cayrou *et al.*, 2012; Dorn & Cook, 2011; Ekundayo & Bleichert, 2019; Prioleau &

MacAlpine, 2016; Vashee *et al.*, 2003). For example, GC-rich regions of DNA, specifically those predicted to form G-quadruplexes, are enriched at replication origins (Costa & Diffley, 2022; Fragkos *et al.*, 2015; Prioleau & MacAlpine, 2016; Valton *et al.*, 2014).

Other features of the DNA landscape, for example the absence of nucleosomes, or chromatin marks such as histone methylation (me) and acetylation (ac), are linked to replication origins (Boos & Ferreira, 2019; Ding & Koren, 2020; Dorn & Cook, 2011). Histone acetylation and methylation can influence whether an origin will fire in early or late S phase. Early-firing origins are more likely to localise with histone (H) 3 lysine (K) 4 me and H3K36me, and H3K9ac, H3K18ac and H3K27ac (Wootton & Soutoglou, 2021). Conversely, late-firing origins are associated with a lack of H3 and H4 acetylation, as well as H3K9me and H3K27me marks (Wootton & Soutoglou, 2021). The 3D structure of the genome also influences origin licensing and firing. Areas of chromatin that cluster together in 3D and are often found in close proximity are known as topological associated domains (TADs), and are held together by CTCF and Cohesin (Liu *et al.*, 2023). CTCF is displaced in G1 phase, leading to chromatin relaxation and the rearrangement of TADs (Liu *et al.*, 2023). TAD boundaries are strongly bound by PCNA, and are enriched for replication origins (Liu *et al.*, 2023). The location of DNA within the nucleus also impacts on replication timing. Early-replicating DNA tends to be found in the nucleoplasm, whereas late-replicating DNA is more likely to be found at the nuclear or nucleolar peripheries, known as lamina-associated domains (LADs) (Liu *et al.*, 2023).

It is likely that a combination of multiple factors determines the location of a replication origin, especially since origin usage varies both from cell to cell, and in the same cell between rounds of replication (Cayrou *et al.*, 2011, 2012).

Replication initiation occurs through origin licensing and activation. Replication origin licensing involves origin binding by origin recognition and replicative machinery proteins in late M and G1 phase (Ekundayo & Bleichert, 2019; Fragkos *et al.*, 2015). Firstly, the origin recognition complex (ORC) is loaded at the origin (Prioleau & MacAlpine, 2016). The ORC consists of ORC1-6 proteins, which have ATPase activity and bind DNA in an ATP-dependent manner (H. Li & Stillman, 2012). CDT1 and CDC6 then bind, followed by the mini chromosome maintenance proteins 2-7 (MCM2-7) which form the helicase core of the replication machinery (Evrin *et al.*, 2009; Remus *et al.*, 2009). MCM2-7 form a hexameric ring, and two complexes are loaded head-to-head on each ORC (Remus *et al.*, 2009). The ORC-CDT1-CDC6-MCM2-7 complex forms the pre-recognition complex (pre-RC), and represents a licensed origin (Nishitani & Lygerou, 2004).

Once the pre-RC is assembled, the origin needs to be activated in order to participate in replication. Origin activation occurs at the G1- S phase boundary by the action of DDK and CDK kinases (Gillespie & Blow, 2022; Heller *et al.*, 2011; N. Li *et al.*, 2023; Prioleau & MacAlpine, 2016; Tanaka *et al.*, 2007). DDK and CDK phosphorylate the MCM complex directly, and also phosphorylate CDC45 and GINS, which bind to MCM2 and MCM5 (Costa *et al.*, 2011) to form the CMG helicase (Fragkos *et al.*, 2015; Prioleau & MacAlpine, 2016). MCM10, TOPBP1, RECQL4 and TRESLIN are also phosphorylated and associate with the CMG helicase to promote activation (Fragkos *et al.*, 2015; Guo *et al.*, 2015; Izumi *et al.*, 2001; Sangrithi *et al.*, 2005). Once activated, the CMG double hexamers separate and unwind double-stranded (ds) DNA bi-directionally into single strands using ATP hydrolysis (Prioleau & MacAlpine, 2016; Reuswig & Pfander, 2019). The CMG helicase is thought to open and release the lagging strand of DNA, encircling only the leading strand (Pellegrini, 2023).

1.1.2 Replication progression

Once the MCM helicase is activated, various factors are recruited to the replication fork to promote DNA synthesis. These factors include proliferating cell nuclear antigen (PCNA), the replicative polymerases α , δ and ϵ , topoisomerases TOP1, TOP2A and TOP3A, and replication factor C (RFC) (Fragkos *et al.*, 2015; Heintzman *et al.*, 2019; Masai *et al.*, 2010; Pommier *et al.*, 2022). Initiation of synthesis requires a short RNA/ DNA primer synthesised by the primase subunit of DNA polymerase (Pol) α (Burgers & Kunkel, 2017; Daigaku *et al.*, 2015; Kunkel & Burgers, 2017; Stillman, 2008). The two main replicative polymerases δ and ϵ displace Pol α via RFC and PCNA, extend the primer at the 3' end, and translocate along the elongating strand in order to add more nucleotides (figure 1.1) (Stillman, 2008). Pol ϵ directly interacts with the CMG helicase and performs leading strand synthesis continuously in the 5'-3' direction with high processivity, following the CMG helicase as it unwinds parental DNA (Daigaku *et al.*, 2015; Loeb & Monnat, 2008; Stillman, 2008). Pol ϵ has intrinsic 3' exonuclease activity, allowing it to efficiently proofread and remove erroneously incorporated nucleotides (Shcherbakova & Pavlov, 1996).

The lagging strand is replicated simultaneous to the leading strand. Unlike the leading strand, the lagging strand is replicated discontinuously in the 5'-3' direction by Pol δ (Prindle & Loeb, 2012). As in leading strand synthesis, Pol α synthesises a short RNA primer and then switches to DNA polymerisation to extend the primer (Chilkova *et al.*, 2007; Deshmukh *et al.*, 2016). Pol δ replaces Pol α when the primer is around 20-30 nucleotides long and extends by hundreds of nucleotides until it reaches the next primer (Prindle & Loeb, 2012). PCNA greatly enhances Pol δ processivity through promoting binding to DNA (Chilkova *et al.*, 2007). Pol δ

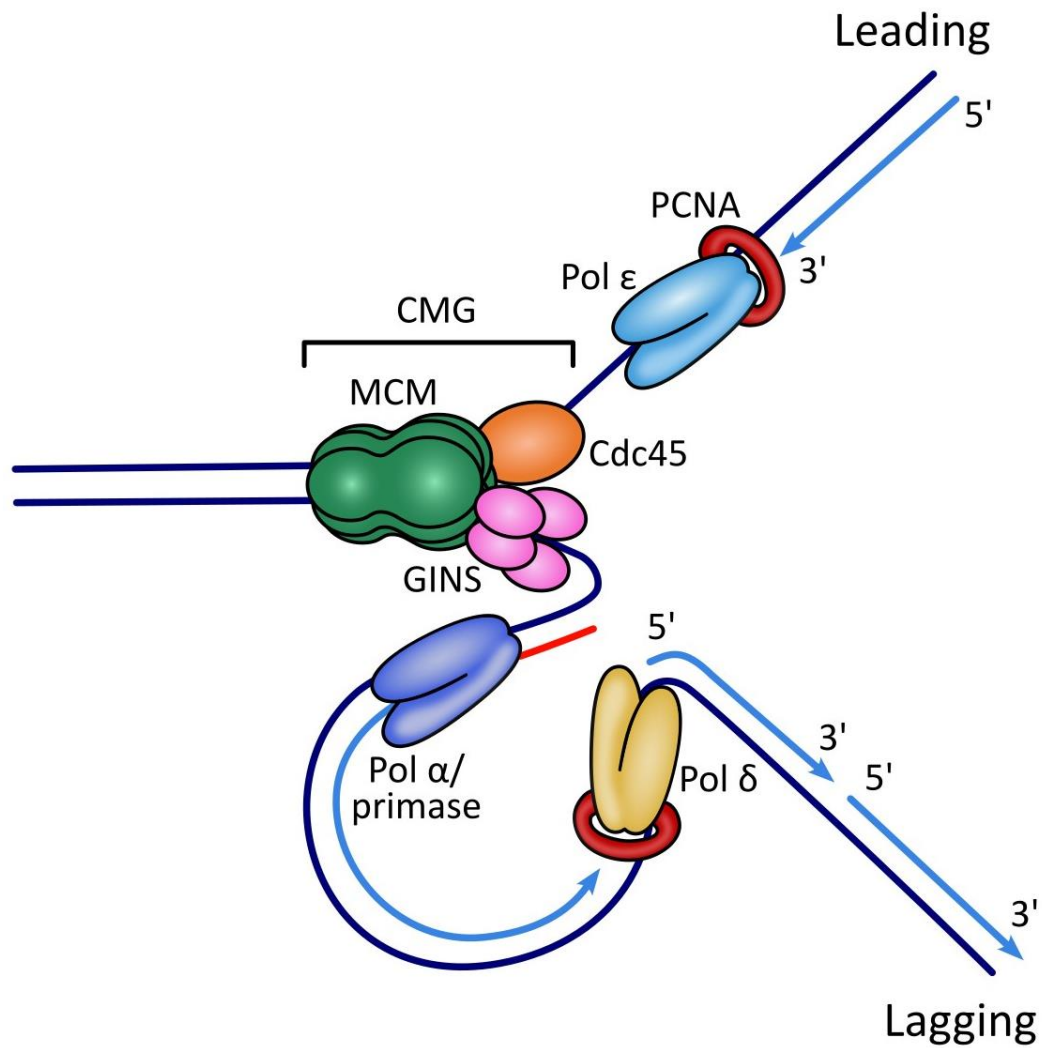


Figure 1.1: The replisome

DNA is replicated semi-conservatively by unwinding of the parental DNA strands by the CMG helicase. Pol α synthesises a short primer which is extended by Pol ϵ on the leading strand and Pol δ on the lagging strand. Synthesis occurs in a 5'-3' direction on both strands, which is achieved by using Okazaki fragments on the lagging strand, resulting in discontinuous replication. Adapted from Aparicio *et al.*, 2009.

proofreads the newly synthesised lagging strand through its exonuclease activity (Bullock *et al.*, 2020; Stillman, 2008). Pol δ may also correct errors in Pol α primers and Pol ϵ leading strand synthesis (Bullock *et al.*, 2020; Dmowski *et al.*, 2022; Zhou & Kunkel, 2022). The length of DNA polymerised by Pol α and δ on the lagging strand is known as an Okazaki fragment. The RNA section of the primer is removed by the concerted action of Pol δ and nucleases, mainly the flap endonuclease FEN1, in a process known as Okazaki fragment maturation (H. Sun *et al.*, 2023; Zheng & Shen, 2011). When Pol δ reaches the primer of the downstream Okazaki fragment it initiates strand displacement synthesis, whereby it displaces one ribonucleotide of the primer and replaces it with a deoxynucleotide triphosphate (dNTP) (H. Sun *et al.*, 2023). Pol δ pauses to allow FEN1 to cleave the displaced flap (H. Sun *et al.*, 2023; Zheng & Shen, 2011). Pol δ continues to slowly displace and replace the primer until the RNA section of the primer is removed (H. Sun *et al.*, 2023; Zheng & Shen, 2011). Some DNA may also be removed by FEN1 exonuclease activity to eliminate errors, as Pol α has low fidelity compared to the other replicative polymerases (Bębenek & Ziuzia-Graczyk, 2018; H. Sun *et al.*, 2023; Zheng & Shen, 2011). DNA ligase I ligates the nicks in the sugar-phosphate DNA backbone between Okazaki fragments, leading to a complete and continuous new DNA strand (H. Sun *et al.*, 2023; Zheng & Shen, 2011).

DNA re-replication can occur when parts of the genome are duplicated more than once during the cell cycle, leading to amplification of genomic regions (Truong & Wu, 2011; Zhang, 2021). As well as leading to loss of heterozygosity, DNA replication is associated with ssDNA formation, DNA double-strand breaks (DSBs) and genomic instability (GIN), so it is important that re-replication is avoided during DNA replication (Truong & Wu, 2011). DNA re-replication is prevented through tight regulation of factors involved in origin firing, especially CDT1 and

CDC6, to avoid the licensing and firing of origins on nascent DNA (Truong & Wu, 2011; Zhang, 2021). Overexpression of either CDT1 or CDC6 is sufficient to cause cells to re-replicate DNA, and the effect is further exacerbated with concurrent loss of the ATR signalling pathway (Truong & Wu, 2011). Loss of Geminin or Cyclin F also leads to re-replication (Walter *et al.*, 2016; Wohlschlegel *et al.*, 2000). CDT1 protein levels are tightly regulated throughout the cell cycle: CDK2 phosphorylates CDT1 during S and G2 phases, leading to ubiquitination by CRL1/SCF-Skp2 and subsequent degradation by the ubiquitin proteasomal pathway (Nishitani *et al.*, 2006). A back-up pathway activated by chromatin-bound PCNA leads to Cul4-Ddb1-Cdt2/CRL4-mediated ubiquitination and degradation of CDT1, linking the activation of replication to CDT1 degradation (Nishitani *et al.*, 2006). CDT1 is also negatively regulated by Geminin during S and G2 phase by preventing CDT1 from associating with the MCM complex, thus preventing origin firing (Wohlschlegel *et al.*, 2000). CDC6 is ubiquitinated by CRL4-Cdt2 in S phase and SCF-Cyclin F in G2 phase, leading to its proteasomal degradation (Clijsters & Wolthuis, 2014; Walter *et al.*, 2016). Similarly to CDT1, ORC1 is ubiquitinated by SCF-Skp2 in S phase and subsequently degraded (Méndez *et al.*, 2002). DOT1L methylates H3K79 during S phase at fired origins, preventing re-replication; loss of DOT1L leads to re-replication (Fu *et al.*, 2013).

1.1.3 Replication termination and completion

Most replication forks terminate by converging with another replication fork, whereby Pol ϵ and the CMG helicase on the leading strand approach an Okazaki fragment on the lagging strand. The PIF1 helicase separates the remaining stretch of unreplicated DNA between the two converging forks, allowing the CMG helicases to move past each other (Moreno &

Gambus, 2020; Xia, 2021). Once the CMG helicase encounters an Okazaki fragment on the lagging strand, it encircles the dsDNA region and translocates along the DNA without unwinding it (Dewar *et al.*, 2015). Pol ϵ finishes the final stretch of synthesis, and displaces and replaces the RNA/ DNA primer of the Okazaki fragment with FEN1. After the gaps in the DNA backbone are ligated, MCM7 is polyubiquitinated by CUL2-LRR1 and subsequently disassembled by p97/ VCP using energy from ATP hydrolysis (figure 1.2) (Dewar & Walter, 2017; Moreno & Gambus, 2020; Wu *et al.*, 2021; Xia, 2021).

As replication proceeds, torsional stress of the DNA backbone leads to supercoiling ahead of the replication fork, and the formation of catenanes behind (Dewar *et al.*, 2015; Dewar & Walter, 2017; Heintzman *et al.*, 2019). Catenanes physically link the two sister chromatids together and must be separated for mitosis, where the chromatids are separated (Charbin *et al.*, 2014). Topoisomerase II contributes to relieving torsional stress through resolving catenanes (McClendon *et al.*, 2005). If catenated chromatids persist through G2 phase and into mitosis, they are separated by the BLM-TOPIII α -RMI1-RMI2 (BTR) complex and PICH to prevent mitotic failure and loss of genetic material (Hertz *et al.*, 2023).

ATR and CHK1 act in late S phase to prevent premature entry into G2 phase by inhibiting CDK2 (Saldivar *et al.*, 2018). TRESLIN and its binding partner MTBP function independently of ATR/ CHK1 to suppress CDK1 activity throughout S phase to ensure that replication is completed before the onset of G2 phase (Zonderland *et al.*, 2022).

Synthesis can continue into G2/ M phase if replication is not completed during S phase. Replication stress can lead to un-replicated DNA, and hard-to-replicate regions/ common fragile sites (CFSs) often remain un-replicated until after S phase, especially in cancer cells

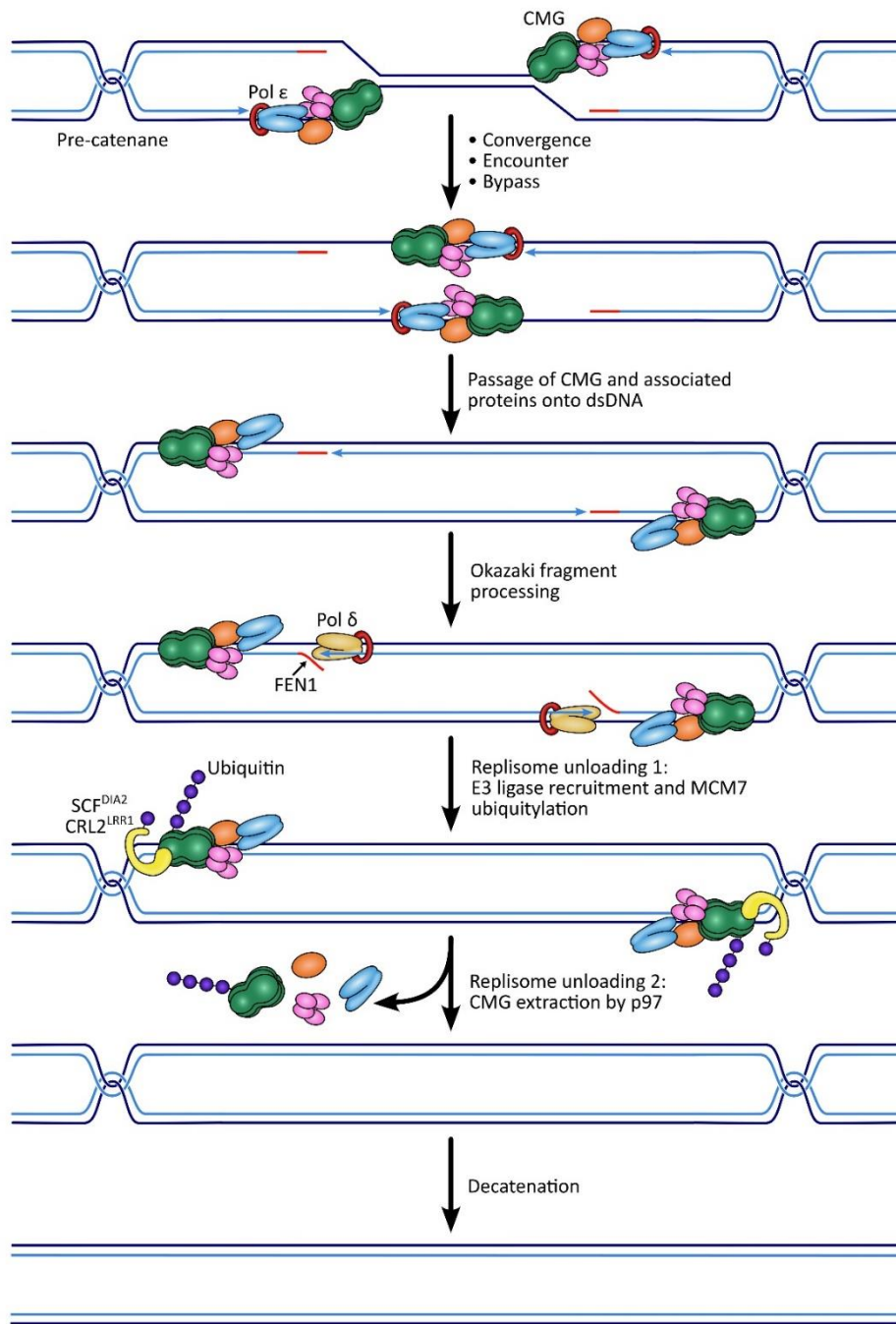


Figure 1.2: Replication termination

Replication is typically terminated through converging replication forks. The converging CMG machineries are thought to bypass each other and continue until they reach dsDNA. The replisome is ubiquitinated and unloaded by p97. Catenanes are removed to remove the physical links between the two dsDNA molecules. Adapted from Dewar & Walter, 2017.

which have less robust cell cycle checkpoints. Mitotic DNA synthesis (MiDAS) is employed during mitosis to finish replicating un-replicated DNA to ensure accurate separation of genetic material to the two daughter cells (Bhowmick *et al.*, 2023; Minocherhomji *et al.*, 2015). Replisomes can be disassembled in mitosis by a process mediated by the E3 ubiquitin ligase TRAP1 to ensure full removal of replisomes when replication is complete (Scaramuzza *et al.*, 2023; Sonnevile *et al.*, 2019).

Telomeres represent a challenge to the replication machinery due to the repetitive nature of the DNA, formation of secondary structure, change in chromatin structure, DNA-RNA hybrids, and the necessity to finish replication without the help of a converging fork (Bonnell *et al.*, 2021; Maestroni *et al.*, 2017). Telomeres are composed of TTAGGG sequence repeats with a single-stranded (ss) DNA overhang at the end (Bonnell *et al.*, 2021; Pfeiffer & Lingner, 2013). The single-stranded overhang can invade the double-stranded telomeric DNA to form a “T-loop”, which is bound by telomere-associating proteins to form the Shelterin complex (Bonnell *et al.*, 2021; Gilson & Géli, 2007). This prevents the ends of chromosomes from being recognised as a DSB and activating repair pathways. The T-loop/ Shelterin complex must be dismantled by RTEL1 to allow the replication fork to proceed (Stroik & Hendrickson, 2020). Replication forks travelling toward the telomere originate at sub-telomeric regions. The majority of the telomere is replicated semi-conservatively with the help of additional helicases such as BLM, WRN, RTEL1 and UPF1 in order to overcome G-quadruplexes, R-loops and other secondary structure (Bonnell *et al.*, 2021; Gilson & Géli, 2007; Maestroni *et al.*, 2017; Stroik & Hendrickson, 2020). A 3' ssDNA overhang is generated by nucleases, and the newly replicated telomeric DNA reforms a T-loop to complete telomere replication (Stroik & Hendrickson, 2020). Generation of the 3' overhang results in shortening of the telomere length, and each

successive round of replication leads to progressively shorter telomeres in most cells (Bonnell *et al.*, 2021). Once telomeres have shortened to a threshold length, cell senescence is induced (Bonnell *et al.*, 2021). However, at least two pathways to maintain or elongate telomeres are active in some circumstances. Telomerase is an enzyme that is expressed in stem cells, gametes, the early stages of gestation, and cancers, and elongates telomeres by synthesising new TTAGGG repeats at telomere overhangs (Udroiu *et al.*, 2022; Zvereva *et al.*, 2010). The separate alternative lengthening of telomeres (ALT) pathway uses a homologous telomere to extend shortened telomeres, and is also employed by cancer cells to escape senescence (J. M. Zhang & Zou, 2020).

As well as maintaining the genetic code during DNA replication, nucleosomes and epigenetic marks need to be copied. DNA is extensively methylated at cytosine residues, especially at CpG islands. DNA methylation is important in the regulation of gene expression, therefore influencing cell differentiation and cell fate (Moore *et al.*, 2012). Each daughter cell receives one methylated parental strand of DNA and one newly synthesised, unmethylated strand (Moore *et al.*, 2012). The nascent strand must be accurately methylated to match the parental strand. DNMT1 is a DNA methyltransferase enzyme that catalyses the transfer of a methyl group from S-adenosyl-L-methionine to cytosine residues (Hermann *et al.*, 2004). DNMT1 is recruited to chromatin through recognition of UHRF1-ubiquitinated H3 (Nishiyama *et al.*, 2013). DNMT1 preferentially recognises and methylates hemi-methylated DNA such as newly replicated DNA (Hermann *et al.*, 2004). DNMT1 travels with the replication fork by interacting with PCNA, allowing rapid methylation of newly synthesised DNA (Hermann *et al.*, 2004).

Histones are removed ahead of the replication fork to allow progression and are assembled again on newly synthesised DNA (W. Zhang *et al.*, 2020). Both parental and new histones are deposited on replicated DNA to ensure continuity in chromatin structure and epigenetic marks (W. Zhang *et al.*, 2020). Histones are deposited with the help of histone chaperones such as CAF-1 (Takami *et al.*, 2007).

1.2 Replication stress and cancer

Replication stress (RS) is defined as any disturbance to the replication fork, leading to slowing or stalling (Gaillard *et al.*, 2015; Macheret & Halazonetis, 2015; Saxena & Zou, 2022; Zeman & Cimprich, 2014). RS can be caused by many endogenous and exogenous factors and is linked to GIN and oncogenesis (Gaillard *et al.*, 2015; Macheret & Halazonetis, 2015; Saxena & Zou, 2022; Zeman & Cimprich, 2014). RS is recognised as a hallmark of cancer: RS has been detected in early pre-cancerous lesions, but not in highly proliferative healthy tissues, and can directly contribute to GIN and further oncogenic transformation (Gaillard *et al.*, 2015; Saxena & Zou, 2022). RS can have serious consequences including cell death through the generation of DSBs at stalled forks (Gaillard *et al.*, 2015; Macheret & Halazonetis, 2015; Zeman & Cimprich, 2014). Additionally, if a stalled replication fork is not rescued by a converging fork, then the intervening DNA may remain unreplicated, leading to loss of genomic material, mis-segregation of chromosomes during mitosis, and chromosomal rearrangements (Gaillard *et al.*, 2015; Macheret & Halazonetis, 2015; Saxena & Zou, 2022; Ubhi & Brown, 2019).

1.2.1 Endogenous and exogenous inducers of replication stress

A leading cause of RS is DNA lesions or unusual DNA secondary structure (Gaillard *et al.*, 2015; Saxena & Zou, 2022; Zeman & Cimprich, 2014). Tens of thousands of DNA lesions occur daily in cells as a by-product of cell metabolism or through replication errors, or from exposure to exogenous agents (Gaillard *et al.*, 2015; J. Wang & Lindahl, 2016; Zeman & Cimprich, 2014). DNA lesions include chemical alterations to DNA bases such as deamination, oxidation and alkylation (Saxena & Zou, 2022; Ubhi & Brown, 2019; Vesela *et al.*, 2017). Replication errors can result in the incorporation of a non-complementary DNA base, distorting the shape of the DNA backbone (Tsegay *et al.*, 2019; S. Yan *et al.*, 2014). ssDNA breaks occur frequently and can arise from oxidative damage from reactive oxygen species (ROS), stalled DNA topoisomerase I activity, unligated Okazaki fragments, or intermediates of DNA repair (Gaillard *et al.*, 2015; Macheret & Halazonetis, 2015; Zeman & Cimprich, 2014). ssDNA breaks can be converted to DSBs during replication, threatening cell viability and genomic stability if not properly repaired (Kuzminov, 2001; Tubbs & Nussenzweig, 2017). Natural features of DNA can create a challenge for the replication machinery, including highly repetitive regions, formation of secondary or tertiary DNA structure, heterochromatin-rich areas, and highly transcribed genes (figure 1.3) (Gaillard *et al.*, 2015; Jones *et al.*, 2012; Zeman & Cimprich, 2014).

There are a number of exogenous sources of DNA damage and RS, including ultraviolet (UV) light and ionising radiation (IR). RS can also be chemically induced with a variety of drugs, some of which physically alter the DNA through introducing intra- and inter-strand crosslinks (ICLs) (mitomycin C, psoralens and cisplatin), alkylating agents such as methyl methane sulphonate (MMS), and agents that mimic radiation damage, such as bleomycin (Vesela *et al.*, 2017). Other chemical inducers of RS do not cause direct changes to the DNA itself but instead target

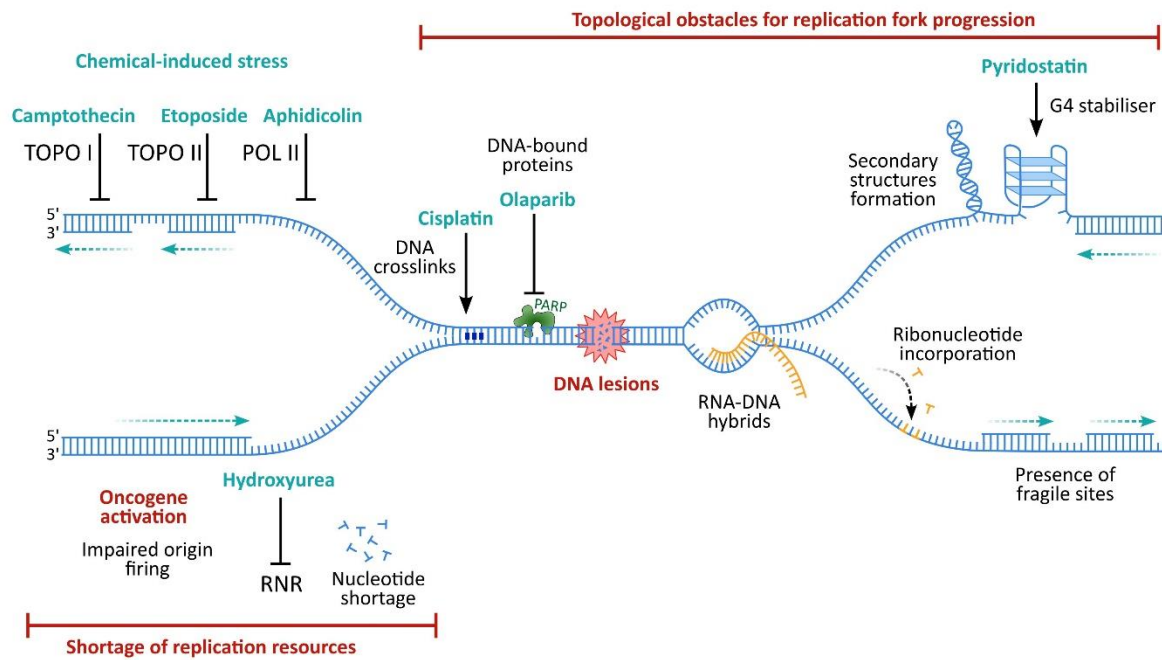


Figure 1.3: Sources of replication stress

RS is caused by a disturbance to replication, leading to slowing or stalling of the replication fork. RS can be induced by many exogenous and endogenous sources. Endogenous sources of RS include DNA damage e.g. DNA inter- or intra-strand crosslinks, DNA-protein complexes or damaged DNA bases. Misincorporation of nucleotides during replication can distort the DNA backbone, as do R-loops formed by RNA hybridising with DNA. Natural features of DNA can perturb replication progression through the generation of DNA secondary structure such as DNA hairpins or G-quadruplexes. Oncogene activation is another endogenous source of RS, limited to cells undergoing oncogenic transformation. Chemical inducers of RS include the topoisomerase poisons camptothecin and etoposide, aphidicolin, HU, and PARP inhibitors. Adapted from Willaume *et al.*, 2021.

enzymes involved in replication. Hydroxyurea (HU) inhibits the enzyme ribonucleotide reductase (RNR), leading to a shortage of dNTPs and halting replication (Koç *et al.*, 2004;

Musiąlek & Rybaczek, 2021). Aphidicolin inhibits B-family replicative and bypass DNA polymerases, blocking nucleotide binding and leading to helicase-polymerase uncoupling and the subsequent generation of long ssDNA stretches (Baranovskiy *et al.*, 2014; Vesela *et al.*, 2017). Olaparib is a poly(ADP-ribose) polymerase (PARP) inhibitor that prevents the PARP-mediated repair of single-stranded breaks (SSBs) (Javle & Curtin, 2011). Camptothecin stabilises DNA topoisomerase I on DNA, causing collisions with the replication machinery (Vesela *et al.*, 2017; Zhao *et al.*, 2012). Finally, etoposide inhibits DNA topoisomerase II, which induces a transient double-strand nick in the DNA (Zhao *et al.*, 2012). Etoposide stabilises the interaction of topoisomerase II with DNA and prevents the re-ligation of the DNA break, causing the DSB to persist and preventing the passage of replication machinery (Zhao *et al.*, 2012). All five drugs described here are most cytotoxic in S phase (Baranovskiy *et al.*, 2014; Koç *et al.*, 2004; Musiąlek & Rybaczek, 2021; Vesela *et al.*, 2017; Zhao *et al.*, 2012).

1.2.2 Oncogene-induced replication stress and genomic instability

A normal, correctly functioning gene product can become oncogenic through mutation of the DNA sequence, fusion with another gene, genomic amplification, or changes to expression patterns (Macheret & Halazonetis, 2015). These alterations can change or enhance the activity of the protein, resulting in oncogenesis (Macheret & Halazonetis, 2015). For example, the oncogene BCR-ABL is caused by chromosomal translocation of chromosomes 9 and 22, which fuses the BCR and ABL genes together, forming a constitutively active kinase with roles in activating multiple signalling pathways involved in proliferation, resistance to apoptosis and differentiation (Amarante-Mendes *et al.*, 2022).

Oncogene activation causes extensive cellular reprogramming, inducing changes in replication, cell cycle, metabolism and transcription (Kotsantis *et al.*, 2018). Oncogene expression can affect replication origin firing and replication fork dynamics, leading to oncogene-induced RS (OIRS) through a variety of oncogene-specific mechanisms. Several oncogenes are known to induce RS, including Cyclin E, MYC, RAS and BCL-2 (Kotsantis *et al.*, 2018). Oncogenes affect replication and induce RS in several ways, for example by misregulation of replication origin firing. Decreased origin firing can be caused by inhibition of replication origin licensing. Overexpression of the oncogene Cyclin E has been shown to reduce levels of MCM2, 4 and 7, impairing origin firing (Ekholm-Reed *et al.*, 2004). Decreased origin firing via oncogenic E1A/ MYC expression corresponds to an increase in fork speed and re-replication of DNA, and a lack of dormant origin firing can lead to failure to rescue stalled forks (Singhal *et al.*, 2013). Conversely, oncogenes can increase origin firing and dysregulate the temporal firing of origins. Unregulated origin firing can affect genomic stability in several ways. Perturbed origin firing can lead to an increase in transcription-replication collisions (TRCs) (where replication factories collide with transcription machinery), exhaustion of replication factors leading to fork stalling, and DNA damage caused by re-replication (Kotsantis *et al.*, 2018). For example, the oncoprotein RAS can cause increased origin firing, contributing to RS (Di Micco *et al.*, 2006). Faulty timing of origin firing can cause TRCs. Cyclin E is also implicated in increased origin firing, decreased speed of replication, and increased transcription and TRCs (Jones *et al.*, 2013). Origin re-firing can also occur through oncogene activation. Oncoproteins such as RAS can promote re-firing through upregulating CDC6, a key regulator of DNA licensing, leading to re-replication of DNA (Di Micco *et al.*, 2006).

Replication and transcription are separated both spatially and temporally to avoid collision of the machineries (Wei *et al.*, 1998). Loss of proper replication regulation by oncogenes can result in increased overlap of the two processes, leading to TRCs and subsequent fork stalling and collapse (Kotsantis *et al.*, 2018). Transcription induces the formation of R-loops between RNA and template DNA, and G-quadruplexes within displaced non-template ssDNA, which can cause replication forks to stall and lead to DNA damage (Bhatia *et al.*, 2014; Duquette *et al.*, 2004). Global transcription can increase upon oncogene activation, leading to an increase in R-loops and OIRS (Kotsantis *et al.*, 2016).

Cellular dNTP levels are inversely proportional to origin firing and are linked to fork speed (Poli *et al.*, 2012). Oncogenes can affect dNTP levels directly: the BCL-2 oncoprotein reduces RNR activity, depleting dNTP pools and leading to replication fork deceleration and OIRS (Xie *et al.*, 2014), whereas MYC has been shown to increase dNTP biosynthesis and enhance proliferation (Mannava *et al.*, 2008). Oncogenic hyperproliferation can indirectly lead to a reduction in dNTPs and subsequent fork slowing if dNTP synthesis cannot keep up with demand due to increased rates of DNA synthesis (Bester *et al.*, 2011).

1.2.3 Replication stress response

Low-level RS, such as the presence of a small number of stalled forks, can elicit a local cellular response in order to restore replication. Conversely, severe RS can induce global, cell-wide responses through ATR activation and the DNA damage response (DDR) (Flynn & Zou, 2011; Gaillard *et al.*, 2015). A stalled fork can generate stretches of ssDNA through the uncoupling of the polymerase to the CMG helicase, which continues to unwind DNA while the polymerase is

blocked (Byun *et al.*, 2005). Stretches of ssDNA are a marker of RS and an effective inducer of the RS response (Byun *et al.*, 2005). ssDNA is coated by RPA, which is subsequently bound by ATR and ATR-interacting protein (ATRIP) to form the ATR-ATRIP kinase complex (figure 1.4) (Cortez *et al.*, 2001; Flynn & Zou, 2011; Ünsal-Kaçmaz & Sancar, 2004). The alternative sliding clamp, composed of RAD9-HUS1-RAD1 (9-1-1), is also loaded via RPA, Pol α , RAD17 and RFC (Awasthi *et al.*, 2015; Flynn & Zou, 2011; Saldivar *et al.*, 2017). 9-1-1 and the MRE11-RAD50-NBS1 (MRN) complex independently recruit TOPBP1, which binds to and activates ATR-ATRIP, stimulating kinase activity and subsequent phosphorylation of downstream targets (Delacroix *et al.*, 2007; Duursma *et al.*, 2013; Kumagai *et al.*, 2006). Once activated, ATR is a potent kinase that phosphorylates a wide range of proteins with the canonical ATR target S/TQ amino acid motif, with the resulting potential to both activate and inhibit its targets (Awasthi *et al.*, 2015; Traven & Heierhorst, 2005). Notable ATR targets include the checkpoint protein CHK1 (serine [S] 317 and S345), p53 (S15), H2AX (S139) and RPA32 (S33) (Koundrioukoff *et al.*, 2013). ATR activation and downstream CHK1 signalling protects cells from the effects of RS through several mechanisms, including pausing S phase progression to allow the replication impediment to be removed or resolved, protecting stalled forks, promoting DNA repair, and pausing firing of new origins until replication is restored (Awasthi *et al.*, 2015; Flynn & Zou, 2011; Saldivar *et al.*, 2017). During RS, activated ATR/CHK1 inhibit global origin firing and simultaneously promote local origin firing in existing replication factories. This fine-tuning of origin firing allows the prevention of further fork stalling while encouraging completion of replication through dormant origin firing in regions with stalled forks (Ge & Blow, 2010). CHK1-

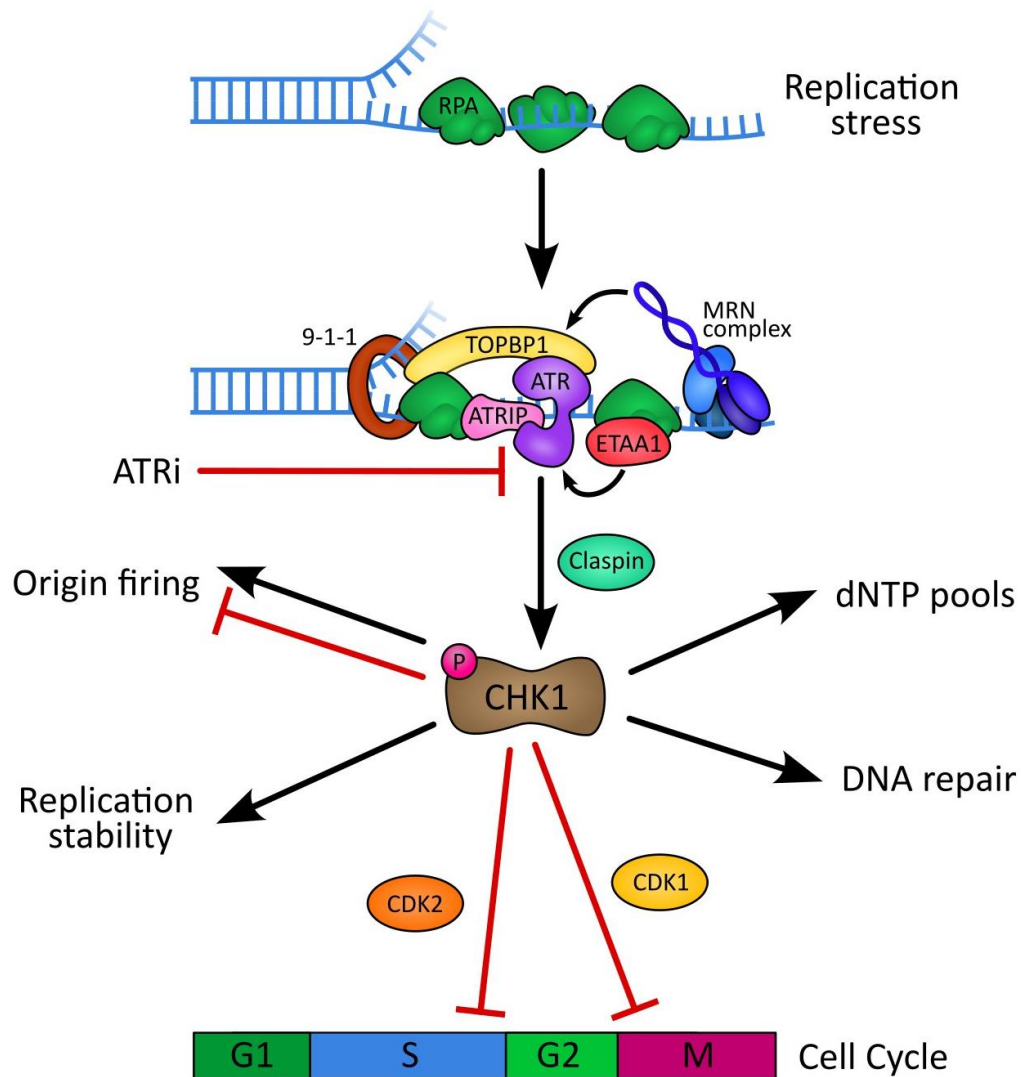


Figure 1.4: ATR signalling after RS.

RS leads to the generation of ssDNA, which is rapidly coated by RPA. ATR and ATRIP are recruited, along with TOPBP1 and the 9-1-1 alternative sliding clamp. Once activated, ATR phosphorylates CHK1, leading to widespread downstream effects including control of origin firing, promoting DNA repair, and halting cell cycle progression. Adapted from Mei *et al.*, 2019.

dependent phosphorylation and inhibition of the CDC25A/B/C phosphatases prevents downstream activation of CDK1 and CDK2 and subsequent entry into mitosis (Furnari *et al.*,

1997; C. Y. Peng *et al.*, 1997; Saldivar *et al.*, 2017; Sanchez *et al.*, 1997). Interestingly, ATR and CHK1 signalling is active in unperturbed cells to prevent excessive and uncontrolled origin firing (Ge & Blow, 2010).

1.3 Mechanisms of replication fork recovery

It is important that a stalled replication fork is restarted so that replication can complete and genomic integrity is maintained. If a replication fork stalls for a prolonged period, it can collapse and be unable to restart (Petermann & Helleday, 2010). This can potentially cause major issues for the cell and needs to be properly responded to. Lesions on the lagging strand do not pose as much of an issue for the replication machinery due to the semi-discontinuous nature of lagging strand synthesis (Cortez, 2015). However, damage or hindrances on the leading strand can cause replication fork stalling and a halt in synthesis until the obstacle is removed (Byun *et al.*, 2005; Cortez, 2015). There are various mechanisms by which stalled replication forks can be restarted (figure 1.5).

1.3.1 Lesion bypass

One method of overcoming replication fork stalling and halting of replication is lesion bypass. There are several mechanisms of lesion bypass currently known: translesion synthesis (TLS), template switching (TS), and repriming (Bainbridge *et al.*, 2021; Cortez, 2015; Ripley *et al.*, 2020; Santa Maria, 2014; Yang, 2011). TLS and TS are both controlled through

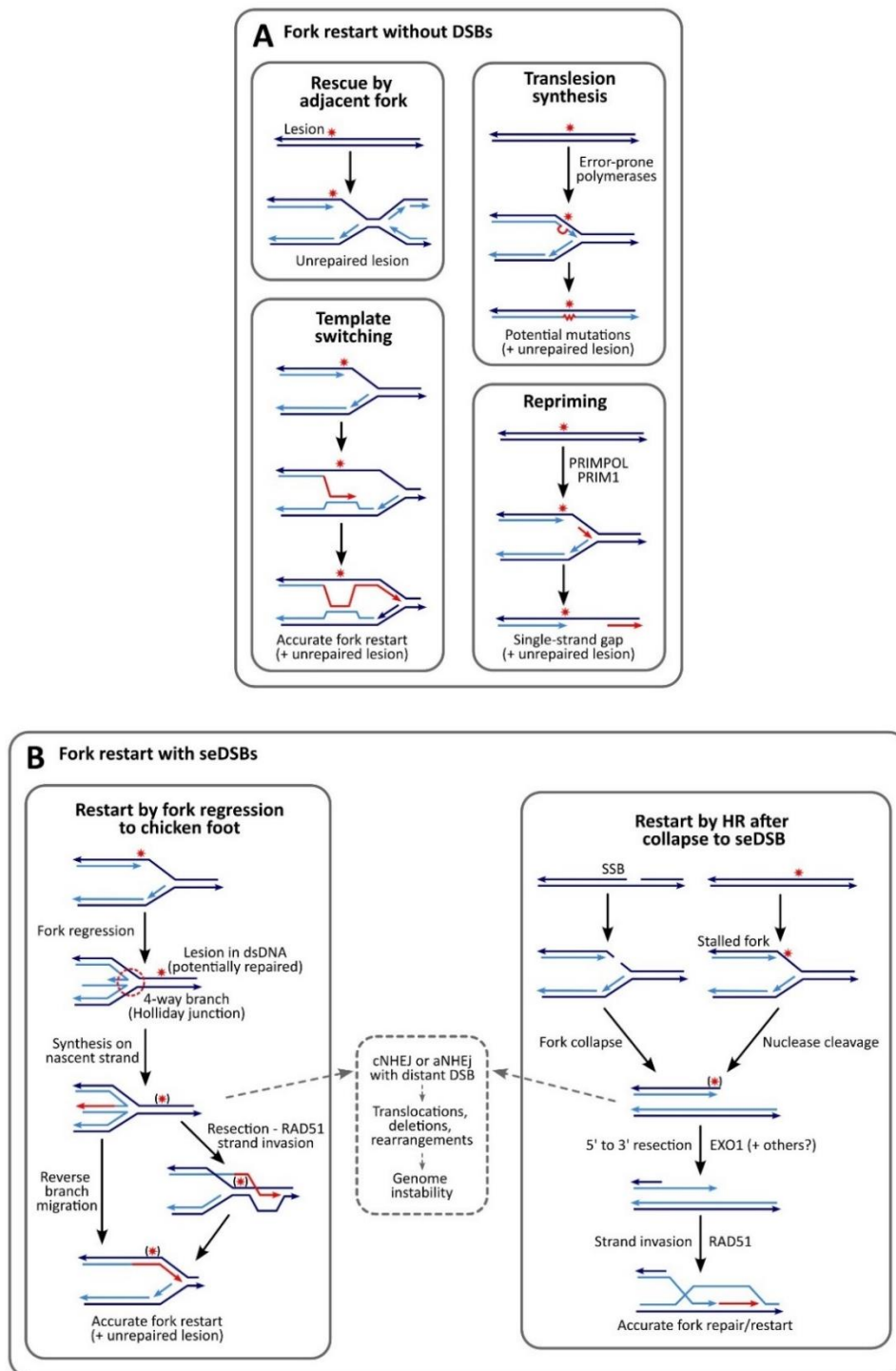


Figure 1.5: Replication fork restart pathways.

There are several pathways to restart stalled replication forks. a) Mechanisms that don't involve fork reversal include passive rescue of replication from a converging fork and lesion bypass (TLS, repriming and TS). b) When the replication fork regresses to form a four-way chicken foot structure, replication

can be rescued by restoration of the four-way structure or through HR-mediated strand invasion. Adapted from Nickoloff *et al.*, 2021.

ubiquitination of PCNA at K164: TLS is activated after monoubiquitination of PCNA by RAD6-RAD18, whereas TS is initiated after polyubiquitination by HLTF and SHPRH (Motegi *et al.*, 2008; Ripley *et al.*, 2020). PCNA ubiquitination is induced by RS and ssDNA but not by DSBs (Motegi *et al.*, 2008; Ripley *et al.*, 2020).

Cells carefully regulate usage of the different DNA damage tolerance (DDT) pathways through ubiquitylation, in order to restrict potentially mutagenic pathways (Cipolla *et al.*, 2016). TLS is usually mutagenic, which can contribute to carcinogenesis and resistance to chemotherapeutics, and its use must therefore be limited (Ler & Carty, 2022). As described previously, DNA replication impediments lead to replication fork stalling, helicase-polymerase uncoupling, generation of ssDNA, and activation of ATR (Byun *et al.*, 2005). INO80 is also recruited to stalled replication forks, where it recruits RAD18, which subsequently recruits RAD6 (Ler & Carty, 2022). RAD6-RAD18 catalyse ubiquitination of PCNA on K164 to determine DDT pathway choice (Ler & Carty, 2022). USP7, USP1 and ELG1 promote PCNA deubiquitination to fine-tune which DDT pathway is chosen (Kashiwaba *et al.*, 2015; K. Y. Lee *et al.*, 2010). If HLTF or SHPRH are recruited to the replication fork along with RAD6-RAD18, the TS pathway is favoured (Xu *et al.*, 2015).

TLS involves the switching of replicative polymerases to bypass polymerases upon PCNA monoubiquitination (A. R. Lehmann *et al.*, 2007; Yang & Woodgate, 2007). In humans, the bypass polymerases are polymerases η , ι , κ , ζ , REV1 and PrimPol (Díaz-Talavera *et al.*, 2022; A.

R. Lehmann *et al.*, 2007; Mourón *et al.*, 2013; Piberger *et al.*, 2020). These polymerases are able to replicate over lesions in the template strand due to having larger active sites compared to replicative polymerases, and are specialised in the types of lesion they are able to tolerate (A. R. Lehmann *et al.*, 2007). TLS has an important role in tolerance to UV-induced damage, which primarily causes DNA backbone-distorting cyclobutane pyrimidine dimers and 6-4 photoproducts (Yang, 2011). UV-induced DNA damage is efficiently removed and repaired by the nucleotide excision pathway (NER). However, when unrepaired UV by-products stall the replication fork, TLS is essential to avoid prolonged stalling and collapse (Yang, 2011; Yang & Woodgate, 2007). TLS polymerases are less faithful than replicative polymerases and lack proofreading activity, leading to inaccurate nucleotide incorporation in nascent DNA. TLS is therefore carefully regulated to avoid unnecessary mutagenesis (A. R. Lehmann *et al.*, 2007).

TS is a method of DDT that utilises recombination, making it a more accurate and less mutagenic pathway than TLS (Gonzalez-Huici *et al.*, 2014; Ortiz-Bazán *et al.*, 2014). 9-1-1 and EXO1 are recruited to polyubiquitinated PCNA, and RAD51 and BRCA2 catalyse strand invasion, allowing replication to proceed using the newly synthesised sister chromatid template strand (Bainbridge *et al.*, 2021; Karras *et al.*, 2013). The resulting sister chromatid junction is resolved by the BTR complex (Fasching *et al.*, 2015). TS is considered to be an error-free pathway in most circumstances (C. P. Lehmann *et al.*, 2020).

Repriming is a mechanism where replication is reinitiated after the lesion, allowing replication to continue but leaving unfilled ssDNA gaps behind the replication fork (Bainbridge *et al.*, 2021). PrimPol, previously mentioned as a TLS polymerase, is both a primase and polymerase that can generate DNA primers from dNTPs to initiate replication (Díaz-Talavera *et al.*, 2022;

Mourón *et al.*, 2013). During RS, PrimPol is deubiquitinated and binds to RPA (Y. Yan *et al.*, 2020). Repriming occurs at leading strand lesions, leaving ssDNA gaps behind the lesion which can be filled in post-replicatively (Bainbridge *et al.*, 2021; Díaz-Talavera *et al.*, 2022; Mourón *et al.*, 2013). It is thought that Pol δ replaces PrimPol to continue replication until it reaches the CMG helicase, whereby Pol ϵ takes over again as the leading strand polymerase (Guilliam *et al.*, 2016; Guilliam & Doherty, 2017).

1.3.2 Replication fork reversal

Replication forks reverse to form a four-way junction known as a chicken foot structure after replication fork stalling (Bhat & Cortez, 2018; Sogo *et al.*, 2002). The nascent daughter strands regress from the parent strands and anneal to one other to form a structure with a one-ended DSB, resembling a Holliday junction (HJ) (Qiu *et al.*, 2021). This reversal reaction can be catalysed by a number of proteins, but relies on RAD51 (Qiu *et al.*, 2021). Replication forks reverse in order to promote DNA repair, fork restart and fork repair mechanisms, but also to protect DNA during RS (Petermann & Helleday, 2010; Rickman & Smogorzewska, 2019). Replication fork reversal can aid DNA repair by moving the DNA lesion from ssDNA back onto dsDNA, allowing access for DNA repair proteins (Cortez, 2015). Fork reversal and stabilisation protects the stalled replication fork from cleavage into a DSB by the endonuclease MUS81, which then requires homologous recombination (HR)-based repair to restart forks (Liao *et al.*, 2018).

When replication forks stall and stretches of ssDNA are generated, the ssDNA is bound by RPA, initiating the ATR-mediated RS response as previously described (Gaillard *et al.*, 2015). RPA-

bound ssDNA also recruits the fork remodeller SMARCAL1 (Poole & Cortez, 2017). RAD51 is also a ssDNA binding protein that quickly displaces RPA, helping to avoid RPA exhaustion and the subsequent formation of unprotected ssDNA that is vulnerable to nucleolytic degradation (Bhat & Cortez, 2018). SMARCAL1, ZRANB3, FBH1 and HLTF are ATP-dependent helicases that can remodel replication forks (Bai *et al.*, 2020; Bhat & Cortez, 2018; Fugger *et al.*, 2015; Kolinjivadi *et al.*, 2017; Neelsen & Lopes, 2015; Vujanovic *et al.*, 2017). Other proteins, such as RAD54, RECQL5, FANCM, WRN and BLM, have been shown to catalyse fork reversal *in vitro*, though it is not known if they also act *in vivo* (Bugreev *et al.*, 2011; Gari *et al.*, 2008; Hu *et al.*, 2009; Islam *et al.*, 2010; Machwe *et al.*, 2007; Ralf *et al.*, 2006). SMARCAL1 is phosphorylated at multiple sites by ATR, with both inhibitory and stimulatory effects, in order to fine-tune and balance fork reversal activity (Couch *et al.*, 2013).

RAD51 is essential for fork reversal as its absence prevents the formation of the chicken foot structure (A. T. Wang *et al.*, 2015; Zellweger *et al.*, 2015). However RAD51 does not appear to be able to catalyse reversal itself, but may be necessary to stimulate reversal by helicases (Bhat & Cortez, 2018; A. T. Wang *et al.*, 2015; Zellweger *et al.*, 2015). PARP1 is recruited to SSBs and promotes fork reversal (Ray Chaudhuri *et al.*, 2012). RAD52 counteracts SMARCAL1 recruitment to forks, and ATR phosphorylates SMARCAL1 at S652 to reduce its activity, likely in order to prevent excessive fork reversal and fork collapse (Malacaria *et al.*, 2019).

1.3.3 Replication fork protection

Once a replication fork is reversed, it needs to be stabilised and protected to avoid nucleolytic degradation and promote prompt restart. The HR proteins BRCA1, BRCA2 and RAD51 are

instrumental in fork protection, a role which is separate from the functions of these proteins in HR (Rickman & Smogorzewska, 2019; Tye *et al.*, 2021). Other fork protection factors include PALB2, BARD1, various Fanconi anaemia (FA) proteins, BOD1L, WRN, WRNIP, and RAD51 paralogues (Billing *et al.*, 2018; Higgs *et al.*, 2015; Leuzzi *et al.*, 2016; M. Peng *et al.*, 2018; Schlacher *et al.*, 2012; Somyajit *et al.*, 2015; Thangavel *et al.*, 2015; S. Xu *et al.*, 2017). Interestingly, the role of RAD51 in fork protection seems to be separate from its role in fork reversal, as a RAD51 mutation with reduced DNA binding is proficient in fork reversal, but deficient in fork protection (Kolinjivadi *et al.*, 2017; A. T. Wang *et al.*, 2015).

The main nucleases that attack the reversed replication fork are MRE11, CtIP, EXO1, DNA2 and MUS81 (Gravel *et al.*, 2008; Mimitou & Symington, 2008; Rickman & Smogorzewska, 2019; Sartori *et al.*, 2007; Symington, 2014; Zhu *et al.*, 2008). Fork reversal protects against MUS81 cleavage as MUS81 prefers to cleave three-way junctions over four-way structures, though it can still nucleolytically degrade a reversed replication fork (Lemaçon *et al.*, 2017). Fork protection proteins are specific in which nucleases they inhibit, and some both inhibit some nucleases and promote or fine-tune others. For example, BRCA1, BRCA2 and RAD51 protect reversed replication forks from MRE11-mediated degradation (Lemaçon *et al.*, 2017; Qiu *et al.*, 2021; Rickman & Smogorzewska, 2019; Tye *et al.*, 2021). Several FA proteins also protect from MRE11 degradation but recruit the nuclease FAN1 (Lachaud *et al.*, 2016). BOD1L, an FA-related protein, protects against DNA2 (Higgs *et al.*, 2015).

Chromatin modifications also play a role in fork protection. EZH2 catalyses the trimethylation of H3K27, which recruits the endonuclease MUS81 to stalled replication forks, promoting degradation. Loss of EZH2-mediated H3K7me3 in BRCA2-deficient cells leads to stabilisation of

the replication fork and acquired resistance to PARP inhibitors (Rondinelli *et al.*, 2017). PTIP, a member of the MLL3/4 complex, promotes methylation of H3K4 and subsequent degradation by MRE11 in cells with a background of BRCA1 loss (Chaudhuri *et al.*, 2016). The lysine methyltransferase SETD1A methylates H3K4 and promotes RAD51-catalysed fork reversal, protecting nascent DNA from extensive degradation by DNA2 (Higgs *et al.*, 2018).

1.3.4 Replication fork recovery/ restart

The reversed replication fork can be restarted by two methods: fork restoration, where the four-way junction is converted back to an active three-way junction, or using HR-mediated restart. RECQL1 restarts forks through its ATPase and branch migration activities (Berti *et al.*, 2013). SMARCAL1 is able to both reverse replication forks into a chicken foot structure and restore this structure back into a three-way junction (Bétous *et al.*, 2013; Bhat & Cortez, 2018; Couch *et al.*, 2013; Lugli *et al.*, 2017). DNA2 in conjunction with WRN helicase processes stalled replication forks, promoting replication fork restart in a manner controlled by RECQL1 (Thangavel *et al.*, 2015). Forks can also be restored via HR, whereby RAD51 bound to ssDNA drives strand invasion of the newly re-annealed template strands, restoring the ongoing replication fork (Nickoloff *et al.*, 2021; Pardo *et al.*, 2020; Y. Xu *et al.*, 2017).

1.3.5 Replication fork recombination repair

If the replication machinery synthesises through a single-stranded nick in the DNA template, the SSB is converted to a DSB. If a replication fork is persistently stalled, it can be cleaved by

MUS81-EME1 to form a one-ended DSB with the broken arm separated from the replication fork, and the replisome can disassemble (Pardo *et al.*, 2020). This structure must be repaired by HR to avoid repair by mutagenic non-homologous end joining (NHEJ) (Kramara *et al.*, 2018; Malkova & Ira, 2013; Sakofsky & Malkova, 2017). The broken arm is resected and RAD51 catalyses strand invasion of the sister chromatid and reinitiates synthesis via a migrating D-loop bubble structure, often until the end of the chromosome (Anand *et al.*, 2013; Kramara *et al.*, 2018; Sakofsky & Malkova, 2017). GINS and Pol ϵ are reloaded onto the replisome via MRE11 and RAD51 (Hashimoto *et al.*, 2012). This type of replication, termed break-induced replication (BIR), results in conservative replication, and is also prone to genomic instability (Deem *et al.*, 2011). BIR is active during S, G2 and M phase as part of MiDAS (Kramara *et al.*, 2018). When RAD51 or other HR factors are not available or are exhausted, a separate BIR pathway dependent on RAD52 exists (Malkova *et al.*, 2005).

1.3.6 Conclusion

There are multiple pathways to promote restart of replication after replication forks encounter obstacles and stall. These pathways include passive rescue of replication through arrival of a converging replication fork, or firing of dormant origins to rescue replication. Other pathways include DDT mechanisms, namely TLS, TS and repriming, in order to bypass the lesion and allow replication to continue, with the lesion repaired and ssDNA gaps filled post-replicatively (Bainbridge *et al.*, 2021; Guillian & Doherty, 2017; Nickoloff *et al.*, 2021; Yang, 2011). Alternatively, the replication fork can be reversed into a chicken foot structure and restored by the fork remodelling enzymes SMARCAL1, RECQL1 or DNA2-WRN once the lesion has been

removed, or through homology-directed restoration via strand invasion and D-loop formation (Berti *et al.*, 2013; Couch *et al.*, 2013; Sturzenegger *et al.*, 2014; Taglialatela *et al.*, 2017; Thangavel *et al.*, 2015). Lastly, a fork that has been nucleolytically processed or “collapsed” into a DSB can be repaired by BIR, which is mediated by HR proteins (J. Kramara, B. Osia, 2018; Pardo *et al.*, 2020).

1.4 RECQ helicase family

The RECQ helicases are conserved from bacteria to metazoans (Croteau *et al.*, 2014). There are five RECQ helicases in humans: RECQL1, BLM, WRN, RECQL4 and RECQL5 (figure 1.6) (Croteau *et al.*, 2014). All have critical roles in genomic stability, with widespread roles in DNA replication, repair, recombination, telomere maintenance and transcription (Croteau *et al.*, 2014). The RECQ helicases prevent genomic instability and oncogenesis (Chu & Hickson, 2009).

1.4.1 WRN helicase/ exonuclease

The gene encoding the Werner helicase/ exonuclease protein is located on chromosome 8p12 and encodes a polypeptide of 1,432 amino acids (Gray *et al.*, 1997; Luo, 2010). WRN is a member of the RECQ family of SF2 helicases along with RECQL1, BLM, RECQL4 and RECQL5 (Croteau *et al.*, 2014). All of the RECQ helicases are intimately involved in DNA replication and repair, and mutations in RECQL1, BLM, WRN and RECQL4 result in distinct diseases (Croteau *et al.*, 2014). Each RECQ helicase has unique roles in DNA metabolism, and the loss of one cannot generally be compensated for by another (Croteau *et al.*, 2014). The RECQ helicases bind to

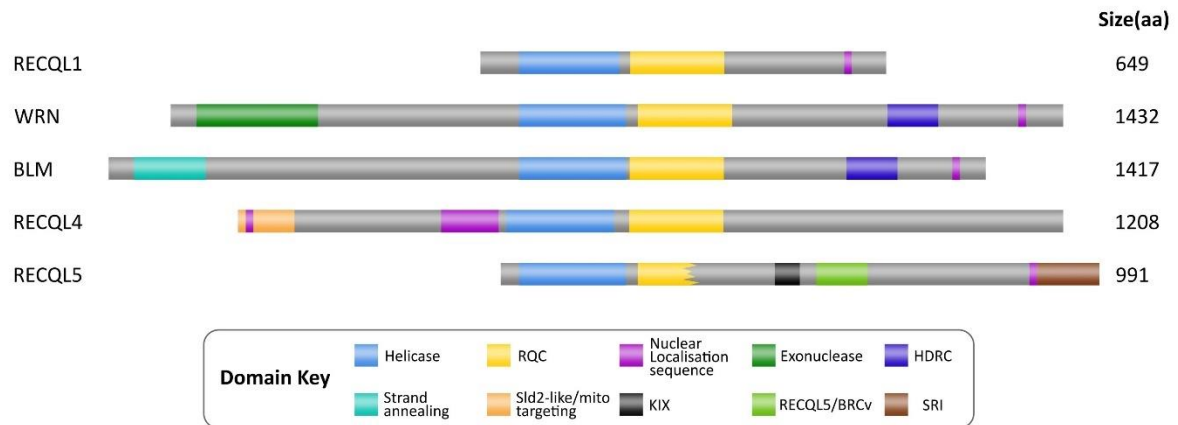


Figure 1.6: Human RECQ helicase family members and their domains.

The human RECQ helicase family consists of RECQL1, WRN, BLM, RECQL4 and RECQL5. All members of the family share the core ATPase/ helicase domain, a zinc-binding domain, NLS and RQC domain. Both WRN and BLM share an HRDC domain. WRN is the only member of the family to have an exonuclease domain. Adapted from Croteau *et al.*, 2014.

and are stimulated by ssDNA, and have a conserved helicase/ ATPase core domain which uses ATP hydrolysis to unwind DNA substrates in a 3'-5' direction (Croteau *et al.*, 2014). The RECQ helicases also share a zinc-binding domain, RecQ-conserved (RQC) domain and nuclear localisation signal (NLS) (Croteau *et al.*, 2014; Friedrich *et al.*, 2010). WRN and BLM share a helicase-and-ribonuclease D/C-terminal (HRDC) domain (Croteau *et al.*, 2014). WRN is unique in the RECQ helicase family by possessing an N-terminal exonuclease domain, which acts in a 3'-5' direction (Luo, 2010). The RQC domain of WRN is located proximal to the helicase domain and is important for DNA binding, directing helicase/ exonuclease activity, and localisation to telomeres (L. Sun *et al.*, 2017; Tadokoro *et al.*, 2012). The HRDC domain of WRN is also

important for localisation to sites of DNA damage and mediating protein-protein interactions (Samanta & Karmakar, 2012).

1.4.2 Werner syndrome

Homozygous or compound heterozygous loss-of-function mutations in the WRN gene cause the progeroid Werner syndrome (WS), first described in 1904 (Gray *et al.*, 1997; Luo, 2010; Yu *et al.*, 1996). WS affects sufferers at the onset of puberty, and is characterised by premature ageing, developmental delays, predisposition to rare mesenchymal cancers, and reduced lifespan (Croteau *et al.*, 2014; Gray *et al.*, 1997; Luo, 2010; Yu *et al.*, 1996). Patients with WS exhibit a reduced growth spurt during puberty leading to short stature and low body weight (Croteau *et al.*, 2014; Gray *et al.*, 1997; Luo, 2010). WS patients also present with alopecia, hypogonadism, and increased predisposition to age-related conditions such as diabetes, cataracts, heart attacks, and cancer (Croteau *et al.*, 2014; Gray *et al.*, 1997; Luo, 2010). Cancer development in WS patients differs from that seen in non-WS elderly populations, with a higher incidence of non-epithelial cancers compared to the rest of the population (Goto *et al.*, 1996). The majority of cancers in WS patients are thyroid epithelial neoplasms, melanoma, meningioma, soft tissue sarcoma, leukaemia and primary bone neoplasms, which may be related to inappropriate use of ALT in WS cells (Laud *et al.*, 2005; Lauper *et al.*, 2013; Multani & Chang, 2007). Over 80 patient mutations in the WRN gene have been identified, spread across the gene and resulting in a truncated, degraded or functionless protein lacking the C-terminal NLS sequence (figure 1.7) (Friedrich *et al.*, 2010). One WS patient was found to carry two compound heterozygous mutations in the helicase/ ATPase domain, each of which are

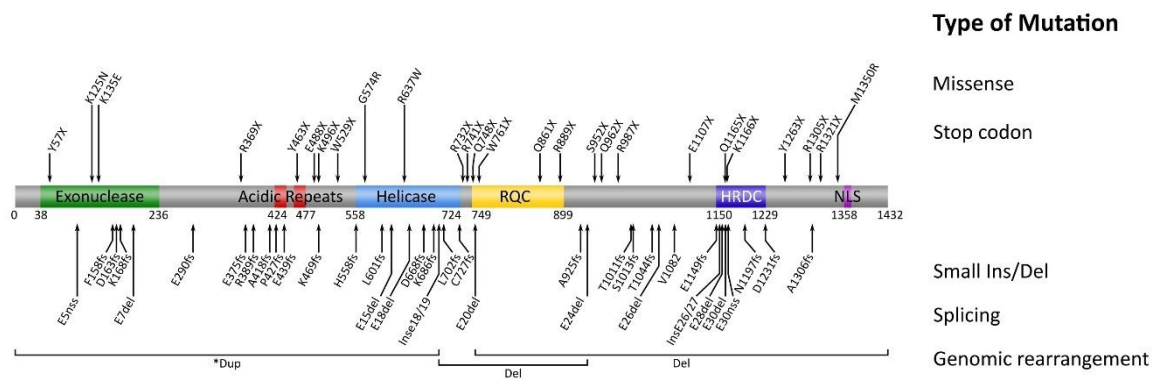


Figure 1.7: Map of location and type of mutation identified in WS patients.

WS is caused by mutation in the WRN gene. Over 80 WRN gene mutations have been identified which span almost the entire length of the gene and include missense mutations, premature stop codons, insertions/ deletions (indels), splicing mutants, and genomic rearrangements. All mutations currently identified occur upstream of the NLS, and most result in a truncated protein product or protein that lacks the ability to shuttle into the nucleus. Adapted from Friedrich *et al.*, 2010.

predicted to abolish enzymatic activity (Friedrich *et al.*, 2010; Huang *et al.*, 2006). These patient mutations highlight that WRN nuclear localisation and ATPase/ helicase activity are essential for WRN function, with catastrophic consequences when mutated.

1.4.3 Werner syndrome cells

Cells isolated from WS patients exhibit marked chromosomal instability (CIN), an increased mutation rate, protracted S phase, hypersensitivity to DNA-damaging agents, and premature senescence due to progressive loss of telomeres (Adelfalk *et al.*, 2005; Gudmundsrud *et al.*, 2021; Laud *et al.*, 2005; Poot *et al.*, 1992; Poot *et al.*, 2001; Takeuchi *et al.*, 1982). Fibroblasts

isolated from WS patients exhibit decreased life span, increased senescence, slower growth, misshapen nuclei, altered heterochromatin structure, lower proportion of S phase cells, S phase arrest and slow S phase kinetics compared to age-matched controls (Adelfalk *et al.*, 2005; Gudmundsrud *et al.*, 2021; Poot *et al.*, 1992; Takeuchi *et al.*, 1982). Analysis of chromosome spreads revealed deletions and variegated chromosomal translocations and rearrangements in WS cells (Poot *et al.*, 1992). WS cells exhibit an increased rate of telomere attrition and telomere-telomere fusions (Laud *et al.*, 2005). WS cells are hypersensitive to camptothecin, 4NQO, ICL inducers, and HU (Lebel & Leder, 1998; Lowe *et al.*, 2004; Ogburn *et al.*, 1997; Pichierri *et al.*, 2000, 2001; Poot *et al.*, 2001).

1.4.4 WRN post-translational modifications

In undamaged cells, WRN localises to the nucleolus, a membrane-less sub-compartment of the nucleus where ribosomal RNA gene repeats cluster and are highly transcribed (Gray *et al.*, 1998; Lindström *et al.*, 2018; Marciniak *et al.*, 1998). Hundreds of proteins involved in the DDR are also localised to the nucleolus, whether to serve a purpose in genomic stability at the ribosomal genes or as storage before translocation to the nucleus (Lindström *et al.*, 2018). During S phase, WRN moves into the non-nucleolar nucleus to aid replication, and immunofluorescent (IF) staining for WRN in replicating cells has revealed its presence diffusely in the nucleoplasm, localised to replication factories, and in the nucleolus (Huang *et al.*, 2006; Rodríguez-López *et al.*, 2003). Upon DNA damage or RS, WRN is acetylated by p300/ CBP at K366, K887, K1117, K1127, K1389 and K1413 (figure 1.8), and translocates from the nucleolus

of DSB formation (Ammazzalorso *et al.*, 2010; Su *et al.*, 2016). Phosphorylation of WRN at S1058, S1141 and S1292 by ATM after RS promotes RAD51 foci formation at broken replication forks by moving WRN away from the break (Ammazzalorso *et al.*, 2010). DNA-PKcs phosphorylates WRN at S440 and S467 after DNA damage (Kusumoto-Matsuo *et al.*, 2014). CDK1 phosphorylates WRN at S1133 after RS (Palermo *et al.*, 2016), and CDK2 phosphorylates WRN at S426 after DSB induction (J. H. Lee *et al.*, 2021). Phosphorylated WRN is also ubiquitinated and targeted for proteasomal degradation to ensure its timely removal from stalled or collapsed forks (M. Li *et al.*, 2020; Liu *et al.*, 2019). MIB1 was recently identified as an interactor and E3 ubiquitin ligase of WRN after camptothecin treatment, and MDM2 has also been shown to ubiquitinate WRN after etoposide treatment, though the exact residues where this occurs is not yet known (M. Li *et al.*, 2020; Liu *et al.*, 2019). Ubiquitination and subsequent degradation of WRN after camptothecin or etoposide treatment leads to cellular senescence (M. Li *et al.*, 2020; Liu *et al.*, 2019). WRN is also SUMOylated by p14ARF at the C-terminus, and by UBC9 at K356, K370, K496 and K898, which affects WRN localisation (Woods *et al.*, 2004).

1.4.5 WRN interactors and partners

WRN interacts with many proteins involved in DNA replication and repair, including the MRN complex (Cheng *et al.*, 2004), RAD51 (Otterlei *et al.*, 2006), BRCA1 (Cheng *et al.*, 2006), RPA (Brosh *et al.*, 1999), ATR (Ammazzalorso *et al.*, 2010), ATM (Ammazzalorso *et al.*, 2010), EXO1 (Aggarwal *et al.*, 2010), PCNA (Rodríguez-López *et al.*, 2003), DNA-PKcs (Karmakar *et al.*, 2002), WRNIP1 (Kawabe *et al.*, 2006), Ku (Cooper *et al.*, 2000; Orren *et al.*, 2001) and p53 (Blander *et al.*, 2004).

et al., 1999). These interactions influence the activity of WRN in several ways. For example, WRN associates with several molecules of the RPA70 subunit with high affinity, which greatly enhances the helicase activity of WRN and stimulates the unwinding of hundreds of base pairs of DNA (Lee *et al.*, 2018). WRN and FEN1 form a complex upon RS at stalled replication forks, and WRN can non-enzymatically and enzymatically stimulate FEN1 cleavage of substrate DNA structures resembling HJs *in vitro* (Sharma *et al.*, 2004). This data suggests that WRN and FEN1 may together be able to process reversed replication fork structures. WRN also collaborates with FEN1 at lagging strand telomeres during replication to ensure telomere replication and maintenance (B. Li *et al.*, 2017; Sparks *et al.*, 2020). WRN interacts with DNA2, another exonuclease/ ATPase-dependent helicase and FEN1 interactor involved in DNA replication and repair (Budd & Campbell, 1997; Sturzenegger *et al.*, 2014). WRN helicase activity promotes DNA2-mediated 5'-3' end resection at DSBs to stimulate HR repair, and WRN and DNA2 act together at stalled replication forks to promote restart (Sturzenegger *et al.*, 2014; Thangavel *et al.*, 2015).

1.4.6 WRN in DNA replication and replication stress

WRN is important in replication progression. WRN was identified at 52% of active sites of replication in one study, indicating that WRN is localised to a subset of replication forks and is important but not essential for replication (Rodríguez-López *et al.*, 2002). Several studies have shown that WRN loss results in a delay in completion of S and G2 phase in cells treated with MMS or HU, and an increase in bidirectional fork asymmetry indicative of fork stalling, but does not affect origin firing or spacing (Rodríguez-López *et al.*, 2002; Sidorova *et al.*, 2008).

WRN is also involved directly in DNA polymerisation through interaction with and support of Pol δ at complex DNA structures such as hairpins and telomeres (Kamath-Loeb *et al.*, 2001; Shah *et al.*, 2010). CFSs are hotspots for mutagenesis during RS, often resulting in microdeletions, metaphase chromosome breaks/ gaps and chromosomal rearrangements (S. Li & Wu, 2020). WRN ATPase/ helicase activity is essential for maintenance of CFSs and preventing the formation of ssDNA gaps (Pirzio *et al.*, 2008; Shah *et al.*, 2010). WRN ATPase/ helicase activity can unwind G-rich, repetitive, hairpin-forming DNA structures *in vitro*, a step that is essential for Pol δ synthesis past these structures (Kamath-Loeb *et al.*, 2001). WRN can also unwind Pol δ -stalling sequences in the FRA16D CFS, including repetitive (AT/TA)_n microsatellite sequences predicted to form DNA secondary structure. This activity is seemingly not dependent on either enzymatic activity of WRN (Shah *et al.*, 2010). WRN co-operates with DNA2 to process and restart stalled replication forks. Like WRN, DNA2 is a helicase and nuclease. However, DNA2 differs from WRN in that its helicase activity is weak and operates in the 5'-3' direction, and DNA2 has primarily 5'-3' endonuclease activity (Masuda-Sasa *et al.*, 2006). Using the DNA fibre assay, Thangavel *et al.* explored the roles of DNA2 and WRN at stalled replication forks (Thangavel *et al.*, 2015), and found that WRN ATPase/ helicase activity and DNA2 nuclease activity promote fork restart after a variety of fork-stalling agent treatments, and inhibit origin firing. DNA2 degrades ssDNA at reversed forks in a 5'-3' direction during HU treatment to promote restart. This mechanism is separate from RECQL1-mediated branch migration and fork restart, and RECQL1 inhibits DNA2-mediated degradation and restart. The pathway is abolished by RAD51 depletion and subsequent loss of reversed fork substrates, implicating the formation of a chicken foot structure as necessary for the WRN-DNA2 pathway of fork restart (Thangavel *et al.*, 2015).

WRN forms a complex with FEN1 at sites of RS and DNA damage (Sharma *et al.*, 2004). WRN stimulates FEN1 cleavage of flap-containing DNA substrates (Sharma *et al.*, 2004). Like WRN, FEN1 depletion leads to telomere instability, and a FEN1 mutant lacking the WRN interaction domain fails to rescue telomeric defects, suggesting that FEN1 and WRN co-operate to restart stalled forks at telomeric regions (Saharia *et al.*, 2010). WRN non-enzymatically stimulates the gap and flap endonuclease activities of FEN1 on replication fork substrates (Zheng *et al.*, 2005). A FEN1 mutant lacking gap endonuclease activity is hypersensitive to UV irradiation, indicating a role in processing DNA structures produced after DNA damage/ fork stalling (Zheng *et al.*, 2005). FEN1 depletion leads to hypersensitivity to HU (Thandapani *et al.*, 2017), loss of fork protection, a fork restart defect, MRE11 degradation and ssDNA accumulation (J. Zhang *et al.*, 2022). A patient variant of FEN1 with no WRN binding ability and reduced gap endonuclease activity is associated with cancer predisposition (Chung *et al.*, 2015).

1.4.7 RECQ helicase-associated diseases

Of the five RECQ helicases, four have so far been associated with human disease when mutated (Abu-Libdeh *et al.*, 2022; Monnat, Jr. & Sidorova, 2014). RECQL1 mutation causes RECON syndrome, BLM mutation causes Bloom syndrome (BS), WRN mutation causes WS, and RECQL4 mutation causes Rothmund-Thomson syndrome (RTS), Baller-Gerold syndrome (BGS), and RAPADILINO (Abu-Libdeh *et al.*, 2022; Monnat, Jr. & Sidorova, 2014). The RECQL-associated diseases share several similarities but also have differences (see table 1). All RECQL-associated diseases are autosomal recessive and are associated with short stature (Abu-Libdeh *et al.*, 2022; Monnat, Jr. & Sidorova, 2014). However, microcephaly has only been reported in

Syndrome	Onset	Bone defects	Skin defects	Cancer risk	Progeroid?
RECON syndrome (RECQL1)	Post-natal	Facial dysmorphism	Xeroderma	Unknown	Unknown
Bloom's syndrome (BLM)	<i>In utero</i>	No	Erythema, photosensitivity	Leukaemia, lymphoma, solid tumours	No
Werner's syndrome (WRN)	Puberty	No	Skin atrophy	Mesenchymal, sarcoma	Yes
Rothmund-Thomson syndrome (RECQL4)	<i>In utero</i> / post-natal	Widespread skeletal defects	Erythema, poikiloderma, photosensitivity	Osteosarcoma, skin cancer	No
Baller-Gerold syndrome (RECQL4)	<i>In utero</i>	Skull and arms	Erythema, poikiloderma	Osteosarcoma, lymphoma, skin cancer	No
RAPADILINO (RECQL4)	<i>In utero</i>	Thumbs, knees, arms, face	No	Osteosarcoma, lymphoma	No

Table 1: Shared and distinct phenotypes between the RECQ helicase-associated diseases.

patients with BS (Renes *et al.*, 2013). Patients with RECON, BS or WS display loss of subcutaneous fat (Abu-Libdeh *et al.*, 2022; Langer *et al.*, 2023; Sawada *et al.*, 2023), and WS patients exhibit deposition of visceral fat and subsequent development of diabetes (Yamaga *et al.*, 2017). RECON, RTS, BGS and RAPADILINO patients exhibit skeletal deformities (Abu-Libdeh *et al.*, 2022; Kellermayer, 2006), whereas BS and WS patients do not. All the RECQL-associated diseases except RAPADILINO are linked to skin issues, especially rashes, and BS and RTS patients exhibit photosensitivity (Abu-Libdeh *et al.*, 2022; Monnat, Jr. & Sidorova, 2014). Only BS is linked with immunodeficiency, with patients suffering repeated infections (Schoenaker *et al.*, 2018). BS, RTS, BGS and RAPADILINO develop in utero, as evidenced by low birth weight, microcephaly and skeletal abnormalities (Monnat, Jr. & Sidorova, 2014), though RTS patients occasionally present with post-natal onset of symptoms (Larizza *et al.*, 2010; Monnat, Jr. & Sidorova, 2014). However, patients with RECON syndrome are reported to be of

normal birth weight and size, with symptom onset in early childhood (Abu-Libdeh *et al.*, 2022). In contrast, WS develops during puberty, and is the only progeroid disease of the RECQL-associated syndromes (though the only RECON patients currently identified are young children, so it is unknown whether RECON syndrome is progeroid or not, and RTS patients are at risk of cataracts, which are age-related) (Abu-Libdeh *et al.*, 2022; Lu *et al.*, 2017; Monnat, Jr. & Sidorova, 2014). All RECQL-associated diseases (except RECON syndrome, due to lack of data) are associated with an increased risk of cancer (Monnat, Jr. & Sidorova, 2014). In BS patients there is a high lifetime risk (around 50%) of developing cancer, and all cancer types are enriched (de Renty & Ellis, 2017; German, 1997). In WS patients, cancers of mesenchymal origin and sarcomas are predominant (Goto *et al.*, 1996; Ozgenc & Loeb, 2006). In RTS, BGS and RAPADILINO, patients are at particular risk of developing osteosarcoma, and RTS and BGS patients are at risk of skin cancer (Kellermayer, 2006; Lu *et al.*, 2017; Siitonen *et al.*, 2009). BGS and RAPADILINO patients also display a higher risk of developing lymphoma (Kellermayer, 2006; Lu *et al.*, 2017; Siitonen *et al.*, 2009).

As highlighted with their roles in DNA metabolism, the RECQ helicase-associated diseases have several common, overlapping features, as well as symptoms that are unique to each disease. The predominance of developmental, skin and skeletal defects, as well as the predisposition to cancer, emphasises the importance of this family of helicases in humans, as well as their inability to fully complement each other.

1.4.8 RECQ helicases in replication

The other RECQ helicases have diverse and important roles in DNA replication. RECQL1 promotes origin firing and restores reversed forks back to a three-way junction to allow replication to continue (Berti *et al.*, 2013; Thangavel *et al.*, 2010). BLM mutation is characterised by slow S phase, CIN and accumulation of unresolved ultra-fine anaphase bridges (K. L. Chan *et al.*, 2007; Hand & German, 1975; Ockey & Saffhill, 1986). BLM binds to RPA and promotes replication fork restart, encourages fork stability and replication progression, and suppresses new origin firing during RS (K. L. Chan *et al.*, 2007; de Renty *et al.*, 2022; Shorrocks *et al.*, 2021). RECQL4 promotes replication initiation through assembling active CMG helicases at replication origins, and prevents re-replication (X. Xu *et al.*, 2023). RECQL5 prevents RS by resolving TRCs (Saponaro *et al.*, 2014), and antagonises RAD51 filament formation to promote MiDAS (Marco *et al.*, 2017; Urban *et al.*, 2016).

1.4.9 WRN in DNA repair

WRN localises to DSBs and has many roles in different DSB repair pathways. Reporter assays suggest that WRN depletion leads to a decrease in the use of NHEJ, single-stranded annealing (SSA), and HR (Chen *et al.*, 2003). NHEJ is used throughout the cell cycle and repairs the majority of DSBs (Karanam *et al.*, 2012). NHEJ proteins tether broken DNA ends to keep them in close proximity, and the DNA ends are then processed for ligation by DNA ligase IV (Stinson & Loparo, 2021). WRN associates with many key classical NHEJ (cNHEJ) proteins, including Ku70/80 (Cooper *et al.*, 2000; Orren *et al.*, 2001), XRCC4 (Kusumoto *et al.*, 2008), DNA ligase IV (Kusumoto *et al.*, 2008) and DNA-PK (Karmakar *et al.*, 2002). The Ku70/80 heterodimer stimulates WRN exonuclease activity, allowing WRN to degrade damaged DNA substrates that

usually inhibit WRN exonuclease activity (Orren *et al.*, 2001). The XRCC4-ligase IV complex also stimulates WRN exonuclease activity to generate ligatable DNA ends (Kusumoto *et al.*, 2008). DNA-PKcs phosphorylates WRN at S440 and S467 to promote nuclear localisation and exonuclease activity (Karmakar *et al.*, 2002; Kusumoto-Matsuo *et al.*, 2014; Yannone *et al.*, 2001). WRN also has roles in alternative NHEJ (alt-NHEJ), which differs from cNHEJ in the use of end resection and microhomology, and shares some proteins with the HR pathway. WRN suppresses alt-NHEJ use through restricting MRE11 and CtIP localisation to DSBs and preventing CtIP-mediated end resection (Shamanna *et al.*, 2016). WRN-depleted cells display CtIP-dependent telomere fusions (Shamanna *et al.*, 2016).

HR repair occurs during late S phase and G2 phase due to the availability of a homologous sister chromatid. WRN associates with several HR pathway proteins including NBS1, EXO1, DNA2, BRCA1, BARD1 and RAD51 (Baynton *et al.*, 2003; Cheng *et al.*, 2004, 2006; Saintigny *et al.*, 2002; Sharma *et al.*, 2003; Sturzenegger *et al.*, 2014). NBS1 binds to and enhances WRN helicase activity (Cheng *et al.*, 2004). WRN helicase activity co-operates with DNA2 nuclease activity to promote long-range end resection at DSBs (Sturzenegger *et al.*, 2014). WRN deficiency leads to accumulation of unresolved recombination intermediates, indicating a role in resolving products of HR repair (Saintigny *et al.*, 2002). BRCA1 associates with WRN and stimulates both helicase and exonuclease activities to repair DNA ICLs (Cheng *et al.*, 2006). SSA repair of DSBs involves extensive end resection to reveal homologous sequences. WRN interacts with RAD52, a key SSA protein, and enhances its strand annealing activity in conjunction with DNA2 (Baynton *et al.*, 2003; Sturzenegger *et al.*, 2014).

1.4.10 Targeting WRN for cancer therapy

WRN is considered to be a tumour suppressor due to its roles in preserving genomic stability. Conversely, targeting WRN in WRN-competent cancer cell lines and tumours has been reported to decrease cellular proliferation and viability, tumour growth and the efficacy of DNA damaging agents (Arai *et al.*, 2011; Futami *et al.*, 2008; Opresko *et al.*, 2007). WRN suppresses senescence in MYC-activated cancers (Moser *et al.*, 2012). WRN is overexpressed in many cancer cell lines (Futami *et al.*, 2008), and overexpression is associated with tumour aggressiveness and relapse in patients with head and neck cancer (Rusz *et al.*, 2017). WRN is therefore considered an attractive target for treating cancer. WRN was also recently found to be a synthetic lethal cancer target in cancers with mismatch repair deficiency and microsatellite instability (MSI), where WRN loss induced DSBs and cell death in MMR-deficient, MSI cells (Chan *et al.*, 2019; Kategaya *et al.*, 2019; Lieb *et al.*, 2019).

1.5 Mismatch repair pathway and Lynch syndrome

The mismatch repair pathway (MMR) detects and corrects replication-associated base-base mismatches and small indels that escaped proof-reading by the replicative polymerases. The core MMR pathway consists of seven proteins: MSH2, MSH3, MSH6, MLH1, MHL2 (PMS1), MLH3 and MLH4 (PMS2) (figure 1.9) (Pećina-Šlaus *et al.*, 2020). MSH2 predominantly forms a heterodimer with MSH6, but also dimerises with MSH3, and both complexes have ATPase activity (Kolodner & Marsischky, 1999). The MSH2-MSH6/3 complexes form a sliding clamp on DNA that scans newly replicated DNA for mismatches (Brown *et al.*, 2016). The MSH2-MSH6

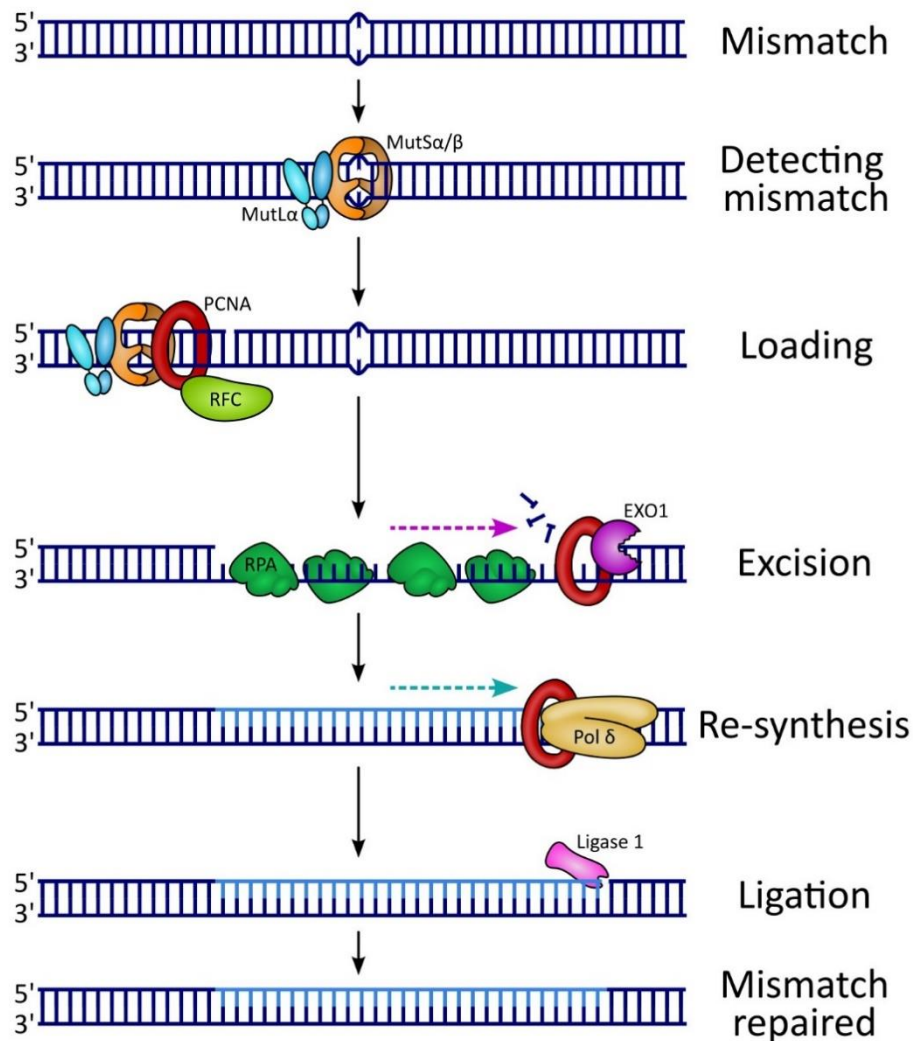


Figure 1.9: The eukaryotic MMR pathway.

Mismatches are detected by the MMR heterodimers MutSα (MSH2-MSH6) or MutSβ (MSH2-MSH3). The MutLα (MLH1-PMS2) complex is recruited along with other factors. Newly synthesised DNA is nicked by MutLα, followed by EXO1-dependent nucleolytic degradation. The gap is filled in by Pol δ, and the template is sealed by DNA ligase I. Adapted from Pećina-Šlaus *et al.*, 2020.

and MSH2-MSH3 complexes have both overlapping and distinct roles: the MSH2-MSH6 complex repairs base-base mismatches, both complexes repair small indels, and MSH2-MSH3

corrects larger indels (Umar *et al.*, 1998). MLH1 heterodimerises with PMS1, MLH3 or PMS2. The MLH1-PMS2 complex is recruited after mismatch detection along with PCNA, RPA, RFC, HMGB1 and EXO1. MLH1-PMS2 has ATPase and nuclease activity (Kadyrov *et al.*, 2006). The non-methylated nascent DNA strand is cut by MLH1-PMS2 and further degraded by EXO1 to initiate post-replicative repair, ensuring that the original parental DNA strand is used as a template. Pol δ is recruited to fill in the gap, and the nicked template is ligated by DNA ligase I (G. M. Li, 2007). Loss of MMR leads to an increased mutation rate and alterations in short repetitive regions known as microsatellites (Schmidt & Pearson, 2016). Inherited mutations or gene silencing in MSH2, MSH6, MLH1 and PMS2 are associated with Lynch syndrome (Niv, 2007). Lynch syndrome patients have a lifetime cancer risk of over 80%, and are at particular risk of developing colorectal cancer (Dominguez-Valentin *et al.*, 2020). Approximately 15% of all colorectal cancer cases are linked to inherited or acquired MMR deficiency (Kim *et al.*, 2013).

1.5.1 Microsatellite instability and cancer

Microsatellites are regions of DNA tandem repeats consisting of a short repeating unit typically one to six nucleotides in length, repeated dozens of times (Rohilla & Gagnon, 2017). Microsatellite repeat number varies widely from human to human. Microsatellites are difficult to replicate: replicative polymerases are prone to slip at repetitive sequences, leading to annealing of parental and daughter strands at the wrong place (Hughes & Queller, 1993). This generates an indel loop where the un-annealed nucleotides bulge out from the DNA backbone, which is detected by the MMR pathway (Martín-López & Fishel, 2013). Correction of the indel

loop leads to maintenance of the number of repeats of the microsatellite. When MMR is deficient, these replication-associated insertions or deletions are maintained and propagated to the daughter cells, where they may then undergo further alteration in length. The changing of microsatellite number between cell divisions is known as microsatellite instability (MSI). MSI is a common occurrence in several subtypes of cancer, with around 15% of colorectal cancers displaying MSI (Hampel *et al.*, 2005). MSI can be divided further into MSI-low and MSI-high, with MSI-high cells showing a higher number of unstable loci compared to MSI-low cells (Boland *et al.*, 1998). Microsatellite instability is referred to as a “hypermuted” state due to the high occurrence of mutations.

Mutations in the POLE (polymerase ϵ) and POLD1 (polymerase δ) genes also lead to a hypermutated phenotype in cells, and are associated with colorectal and endometrial cancer (Strauss & Pursell, 2023). However, the mutational landscape caused by POLE or POLD1 mutation differ significantly to those in MSI cells. Firstly, cancer cells with POLE/ POLD1 mutation are generally microsatellite stable (MSS) (though tumours with dual mutations in MMR and POLE/ POLD1 have been identified) (Chung *et al.*, 2021; Muzny *et al.*, 2012; Strauss & Pursell, 2023). Secondly, the mutation rate in POLE/ POLD1-mutated cancers is significantly higher than in MSI cells (>100 mutations vs >10 mutations per megabase of DNA, respectively) (Barbari & Shcherbakova, 2017; Chung *et al.*, 2021; Strauss & Pursell, 2023; Xing *et al.*, 2022). Thirdly, the mutational signature differs between cells with MSI and cells with POLE/ POLD1 mutations. POLE/ POLD1 mutations lead to an increase in the incidence of specific single nucleotide substitutions at distinct trinucleotide sequences (Chung *et al.*, 2021; Strauss & Pursell, 2023).

1.5.2 WRN synthetic lethality with mismatch repair deficiency

Synthetic lethality describes the phenomenon where the combined loss or alteration of two proteins causes cell death, whereas either event alone does not. This indicates a promising opportunity to exploit synthetic lethality to selectively kill cancer cells due to the propensity for cancer cells to possess mutations, exhibit oncogene dependency, and have altered cellular pathways. Identifying synthetic lethal interactions in cancer cells opens new areas of therapeutic potential. Targeting synthetic lethal relationships has already been used in patients for the treatment of BRCA-deficient cancers with PARP inhibitors (Lord & Ashworth, 2017).

Analysis of data from two large-scale CRISPR knockout/ shRNA knockdown screens in cancer cell lines revealed that WRN loss is synthetic lethal with MMR deficiency (Chan *et al.*, 2019; Kategaya *et al.*, 2019; Lieb *et al.*, 2019; McDonald *et al.*, 2017; Meyers *et al.*, 2017). Sensitivity to WRN depletion corresponds to the severity of MSI in the 51 MSI cell lines represented across the two studies, whereas viability of 541 MSS cell lines is not affected (Chan *et al.*, 2019; Kategaya *et al.*, 2019; Lieb *et al.*, 2019). The majority of the MSI cell lines in the studies are of colorectal, endometrial, gastric and ovarian origin, and all exhibit WRN dependency (Chan *et al.*, 2019; Kategaya *et al.*, 2019; Lieb *et al.*, 2019). Loss of cell viability in WRN-depleted MSI cells can be rescued by complementation with wild-type or exonuclease-dead WRN constructs, but not ATPase/ helicase-dead WRN, implicating WRN helicase activity specifically in the synthetic lethal relationship (Chan *et al.*, 2019; Kategaya *et al.*, 2019; Lieb *et al.*, 2019; Newman *et al.*, 2021). Interestingly, restoring MMR proficiency to MSI cells does not fully rescue cell viability after WRN depletion, suggesting that the genetic changes caused by MMR deficiency are irreversible (Chan *et al.*, 2019; Kategaya *et al.*, 2019; Lieb *et al.*, 2019). Similarly,

transient depletion of WRN and MLH1 or MSH3 does not lead to cell death in MSS cells, indicating that an intermediate step is required for WRN dependency to develop in MMR-deficient cells (Lieb *et al.*, 2019). MSI cells depleted of WRN exhibit an increase in DSBs, chromatin bridges, lagging chromosomes, micronuclei and broken chromosomes, and a decrease in cells in S phase (Chan *et al.*, 2019; Kategaya *et al.*, 2019; Lieb *et al.*, 2019). Intriguingly, telomere-specific defects are not seen in WRN-depleted MSI cells, suggesting that the role of WRN in telomere maintenance does not drive the synthetic lethal relationship (Chan *et al.*, 2019). p53-mediated apoptosis is induced in MSI cells after WRN depletion, though cell death is also seen in p53-depleted or p53-mutant MSI cells (Chan *et al.*, 2019; Kategaya *et al.*, 2019; Lieb *et al.*, 2019).

A report by van Wietmarschen *et al.* describes that knockout of MLH1 or MSH2 fails to sensitise human primary stomach epithelial cells to WRN loss after four months of continuous culture. This finding strengthens the hypothesis that the synthetic lethal relationship between WRN loss and MMR deficiency requires the development of downstream genomic events (van Wietmarschen *et al.*, 2020). The authors observe widespread DSBs and complete chromosome shattering (chromothripsis) in WRN-depleted MSI colorectal cancer cells. Analysis of the genomic location of DSBs in WRN-depleted MSI cells reveals that DSBs occur at extended (TA)_n microsatellites with tandem repeats of 25+ units, with extensive end resection occurring around the breaks. DSBs are only seen at ~ 8% of the almost 70,000 TA repeats in the genome, indicating that only a subset of TA repeats forms DSBs in WRN-depleted MSI cells. The TA repeats associated with DSB formation are longer and contain fewer interruptions, suggesting that (TA)_n repeat number and purity is linked to DSB formation after WRN depletion. DSB formation at TA repeats is suppressed by depletion of MUS81 or SLX4, indicating that DSBs

result from cleavage of stalled replication forks. Repetitive sequences are predicted to form thermodynamically favourable cruciform or hairpin structures, contributing to difficulty in replication (Bowater *et al.*, 2022). The authors suggest that extended (TA)_n tracts in MSI-high cells form highly stable cruciform structures that block the replication machinery, requiring WRN helicase activity to rescue replication and prevent DSB formation (figure 1.10).

Building on the hypothesis that extended TA repeats form DNA cruciforms that are cleaved in WRN-depleted MSI cells, Mengoli *et al.* interrogated the effects of MMR proteins and WRN at cruciform structures *in vitro* (Mengoli *et al.*, 2023). The researchers utilised a plasmid carrying an EcoRI restriction site flanked by non-TA inverted repeats, placing the restriction site at the single-stranded loop of the cruciform arm and thus rendering it unable to be cleaved by EcoRI. The effect of WRN and MMR proteins on cruciform formation was subsequently assessed by looking at the ratio of EcoRI-resistant (cruciform) to EcoRI-digested (non-cruciform) DNA products. Incubation of the DNA substrate with ATPase-proficient WRN leads to an EcoRI digestion product, indicating that the cruciform has been unwound by WRN. This activity is enhanced by co-incubation with RPA. Another construct with 23 TA repeats flanking the EcoRI site has a high propensity to spontaneously form cruciform DNA. Incubation with WRN leads to less efficient unwinding compared to the first substrate, implying that the TA cruciform rapidly re-forms after WRN unwinding. The MSH2-MSH6 and MSH2-MSH3 complexes are also able to unwind the TA cruciform substrate, as are MLH1-PMS2 and MLH1-MLH3, to a lesser extent. However, this unwinding is independent of ATP hydrolysis or RPA stimulation, implying use of a different cruciform-unwinding mechanism to that used by WRN. The authors theorise that the MMR complexes may stabilise the dsDNA structure over the cruciform, thus favouring the dsDNA form produced from spontaneous unfolding of the dynamic cruciform. Co-

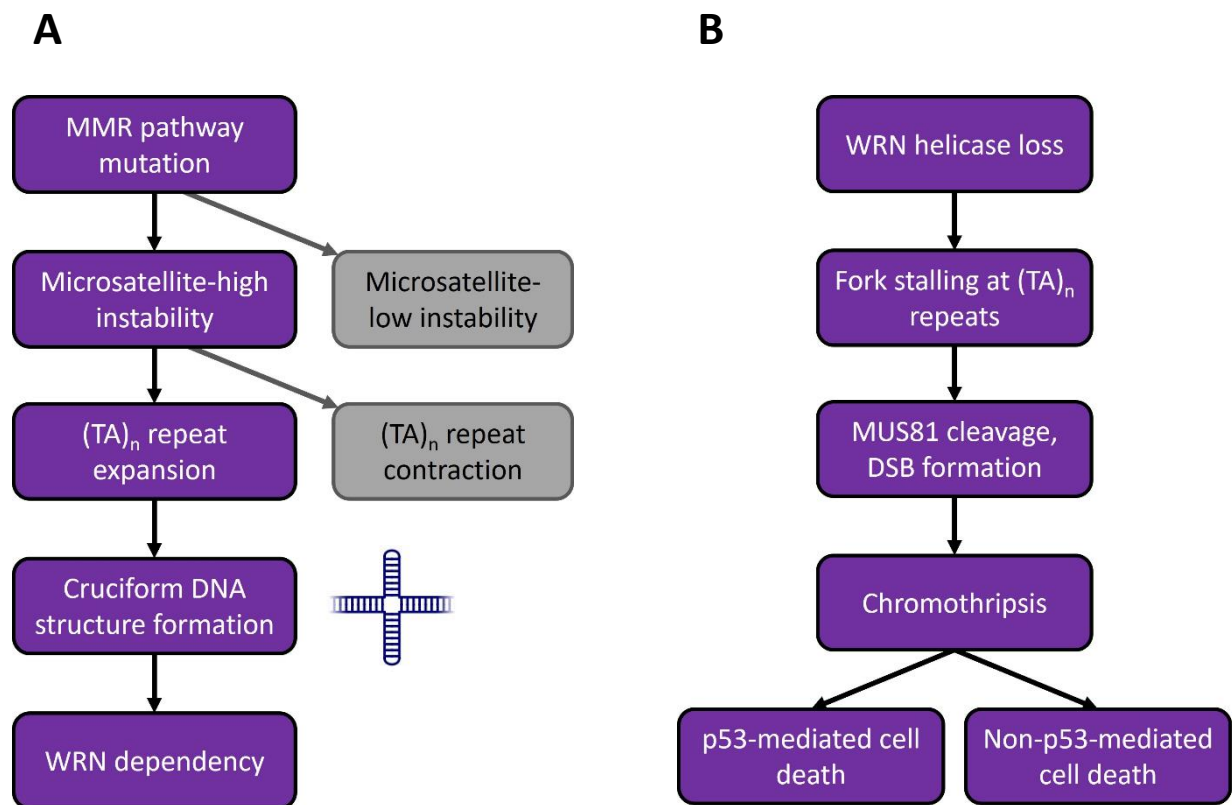


Figure 1.10: Development of WRN dependence and consequences of WRN loss.

a) MMR pathway deficiency can lead to MSI, where repetitive microsatellite sequences expand or contract due to replication errors. If TA repeats expand to a critical length, it is thought that the DNA folds into cruciform secondary structure, which relies on WRN unwinding to allow the replication fork to progress. b) Loss of WRN helicase function is thought to lead to fork stalling at cruciform-forming TA repeats, leading to MUS81 cleavage and DSB formation. Chromothripsis occurs, and cells die from p53-mediated apoptosis or non-p53-mediated cell death.

incubation of the TA cruciform substrate with WRN and MMR complexes synergistically enhances cruciform unwinding, independently of WRN ATPase/ helicase activity. Curiously,

BLM is also capable of unwinding the TA-containing cruciform, yet is dispensable *in vivo* for survival of MSI cells. These data suggest that some other physiological property of WRN beyond cruciform unwinding, such as localisation to stalled replication forks at cruciforms, is unique and necessary for survival of MSI cells.

A study by Zong *et al.* examined the effects of acute WRN depletion by PROTAC-mediated degradation on cell division and death in MSI colorectal and ovarian cells (Zong *et al.*, 2023). DSB formation and ATM activation are detected within two hours of WRN degradation, but cells continue replication. Cells then accumulate in G2, with RAD51 and 53BP1 foci observed. Subsequent rounds of cell division lead to increased numbers of 53BP1 bodies, mitotic defects and chromosomal abnormalities. Most cells proceed through two to three rounds of cell division before dying. A CRISPR knockout screen identified three genes (IPKK, c19orf43 and p53) that were enriched in WRN-depleted MSI cells, suggesting that loss of these genes could confer resistance to WRN depletion. However, co-depletion of WRN and any of these genes does not significantly rescue cell viability. MSI cells are sensitive to low-dose ATR inhibition compared to MSS cells, and combination with partial WRN depletion leads to additive hypersensitivity, suggesting the possibility of combination therapy with WRN and ATR inhibition in patients.

Picco *et al.* analysed 55 MSI colorectal cancer cell lines and organoids to assess whether previous chemotherapy treatment and resistance affects WRN dependency (Picco *et al.*, 2021). Depletion of WRN in treatment-resistant MSI cancer cells leads to cell death, suggesting that strategies employed by cancer cells to overcome chemotherapy and immunotherapy do not lead to resistance to WRN targeting.

1.5.3 Current treatments for microsatellite unstable cancers

Until recently, MSI cancers had been treated similarly to MSS cancers, with a standard regimen of platinum-based chemotherapy (oxaliplatin combined with 5-fluorouracil) (Chau & Cunningham, 2009). Oxaliplatin is a derivative of cisplatin, and both induce inter- and intra-strand crosslinks and DNA-protein crosslinks through inducing DNA-platinum adducts (Faivre *et al.*, 2003). However, most cancers progress within a year of this treatment (Choucair *et al.*, 2021). New advances in MSI cancer treatment have shown that immune checkpoint inhibitors (ICIs) have therapeutic potential in patients with MMR-deficient, MSI-high tumours.

Polymerase slippage and microsatellite expansion/ contraction due to MMR deficiency can result in the generation of frame-shift mutations in protein-coding genes. This can result in novel, mutated proteins that are digested by the proteasome and presented via HLA/ MHC on the cell surface of an MSI tumour cell (Choucair *et al.*, 2021). These unnatural peptides can be recognised by T cells and activate the innate immune system to destroy the cancer cells (Choucair *et al.*, 2021). Cancers evade the immune system in several ways, for example by overexpressing immune checkpoint ligands such as PD-L1 that act to dampen the immune response and prevent cancer cell apoptosis (Llosa *et al.*, 2015). ICIs such as pembrolizumab and nivolumab are monoclonal antibodies that bind to and block PD-L1 to encourage T cell activation and cytotoxicity (André *et al.*, 2020; Le *et al.*, 2015; Llosa *et al.*, 2015; Overman *et al.*, 2017). ICI treatment response is associated with increased tumour mutational burden. In a phase II trial of pembrolizumab, 40% of patients with MSI colorectal cancer showed responses vs 0% of patients with MSS colorectal cancer (Le *et al.*, 2015). Patients with MSI cancers treated with pembrolizumab showed improved survival and disease-free progression

in phase III trials when compared to patients treated with chemotherapy treatment only (André *et al.*, 2020; Le *et al.*, 2015, 2017). Nivolumab has also showed promising efficacy in trials (Overman *et al.*, 2017). Pembrolizumab is the first anti-cancer treatment to be approved in the USA based on cancer biomarkers alone rather than location of the tumour.

Despite these recent advancements, less than half of patients with MSI cancers respond to ICI treatment. Targeted treatment of MSI cancers through small molecule inhibition of WRN could represent an effective therapy option, with no resistance mechanisms as yet identified. More research is needed to better understand the mechanisms behind WRN synthetic lethality in MSI cancers and how to target these cancers effectively to improve patient survival and disease-free progression.

1.6 USP50 in replication

USP50 is a member of the ubiquitin-specific protease (USP) family of deubiquitinating enzymes (DUBs), which remove ubiquitin from target proteins with wide-ranging cellular effects including influencing protein localisation and proteasomal degradation (Cruz *et al.*, 2021). The USP family are cysteine proteases due to the presence of a cysteine residue in the catalytic triad that is critical for DUB activity, which is common to the majority of USPs (Snyder and Silva). The catalytic triad is composed of a cysteine, histidine and asparagine/ aspartic acid residue (Quesada *et al.*, 2004; Snyder & Silva, 2021). However, USP50 lacks the asparagine/ aspartic acid residue and the downstream C-terminal region found in other USP family members (Quesada *et al.*, 2004). USP50 showed no enzymatic activity on a ubiquitin recombinant substrate, indicating that the incomplete catalytic triad of USP50 renders it

inactive (Quesada *et al.*, 2004). USP50 is a poorly annotated gene, with a short N-terminal stretch of DNA followed by the identified, truncated USP domain containing the incomplete catalytic triad, which spans the rest of the USP50 gene length (uniprot.org; Q70EL3) (figure 1.11a). The USP domain in active USP family members contains multiple ubiquitin binding motifs and is able to cleave the isopeptide bond linking ubiquitin to target proteins (or to another ubiquitin molecule) (Snyder & Silva, 2021). The USP50 gene is located on chromosome 15 and lies head-to-head and partially overlapping with another USP, USP8 (ncbi.nlm.nih.gov; gene 373509). Proteins that have been demonstrated to physically interact with USP50 include HSP90 (Aressy *et al.*, 2010), ASC, NLRP3 (J. Y. Lee *et al.*, 2017), WEE1, KU70, HnRPNH3, FHL2 (Cai *et al.*, 2018), and ACE2 (Zuo *et al.*, 2023). USP50 has been implicated in control of the G2/M checkpoint (Aressy *et al.*, 2010), inflammasome regulation (Jiang *et al.*, 2024; J. Y. Lee *et al.*, 2017; Zhao *et al.*, 2024), erythropoiesis (Cai *et al.*, 2018), and SARS-CoV-2 infection (Zuo *et al.*, 2023).

USP50 has been identified as having an important role in the cellular response to HU-induced RS in two screens of deubiquitinases (DUBs) (Butler *et al.*, 2012; Yuan *et al.*, 2014), suggesting that USP50 has an important role in the replication stress response. Previous work in our laboratory using the DNA fibre assay showed that depletion of USP50 led to a decrease in ongoing replication forks and an increase in stalled replication forks (figure 1.11b). USP50 depletion led to an increase in the DNA DSB marker 53BP1 in S phase cells, suggesting that USP50 prevents DSB formation during replication (figure 1.11c). These S phase DSBs in USP50-depleted cells could be rescued by co-depletion of the structure-specific endonuclease MUS81, implying that USP50 prevents stalled replication forks from being cleaved into DSBs

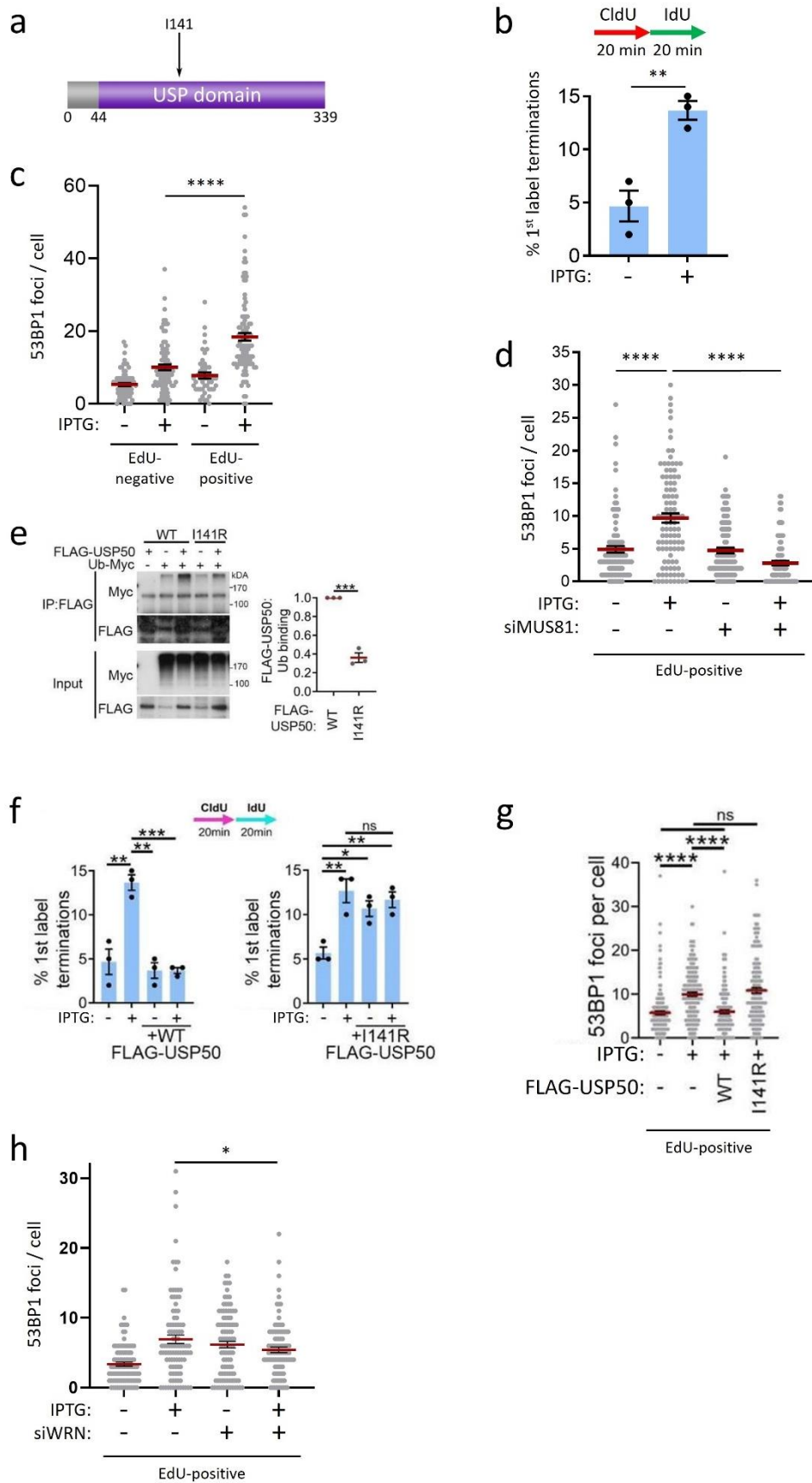


Figure 1.11

a) Annotated domains of the USP50 protein. The USP domain spans from amino acids 44 to 339. Residue isoleucine 141 is highlighted.

b) 1st label terminations were examined using the DNA fibre assay in HeLa cells treated with shRNA targeting USP50. shUSP50 expression was induced with IPTG; untreated cells were given vehicle (water). Results are from 3 independent repeats, with n >200 fibres per condition, per repeat. Bars indicate the mean, error bars are standard error of mean (SEM). Performed by Dr Helen Stone.

c) 53BP1 foci were examined using IF in EdU-negative and EdU-positive HeLa cells with USP50 depletion. shUSP50 expression was induced with IPTG; untreated cells were given vehicle (water). Results are from 2 independent repeats, with n >100 cells per condition, per repeat. Red lines indicate the mean, error bars are SEM. Performed by Dr Helen Stone.

d) 53BP1 foci were examined using IF in EdU-positive HeLa cells with USP50 and MUS81 depletion. shUSP50 expression was induced with IPTG; untreated cells were given vehicle (water). Transfection control was with siRNA targeting Luciferase. Results are from 3 independent experiments, with n >100 cells per condition, per repeat. Red bars indicate the mean, error bars are SEM. Performed by Dr Helen Stone.

e) Immunoprecipitation of FLAG epitopes from HeLa cells expressing FLAG-USP50 or I141R-FLAG-USP50 and Myc-Ub, probed for FLAG and Myc (left) and quantification (right) of Myc-Ub from 3 independent experiments, and normalised to both Myc-Ub and FLAG-USP50 expression in the whole cell lysate. Red bars indicate mean, error bars are SEM. Performed by Dr Hannah Mackay.

f) 1st label terminations were examined using the DNA fibre assay in HeLa cells treated with shRNA targeting USP50 and complemented with FLAG-USP50 (left) or I141R-FLAG-USP50 (right) or uninduced (-). shUSP50 expression was induced with IPTG; untreated cells were given vehicle (water). Results are

from 3 independent repeats, with $n > 200$ fibres per condition, per repeat. Bars indicate the mean, error bars are SEM. Performed by Dr Hannah Mackay.

g) 53BP1 foci were examined using IF in EdU-positive HeLa cells treated with shRNA targeting USP50 and complemented with FLAG-USP50 or I141R-FLAG-USP50. shUSP50 expression was induced with IPTG; untreated cells were given vehicle (water). Data is from 3 independent experiments ($n > 150$ cells per condition). Red bars indicate the mean, error bars are SEM. Performed by Dr Hannah Mackay.

h) 53BP1 foci were examined using IF in EdU-positive HeLa cells with USP50 and WRN depletion. shUSP50 expression was induced with IPTG; untreated cells were given vehicle (water). Transfection control was with siRNA targeting Luciferase. Results are from 3 independent experiments, with $n > 100$ cells per condition, per repeat. Red bars indicate the mean, error bars are SEM. Statistical analysis done with unpaired two-tailed t -test; $* = p \leq 0.05$. Performed by Dr Helen Stone.

(figure 1.11d). USP50 is predicted to bind to ubiquitin at the putative ubiquitin binding face located near isoleucine 141, and this residue is highly conserved evolutionarily. Previous results from our laboratory suggest that USP50 binds ubiquitin via isoleucine 141, as a mutant USP50 protein with arginine at position 141 shows reduced ubiquitin binding (figure 1.11e). Interestingly, this function of USP50 appears to be critical for its roles in promoting ongoing replication and suppressing replication-associated DSBs, as expression of a USP50 mutant with a substituted arginine residue at position 141 fails to rescue these phenotypes in USP50-depleted cells (figure 1.11f, g).

To test which pathways USP50 might be involved in, co-depletions were performed with proteins with similar roles in preventing DSB formation, and it was observed that USP50 and the RECQ helicase/ exonuclease WRN were epistatic in DSB formation (figure 1.11h). It is not

currently clear whether USP50 and WRN interact physically, as well as functionally. Previous work in the laboratory suggested that USP50 acts epistatically to WRN in the prevention of replication-associated DSBs, indicating a role in replication fork progression and genomic stability. This thesis explores the relationship between WRN and USP50 during replication.

1.6.1 Thesis aims

- 1) Investigate the relationship between USP50 and WRN in unperturbed replication and replication stress
- 2) Identify potential roles of USP50 in MSI cells with WRN synthetic lethality
- 3) Analyse consequences of USP50 loss on genome stability

2 Materials and Methods

2.1 Molecular biology

2.1.1 Bacterial transformation

Fifty ng plasmid or 5 µl ligation mix was added to 50 µl *E.coli* NEB5α competent cells (New England Biolabs; C29871) on ice and mixed gently by tapping. The transformation mixture was incubated on ice for 30 mins, then heated at 42°C for 45 seconds, and then returned to ice for 5 mins. Five hundred µl SOC outgrowth media (New England Biolabs; B9020) was added and the cells were incubated at 37°C with shaking at 600 rpm for 1 hour. Cells were plated onto agar (Sigma Aldrich; L7025) plates containing 100 µg/ml ampicillin (MP Biomedicals; 190146) and incubated in a standing incubator overnight at 37°C.

2.1.2 Plasmid DNA purification

A single colony was picked and grown overnight in 5 ml (miniprep) or 200 ml (maxiprep) LB-broth (Melford; L24066) containing 100 µg/ml ampicillin at 37°C at 200 rpm. Cultures were spun at 4100 g for 15 mins and the supernatant was poured off. DNA was extracted from the bacterial pellet according to the GenElute (Sigma Aldrich; PLN10) or QIAprep (Qiagen; 27104, 12963) Miniprep or Maxiprep kit instructions.

2.1.3 DNA quantification

DNA concentration was quantified using a Nanodrop 2000 machine. A blank measurement was taken using elution buffer. A 1.5 µl sample was loaded onto the machine and the DNA-50 programme was used to determine concentration.

2.1.4 Guide RNA (gRNA) design

To design the CRISPR gRNA sequences, the USP50 gene sequence and flanking upstream sequence was obtained from Ensembl (ensembl.org/index.html), and all protospacer adjacent motifs (PAM) (GG and CC motifs) and corresponding cut sites within 30 nucleotides of the edit site were noted. gRNA sequences were identified from the corresponding PAM, and on-target and off-target effects of each were predicted using the Integrated DNA Technologies gRNA design checking software (eu.idtdna.com/site/order/designtool/index/CRISPR_SEQUENCE). The two best-scoring gRNAs were commercially cloned into the pX459 vector, which uses the U6 promoter. The U6 terminator minimum consensus sequence is TTTT, so any TTTT sequences in the gRNA or resulting from cloning must be silently mutated to avoid premature transcription termination.

2.1.5 Double stranded homology directed repair (HDR) template design

The flanking 500 bp of the USP50 gene start site were obtained from Ensembl as before, and the chosen gRNA sites and PAM sequences highlighted. To avoid cutting of the HDR template by Cas9, the PAM sites or gRNA-binding sites were silently mutated. The 3x FLAG-tag sequence contains three repeats of the FLAG-tag sequence. To avoid recombination within the HDR

template, each FLAG-tag sequence was silently mutated. The HDR template was reduced to under 500 bp for higher efficiency of transfection. The construct was synthesised and cloned by GenScript.

2.1.6 Genomic DNA (gDNA) extraction

Once cells were confluent in a 6 well dish, media was removed, the cells washed twice with PBS (Sigma Aldrich; P4417) and 200 µl trypsin added. Once cells were detached, they were transferred to an Eppendorf tube and spun at 13,000 g for 5 mins to pellet the cells. The supernatant was removed and 100 µl Tail buffer (Viagen Biotech; 101-T) added and mixed to lyse the cells. One unit of proteinase K (Thermo Fisher; 11501515) was added to the cell suspension and incubated at 55°C for 1 hour. The proteinase K was then denatured by incubation at 75°C for 10 mins.

2.1.7 gDNA screening

PCR was set up with a forward primer annealing to the CRISPR plasmid sequence and a reverse primer annealing to genomic DNA downstream of the edit site, to identify clones which had incorporated the CRISPR edit into the genome. The PCR was run on an agarose gel and clones which produced a band of correct molecular weight were chosen for further screening. PCR products from successful clones were purified using a QIAquick PCR purification kit and were ligated into the pJET1.2/blunt vector using the CloneJET PCR cloning kit (Thermo Fisher; K1231) according to the manufacturer's instructions. The ligation mixture was transformed as before.

Twelve to fifteen individual bacterial colonies were picked, grown and the DNA extracted and sent for sequencing to confirm the presence of the CRISPR edit in the original clone.

PCR reaction:

Constituent	Concentration	Volume (μl)
GoTaq Green master mix	2x	10
Forward primer	10 μM	1
Reverse primer	10 μM	1
Template DNA	-	1
Nuclease-free water	-	7

Step	Temperature (°C)	Time (mins)	Cycles
Initial denaturation	95	5	1
Denaturation	95	1	35
Anneal	60	0.5	
Extension	72	1	
Final extension	72	5	1
Hold	4	Infinite	-

2.1.8 Gel electrophoresis

A 1% agarose gel was prepared by mixing 1 g agarose (Sigma Aldrich; A9539) per 100 ml 1x TAE buffer and heating in a microwave until the agarose had dissolved. Ethidium bromide (1:50,000) (BioRad; 1610433) was added to the 1% agarose solution. Gels were run with 1kb plus DNA ladder (Thermo Fisher; 10787018) for 30 mins at 120 volts. DNA was visualised in a GeneFlash UV transilluminator (Syngene).

2.1.9 Gel extraction

DNA run on an agarose gel was visualised using a UV transilluminator and excised. DNA was extracted using the QIAquick gel extraction kit (Qiagen; 28706X4) following manufacturer's instructions.

2.1.10 DNA sequencing

DNA was diluted to 100 μ M and 5 μ l sample sent to Source Bioscience with 5 μ l primers per reaction at 5 μ M. Sequencing data was analysed using SeqMan and Chromas software.

2.2 Protein biology

2.2.1 SDS-PAGE

Polyacrylamide gels were made up according to the recipe below. Acrylamide percentage was chosen based on protein size. Gels were made in BioRad gel pouring equipment.

Resolving layer (10ml)	6%	8%	10%	12%
Water (ml)	5.3	4.6	4	3.3
30% Acrylamide (ml)	2	2.7	3.3	4
1.5 M Tris pH 8.8 (ml)	2.5	2.5	2.5	2.5
10% SDS (ml)	0.1	0.1	0.1	0.1
10% APS (ml)	0.1	0.1	0.1	0.1
TEMED (ml)	0.01	0.01	0.01	0.01

Stacking layer (1ml)	5%
Water (ml)	0.68
30% Acrylamide (ml)	0.17
1M Tris pH 6.8 (ml)	0.13
10% SDS (ml)	0.01
10% APS (ml)	0.01
TEMED (ml)	0.001

Cells were harvested in 4x sample buffer, sonicated 3 times for 10 seconds, and boiled for 5 mins at 95°C. Polyacrylamide gels were run at 180 volts until the dye front had run to the bottom of the gel. PageRuler Plus prestained protein ladder (Thermo Fisher; 26619) was run alongside samples to ascertain molecular weight.

2.2.2 Western blotting

Proteins were transferred onto methanol-soaked PVDF membranes (Thermo Fisher; 88518) in 1x transfer buffer (20% methanol) at 100 volts for 2 hours. Membranes were blocked in 5% milk (Marvel) in PBST for 30 mins, then primary antibodies in 5% milk were added and incubated overnight at 4°C. Membranes were washed 3 times in PBST for 5 mins, then secondary antibodies in 5% milk were added and incubated at room temperature for 1 hour. Membranes were washed 3 times in PBST for 5 mins, then incubated with ECL (GeneFlow; 20-500-500B) at room temperature for 1 min. In a dark room, X-ray sensitive films (Scientific Laboratory Supplies; MOL-7016) were exposed to the membrane and developed in a Konica-Minolta SRX-101A medical film processor. Constitutively expressed proteins were used as loading controls. Protein signal was analysed in ImageJ.

2.3 Cell biology

2.3.1 Tissue culture

All colorectal cancer cell lines were sourced from Professor Andrew Beggs, University of Birmingham.

Cell line	RRID	Microsatellite status	Growth medium
HT29	CVCL_0320	Stable	McCoy's 5A medium + 10% FBS + 1% PenStrep
HT55	CVCL_1294	Stable	MEM + 20% FBS + 2 mM L-glutamine + 1% NEAA + 1% PenStrep
C80	CVCL_5249	Stable	Iscove's medium + 10% FBS + 2 mM L-glutamine + 1% PenStrep
HCT116	CVCL_0291	Unstable	McCoy's 5A medium + 10% FBS + 1% PenStrep
RKO	CVCL_0504	Unstable	MEM + 10% FBS + 2 mM L-glutamine + 1% PenStrep
LS411N	CVCL_1385	Unstable	RPMI + 10% FBS + 1% PenStrep

HeLa cells were grown in DMEM + 10% tetracycline-free FBS + 1% PenStrep.

Capan-1 cells were grown in DMEM + 20% FBS + 1% PenStrep.

All cell lines were maintained in T75 flasks at 37°C and 5% CO₂.

2.3.2 siRNA transfection

siRNA was transfected using DharmaFECT 1 (Horizon Discovery; T-2001-03). Per ml of media, 0.1-0.3 µl siRNA (100 µM) was mixed gently in 25 µl OptiMEM™ (Thermo Fisher; 31985070).

In a separate tube, 1 µl DharmaFECT 1 was mixed gently in 25 µl OptiMEM™. The two mixtures were combined, mixed gently, and incubated at room temperature for 20-25 mins before adding slowly to the cell media and mixed by swirling.

In HeLa and HCT116 cells, 10 nM siRNA was used. In HT29 cells, 30 nM siRNA was used. In HT55, C80, RKO and LS411N cells, 30 nM siRNA was added on two consecutive days (60 nM siRNA total).

2.3.3 CRISPR cell line generation

Flp-In™ HeLa cells were chosen for CRISPR editing. On day 0, 1×10^6 low passage cells were plated into 10 cm dishes. On day 1, 250 µl OptiMEM, 5 µg pX459 and 5 µg HDR template were mixed gently. In a separate tube, 125 µl of OptiMEM and 30 µl FuGENE6 (Promega; E2691) were mixed gently. The two mixes were combined, mixed gently and incubated at room temperature for 15 mins. The transfection mixture was added directly to cells and mixed gently. On day 4, cells were pulsed for 24 hours with 3 µg/ml puromycin. On day 7, cells were collected and plated out at low densities for single colony isolation, screening and cell line establishment. gDNA was extracted and screened by PCR as described.

2.3.4 Stable cell line generation

The pcDNA5/FRT/TO-EGFP-WRN WT, E84A and K577M plasmids were synthesised by GenScript and include siRNA resistance to WRN exon 9 and exon 17 siRNA.

Flp-In™ HeLa cells were transfected using FuGENE6 (Promega; E2691) with pcDNA5/FRT/TO-EGFP-WRN variants and pOG44 in a 4:1 plasmid: FuGENE6 ratio ratio. On day 0, 1×10^6 low passage cells were plated into 10 cm dishes. On day 1, 100 μ l OptiMEM™, 5 μ g pcDNA5/FRT/TO-EGFP-WRN and 1 μ g pOG44 were mixed gently. In a separate tube, 100 μ l of OptiMEM™ and 24 μ l FuGENE6 (Promega; E2691) were mixed gently. The two mixtures were combined, mixed gently and incubated at room temperature for 15 mins. The transfection mixture was added directly to cells and mixed gently. On day 2, the media was removed and replaced with fresh media. On day 4, 100 μ g/ml hygromycin was added to the media. Successfully transfected clones were selected with hygromycin until the untransfected control cells had died (10-14 days). Expression of siRNA-resistant inducible genes was confirmed by Western blot after incubation with 2 μ g/ml doxycycline (Sigma Aldrich; D9891) for 72 hours.

2.3.5 Plasmid transfection

The pcDNA5/FRT/TO-FLAG-USP50 plasmid with resistance to USP50 #5 and #7 siRNA was synthesised by GenScript. FuGENE6 (Promega; E2691) was used to transfect DNA plasmids into cells at a 4:1 plasmid: FuGENE6 ratio. Per ml of media, 1 μ g of pcDNA5/FRT/TO-FLAG-USP50 plasmid was mixed with 25 μ l OptiMEM™ (Thermo Fisher; 31985070). In a separate tube, 4 μ l FuGENE6 was mixed gently in 25 μ l OptiMEM™. The two mixtures were combined, mixed gently, and incubated at room temperature for 15 mins before adding slowly to the cell media and mixed by swirling.

2.3.6 Inducible shRNA expression

Flp-In™ HeLa cells expressing IPTG-inducible (Promega; V395A) shRNA targeting USP50 were obtained from Dr Helen Stone.

2.3.7 Immunofluorescence staining

Cells were plated in 24 well plates on 13 mm circular glass coverslips. Cells were treated according to the specific experiment, then fixed with 4% PFA. For EdU labelling of S phase cells, cells were incubated with 10 µM EdU for 10-15 mins prior to fixation with 4% PFA. Once fixed, cells were permeabilised with 0.5% Triton-X100 in PBS for 15 mins, then blocked using 10% FBS in PBS for 20 mins. EdU was labelled with Alexa Fluor 647 azide using Click-IT technology: cells were incubated with the Click-IT reaction mix for 30 mins at room temperature in the dark. Cells were washed with PBST and incubated with blocking solution for 40 mins, then incubated with primary antibody for 1 hr at room temperature in blocking solution. Cells were then washed 3 times with PBST before being incubated for 1 hour with Alexa Fluor 488 antibody. Cells were washed 3 times in PBST and DNA was stained using Hoechst at 1:20,000 for 5 mins. Cells were washed 3 times in PBST, fixed for 10 mins in 4% PFA, and washed 2 times in PBS. Coverslips were mounted onto SuperFrost microscope slides with mounting medium. Cells were imaged using a 100x oil immersion lens. Foci were analysed using LASX software. Overall nuclear fluorescence was analysed using ImageJ.

2.3.8 DNA fibre labelling

Cells were seeded in 6 well plates and treated according to the specific experiment. Cells were incubated at 37°C with 25 µM CldU (Sigma Aldrich; C6891) and then with 250 µM CO₂-equilibrated IdU (Sigma Aldrich; I7125) according to the experimental design. Cells were washed twice with ice-cold PBS, trypsinised and resuspended in PBS to a cell density of 50x10⁴ cells/ ml. Two µl of cells was spotted at the top of a SuperFrost microscope slide and left to partially dry. Seven µl of fibre spreading buffer was mixed with the sample and incubated for 2 mins. Slides were gradually tilted to spread the liquid drop to the bottom, then left to dry for 2 mins. Slides were fixed in 3:1 methanol: acetic acid for 10 mins then left to air-dry. Dried slides were stored at 4°C in the dark.

2.3.9 Fibre immunostaining

Slides were washed twice for 5 mins with dH₂O and rinsed with 2.5 M HCl before incubation with 2.5 M HCl for 1 hour 15 mins. Slides were then rinsed twice with PBS and washed twice for 5 mins in blocking solution (PBS, 1% BSA, 0.1% Tween20). Slides were incubated for 30 mins in blocking solution. Slides were incubated with 130 µl of primary antibodies in blocking solution (1:2000 rat anti-BrdU [anti-CldU] [Abcam; ab6326] and 1:500 mouse anti-BrdU [anti-IdU] [BD Biosciences; 347580]). Slides were covered with large coverslips and incubated for 1 hour. Slides were rinsed 3 times with PBS and fixed with 4% PFA for 10 mins. Slides were then incubated with blocking solution for 1 min, 5 mins and 25 mins. Slides were incubated with 130 µl of secondary antibodies in blocking solution (1:500 anti-rat Alexa Fluor 555 [Invitrogen; A21434] and 1:500 anti-mouse Alexa Fluor 488 [Invitrogen; A21202]) with a coverslip on each slide, protected from light, for 2 hours. Slides were rinsed 3 times with PBS and incubated with

blocking solution for 1 min, 5 mins and 25 mins. Slides were rinsed 2 times with PBS and left to air-dry. Mounting medium (Thermo Fisher; 10622689) was applied, and the slides were covered with coverslips and allowed to air-dry. Slides were stored at 4°C in the dark.

2.3.10 Fibre scoring and analysis

Slides were imaged using a 40x oil immersion lens and green and red channels. One channel was used to identify regions for image acquisition to minimise bias. Images were taken across the length of the slide with two slides were imaged per condition. Fibres were analysed using ImageJ software.

2.3.11 Clonogenic survival assay

Cells were seeded in 24 well plates and treated according to the specific experiment. Cells were plated out in 6 well plates at a low density (300-1000 cells per well, depending on plating efficiency). Plates were incubated for 7-14 days at 37°C, 5% CO₂ until colonies of 50+ cells formed. Colonies were stained using 1% methylene blue (Sigma Aldrich; 66719) or 0.5% crystal violet (Acros; 405831000) and counted. Alternatively, cells were plated into 24 well plates at a low density, incubated as before and stained with 0.5% crystal violet. The plates were thoroughly washed to remove unbound crystal violet, left to dry, and resuspended in 3:1 methanol: acetic acid. Resuspended crystal violet was measured on a plate reader at 595 nm.

2.3.12 Cell viability assay

Cells were seeded in 24 well plates and treated according to the specific experiment. Cells were plated out in 24 well plates at a low density. Plates were incubated for 5-10 days at 37°C, 5% CO₂ until siNTC-treated wells were around 50% confluent. Media was removed and replaced with fresh media with 10% resazurin (Scientific Laboratory Supplies; 199303-5G) and incubated at 37°C, 5% CO₂ for 2 hours. Plates were shaken gently to mix the media. Absorbance was measured on a Varioskan plate reader at 570 and 600nm, and fluorescence was measured on an Enspire multimode plate reader (Perkin Elmer) with excitation at 560nm and emission at 590nm.

2.3.13 Broken String Biosciences double strand break site mapping

HeLa cells were plated into 24 well plates and treated with siRNA for 72 hours. Cells were harvested and counted. One hundred and twenty thousand cells were plated onto poly-L-lysine-coated 96 well plates. Once cells had attached to the plate, 100 µl of 8% methanol-free PFA (Thermo Scientific, 28908) was slowly added to the cells and incubated at room temperature for 10 mins. The liquid was then removed and the cells washed twice with 1x PBS. Two hundred µl PBS was added to the cells, and the plate was sealed with an adherent plate seal and stored at 4°C before shipping to Broken String Biosciences for INDUCE-seq analysis. Data was analysed using Galaxy and Integrative Genome Viewer.

2.4 Microscopy

IF staining was imaged using the Leica DM6000B microscope using an HBO lamp with 100W mercury short arc UV bulb light source and four filter cubes, A4, L5, N3 and Y5, which produce excitations at wavelengths 360, 488, 555 and 647 nm respectively.

2.5 Chromatin fractionation

Cells were harvested and kept on ice at all times. Cells were pelleted in a cold centrifuge at 500x g for 5 mins. Supernatant was removed and the pellet was resuspended in 500 µl PBS. Fifty µl of resuspended cells was separated into a new tube and kept as the whole cell extract. Cells were spun at 500x g for 5 minutes, the supernatant was discarded and the pellet was resuspended in 500 µl cold sucrose buffer. Triton-X100 was added to 0.3% of final volume. The samples were vortexed 3x for 5 seconds. The cells were spun at 500x g for 5 mins, and the supernatant was transferred into a separate tube and kept as the cytoplasmic fraction. The pellet was resuspended in 200 µl NETN buffer. Cells were incubated on ice for 30 mins. Cells were spun at 1700x g for 5 mins, and the supernatant was transferred to a separate tube and kept as the nuclear soluble fraction. The pellet was resuspended in 200 µl NETN buffer as the chromatin fraction.

2.6 Buffers

1x SDS running buffer: 10% 10x Tris/ glycine/ SDS in 90% dH₂O.

1x transfer buffer: 10% 10x Tris/ glycine, 20% methanol, 70% dH₂O.

4x SDS sample buffer: 8% SDS, 40% glycerol, 0.2 M Tris-HCl pH 6.8, 5% β -mercaptoethanol, 6 M urea, bromophenol blue.

Click-IT reaction mix: 10 μ M biotin azide, 10 mM sodium ascorbate, 1 mM CuSO₄ in PBS

Crystal violet: 0.5% crystal violet, 49.5% dH₂O, 50% methanol.

Fibre fixative: 75% methanol, 25% glacial acetic acid.

Fibre spreading buffer: 200 mM Tris pH 7.4, 50 mM EDTA, 0.5% SDS.

Methylene blue: 1% methylene blue, 49% dH₂O, 50% ethanol.

NETN buffer: 50 mM Tris-HCl pH 8.0, 150 mM NaCl, 2 mM EDTA, 0.5% NP-40, protease inhibitor.

PBS: 1 PBS tablet (Sigma Aldrich) in 200ml dH₂O.

PBST: PBS + 0.1% Tween 20.

Sucrose buffer: 10 mM Tris-HCl pH 7.5, 20 mM KCl, 250 mM sucrose, 2.5 mM MgCl₂, protease inhibitor.

2.7 Primer sequences

Primer name	Sequence	Purpose
Forward primer 1	CAACCCAGTAACAGTGTCTCA	CRISPR screening
Forward primer 2	TCTCTGGAGCCTAATCTTTCTA	CRISPR screening
Int for 1	GATCATGATGGTGACTACAAGG	CRISPR screening
Int for 2	GACATTGATTACAAAGACGATGA	CRISPR screening

Rev 1	TCTCGGATTTTCTTTCCATAT	CRISPR screening
Rev 2	TGGGGCTCCATGAGAC	CRISPR screening
Rev 3	CAAGCTACTTGACACAGGTTC	CRISPR screening
Rev 4	GAGGATTATGCAGGTATCATG	CRISPR screening

2.8 siRNA sequences

Target	Sequence
Luciferase (NTC)	CUUACGCUGAGUACUUCGA
MUS81 ex 1	ACGCGCUUCGUUUUCAGA
MUS81 ex 13	GCAGGAGCCAUAAGAAUA
RECQL4	ACCUCGAUUCCAUUAUCAUUU
RECQL5	GAGGAGAAGGUCCCUGUAAUU
SMARCA1	Dharmacon On-targetPLUS SMARTpool L-013058-00-0005
USP50 #5	UAUGAUACCCUCCAGUUA
USP50 #7	CUACCCAGCAUUUACGAAA
WRN ex 11	AUACGUAACUCCAGAAUAC
WRN ex 9	GAGGGUUUCUAUCUUACUA

2.9 gRNA sequences

Name	Sequence
gRNA 3	ATAGAAGCAAAAGTCCAACG
gRNA 7	TAGATATCGAAGTCATCTGC

2.10 Antibodies

Target	Animal	Supplier	Code	RRID	Assay	Dilution
53BP1	Rabbit	Abcam	ab36823	AB_722497	IF	1:1000
Abraxas	Rabbit	Novus Biologicals	NBP2-38356	-	WB	1:1000
Alexa Fluor 647 azide	-	Thermo Fisher	A10277	-	IF	1:2000
ATM	Rabbit	Abcam	ab199726	-	WB	1:1000
BARD1	Rabbit	Abcam	ab226854	-	WB	1:1000
BrdU (CldU)	Rat	Abcam	ab6326	AB_305426	Fibres	1:2000
BrdU (IdU)	Mouse	BD Biosciences	347580	AB_10015219	Fibres	1:500
EXO1	Rabbit	Abcam	ab155553	-	WB	1:1000
FANCD2	Rabbit	Abcam	ab108928	AB_10862535	WB	1:1000
FEN1	Rabbit	Abcam	ab17994	AB_444168	WB	1:1000
FLAG (M2)	Mouse	Sigma Aldrich	F1804	AB_262044	WB, IF	1:500
GAPDH	Mouse	Abcam	ab8245	AB_2107448	WB	1:5000
H3	Rabbit	Abcam	ab1791	AB_302613	WB	1:1000
HUS1	Rabbit	Proteintech	11223-1-AP	-	WB	1:1000
MUS81	Mouse	Novus Biologicals	NB100-2064	AB_2147134	WB	1:1000
PALB2	Rabbit	Bethyl Laboratories	A301-246A	-	WB	1:1000
PCNA	Mouse	Santa Cruz	PC-10	-	WB	1:1000
PIN1	Mouse	R&D Systems	MAB2294	AB_2163944	WB	1:1000
RAD51	Rabbit	Millipore	PC130	AB_569857	WB	1:2000
RFWD3	Rabbit	Abcam	ab138030	AB_2687568	WB	1:1000
RNF168	Rabbit	Abcam	ab367	-	WB	1:1000
RPA32	Mouse	Abcam	ab2175	-	WB	1:1000

Vinculin	Rabbit	Abcam	ab129002	AB_11144129	WB	1:2000
WRN	Mouse	Novus Biologicals	H00007486-M09	AB_830410	WB	1:1000
α mouse Alexa Fluor 488	Donkey	Thermo Fisher	A21202	AB_2762823	Fibres	1:500
α mouse Alexa Fluor 488	Donkey	Thermo Fisher	A21206	AB_2535792	IF	1:5000
α mouse HRP	Rabbit	Agilent	P0161	AB_2687969	WB	1:5000
α rabbit HRP	Swine	Agilent	P0217	AB_2728719	WB	1:5000
α rat Alexa Fluor 555	Goat	Thermo Fisher	A21434	AB_2535855	Fibres	1:500
α-tubulin	Mouse	Santa Cruz	sc-5286	AB_628411	WB	1:1000
β-actin	Rabbit	Abcam	ab115777	AB_10899528	WB	1:5000
γ-H2AX	Mouse	Abcam	ab22551	AB_447150	IF	1:1000

2.11 Chemicals

Name	Activity	Concentration	Supplier	CAS number
B02	RAD51 inhibitor	0.25-10 μ M	Sigma Aldrich	1290541-46-6
CldU	Thymidine analogue	25 μ M	Sigma Aldrich	50-90-8
EdU	Thymidine analogue	10 μ M	Thermo Fisher	61135-33-9
Hydroxyurea	RNR inhibitor	1-5 mM	Alfa Aesar	127-07-1
IdU	Thymidine analogue	250 μ M	Sigma Aldrich	54-42-2
KU-55933	ATM inhibitor	1-10 μ M	Abcam	ab120637
NSC 617145	WRN helicase inhibitor	250 nM	Sigma Aldrich	203115-63-3
VE-821	ATR inhibitor	0.1-1 μ M	Selleck	58007

2.12 Statistical methods

All statistical tests, unless indicated otherwise, used an unpaired two-tailed *t*-test. n.s.= not significant, * = $p \leq 0.05$, ** = $p \leq 0.01$, *** = $p \leq 0.001$, **** = $p \leq 0.0001$.



3 USP50 regulates WRN at ongoing and stalled forks

3.1 Introduction

Faithful DNA replication is paramount for ensuring the preservation of the genome and avoiding potentially deleterious mutations or loss of genomic material. Cells have evolved several pathways for promoting error-free replication and repair of DNA after damage. The replication fork encounters many obstacles from exogenous and endogenous sources, including UV damage, ICLs, G-quadruplexes and DNA-RNA hybrids (Macheret & Halazonetis, 2015). There is significant overlap between the RS response and DNA repair and the proteins that participate in these processes, highlighting the importance of replication to cell viability (Tye *et al.*, 2021).

Previous work carried out in the laboratory identified USP50 as an inactive DUB with roles in the RS response. Using the DNA fibre assay, it was seen that depletion of USP50 led to a decrease in ongoing replication forks and an increase in stalled replication forks, without affecting the firing of new replication origins (figure 1.11b). USP50 depletion led to an increase in the DNA DSB marker 53BP1 in S phase cells, suggesting that USP50 prevents DSB formation during replication (figure 1.11c). These S phase DSBs in USP50-depleted cells could be rescued by co-depletion of the structure-specific endonuclease MUS81, implying that USP50 prevents stalled replication forks from being cleaved into DSBs (figure 1.11d). To test which pathways USP50 might be involved in, co-depletions were performed with proteins with similar roles in preventing DSB formation, and it was observed that USP50 and the RECQ helicase/exonuclease WRN were epistatic in DSB formation (figure 1.11h).

WRN is a multifunctional enzyme with roles in DNA replication, repair and gene expression regulation. WRN associates with many other replication and repair proteins such as ATR, BLM, KU70, MRE11, NBS1, RAD50, PCNA and RPA (Lachapelle *et al.*, 2011). During replication, WRN has roles in prevention of fork stalling, restart of stalled forks and protection of nascent DNA at reversed forks. Given previous data suggesting that USP50 and WRN are epistatic in DSB formation in S phase cells, and evidence that USP50 promotes ongoing replication, we wondered whether USP50 and WRN collaborate in other aspects of replication.

The aims of this chapter are to identify pathways where USP50 and WRN are epistatic, in order to better understand the relationship between these two proteins in replication. WRN is a well-known and important protein in DNA replication and repair, so learning more about how it is regulated is of benefit. USP50 is a poorly understood protein and lacks ubiquitin protease function, unlike other members of the USP family. Understanding how this inactive USP exerts its influence in cells could provide further insights into the mode of action of active and inactive DUBs.

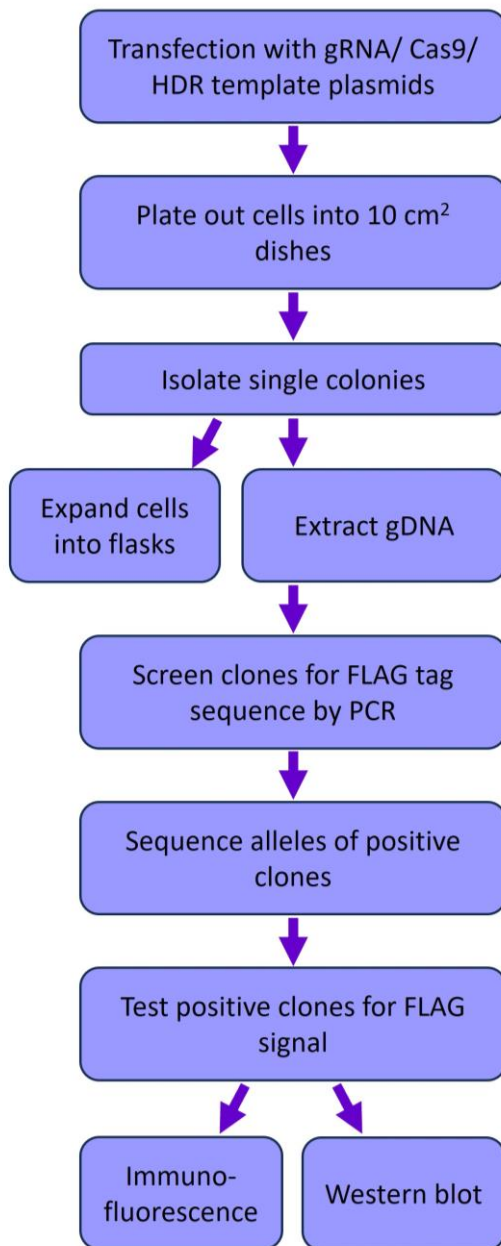
3.2 3xFLAG-tagged USP50 HeLa cells engineered using homology-directed CRISPR

USP50 is expressed at very low levels in several tissues, and our laboratory has not been able to detect endogenous USP50 expression with a variety of antibodies. The generation of a stable HeLa cell line expressing doxycycline-inducible FLAG-USP50 has allowed the study of interactions between USP50 and other proteins, for example through FLAG-immunoprecipitation and the proximity ligation assay with anti-FLAG antibodies. A caveat of this approach is that the doxycycline-induced expression of USP50 is orders of magnitude higher than the expression of endogenous protein. This could influence cellular phenotypes in a way that does not reflect physiological conditions.

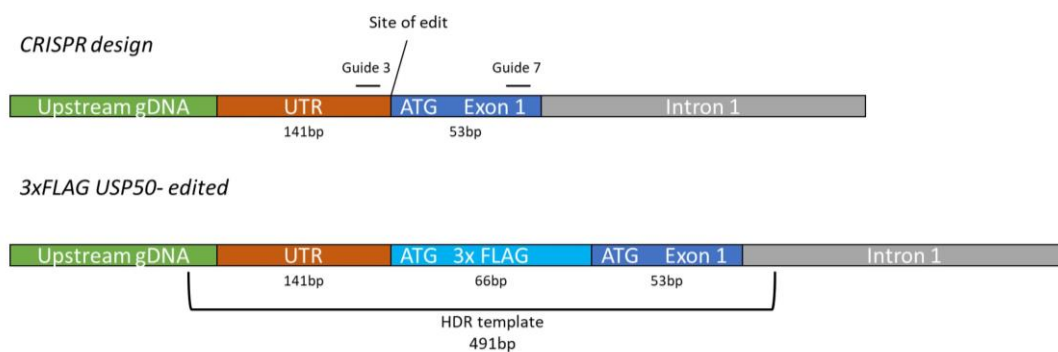
To address this problem, we used HDR CRISPR to engineer a HeLa cell line with a 3xFLAG-tag at the N-terminus of USP50. HDR CRISPR works through creating a DSB with Cas9 at a known locus, and simultaneously transfecting cells with DNA carrying the desired insert sequence flanked by homology to the upstream and downstream sequence at the cut. If the cell repairs the DSB through HR and uses the transfected DNA as a homology template, the cell will repair the DSB and introduce the inserted sequence at the DSB. To generate the edited cell line, HeLa cells were transfected with a plasmid encoding the Cas9 enzyme and gRNA sequence, and with the HDR template (figure 3.1a, b). Individual cells were isolated and grown, and PCR and sequencing was used to determine the approximate ratio of edited to unedited alleles in the HeLa cells, as well as the presence of introduced mutations. Of 270 clones tested, five HeLa clones tested positive for the 3x FLAG-tag DNA sequence by sequencing, however four of the five had mutations up- or downstream of the edit site, resulting in a mutant protein. Clone 22 did not have any mutations detected and was predicted to have around one in five USP50

alleles tagged with FLAG-tag. This suggests that this particular HeLa clone has five USP50 alleles, one of which was successfully FLAG-tagged using HDR-CRISPR. Clone 22 HeLa cells were plated and treated with siRNA targeting USP50 and were examined using Western blotting and IF for FLAG-tag (figure 3.1c-e). No FLAG-USP50 signal, or reduction in signal with USP50 depletion, was detected in clone 22 by Western blotting or IF. This suggests that the expression of FLAG-USP50 in the HeLa cells is too low to detect FLAG-tag expression by Western blotting or IF.

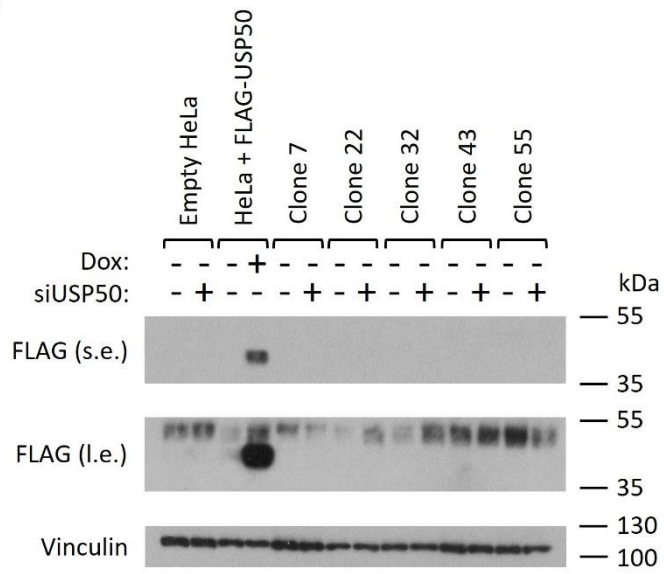
a



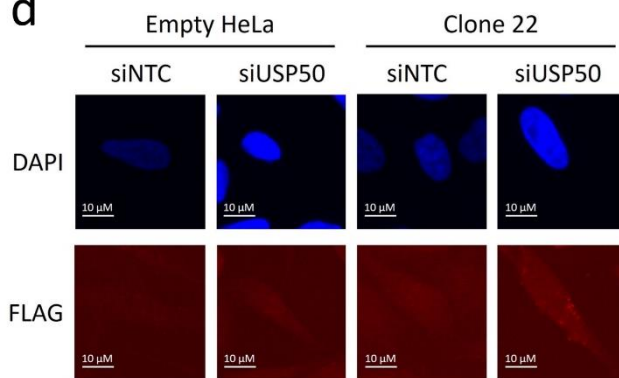
b



c



d



e

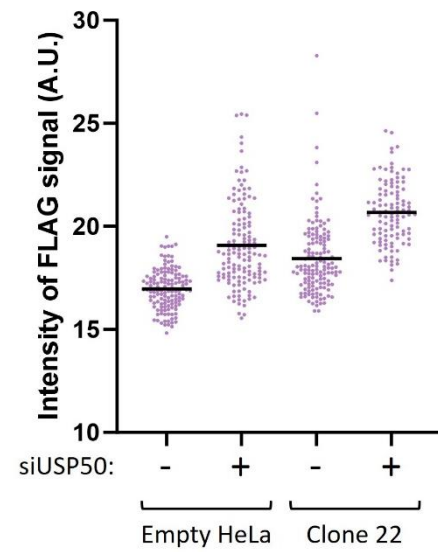


Figure 3.1

- Schematic of the CRISPR workflow.
- Diagram of the CRISPR site and HDR template.

c) Western blot showing FLAG-tag expression after 72 hours of treatment with siRNA targeting USP50 in HeLa CRISPR cells. USP50 expression was induced with doxycycline; control cells were treated with vehicle. Transfection control was with siRNA targeting Luciferase.

d) FLAG-tag expression was examined using IF in HeLa CRISPR cell lines with USP50 depletion. Transfection control was with siRNA targeting Luciferase. Representative images shown.

e) FLAG-tag expression was examined using IF in HeLa CRISPR cell lines with USP50 depletion. Transfection control was with siRNA targeting Luciferase. Results are from 1 repeat, with n >100 cells per condition. Black lines indicate the mean. A.U.= arbitrary units.

3.3 USP50-deficient cells are not hypersensitive to UV treatment

When a replication fork stalls due to a lesion on the leading strand, TLS may be employed to allow replication to quickly continue without the generation of potentially deadly DSBs. The use of TLS polymerases reduces fork reversal, fork collapse, and the generation of single-strand gaps during RS (Nayak *et al.*, 2020). UV-induced DNA damage is repaired primarily by NER, but during S phase, unrepaired lesions are bypassed using TLS (Yang, 2011). TLS is initiated by the monoubiquitination of PCNA by the E3 ubiquitin ligase RAD18 (Yoon *et al.*, 2012).

We saw previously that USP50 depletion led to an increase in fork stalling and DSBs (figure 1.11b, c), suggesting a role for USP50 in DDT. We therefore wondered whether USP50 may have a role in promoting TLS and lesion bypass. To test this, HeLa cells were treated with siRNA targeting USP50, then exposed to increasing doses of UV-C radiation. Cells were then plated out at a low density and left to grow into colonies, then stained and counted. RAD18 knockdown was used as a positive control for UV sensitivity. Western blotting for RAD18 to check the level of protein depletion was unsuccessful, possibly because RAD18 is endogenously expressed at low levels. Despite this, cells treated with siRNA targeting RAD18 were hypersensitive to UV treatment compared to NTC siRNA-treated cells. Cells depleted of USP50 were not hypersensitive to UV treatment compared to siNTC-treated cells (figure 3.2a). This indicates that USP50 does not promote TLS to overcome UV-induced DNA damage.

a

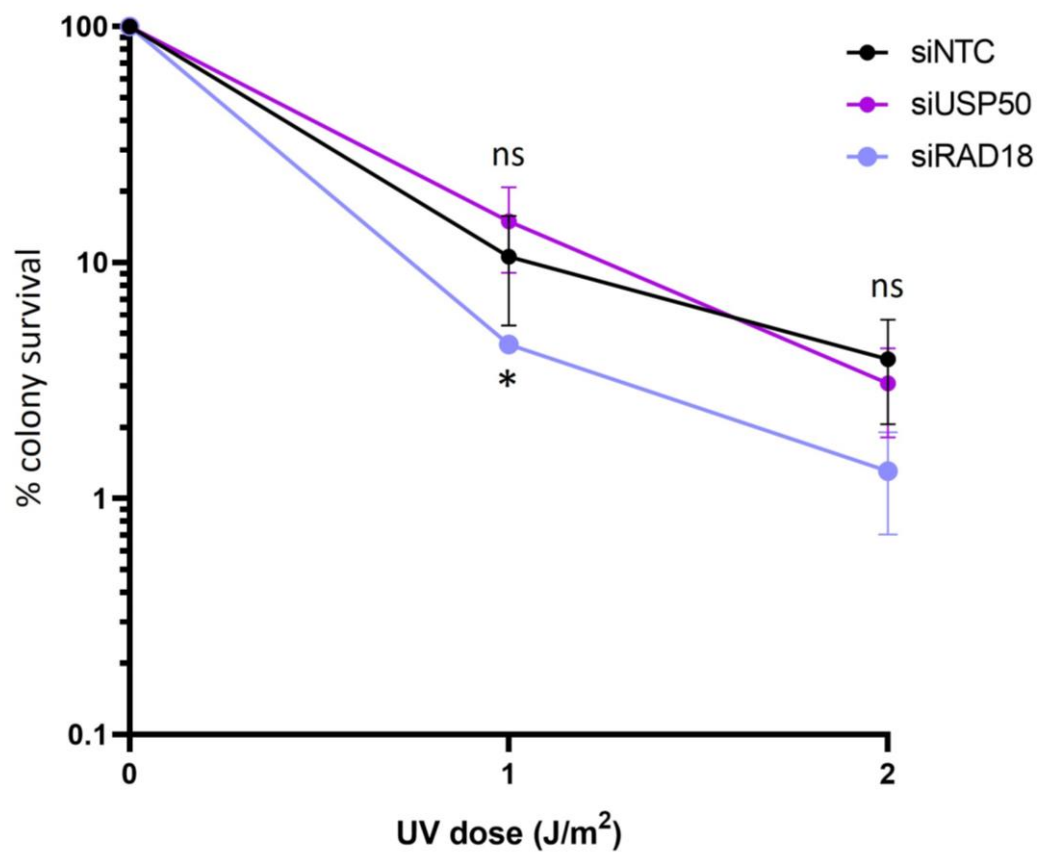


Figure 3.2

a) Cell survival was measured using the clonogenic survival assay. HeLa cells were treated for 72 hours with siRNA targeting USP50 and RAD18, then exposed to increasing doses of UV radiation (joules/metre²). Transfection control was with siRNA targeting Luciferase. Results are from 3 independent repeats. Points indicate the mean, error bars are SEM. Statistical analysis done with two-way ANOVA; ns= not significant, *= p≤0.05.

3.4 USP50 acts to prevent fork stalling before MUS81 cleavage of stalled replication forks

Previous unpublished work using the DNA fibre assay showed that depleting USP50 led to an increase in the levels of replication fork stalling (figure 1.11b). We also saw that depleting USP50 led to an increase in DSBs in S phase cells, but that co-depletion of MUS81 rescued 53BP1 foci levels to that seen in untreated cells (figure 1.11d). These data suggest that the DSBs formed when USP50 is depleted are the product of MUS81 cleavage of stalled replication forks. Given this, we asked ourselves whether USP50 acts before or after MUS81 cleavage to prevent replication fork stalling, using the DNA fibre assay. HeLa cells were treated with shRNA targeting USP50 and siRNA targeting MUS81 for 72 hours before labelling with CldU and IdU nucleotide analogues (figure 3.3a, b). CldU and IdU were added sequentially for 20 minutes each before cells were harvested and DNA fibres were spread and stained. The replication structures shown in figure 3.3c were counted.

In USP50-depleted cells there was a significant increase in the proportion of stalled forks, in accordance with previous experiments. MUS81 depletion alone did not affect fork stalling levels compared to cells treated with NTC siRNA. When USP50 and MUS81 were co-depleted, the levels of stalled forks were comparable to those in USP50-depleted cells (figure 3.3d). This data indicates that abolishing MUS81 cleavage of stalled forks does not affect fork stalling in USP50-depleted cells. This suggests that the role of USP50 in promoting ongoing replication and preventing fork stalling occurs before MUS81-mediated cleavage of stalled forks into DSBs.

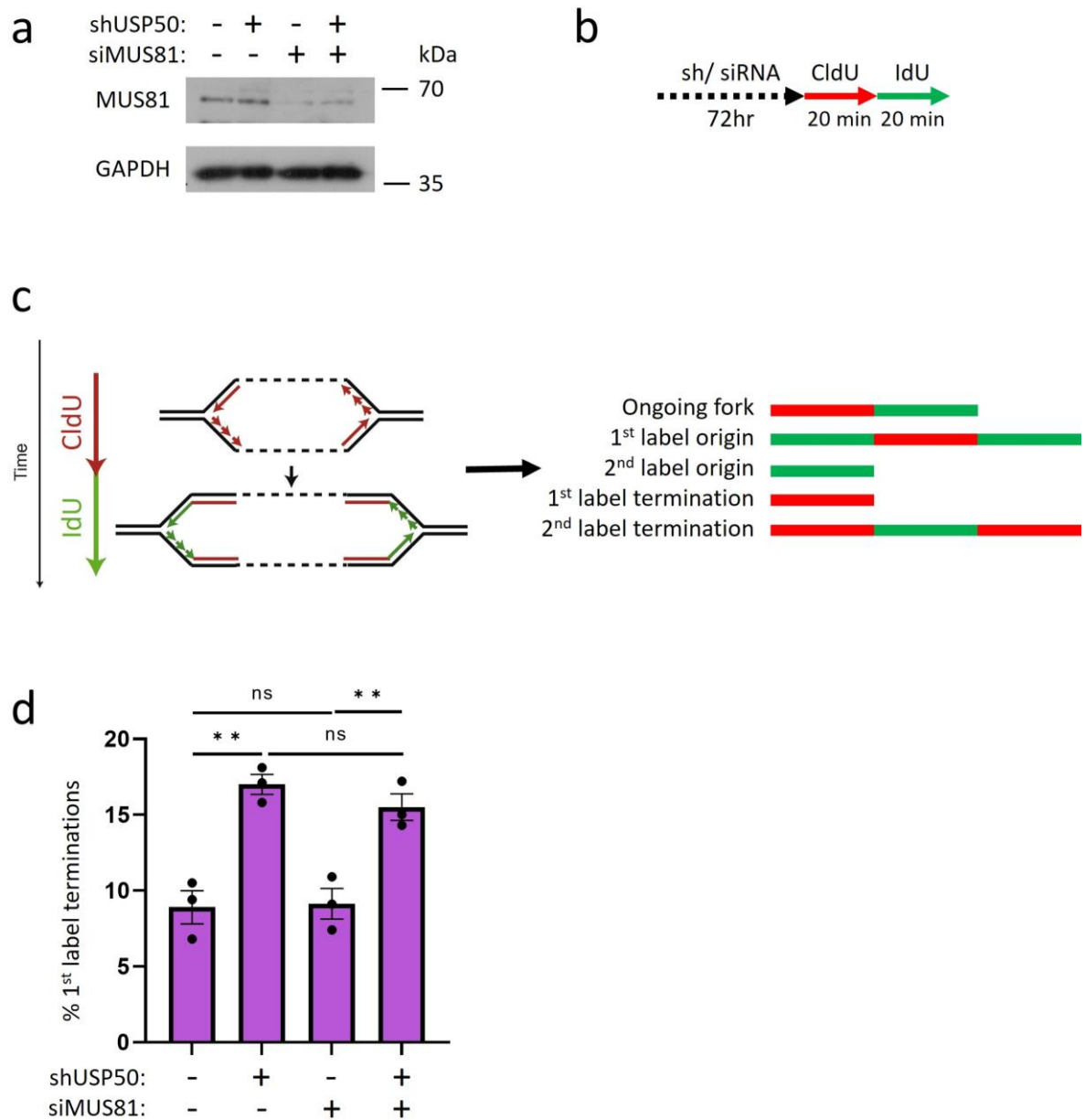


Figure 3.3

a) Western blot showing MUS81 protein levels after 72 hours of treatment with sh/ siRNA targeting MUS81 and USP50 in HeLa cells. shUSP50 expression was induced with IPTG; control cells were treated with vehicle. Transfection control was with siRNA targeting Luciferase.

b) Schematic of the DNA fibre assay. HeLa cells were treated with sh/ siRNA targeting USP50 and MUS81 for 72 hours before incubation with CldU and IdU for 20 minutes each.

c) Schematic of the DNA fibre assay. Cells are incubated sequentially with the nucleotide analogues CldU and IdU, which are incorporated into replicating DNA. The five types of structures shown were counted.

d) 1st label terminations were examined using the DNA fibre assay in HeLa cells treated with siRNA targeting MUS81 and shRNA targeting USP50. shUSP50 expression was induced with IPTG; control cells were treated with vehicle. Transfection control was with siRNA targeting Luciferase. Results are from 3 independent repeats, with n >200 fibres per condition, per repeat. Bars indicate the mean, error bars are SEM. Statistical analysis done with unpaired two-tailed *t*-test; ns= not significant, **= $p \leq 0.01$.

3.5 WRN depletion/ inhibition rescues fork stalling in USP50-depleted cells

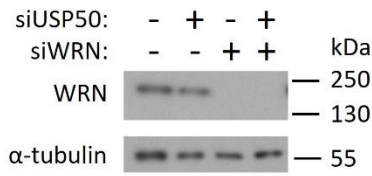
Previous work by the Morris group showed that cells depleted of USP50 have a higher proportion of stalled forks and an increase in S phase DSBs (figure 1.11b, c). We also saw that co-depletion of USP50 and WRN led to a reduction in the number of 53BP1 foci in cells (7.0 average foci in USP50-depleted cells vs 5.4 average foci in USP50- and WRN-depleted cells) (figure 1.11h). WRN has known roles in replication fork progression and protecting forks from stalling, both in untreated cells and cells treated with RS inducers (Palermo *et al.*, 2016; Rodríguez-López *et al.*, 2002; Sidorova *et al.*, 2008). Similar to USP50, WRN prevents DSB formation in S phase cells (Franchitto *et al.*, 2008). Given these data, we wondered how USP50 and WRN co-depletion would affect replication fork dynamics using the DNA fibre assay. HeLa cells were treated with siRNA targeting USP50 and WRN (figure 3.4a) before labelling (figure 3.4b). USP50 or WRN depletion alone caused an increase in 1st label terminations compared to cells treated with NTC siRNA (figure 3.4c). Surprisingly, co-depletion of USP50 and WRN restored the level of 1st label terminations to that seen in untreated cells. This result bears similarity to the reduction in 53BP1 foci levels seen with USP50 and WRN co-depletion in EdU-positive cells observed previously (figure 1.11h).

A commercially available small molecule inhibitor of WRN, NSC 617145, is reported to specifically inhibit WRN helicase activity *in vitro*, through disrupting ATPase activity without affecting exonuclease activity, and with minimal effects on other helicases (Aggarwal *et al.*, 2013). To test the specificity of the WRN inhibitor (WRNi), we combined WRN siRNA knockdown and WRN inhibition and looked at fork stalling using the DNA fibre assay. A concentration of 250 nM NSC 617145 was chosen as this dose has been previously reported

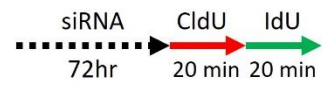
to induce DSBs in HeLa cells (Aggarwal *et al.*, 2013). HeLa cells were treated with siRNA targeting WRN for 72 hours, and NSC 617145 at 250 nM for 24 hours prior to labelling (figure 3.4d, e). Depletion of WRN caused an increase in 1st label terminations, as did treatment with the WRNi to a comparable degree (19.7% vs 20.2% respectively). The combination of WRN depletion and WRNi treatment did not significantly alter the proportion of stalled forks compared to either treatment alone (figure 3.4f). This suggests that WRNi treatment leads to fork stalling due to its effects on WRN activity, rather than off-target effects. This data supports previous literature demonstrating the specificity of NSC 617145 to WRN.

Having observed a restoration of fork stalling levels in HeLa cells when co-depleting USP50 and WRN, we wondered whether treatment with NSC 617145 would affect replication fork stalling in USP50-depleted cells. HeLa cells were treated with siRNA targeting USP50 and WRNi at 250 nM for 72 hours before labelling (figure 3.5g). WRNi treatment alone caused an increase in 1st label terminations, as seen before. Intriguingly, the combination of USP50 depletion and WRNi treatment rescued fork stalling levels to that seen in cells treated with NTC siRNA and vehicle (9.5% vs 10.6% respectively) (figure 3.4h). This result is comparable to the effect seen with siRNA depletion of WRN, indicating that when USP50 is depleted, WRN depletion or helicase inhibition causes the increase in stalled forks to be restored.

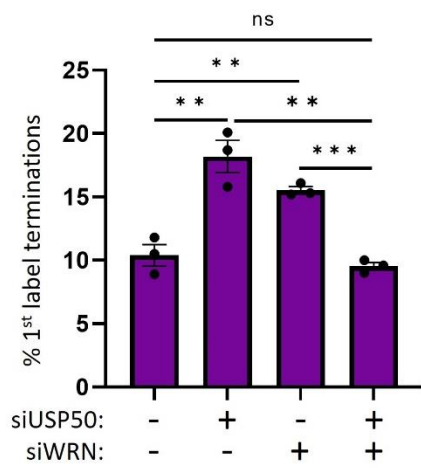
a



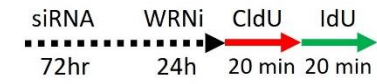
b



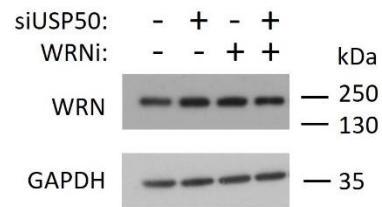
c



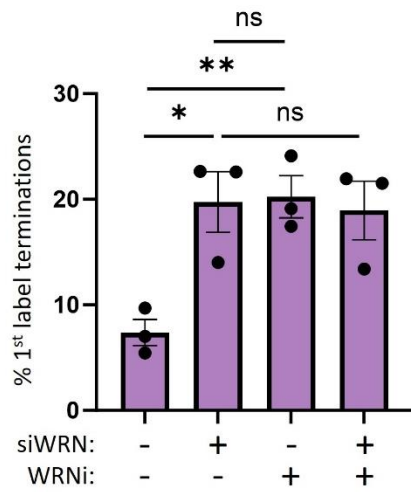
d



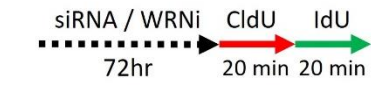
e



f



g



h

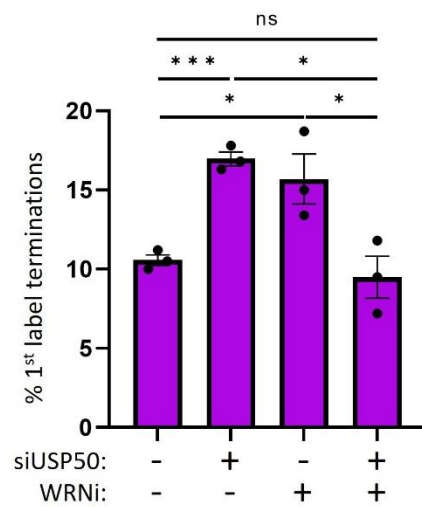


Figure 3.4

a) Western blot showing WRN protein levels after 72 hours of treatment with siRNA targeting WRN and USP50 in HeLa cells. Transfection control was with siRNA targeting Luciferase.

b) Schematic of the DNA fibre assay. HeLa cells were treated with siRNA targeting USP50 and WRN for 72 hours before incubation with CldU and IdU for 20 minutes each.

c) 1st label terminations were examined using the DNA fibre assay in HeLa cells treated with siRNA targeting USP50 and WRN. Transfection control was with siRNA targeting Luciferase. Results are from 3 independent repeats, with $n > 200$ fibres per condition, per repeat. Bars indicate the mean, error bars are SEM. Statistical analysis done with unpaired two-tailed t -test; ns= not significant, **= $p \leq 0.01$, ***= $p \leq 0.001$.

d) Schematic of the DNA fibre assay. HeLa cells were treated with siRNA targeting WRN for 72 hours and 250 nM WRNi for 24 hours before incubation with CldU and IdU.

e) Western blot showing WRN protein levels after 72 hours of treatment with siRNA targeting USP50 and 24 hours of WRNi treatment in HeLa cells. Transfection control was with siRNA targeting Luciferase. Control cells were treated with vehicle (DMSO).

f) 1st label terminations were examined using the DNA fibre assay in HeLa cells treated with siRNA targeting WRN and 250 nM WRNi. Transfection control was with siRNA targeting Luciferase. Control cells were treated with vehicle (DMSO). Results are from 3 independent repeats, with $n > 200$ fibres per condition, per repeat. Bars indicate the mean, error bars are SEM. Statistical analysis done with unpaired two-tailed t -test; ns= not significant, *= $p \leq 0.05$, **= $p \leq 0.01$.

g) Schematic of the DNA fibre assay. HeLa cells were treated with siRNA targeting USP50 and 250 nM WRNi for 72 hours before incubation with CldU and IdU.

h) 1st label terminations were examined using the DNA fibre assay in HeLa cells treated with siRNA targeting USP50 and 250 nM WRNi. Transfection control was with siRNA targeting Luciferase. Control cells were treated with vehicle (DMSO). Results are from 3 independent repeats, with n >200 fibres per condition, per repeat. Bars indicate the mean, error bars are SEM. Statistical analysis done with unpaired two-tailed *t*-test; ns= not significant, *= $p \leq 0.05$, ***= $p \leq 0.001$.

3.6 Both enzymatic activities of WRN are needed to rescue fork stalling in USP50-depleted cells

WRN is a member of the RECQ family of ATP-driven helicases, with diverse roles in DNA repair and replication (Croteau *et al.*, 2014). WRN is the only member of the RECQ helicase family to also possess exonuclease activity (Shen & Loeb, 2000). In addition, WRN has known non-enzymatic roles, including DNA binding, protecting reversed forks from MRE11-dependent degradation, and removal of camptothecin-induced lesions (P. Gupta *et al.*, 2022; Kamath-Loeb *et al.*, 2012; Su *et al.*, 2014). Given the similarity in substrates between the helicase and exonuclease domains, it is thought to be likely that the two enzymatic activities of WRN co-ordinate to process DNA structures (Opresko *et al.*, 2004).

Previous data (figure 3.4g) implicated WRN helicase activity in causing fork stalling in USP50-depleted cells, however the potential role for exonuclease activity was not explored due to lack of an exonuclease-specific inhibitor. To answer this question, we generated HeLa FlpIn cell lines stably expressing doxycycline-inducible, siRNA-resistant, GFP-tagged WRN constructs: wild-type, exonuclease-dead (E84A) and helicase-dead (K577M). To test for expression of the WRN constructs, HeLa cells were treated with siRNA targeting WRN and doxycycline for 72 hours, then analysed by Western blotting. The samples showed strong expression of the GFP-tagged WRN constructs in each stable cell line, with each WRN construct showing expression levels higher than the endogenous WRN protein (figure 3.5a).

We used the DNA fibre assay in the stable cell lines to assess the effect of expression of the WRN constructs on fork stalling in cells depleted of USP50 and/ or WRN. Cells were treated with siRNA targeting USP50 or WRN and doxycycline for 72 hours (figure 3.5b), with empty

HeLa FlpIn cells used as a control cell line. As seen before, depleting WRN led to increased fork stalling compared to untreated cells, which was rescued upon expression of the wild-type WRN construct (figure 3.5c). Interestingly, neither the helicase-dead nor exonuclease-dead WRN constructs could reduce the levels of stalled forks in WRN-depleted cells. In cells depleted of USP50 and WRN, expression of wild-type WRN unexpectedly rescued fork stalling levels, whereas expression of either the helicase-dead or exonuclease-dead WRN constructs did not (figure 3.5d). This result is intriguing as it suggests that when USP50 is depleted, either loss of WRN or expression of exogenous wild-type WRN rescues fork stalling, which appears to be contradictory. This could potentially be explained by the observation that the expression of exogenous WRN is much higher than that of endogenous WRN, meaning that the WRN defect seen in USP50-depleted cells could be overcome by overexpressing WRN beyond endogenous levels.

Given this possible WRN overexpression-driven phenotype, we wondered whether the effect on fork stalling in cells expressing either WRN mutant was due to the lack of one enzymatic activity, or the excess activity of the intact enzymatic function due to increased protein levels. To address this question, we generated another stable HeLa FlpIn cell line expressing doxycycline-inducible WRN with both K577M and E84A point mutations, rendering the resulting protein both helicase- and exonuclease-dead. We refer to this mutant as enzymatic-dead (ed) WRN. Western blotting of cells treated with doxycycline for 72 hours showed that the edWRN mutant was expressed (figure 3.5e). We repeated the DNA fibre assay in these cells as before to investigate the effect of non-enzymatic WRN expression on replication fork stalling. As before, in empty HeLa cells the co-depletion of USP50 and WRN rescued fork stalling levels. In cells depleted of WRN, expression of edWRN was not able to reduce stalled

fork numbers. Nor was the edWRN mutant able to rescue fork stalling in cells depleted of both USP50 and WRN (figure 3.5f). These results suggest that in cells depleted of WRN, only wild-type WRN can rescue fork stalling. On a background of USP50 and WRN co-depletion, the overexpression of wild-type WRN restored levels of fork stalling to that seen in untreated cells, unlike the overexpression of helicase- dead, exonuclease-dead WRN or enzymatic-dead WRN. Again, this implies that both enzymatic functions of WRN are needed to rescue fork stalling when USP50 is depleted, and that overexpression of wild-type WRN can overcome the replication defect caused by WRN activity in cells lacking USP50.

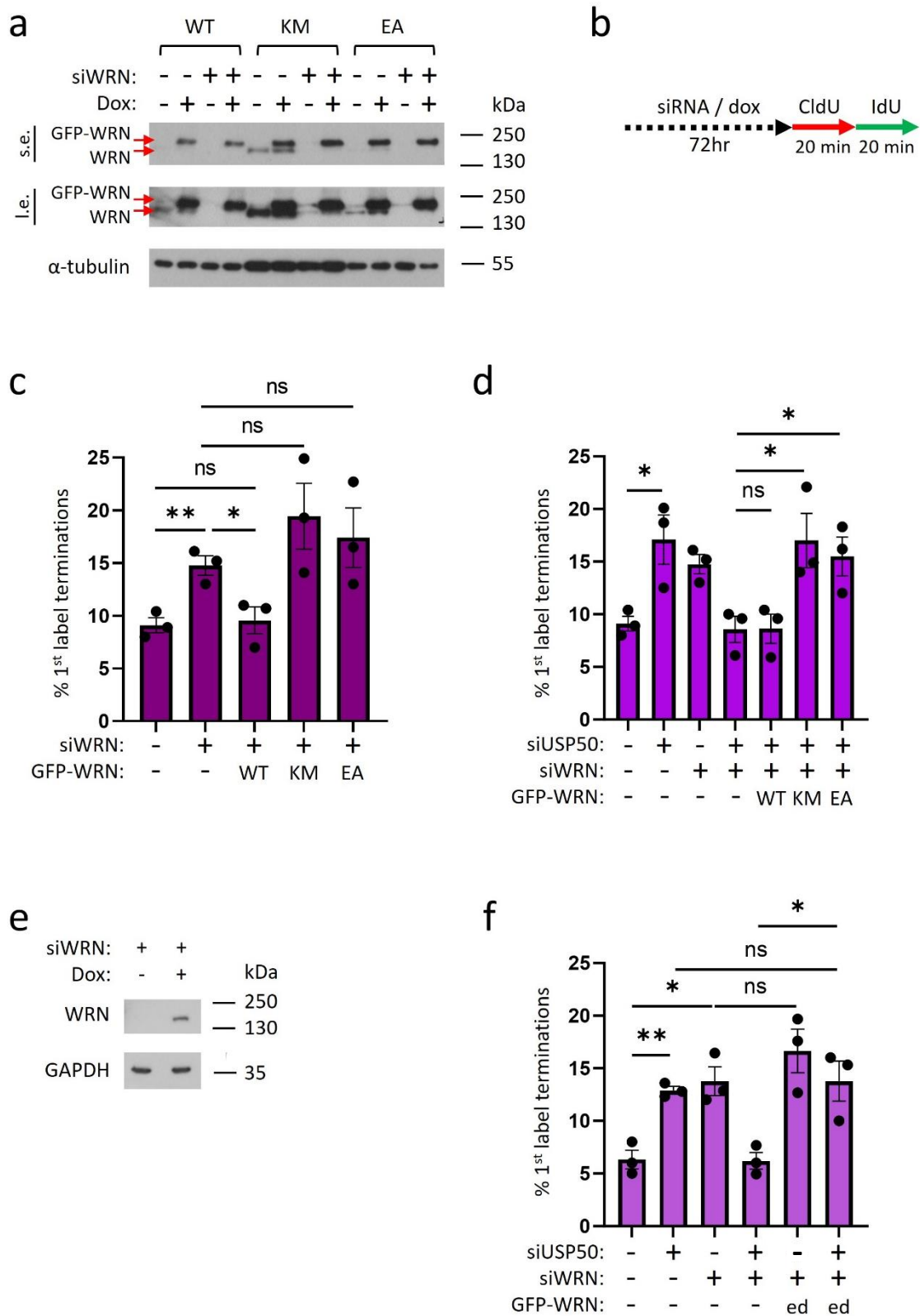


Figure 3.5

a) Western blot showing WRN protein levels after 72 hours of treatment with siRNA targeting WRN and doxycycline in HeLa FlpIn stable cells. GFP-WRN expression was induced with doxycycline; control cells were treated with vehicle. Transfection control was with siRNA targeting Luciferase. S.e.= short exposure, l.e.= long exposure.

b) Schematic of the DNA fibre assay. HeLa FlpIn cells were treated with siRNA targeting USP50 or WRN and doxycycline for 72 hours before incubation with CldU and IdU for 20 minutes each.

c) 1st label terminations were examined using the DNA fibre assay in HeLa FlpIn stable cells treated with siRNA targeting WRN, and doxycycline. GFP-WRN expression was induced with doxycycline; control cells were treated with vehicle. Transfection control was with siRNA targeting Luciferase. WT= wild-type, KM= helicase-dead (K577M), EA= exonuclease-dead (E84A). Results are from 3 independent repeats, with n >200 fibres per condition, per repeat. Bars indicate the mean, error bars are SEM. Statistical analysis done with unpaired two-tailed *t*-test; ns= not significant, *= $p \leq 0.05$, **= $p \leq 0.01$.

d) 1st label terminations were examined using the DNA fibre assay in HeLa FlpIn stable cells treated with siRNA targeting USP50 and WRN, and doxycycline. GFP-WRN expression was induced with doxycycline; control cells were treated with vehicle. Transfection control was with siRNA targeting Luciferase. WT= wild-type, KM= helicase-dead (K577M), EA= exonuclease-dead (E84A). Results are from 3 independent repeats, with n >200 fibres per condition, per repeat. Bars indicate the mean, error bars are SEM. Statistical analysis done with unpaired two-tailed *t*-test; ns= not significant, *= $p \leq 0.05$.

e) Western blot showing WRN protein levels after 72 hours of treatment with siRNA targeting WRN and doxycycline in HeLa FlpIn stable cells.

f) 1st label terminations were examined using the DNA fibre assay in HeLa FlpIn stable cells treated with siRNA targeting USP50 and WRN, and doxycycline. ed= enzymatic dead (K577M/ E84A). GFP-WRN

expression was induced with doxycycline; control cells were treated with vehicle. Transfection control was with siRNA targeting Luciferase. Results are from 3 independent repeats, with $n > 200$ fibres per condition, per repeat. Bars indicate the mean, error bars are SEM. Statistical analysis done with unpaired two-tailed t -test; ns= not significant, *= $p \leq 0.05$, **= $p \leq 0.01$.

3.7 Targeting USP50 and WRN together rescues formation of DSBs in replicating cells

WRN has known roles in preventing the formation of DSBs. WRN is a target of ATM and ATR, and accumulates at stalled forks to prevent collapse into DSBs (Ammazzalorso *et al.*, 2010). WRN also has roles in DSB repair: WRN loss leads to a defect in NHEJ and HR repair (Saintigny *et al.*, 2002; Shamanna *et al.*, 2016), and WRN-depleted cells are sensitive to DNA-damaging drugs (Ammazzalorso *et al.*, 2010; Imamura *et al.*, 2002; Yannone *et al.*, 2001; Zecevic *et al.*, 2009). 53BP1 and γ -H2AX foci are frequently used as markers for DSBs (A. Gupta *et al.*, 2014; Kuo & Yang, 2008).

Given data showing that USP50 depletion led to the increased formation of 53BP1 foci in S phase cells (figure 1.11c), we wanted to confirm this data with another marker of DSBs. HeLa cells plated onto coverslips were treated with siRNA targeting USP50 for 72 hours, then cells were pulsed with the nucleotide analogue EdU for 15 minutes to label replicating cells. Cells were fixed and γ -H2AX foci were examined using IF (figure 3.6a). The number of γ -H2AX foci per non-replicating cell increased from an average of 2.6 foci in untreated cells to 3.1 foci per cell in USP50-depleted cells, an increase of 19% (figure 3.6b). The average foci numbers in USP50-depleted cells increased by 84% to 5.7 foci per cell in S phase USP50-depleted cells, which agrees with our previous finding that USP50 depletion leads to an increase in primarily S phase DSBs.

Next, we wanted to examine how USP50 and WRN influence DSB formation. We had previously seen that co-depletion of USP50 and WRN did not have an additive effect on 53BP1 foci formation, and in fact led to a small but significant reduction in average foci numbers (figure 1.11h). We decided to test whether the WRNi NSC 617145 affects DSB formation in USP50-

depleted cells. HeLa cells plated onto coverslips were treated with siRNA targeting USP50 and NSC 617145 at 250 nM for 72 hours, then cells were pulsed with EdU for 15 minutes. Cells were fixed and 53BP1 foci were examined using IF (figure 3.6c, d). As seen before, replicating cells depleted of USP50 had a higher number of 53BP1 foci, though the effect seen was less dramatic than previously observed (3.8 vs 2.6 average foci per cell respectively). Treatment with the WRNi led to an increase in 53BP1 foci from 2.6 to 5.8 average foci per cell, consistent with evidence that losing WRN helicase activity contributes to DSB formation. Depletion of USP50 in combination with WRNi treatment reduced levels of 53BP1 foci compared with WRNi treatment alone to 3.1 foci per cell (figure 3.6d), suggesting that the DSBs formed upon WRN helicase inhibition are in part caused by USP50 activity during replication, or vice versa.

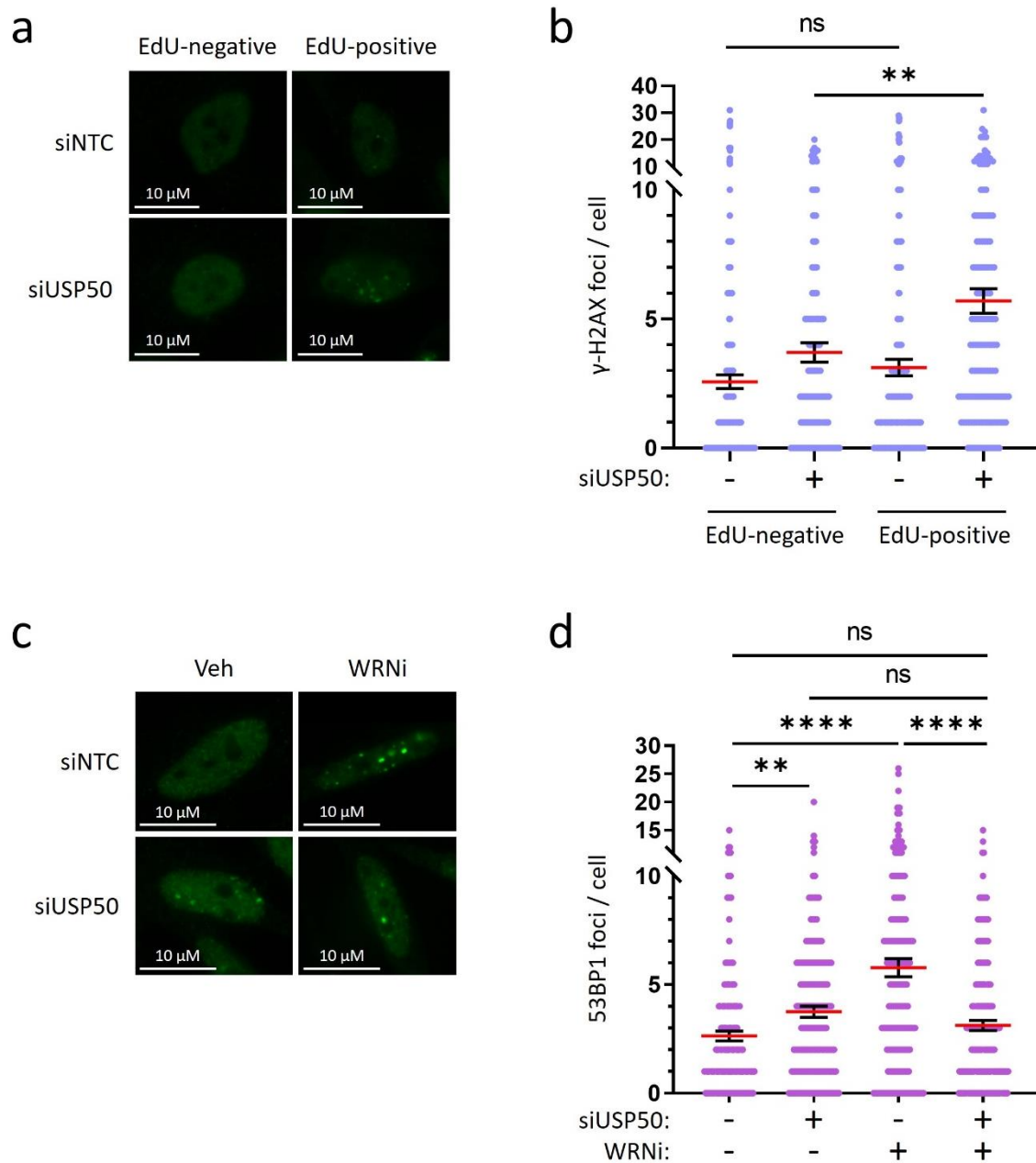


Figure 3.6

a) Representative images of γ -H2AX foci and EdU-labelled HeLa cells.

b) γ -H2AX foci were examined using IF in HeLa cells with USP50 depletion and EdU labelling. Transfection control was with siRNA targeting Luciferase. Results are from 3 independent repeats, with $n > 50$ cells per condition, per repeat. Red lines indicate the mean, error bars are SEM. Statistical analysis done with unpaired two-tailed t -test; ns= not significant, **= $p \leq 0.01$.

c) 53BP1 foci were examined using IF in EdU-positive HeLa cells with USP50 depletion and WRNi treatment. Transfection control was with siRNA targeting Luciferase. Control cells were treated with vehicle (DMSO). Representative images shown.

d) 53BP1 foci were examined using IF in EdU-positive HeLa cells with USP50 depletion and WRNi treatment. Transfection control was with siRNA targeting Luciferase. Control cells were treated with vehicle (DMSO). Results are from 3 independent repeats, with $n > 50$ cells per condition, per repeat. Red lines indicate the mean, error bars are SEM. Statistical analysis done with unpaired two-tailed t -test; ns= not significant, **= $p \leq 0.01$, ****= $p \leq 0.0001$.

3.8 Co-depletion of USP50 and WRN does not rescue cell survival in HeLa cells

We previously saw that depletion or inhibition of WRN led to accumulation of DSBs in HeLa cells (figure 1.11c, figure 3.6d). DSBs are the most lethal form of DNA break, and a single unrepaired DSB in yeast cells can lead to cell death (Featherstone & Jackson, 1999). WRN loss has been reported to affect cell proliferation and survival: cells isolated from WS patients have reduced proliferative potential and a higher rate of apoptosis (Pichierri *et al.*, 2001), and WS cells induce apoptosis hours quicker than non-WS cells after a short treatment with camptothecin (Pichierri *et al.*, 2001).

Given previous data suggesting that co-depletion of USP50 and WRN had a rescue effect on fork stalling and DSB formation, we investigated whether co-depletion could be beneficial for cell survival using the clonogenic survival assay. HeLa cells were treated with siRNA targeting USP50 and WRN, and cells were plated out at a low density and left to grow into colonies, then stained and counted. USP50 or WRN depletion alone caused 7.7% and 22.0% of cells to die respectively. When USP50 and WRN were co-depleted there was a trend towards increased cell death, with 31.4% cell death, though the difference in cell survival between the co-depletion and either single depletion was not statistically significant (figure 3.7a). This suggests that despite appearing to improve potentially harmful events such as replication fork stalling and DSB formation, depleting both USP50 and WRN does not improve cell survival.

a

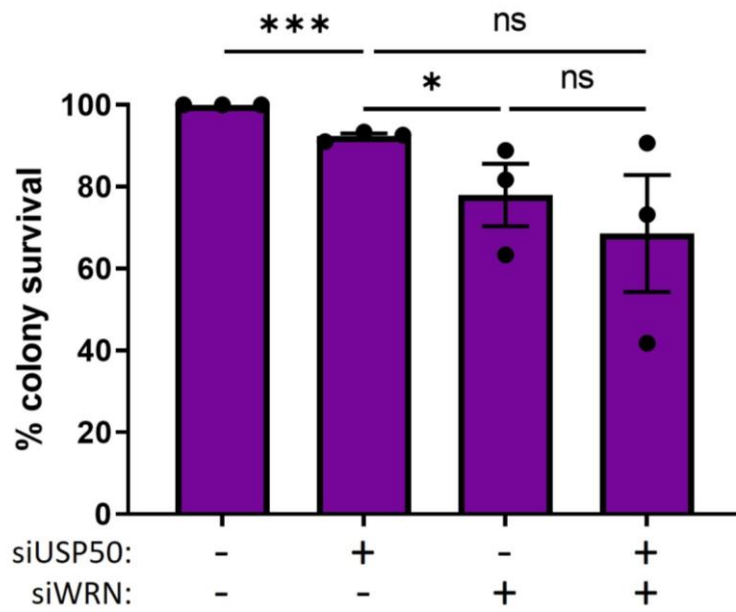


Figure 3.7

a) Cell survival was measured using the clonogenic survival assay. HeLa cells were treated for 72 hours with siRNA targeting USP50 and WRN. Transfection control was with siRNA targeting Luciferase. Results are from 3 independent repeats. Bars indicate the mean, error bars are SEM. Statistical analysis done with unpaired two-tailed *t*-test; ns= not significant, *= $p \leq 0.05$, ***= $p \leq 0.001$.

3.9 USP50 regulates WRN localisation to chromatin after hydroxyurea treatment

WRN is localised to the nucleolus in unstressed conditions (Gray *et al.*, 1998; Marciniak *et al.*, 1998; Yankiwski *et al.*, 2000). Several post-translational modifications regulate the shuttling of WRN between the nucleolus and nucleus after DNA damage or RS, including acetylation, phosphorylation and SUMOylation (Cheng *et al.*, 2003; Lee *et al.*, 2015; Woods *et al.*, 2004). DNA-PK_{CS} phosphorylates WRN after DSB formation after IR, bleomycin or 4NQO treatment (Karmakar *et al.*, 2002; Yannone *et al.*, 2001). ATR phosphorylates WRN after treatment with HU, CPT, MMC and UV (Ammazzalorso *et al.*, 2010; Su *et al.*, 2016). ATM phosphorylates WRN after replication stress (Ammazzalorso *et al.*, 2010), and CDK1 phosphorylates WRN after etoposide treatment (Palermo *et al.*, 2016). WRN is acetylated by p300/ CBP after MMC treatment (K. Li *et al.*, 2010). Once in the nucleoplasm, WRN congregates at sites of DNA damage and replicative stress (Li *et al.*, 2008; Zecevic *et al.*, 2009).

We asked whether USP50 could be regulating WRN through localisation to cellular compartments, and whether this could explain the phenotypes previously seen. To address this question, HeLa cells were treated with siRNA targeting USP50 for 72 hours before the cells were harvested and separated into cytoplasmic, nuclear and chromatin-enriched fractions. The samples were then analysed by Western blot. As seen in figure 3.8a, the cellular compartments were separated well, with α -tubulin seen in only the whole cell extract and cytoplasmic fraction, and histone H3 found only in whole cell extract and chromatin fraction, as expected. In the whole cell extract and chromatin fraction, USP50 depletion did not affect levels of WRN protein (figure 3.8b, lane 1 vs 2; lane 5 vs 6). The experiment was repeated with the addition of a 3-hour treatment with 5 mM HU to induce fork stalling and RS (Koç *et al.*,

2004). Interestingly, USP50 depletion in HU-treated cells led to a 50.3% reduction of WRN at chromatin, but not in the whole cell extract (figure 3.8c, lane 1 vs 2 of WCE blot; lane 1 vs 2 of chromatin blot). This effect was seen again in a second biological repeat (data not shown).

The WRNi NSC 617145 has been reported to alter WRN protein levels and localisation through promoting WRN proteasomal degradation and trapping WRN protein on chromatin (Aggarwal *et al.*, 2013). To test how WRNi treatment and USP50 depletion could affect WRN at chromatin, we repeated the cell fractionation protocol as before, with the addition of 24-hour WRNi treatment at 250 nM. In untreated cells, WRNi treatment did not affect WRN protein levels in the whole cell extract or chromatin fraction, contrasting with previous reports (figure 3.8b, lane 1 vs 3; lane 5 vs 7). After HU treatment, WRNi treatment did not affect WRN levels in the whole cell extract (figure 3.8c, lane 1 vs 3). However, in HU-treated cells depleted of USP50, the addition of WRNi led to higher levels of WRN in the chromatin fraction compared to USP50-depleted cells (figure 3.8c, lane 2 vs 4 of chromatin blot; 49.7% vs 89.2%). This indicates that WRNi treatment counteracts the loss of WRN at chromatin when USP50 is depleted, perhaps by trapping WRN on chromatin as previously reported.

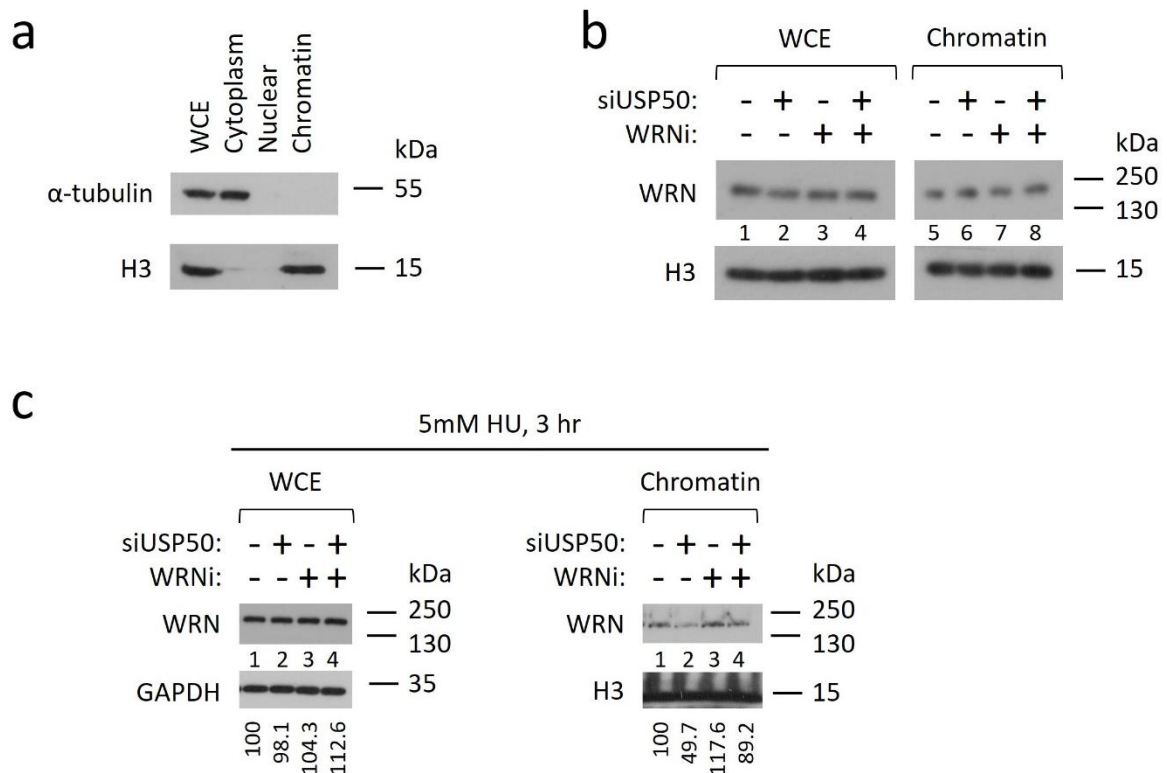


Figure 3.8

a) Western blot showing cytoplasmic and chromatin markers in cellular fractions. WCE= whole cell extract.

b) Western blot showing WRN protein levels after 72 hours of treatment with siRNA targeting USP50 and 250 nM WRNi for 24 hours in HeLa cells. Transfection control was with siRNA targeting Luciferase. Control cells were treated with vehicle (DMSO). WCE= whole cell extract. Experiment was performed twice; images shown are representative of the effect seen.

c) Western blot showing WRN protein levels after 72 hours of treatment with siRNA targeting USP50, 250 nM WRNi for 24 hours, and 5 mM HU for 3 hours in HeLa cells. Transfection control was with siRNA targeting Luciferase. Control cells were treated with vehicle (DMSO). Numbers below H3 loading controls show relative WRN signal normalised to untreated cells and loading control from one

experiment. WCE= whole cell extract. Experiment was performed twice; images shown are representative of the effect seen.

3.10 WRN and USP50 operate in the same pathway to restart stalled forks after hydroxyurea treatment

WRN has known roles in restarting stalled replication forks. It has been reported that WRN coordinates with the nuclease/ helicase DNA2 to promote fork restart, a process that relies on WRN ATPase/ helicase activity and DNA2 nuclease activity (Thangavel *et al.*, 2015). Depletion of WRN or DNA2 leads to a replication fork restart defect after HU treatment, and the two proteins are epistatic with one another in fork restart assays (Franchitto *et al.*, 2008; Thangavel *et al.*, 2015).

We wondered whether USP50 has a role in fork restart, and if so, whether it is epistatic with WRN. A modified version of the DNA fibre assay was used where cells are incubated with CldU for 30 minutes, incubated with HU for 3 hours, then incubated with IdU for 1 hour before harvesting (figure 3.9a). Replication forks that restarted after HU treatment will have incorporated both CldU and IdU labels into the DNA tract, whereas forks that did not restart will only have CldU incorporated. New origins that fired after HU treatment will only have the IdU label.

Previous unpublished data from the laboratory showed that depletion of USP50 led to an increase in stalled forks (7.7% in untreated cells to 13.7%) (figure 3.9b). As reported previously, WRN depletion also led to a decrease in the proportion of restarted forks to a similar level of that seen in USP50 depletion (13.0% vs 13.7% respectively), supporting evidence that WRN promotes fork restart. Interestingly, when USP50 and WRN were co-depleted the proportion of stalled forks did not change compared to either depletion alone. Together this data implies

that USP50 has an important role in replication fork restart after arrest, and that it operates in the same pathway as WRN in this regard.

We then asked whether WRN helicase activity specifically is epistatic with USP50 in promoting fork restart. To test this, the DNA fibre assay was repeated with USP50 siRNA depletion and WRNi treatment at 250 nM for 24 hours before incubation with CldU, HU and IdU (figure 3.9a). As seen before, depletion of USP50 led to an increase in the proportion of stalled/ unrestarted forks after HU treatment (24.3% vs 16.8% in untreated cells). Interestingly, WRNi treatment did not alter the proportion of restarted or stalled forks (15.0% vs 16.8% in untreated cells). Co-treatment of USP50 depletion and WRN helicase inhibition did not affect fork restart compared to USP50 depletion alone (figure 3.9c). This result suggests that the helicase function of WRN is not involved in replication fork restart, contradicting previous reports (Franchitto *et al.*, 2008; Thangavel *et al.*, 2015).

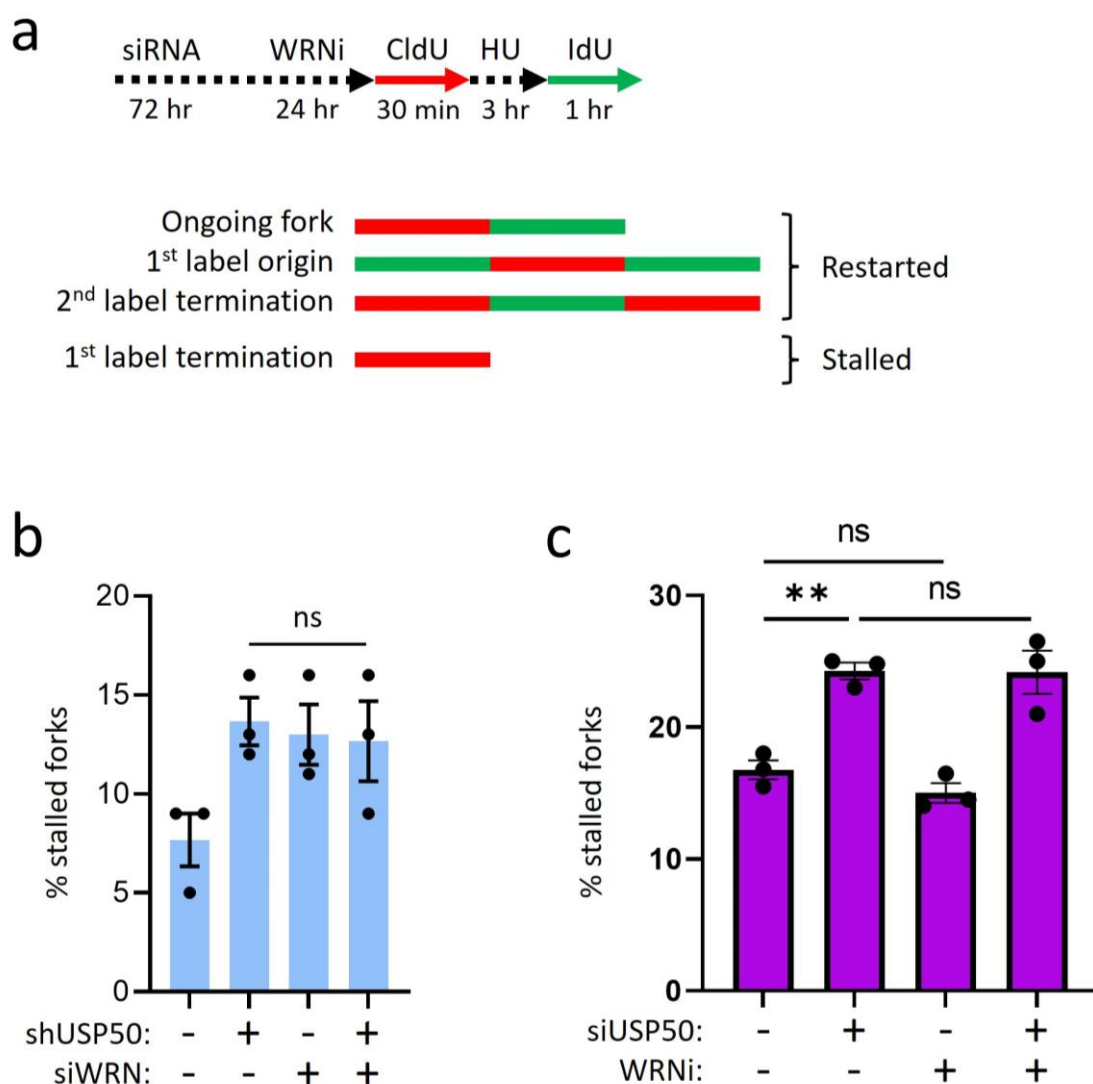


Figure 3.9

a) Schematic of the DNA fibre assay. HeLa cells were treated with siRNA targeting USP50 for 72 hours and 250 nM WRNi for 24 hours before incubation with CldU, 5 mM HU and IdU.

b) Stalled forks were examined using the DNA fibre assay in HeLa cells treated with shRNA targeting USP50 and siRNA targeting WRN. shUSP50 expression was induced with IPTG; control cells were treated with vehicle. Transfection control was with siRNA targeting Luciferase. Results are from 3 independent repeats, with $n > 200$ fibres per condition, per repeat. Bars indicate the mean, error bars are SEM.

Statistical analysis done with unpaired two-tailed *t*-test; ns= not significant. Performed by Dr Hannah Mackay.

c) Stalled forks were examined using the DNA fibre assay in HeLa cells treated with siRNA targeting USP50 and treated with 250 nM WRNi for 24 hours. Transfection control was with siRNA targeting Luciferase. Control cells were treated with vehicle (DMSO). Results are from 3 independent repeats, with $n > 100$ fibres per condition, per repeat. Bars indicate the mean, error bars are SEM. Statistical analysis done with unpaired two-tailed *t*-test; ns= not significant, **= $p \leq 0.01$.

3.11 Replication fork progression during hydroxyurea treatment is promoted by USP50 and WRN

Replication fork reversal is an important protective feature that is essential for ensuring genomic integrity (Poole & Cortez, 2017). The halting of replication fork progression through fork reversal allows time for the cell to remove the replication impediment, upon which the reversed fork can be restarted. If the fork is restarted in a timely manner, this pathway avoids the generation of a replication-associated DSB (Qiu *et al.*, 2021). Several enzymes have been reported to catalyse fork reversal *in vivo*, including SMARCAL1 (Tye *et al.*, 2021). There is evidence that WRN can regress forks *in vitro* and may have the ability to do so *in vivo* as well (Iannascoli *et al.*, 2015; Machwe *et al.*, 2006, 2007).

We wondered whether USP50 and WRN affect the ability of replication forks to progress during RS conditions, which could indicate an effect on fork reversal. We used a modified version of the DNA fibre assay to address this question. In this version of the assay, cells were incubated with CldU for 30 minutes, then with IdU and 5 mM HU together for 3 hours before cells were harvested (figure 3.10a). The length of the IdU tract was compared to the length of the CldU tract to determine how far the replication fork was able to travel during HU treatment before it stopped, while controlling for effect of the treatment on fork speeds. SMARCAL1 depletion was used as a positive control of inhibition of fork reversal (figure 3.10b). Cells depleted of SMARCAL1 showed an increase in IdU: CldU tract length from 0.14 to 0.2, indicating that replication forks travelled further on average during HU treatment compared to the NTC condition (figure 3.10c).

To measure the effect of USP50 and WRN on fork progression during HU treatment, HeLa cells were plated and treated with siRNA targeting USP50 and WRN and with WRNi at 250 nM for 24 hours prior to incubation with CldU, IdU and HU (figure 3.10d). Depletion of USP50 led to an increase in the IdU: CldU ratio compared to cells treated with NTC siRNA (0.28 vs 0.21 respectively), indicating that the replication forks travelled further in the presence of HU when USP50 was depleted. Depletion of WRN also led to an increase in the IdU: CldU ratio, to a greater extent than with USP50 depletion (0.33 vs 0.28 respectively), indicating a greater effect of WRN on the ability of forks to progress during HU treatment. The combination of USP50 and WRN depletion reduced the IdU: CldU ratio compared to either depletion alone (0.25), though did not rescue fully back to levels seen in untreated cells. WRNi treatment had a similar effect to WRN knockdown, with an increase in length of replication fork progression during HU block (0.33). Combining WRNi and USP50 depletion led to a slight decrease in IdU: CldU ratio to 0.28, similar to that seen in the condition with co-depletion of USP50 and WRN. This data suggests that during HU-induced RS, WRN and USP50 encourage active replication forks to stop travelling, possibly by encouraging fork reversal.

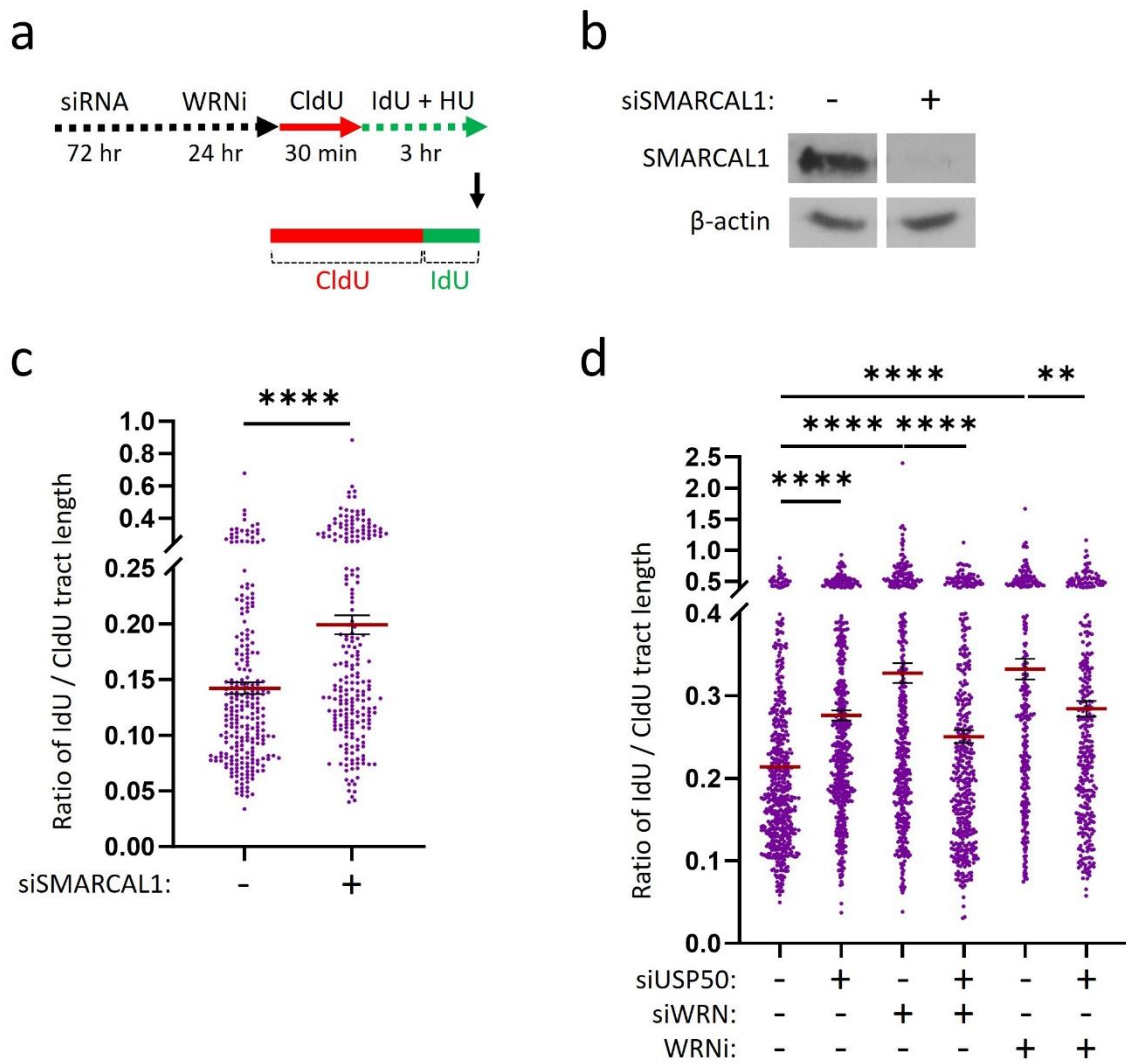


Figure 3.10

a) Schematic of the DNA fibre assay. HeLa cells were treated with siRNA targeting SMARCAL1, USP50 and WRN for 72 hours, and 250 nM WRNi for 24 hours, before incubation with CldU, IdU and 5 mM HU.

b) Western blot showing SMARCAL1 protein levels after 72 hours of treatment with siRNA targeting SMARCAL1 in HeLa cells. Transfection control was with siRNA targeting Luciferase. Performed by Dr Hannah Mackay.

c) IdU: CldU lengths were examined using the DNA fibre assay in HeLa cells treated with siRNA targeting SMARCAL1. Transfection control was with siRNA targeting Luciferase. Results are from 2 independent repeats, with $n > 100$ fibres per condition, per repeat. Red lines indicate the mean, error bars are SEM. Statistical analysis done with unpaired two-tailed t -test; ****= $p \leq 0.0001$.

d) IdU: CldU lengths were examined using the DNA fibre assay in HeLa cells treated with siRNA targeting USP50 and WRN, and 250 nM WRNi for 24 hours. Transfection control was with siRNA targeting Luciferase. Control cells were treated with vehicle (DMSO). Results are from 3 independent repeats, with $n > 100$ fibres per condition, per repeat. Bars indicate the mean, error bars are SEM. Statistical analysis done with unpaired two-tailed t -test; **= $p \leq 0.01$, ****= $p \leq 0.0001$.

3.12 RECQL4 and RECQL5 can compensate for loss of WRN and USP50 to rescue stalled replication forks

WRN is a member of the RECQ family of helicases, along with RECQL1, BLM, RECQL4 and RECQL5. The RECQ helicases share a conserved ATPase/ helicase domain, zinc-binding region, RQC domain and NLS (Croteau *et al.*, 2014). BLM and WRN also share a conserved HRDC domain (Croteau *et al.*, 2014). The RECQ helicases share many DNA replication and repair substrates and have several similar roles. Despite sharing protein domains and substrates, it is thought that the RECQ helicases cannot compensate for each other when one is missing or mutated (Kitano, 2014).

Previous work in the laboratory using the DNA fibre assay looked at the role of BLM, RECQL1, RECQL4 and RECQL5 in fork restart when USP50 is depleted. We saw that neither BLM nor RECQL1 depletion improved fork restart in USP50-depleted cells. However, RECQL4 or RECQL5 depletion could rescue the fork restart defect seen in USP50-depleted cells (figure 3.11a, b). We were curious to see whether the other RECQ helicases behaved similarly to WRN in the context of USP50 depletion and replication fork stalling in untreated cells. We used the DNA fibre assay to look at replication fork stalling with USP50 and RECQL4 or RECQL5 co-depletion. HeLa cells were plated and treated with siRNA targeting USP50, WRN, RECQL4 and RECQL5, then incubated with CldU and IdU for 20 minutes each before harvesting (figure 3.11c, d). As seen before, depletion of USP50 or WRN alone led to an increase in 1st label terminations, and the co-depletion of both rescued 1st label terminations back to levels seen in untreated cells. Depletion of RECQL4 alone caused a small increase in 1st label terminations (figure 3.11e). Interestingly, USP50 and RECQL4 co-depletion rescued 1st label terminations to untreated

levels. When RECQL4 was depleted on top of USP50 and WRN, the proportion of 1st label terminations increased, suggesting that when USP50 and WRN are depleted, RECQL4 acts to suppress fork stalling. RECQL5 depletion alone caused an increase in 1st label terminations (figure 3.11f). Similar to RECQL4, co-depletion of USP50 and RECQL5 rescued 1st label terminations. Co-depletion of USP50, WRN and RECQL5 led to an increase in 1st label terminations. Together, this data suggests that when USP50 is depleted, the increase in 1st label terminations can be rescued by depleting either WRN, RECQL4 or RECQL5. When USP50 and WRN are depleted, depleting either RECQL4 or RECQL5 in addition causes 1st label terminations to increase, suggesting that RECQL4 or RECQL5 promote fork progression in the absence of USP50 and WRN, perhaps acting together.

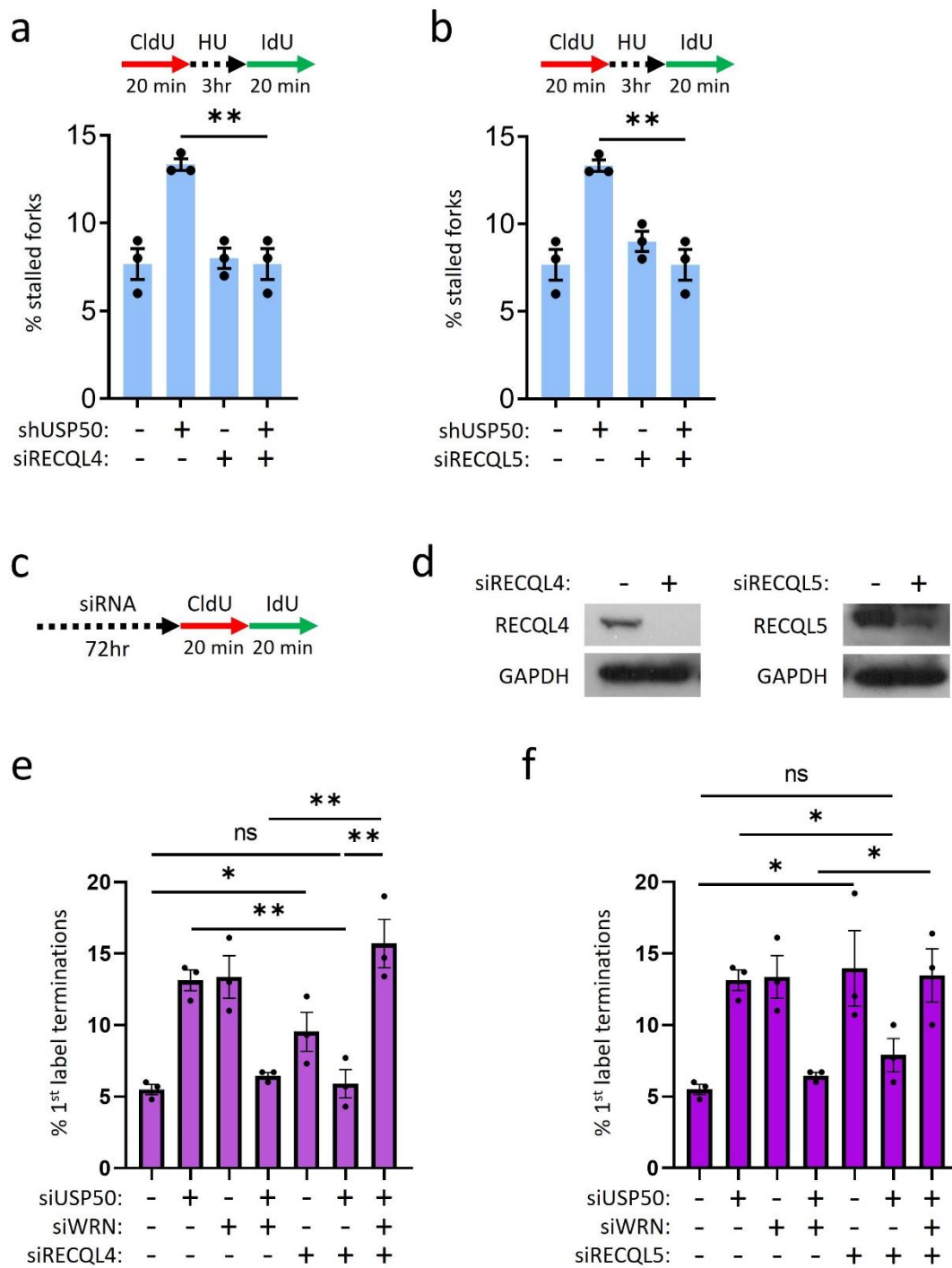


Figure 3.11

a) Stalled forks were examined using the DNA fibre assay in HeLa cells treated with sh/ siRNA targeting USP50 and RECQL4, and 5 mM HU. shUSP50 expression was induced with IPTG; control cells

were treated with vehicle. Transfection control was with siRNA targeting Luciferase. Results are from 3 independent repeats, with $n > 200$ fibres per condition, per repeat. Bars indicate the mean and error bars are SEM. Statistical analysis done with unpaired two-tailed t -test; **= $p \leq 0.01$. Performed by Dr Hannah Mackay.

b) Stalled forks were examined using the DNA fibre assay in HeLa cells treated with sh/ siRNA targeting USP50 and RECQL5, and 5 mM HU. shUSP50 expression was induced with IPTG; control cells were treated with vehicle. Transfection control was with siRNA targeting Luciferase. Results are from 3 independent repeats, with $n > 200$ fibres per condition, per repeat. Bars indicate the mean and error bars are SEM. Statistical analysis done with unpaired two-tailed t -test; **= $p \leq 0.01$. Performed by Dr Hannah Mackay.

c) Schematic of the DNA fibre assay. HeLa cells were treated with siRNA targeting USP50, WRN, RECQL4 and RECQL5 for 72 hours before incubation with CldU and IdU for 20 minutes each.

d) Western blot showing RECQL4 and RECQL5 protein levels after 72 hours of treatment with siRNA targeting RECQL4 and RECQL5 in HeLa cells. Performed by Dr Hannah Mackay.

e) 1st label terminations were examined using the DNA fibre assay in HeLa cells treated with siRNA targeting USP50, WRN and RECQL4. Transfection control was with siRNA targeting Luciferase. Results are from 3 independent repeats, with $n > 200$ fibres per condition, per repeat. Bars indicate the mean, error bars are SEM. Statistical analysis done with unpaired two-tailed t -test; ns= not significant, *= $p \leq 0.05$, **= $p \leq 0.01$.

f) 1st label terminations were examined using the DNA fibre assay in HeLa cells treated with siRNA targeting USP50, WRN and RECQL5. Transfection control was with siRNA targeting Luciferase. Results are from 3 independent repeats, with $n > 200$ fibres per condition, per repeat. Bars indicate the mean, error bars are SEM. Statistical analysis done with unpaired two-tailed t -test; ns= not significant, *= $p \leq 0.05$.

3.13 Discussion

Replication fork progression and recovery after RS is key to avoid deleterious consequences such as DSB formation, incomplete replication and mutations. USP50, a poorly understood inactive DUB, was previously shown in the laboratory to have a role in the RS response, with evidence that it was epistatic with WRN in certain aspects of replication. WRN has known roles in DNA replication and repair, but its possible relationship with USP50 is unexplored. In this chapter, we shed light on the specific areas of replication that USP50 and WRN are involved in, and assessed cellular consequences of loss of the USP50-WRN axis in HeLa cells.

A possible source of the MUS81-dependent DSBs seen in USP50-depleted cells is the nucleolytic processing by MUS81 of stalled replication forks to aid HR-mediated repair. Having seen that MUS81 depletion on top of USP50 depletion reversed the increase in 53BP foci, I used the DNA fibre assay to assess whether USP50 acts before or after MUS81 in preventing replication fork stalling. Co-depletion of MUS81 and USP50 had no effect on fork stalling compared to USP50-depleted cells, suggesting that MUS81 processing of stalled replication forks occurs after USP50 action at the replication fork, meaning that USP50 plays an earlier role in promotion of fork progression. This data implicates USP50 in preventing the formation of DNA structures that are MUS81 cleavage substrates. USP50 could therefore play a role in any or several of the processes occurring between a progressing replication fork and a persistently stalled fork, e.g. in supporting the replication machinery, clearing replication impediments ahead of the fork, fork reversal to generate a structure that can be cleaved by MUS81, prevention of fork restart, or inhibition of DDT mechanisms. Loss of any of these processes could potentially explain the increase in stalled forks and MUS81-dependent DSB

formation seen. We saw that USP50-depleted cells were not hypersensitive to UV radiation, suggesting that USP50 is not involved in TLS-driven DDT. Further experiments would be needed to elucidate which process or processes USP50 is involved in that promote fork progression, and whether this is direct or indirect. It would be interesting to analyse interactors of USP50 to identify whether any components of the replication fork complex associate with USP50. Similarly, it would be useful to know which, if any, physical DNA lesions cause stalling of replication forks in the absence of USP50. Combining USP50 depletion with inducers of specific types of DNA damage and analysing the effect on fork stalling could be one way to address this question.

The DNA fibre assay was used to assess the relationship between USP50 and WRN in preventing fork stalling. As reported by other groups, WRN depletion/ inhibition led to an increase in stalled replication forks. Surprisingly, we found that co-depletion of USP50 and WRN rescued the fork stalling defect seen with either depletion alone. This result suggests that in the absence of USP50, WRN activity contributes to increased fork stalling, and vice versa. Intriguingly, treating cells with the small molecule inhibitor NSC 617145 to inhibit WRN helicase activity had a similar effect on fork stalling in USP50-depleted cells, leading to a decrease in stalled forks to levels seen in untreated cells. The effects of the inhibitor treatment seem to be specific to WRN activity, as combining WRN knockdown with WRN inhibitor treatment did not exacerbate stalled fork levels. This implies that the fork stalling seen in WRNi-treated cells is indeed due to WRN inhibition and not an off-target effect. This observation strengthens the finding that WRN activity has a deleterious effect on fork stalling in the absence of USP50, and points towards the helicase function of WRN specifically.

To corroborate this, stable cell lines expressing doxycycline-inducible WRN constructs were utilised to examine the effect of WRN enzymatic mutants on fork stalling, in the presence and absence of USP50. Using the DNA fibre assay again, we saw that when WRN was depleted, only the exogenous expression of wild-type WRN could rescue the increase in fork stalling. Unexpectedly, in USP50-depleted cells both the loss and exogenous expression of wild-type WRN rescued the increase in fork stalling seen upon USP50 depletion. This result appears contradictory as it implies that when USP50 is lost, either loss of WRN or restoration of WRN can rescue fork stalling. A possible explanation for this phenotype is that the protein levels of exogenous WRN are higher than endogenous WRN, and overexpression of WRN behaves differently to endogenous WRN expression in that it can rescue the fork stalling defect in USP50-depleted cells. This would imply that WRN protein levels are critical to determining the outcomes of progressing forks when USP50 is depleted, perhaps through increased enzymatic activity at the replication fork due to increased WRN protein, or through the increased localisation/ presence of a WRN binding partner. Another explanation for the rescue of stalled forks seen in USP50-depleted, exogenous WRN-expressing cells is that the exogenous WRN construct used behaves differently to wild-type WRN and therefore affects fork stalling differently. However in cells depleted of WRN, expression of the wild-type WRN construct was able to rescue fork stalling, thus behaving at least in this scenario as wild-type WRN.

Given that the effect of WRN on fork stalling appeared to depend at least in part on WRN cellular levels, we wondered whether the phenotype seen when helicase-dead or exonuclease-dead WRN was expressed was due to the loss of the mutated enzymatic activity, or instead the over-activity of the intact enzymatic activity due to increased WRN protein at replication forks. To test for this, we created a fourth WRN construct with two point mutations,

rendering both helicase and exonuclease activities dead. This double mutant should therefore have lost all enzymatic activity, but should still retain non-enzymatic WRN functions. Using the DNA fibre assay to assess fork stalling, we saw that enzymatic-dead WRN could not rescue fork stalling in WRN-depleted or USP50- and WRN-depleted cells. Together, these DNA fibre assay experiments suggest that when USP50 is depleted, the helicase and exonuclease functions of WRN act together to cause fork stalling. When both helicase and exonuclease activity is lost, fork stalling levels are reduced. The use of stable cell lines expressing WRN constructs is useful for assessing the impact of WRN mutations on cellular phenotypes. A drawback of the system is that expression of the inducible protein may not match that of the endogenous protein, which may affect phenotypes in unexpected ways. Expression levels can also vary between exogenous constructs, which risks conflating the effect of a mutation with the expression level of the construct. Identification and isolation of clones with comparable levels of exogenous and endogenous WRN expression could address this issue.

The RECQ helicases have similar cellular roles but are not thought to be able to compensate for each other when one is missing. Despite this, we were curious to see whether USP50 affected other RECQ helicases and if so, whether this was related to the USP50-WRN axis. We used the DNA fibre assay to assess the impact of RECQL4 and RECQL5 depletion combined with USP50 depletion. RECQL4 or RECQL5 depletion rescued the increase in 1st label terminations in USP50-depleted cells, mirroring the effect seen with USP50 and WRN depletion. However, the additional depletion of WRN caused 1st label terminations to increase again. This data implies that when USP50 is depleted, the subsequent increase in stalled forks is due to WRN/ RECQL4/ RECQL5 activity, as depleting any of these helicases rescues fork stalling back to levels of untreated cells. This could point to a dysregulation of these RECQ

helicases when USP50 is depleted that contributes to fork stalling, perhaps through an alteration in protein levels, activity or binding partners. Given that when USP50 and WRN are depleted, RECQL4 or RECQL5 depletion causes an increase in fork stalling again, this could indicate that both RECQL4 and RECQL5 need to act together to compensate for loss of WRN and USP50.

The observation that depletion of RECQL4 or RECQL5 reverses the rescue in fork stalling with USP50 and WRN depletion suggests that RECQL4 and RECQL5 can compensate for WRN depletion to restore fork progression. Which roles of RECQL4 and RECQL5 could be responsible for restoration of replication when USP50 and WRN are lost? RECQL4 has important roles in control of replication initiation, and RECQL4 knockout is embryonic lethal in mice (Luong & Bernstein, 2021; Smeets *et al.*, 2014). RECQL4 localises to replication origins and interacts with components of the CMG helicase to promote stabilisation and activation (Luong & Bernstein, 2021; Masai, 2011; Sangrithi *et al.*, 2005). RECQL4 fine-tunes replication initiation through interactions with and control of APC/C (Xu *et al.*, 2023). Loss of RECQL4 leads to destabilisation of the CMG helicase and a decrease in DNA synthesis (Arora *et al.*, 2016; Im *et al.*, 2009). RECQL5 has roles in replication and transcription, particularly in preventing TRCs. RECQL5 is thought to suppress TRCs by limiting transcription elongation and transcription machinery stalling (Saponaro *et al.*, 2014; Urban *et al.*, 2016). RECQL5 helicase activity promotes PCNA ubiquitination and unloading at TRCs, allowing the transcription machinery to proceed (Urban *et al.*, 2016). RECQL5 acts at CFSs to remove RAD51 filaments, promoting MUS81 cleavage and subsequent fork restart (Di Marco *et al.*, 2017). RECQL5 interacts with WRN, especially during replication stress, and stimulates WRN helicase activity (Popuri *et al.*, 2013). In the absence of WRN, RECQL5 is retained at DSBs for longer and is required for replication progression, DSB

repair and cell survival, especially after HU treatment (Popuri *et al.*, 2013). It is possible that RECQL4 and RECQL5 co-operate in the absence of USP50 and WRN to promote replication by promoting origin firing to rescue stalled forks and encouraging fork restart through MUS81 cleavage. Further experiments are needed to confirm this hypothesis.

We had previously seen that depletion of USP50 led to an increase in 53BP1 foci in S phase cells. To corroborate this, the experiment was repeated with immunostaining for another DSB and replication stress marker, γ -H2AX, in S phase cells (Katsube *et al.*, 2014). We observed that loss of USP50 led to an increase in γ -H2AX foci in replicating cells, strengthening the theory that USP50 protects cells from replication stress and prevents replication-associated DSBs. Furthermore, analysis of 53BP1 foci in S phase cells revealed that depletion of USP50 and WRNi treatment led to a reduction in 53BP1 foci compared to WRNi treatment alone, indicating that the increase in DSBs upon loss of WRN helicase activity can be reduced by losing USP50 (and vice versa). It is known that stalled replication forks can be converted to DSBs through the nucleolytic activity of MUS81, necessitating repair by HR. Paired with the DNA fibre assay data showing that co-depletion or inhibition of USP50 and WRN rescues fork stalling, this could infer that the reduction in stalled forks corresponds to at least a partial reduction in broken replication forks and DSB formation. Replication-associated DSBs can be repaired by HR, but the replication machinery is disassembled, and replication is completed by a converging replication fork. Broken forks can also be repaired by microhomology-mediated end joining, a highly mutagenic process (Cannan & Pederson, 2016). DSBs impact on cell survival, as a single unrepaired DSB can cause cell death due to chromosome mis-segregation and the initiation of apoptosis. We used the clonogenic survival assay to assess the impact of USP50 and WRN depletion on cellular viability. USP50 and WRN co-depletion neither improved nor had an

additive effect on cell survival, highlighting a discrepancy between DSB levels and cell viability. This data therefore suggests that roles of USP50 and WRN unrelated to DSB formation have an impact on cell survival. WRN has many functions, so WRN depletion affects many pathways in the cell, with corresponding effects on cellular viability.

We know little about how USP50 may exert its cellular roles. Previous data from the laboratory suggests that USP50 binds ubiquitin but cannot catalyse its removal from proteins, rendering it an inactive DUB. The ubiquitin-binding activity of USP50 seems to be important for most phenotypes observed with USP50 depletion by our group, as a mutant USP50 construct deficient in ubiquitin binding is not able to rescue fork stalling, DSB formation and other phenotypes seen with USP50 depletion. Outside of this function, little is known about USP50 activity. There are many ways that USP50 could affect WRN activity in the assays used: USP50 could affect WRN enzymatic activity, or could indirectly affect WRN through interactions with WRN partners. It could affect WRN localisation or interaction with proteins, or regulate WRN degradation. We had previously seen that knockdown of USP50 did not affect WRN protein levels in whole cell extracts, however we wondered whether USP50 regulated WRN localisation to cellular compartments. To answer this question, we fractionated cells into cytoplasm, nucleoplasm and chromatin fractions. In cells treated with siRNA targeting USP50, WRN levels were not altered in either WCE or in the chromatin fraction. However, when we combined USP50 depletion with 5 mM HU treatment for 3 hours to stall replication forks and induce RS, the amount of WRN in the chromatin fraction was reduced by 50% compared to NTC-treated cells with HU. This result suggests that when cells are experiencing RS, USP50 regulates localisation of WRN to the chromatin and to sites of stress/ damage, through an as yet unknown mechanism. It also suggests that there is a switch in function of USP50 regarding

WRN in untreated versus replicatively stressed cells, or possibly at unstressed versus stressed/stalled forks. The WRNi NSC 617145 has been reported to affect WRN protein levels in two ways: lowering WRN protein levels through protein degradation, and “trapping” WRN on chromatin. We were curious to see how USP50 depletion and WRNi treatment might affect WRN levels at chromatin, so USP50 depletion was combined with 24-hour WRNi treatment at 250 nM. In untreated cells, WRNi treatment alone or in combination with USP50 depletion did not appear to affect the amount of WRN either in whole cell extracts or in chromatin fractions, contrary to previous reports. When combined with a 3-hour treatment of 5 mM HU to induce RS, WRNi treatment restored WRN levels at chromatin in USP50-depleted cells, suggesting that loss of USP50-dependent WRN localisation to stalled forks can be overcome by WRNi treatment. This could be through a mechanism of WRN “trapping” on chromatin as was previously described, and could also imply that USP50 may specifically promote WRN retention or inhibit WRN removal from chromatin.

Given the potential for a switch in USP50 activity upon HU treatment, we decided to delve deeper into the roles of USP50 and WRN at stalled replication forks. We used a variation of the standard DNA fibre assay labelling scheme to specifically look at whether USP50 and WRN affect the ability of replication forks to restart after HU-induced stalling. We saw that USP50 depletion led to a decrease in restarted forks and an increase in stalled forks, indicating that USP50 plays an important role in fork restart after HU-induced stalling. Interestingly, treatment with WRNi did not affect the ability of stalled forks to restart, with or without USP50 depletion. This could imply that WRN helicase activity is not needed for fork restart, contrary to previous reports. We had previously seen that WRN depletion led to a decreased ability of forks to restart, and that this was epistatic with USP50 depletion. Together these data could indicate

that WRN does have roles in fork restart related to USP50, but that helicase activity is not involved in this, thus implicating exonuclease or a non-enzymatic function of WRN in fork restart. As we saw previously, USP50 depletion in combination with HU treatment leads to a loss of WRN at chromatin, but WRNi treatment reverses this and restores WRN at chromatin. Therefore the WRN protein levels at the stalled forks in the USP50-depleted, WRNi-treated cells could be equivalent to endogenous WRN levels. If a non-enzymatic function of WRN is involved in fork restart in USP50-depleted cells, treating with the WRNi may not affect this ability due to antagonising the effects of USP50 depletion on WRN levels. It is interesting to note that co-depletion of USP50 and WRN rescues fork stalling in untreated but not HU-treated cells. This could indicate that while RECQL4 and RECQL5 are able to rescue ongoing fork progression in the absence of USP50 and WRN, they are not able to restart HU-stalled replication forks. This suggests that the ability of RECQL4-RECQL5 to compensate for WRN loss in USP50-depleted cells is limited to ongoing replication only.

When a replication fork encounters an obstacle or is unable to progress, it reverses to form a four-way structure. This is in order to protect nascent DNA from degradation by nucleases such as MRE11 and EXO1, which are capable of long-range resection and could cause loss of genomic material. Fork reversal is regulated by RECQL1, and a number of fork-remodelling proteins are thought to be able to regress replication forks *in vivo*, including SMARCAL1. WRN and BLM are among helicases able to regress model forks in *in vitro* assays. We wondered whether USP50 may influence the ability of forks to reverse in a WRN-dependent or WRN-independent manner, and whether this could explain the defect in fork restart seen previously upon USP50 depletion. To answer this question, we performed another variation of the DNA fibre assay to measure how far replication forks travel during HU treatment. Cells were treated

with siRNA and WRNi, then pulsed with CldU for 30 minutes, then incubated with 5 mM HU and IdU for 3 hours. The length of the IdU tract was compared to the CldU tract length to obtain a ratio, and to internally control for the effect of treatment on fork speed. A decrease in the ratio could indicate that forks stop travelling sooner during an HU block, and an increase in the ratio could indicate that forks are travelling further and not reversing. In untreated cells, the length of the IdU tract was much shorter than the CldU tract despite the pulse being six times longer, indicating that the HU treatment was effective at slowing or stalling replication forks. SMARCAL1 knockdown was used as a positive control, and we observed an increase in the IdU: CldU ratio compared to NTC-treated cells, indicating that forks were travelling further during HU treatment than in untreated cells. When USP50 was depleted, the IdU: CldU ratio increased, and WRN depletion led to a greater increase in IdU: CldU length. This could indicate that when USP50 or WRN is depleted, replication forks were able to travel further during HU treatment, and could indicate that fork reversal was inhibited by loss of these proteins. This could indicate a role for USP50 and WRN in promoting fork reversal during RS. Co-depletion of USP50 and WRN reduced the IdU: CldU ratio to near-untreated levels, implying that in the absence of USP50, WRN activity causes forks to travel further during HU treatment, and vice versa. We know that USP50 depletion during HU treatment causes WRN levels to decrease on chromatin, so the effect could be caused by a lack of adequate WRN levels at the replication fork. When WRNi was added to the cells, the IdU: CldU ratio increased to a similar degree to the WRN depletion condition, suggesting that WRN helicase activity is involved in producing this phenotype. The combination of USP50 depletion and WRN inhibitor treatment did not increase the IdU: CldU ratio beyond that of USP50-depleted cells only. We saw previously that WRNi treatment restored WRN to chromatin when USP50 was depleted, implying that the

effect of the WRNi here was due to inhibition of helicase activity rather than altered protein levels.

3.14 Experimental limitations

DNA fibre assay:

The DNA fibre assay was employed heavily in this chapter to assess how USP50 and WRN affect replication dynamics. Several limitations and drawbacks to the DNA fibre exist. There is innate variability in how the DNA fibres spread, e.g. depending on the angle of the microscope slide during spreading. While this should not affect the analysis of replication structures, it can affect measurement of fork length/ speed. Use of an automated spreading method, such as DNA combing, can help limit the variability between experimental repeats and conditions. Secondly, resolution of the fluorescent signal is poor, meaning that subtle differences of a few hundred base pairs of DNA may not be detected/ measurable (Quinet *et al.*, 2017). This will disproportionately affect shorter fibres, such as when measuring CldU: IdU lengths during HU treatment, where the IdU tract length is significantly shorter than the CldU label, and therefore subject to a higher level of variability. Thirdly, when analysing fork stalling/ restart, careful consideration is needed when deciding which DNA structures to count. Fork stalling can lead to the firing of new replication origins in order to rescue replication, which manifests as an increase in IdU/ green-only labels. Including these structures in the DNA fibre analysis could mask a change in the proportion of other structures. Finally, IdU has been reported to induce DNA damage in cells (C. Li *et al.*, 2024; Rosina *et al.*, 2019), so “endogenous” levels of fork stalling in untreated cells may be affected by cellular sensitivity to IdU.

Specifically regarding the DNA fibre methodologies employed in this chapter, interpretation of the results obtained from the assay is limited because the assay does not inform on why replication forks have stalled. When looking at fork restart after HU treatment, forks were only analysed one hour post-release from HU, providing a snapshot of the number of forks that have/ have not restarted in this time. However, the efficiency of fork restart was not analysed here. Measurement of IdU length of restarted forks would give insight into this. Further, it was not shown whether the forks in USP50- or WRN-depleted cells had delayed or defective restart. A time-course showing level of fork restart after several hours of HU treatment could shed light on whether the forks eventually all restarted, or whether there were stalled forks that were unable to be restarted. When analysing CldU: IdU tract lengths, the data provides only a snapshot of length of the IdU tract in cells during HU treatment. However we do not know whether this is due to slowing of replication during HU treatment, or whether the forks have truly stopped moving. A time-course over several hours could reveal whether forks continue to move after 3 hours of HU treatment, or whether they stop before 3 hours and do not progress any further. However due to poor resolution of the technique, very short fibres are harder to measure accurately, and this could influence the validity of any results seen.

Immunofluorescence:

As mentioned previously, γ -H2AX is a marker of DNA damage and replication stress, so examining γ -H2AX foci in S-phase cells means that both DSBs and replication stress are likely to cause γ -H2AX foci formation (Katsube *et al.*, 2014). The IF experiments in this chapter represent a snapshot of DSBs in the cell, but do not offer information on how USP50 and WRN

depletion/ inhibition affect repair dynamics. A time-course of 53BP1 foci after DNA damage with USP50 or WRN depletion could offer information on how these proteins affect repair dynamics, and therefore whether the increase in 53BP1 and γ -H2AX foci seen in USP50-depleted cells is due to an increase in DSBs or a delay in their repair. In addition, pre-extraction of cells with CSK buffer or similar can reduce nuclear staining while retaining chromatin-bound protein signal, leading to reduced background fluorescence and better distinction of foci.

Clonogenic survival assay:

The clonogenic survival assay offers vital information on the impact of cellular treatments on the ability of cells to form colonies. However, the assay does not provide data on how the cells die, or whether cells that fail to form colonies have died or are senescent.

Western blot:

The Western blot does not provide information on why protein levels are altered. Protein levels are affected by many factors, including protein degradation and changes in transcription.

WRN addback expression system:

Introducing genes with the ability to be inducibly expressed allows the researcher to deplete the endogenous protein, replace it with an altered version of the protein, and examine how this affects cellular phenotypes. In this chapter, we introduced variants of the WRN gene into

FlpIn™ cells assess how loss of WRN enzymatic functions affect fork stalling. However, a drawback to the assay is that expression level of the protein cannot generally be controlled, and overexpression of a protein compared to endogenous expression can lead to unexpected phenotypes. It is possible to screen individual clones to find one with comparable expression of the exogenous gene, but this takes extra work and time.

3.15 Future experiments

Given the uncovering of a USP50-WRN-RECQL4-RECQL5 axis in replication, we would be interested to conduct further experiments to learn more about how the RECQ helicases are able to compensate for each other, and how USP50 regulates this process.

- 1) Does rescue of fork stalling with USP50 depletion and WRN inhibition depend on RECQL4/ RECQL5?

We have shown that USP50 and WRN co-depletion or inhibition rescues the increase in fork stalling seen with either condition alone (figure 3.5c, h). RECQL4 and RECQL5 appear to be responsible for this rescue when WRN is depleted, but we don't know if they are capable of restoring replication when WRN is inhibited. To test this, we would repeat the DNA fibre assay to look at levels of stalled forks with USP50 depletion and WRNi treatment, with additional knockdown of RECQL4 or RECQL5.

- 2) Does rescue of fork stalling when USP50 and WRN are co-depleted depend on co-operation of RECQL4 and RECQL5?

We saw previously (figure 3.12e, f) that when USP50 and WRN are co-depleted, the reduction in fork stalling can be reversed by depleting RECQL4 or RECQL5. This suggests that both may be required to rescue fork progression in cells co-depleted of USP50 and WRN. To test this, we would repeat the DNA fibre assay with USP50, WRN, RECQL4 and RECQL5 co-depletion. We would expect the fork stalling levels to remain increased, indicating that RECQL4 and RECQL5 co-operate together to rescue fork progression in the absence of USP50 and WRN.

- 3) Does rescue of fork stalling with USP50 and WRN co-depletion depend on RECQL4/RECQL5 helicase activity?

It would be interesting to see whether the helicase activity of RECQL4 or RECQL5 is required for the rescue in fork progression seen with USP50 and WRN co-depletion (figure 3.12e and f). To test this, we could generate constructs of the RECQL4 and RECQL5 genes with mutations in the ATPase/ helicase domain to eliminate helicase function. RECQL4 helicase function can be abolished by mutating K508 to a methionine (Rossi *et al.*, 2010), and RECQL5 can be rendered helicase-dead through substitution of K58 to an arginine residue (Garcia *et al.*, 2004). Repeating the DNA fibre assay in stable cell lines expressing inducible RECQL4 or RECQL5 constructs would provide insights into the importance of the helicase activities of these proteins in the USP50-WRN-RECQL4-RECQL5 axis.

4) Do RECQL4/ RECQL5 rescue DSB formation in USP50- and WRN-depleted cells?

We wonder whether RECQL4 and RECQL5 can also suppress DSB formation when USP50 and WRN are depleted. We would use IF to examine levels of DSB markers in cells depleted of USP50, WRN and RECQL4/ 5.

5) Does USP50 depletion affect RECQL4/ RECQL5 localisation to chromatin?

We previously used chromatin fractionation to determine that USP50 promotes WRN localisation/ retention to chromatin after HU treatment (figure 3.9c). It would be interesting to test whether USP50 also regulates the localisation of RECQL4 and RECQL5 to chromatin, and whether this is further affected by WRN co-depletion. We would repeat the chromatin fractionation protocol on cells depleted of USP50 and WRN, with and without HU treatment, and probe for RECQL4 and RECQL5.

6) Can the effects of USP50 depletion be phenocopied by partial loss of WRN?

As previously shown, USP50 depletion leads to a reduction in WRN on chromatin after HU treatment (figure 3.9c). This could suggest that USP50 is required for WRN to localise to stalled forks. We wonder whether the cellular effects of USP50 loss could be phenocopied by partial depletion, but not complete loss, of WRN. To test this, we would titrate siRNA targeting WRN into cells to identify a concentration of siRNA that results in a 50% loss of WRN. We would then examine how this level of WRN depletion affects fork stalling, fork restart and DSB formation using the DNA fibre assay and IF.

7) Can the effects of USP50 depletion be rescued by overexpression of RECQL4/ RECQL5?

We saw previously that overexpression of wild-type WRN rescued fork stalling in USP50-depleted cells (figure 3.6d). We therefore hypothesise that the effects of loss of USP50 are due to partial loss of WRN, and that complete loss of WRN allows RECQL4 and RECQL5 to rescue fork progression. We wonder whether combining USP50 depletion with RECQL4 and RECQL5 overexpression would rescue fork stalling by promoting RECQL4/ RECQL5-dependent fork progression. We would perform the DNA fibre assay in cells depleted of USP50, inducibly overexpress RECQL4 and RECQL5, and examine levels of stalled forks.

4 USP50 and WRN in replication in MSS vs MSI cells

4.1 Introduction

The concept of synthetic lethality describes the phenomenon where the mutation or alteration of two genes leads to cell death, but either mutation/ alteration alone can be tolerated (Topatana *et al.*, 2020). Cancers by nature carry mutations and can be highly prone to acquiring further alterations. WRN loss was recently discovered to be a synthetic lethal target in a subset of cancers with MMR pathway mutation and subsequent high levels of MSI. Microsatellites are short, repetitive sequences of DNA, with the repeating unit being between one and six nucleotides long (Garrido-Ramos, 2017), and represent around 3% of the human genome (Eckert & Hile, 2009). Microsatellites are present in every chromosome, are distributed non-randomly and have roles in gene expression (Vieira *et al.*, 2016). Microsatellite length is intrinsically hypermutable as the replication machinery can slip at highly repetitive regions, leading to over- or under-replication of microsatellite repeats (Hughes & Queller, 1993; Martín-López & Fishel, 2013). The resulting unpaired nucleotides form extrahelical loops which are detected and corrected by the MMR pathway (Martín-López & Fishel, 2013). In the absence of a functional MMR pathway through mutation or inactivation of MLH1, MLH3, MSH2, MSH3, MSH6 or PMS2, the indel is maintained, leading to a change in the microsatellite length (Pećina-Šlaus *et al.*, 2020). Over many cell cycles, the microsatellites can expand or contract dramatically (known as MSI-high). The WRN-MSI synthetic lethality arises due to expansion of TA microsatellite repeats specifically (van Wietmarschen *et al.*, 2020). It is thought that when TA repeats are long enough, the DNA forms a secondary structure known as cruciform DNA.

When MSI-high cells with expanded TA repeats lose WRN helicase activity, DSBs form at TA repeats and chromosome shattering occurs, leading to cell death (van Wietmarschen *et al.*, 2020). It is therefore hypothesised that WRN helicase is required to unwind the cruciform structures to allow replication to proceed, and the failure to do so leads to replication fork stalling, DSB formation and subsequent cell death.

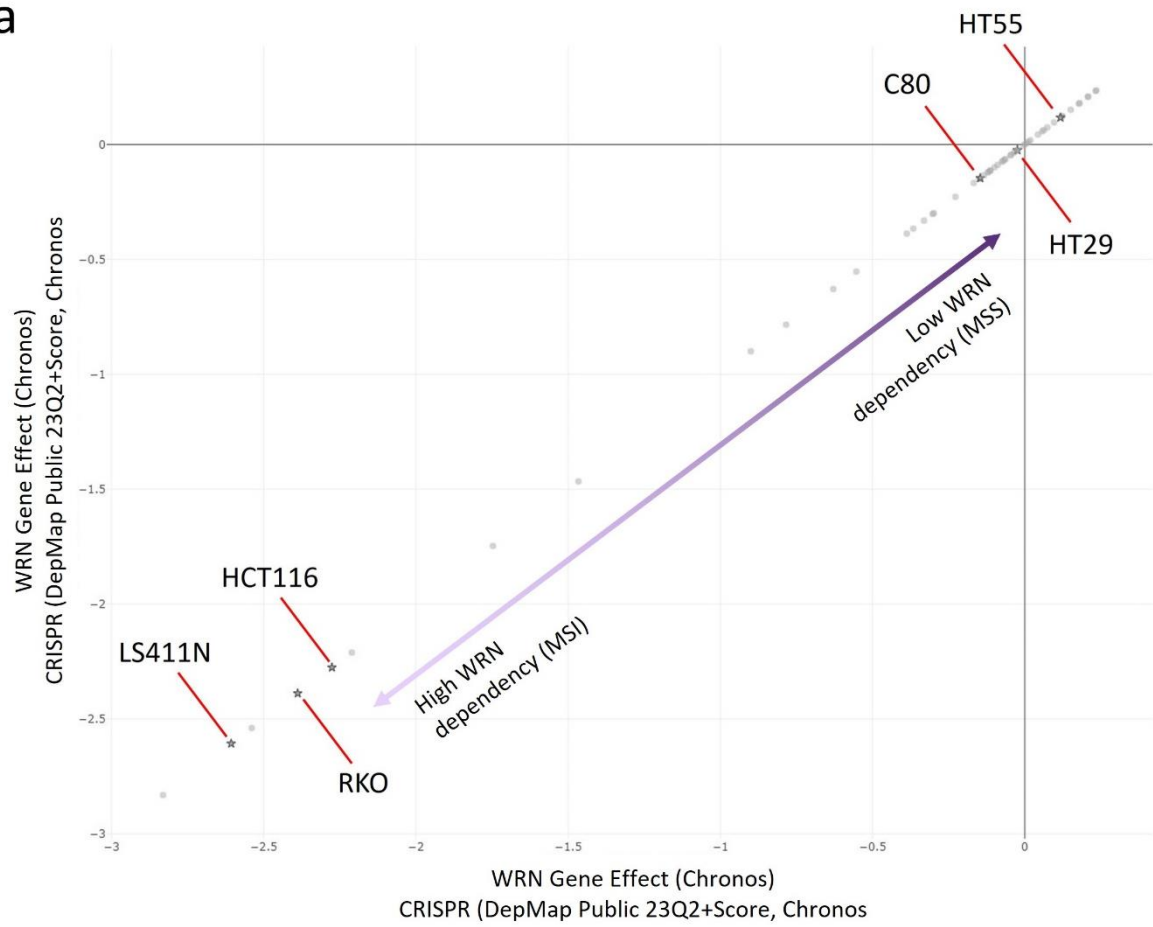
We had previously seen that USP50 and WRN have a close relationship in promoting replication fork progression and preventing DSBs during replication in HeLa cells, which are microsatellite stable (MSS) and of cervical origin. We wanted to investigate whether USP50 behaves differently in cells with high MSI, and how cellular WRN dependency could affect the USP50-WRN axis. MSI has been found in many cancer types, and is particularly common in colorectal, gastric and ovarian cancers, representing around 15% of all colorectal cancers (Kim *et al.*, 2013). Lynch syndrome is a disease caused by mutations in the MMR pathway, and patients have a high lifetime risk of developing colorectal cancer (Dominguez-Valentin *et al.*, 2020; Niv, 2007). We therefore selected a panel of colorectal cancer cell lines with MSS or MSI-high to examine the roles of USP50 and WRN in cells with a background of WRN dependency.

4.2 Optimisation of siRNA transfection in a panel of colorectal cancer cell lines with and without WRN dependency

We wanted to use a panel of cancer cell lines to study the USP50-WRN axis in the context of WRN dependency. We utilised data from the Cancer Dependency Map (depmap.org/portal/) to assess WRN dependency in colorectal cancer cell lines, as MMR deficiency and microsatellite instability is common in cancers of the gastric system. Six colorectal cancer cell lines were chosen, three with a high dependency on WRN (HCT116, RKO and LS411N [MSI]), and three with low WRN dependency (HT29, HT55 and C80 [MSS]) (figure 4.1a).

Cell lines vary in transfection efficiency, so we tested the efficacy of siRNA-mediated WRN depletion in the cell line panel. The aim was to obtain a comparable level of protein knockdown in each cell line, to allow better comparison of data between cell lines. To achieve this, cells were plated and treated with increasing concentrations of siRNA targeting WRN for 72 hours before cells were harvested. Lysates were analysed by Western blot to assess WRN protein levels (figure 4.1b). We observed that individual cell lines needed different concentrations of siRNA to achieve a consistent and effective level of protein reduction across the cell line panel.

a



b

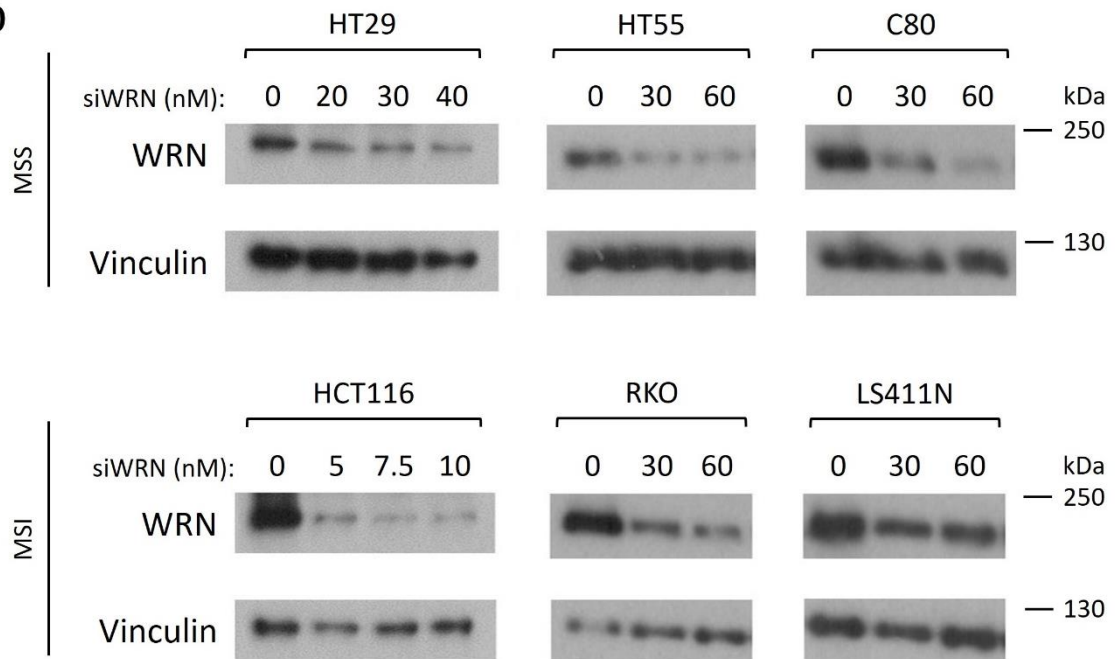


Figure 4.1

a) DepMap data was analysed for WRN dependency in colorectal cancer cell lines. Relevant cell lines are highlighted.

b) Western blot showing WRN protein levels after 72 hours of treatment with siRNA targeting WRN in colorectal cancer cell lines. Transfection control was with siRNA targeting Luciferase.

4.3 WRN-dependent MSI cells are not hypersensitive to USP50 depletion compared to MSS cells

Analysis of DepMap data suggested that the cell lines in our panel consisted of three highly WRN-dependent MSI cell lines, and three MSS cell lines with low or no WRN dependency. Given the previously characterised relationship between USP50 and WRN, we wondered whether cell lines dependent on WRN for survival were also selectively sensitive to USP50 depletion. To test this, cells were plated out and treated with siRNA targeting USP50 and WRN for 48 hours, then plated out at low density and incubated for 7-14 days to grow into colonies. We saw that USP50 depletion led to a similar level of cell death in MSS cell lines (3.9 - 25.5%) compared to MSI cell lines (18.0 - 25.7%) (figure 4.2a). In cells depleted of WRN, we saw that MSI cells exhibited higher levels of cell death (89.8 - 90.8%) compared to MSS cells (19.4 - 37.6%), confirming the DepMap data and previous findings (Chan *et al.*, 2019; Kategaya *et al.*, 2019; Lieb *et al.*, 2019). When USP50 and WRN were co-depleted, there was no appreciable difference in impact on survival between MSS and MSI cell lines. HT29 (MSS) cells and RKO (MSI) cells both showed a trend towards increased survival with USP50 and WRN co-depletion compared to WRN depletion alone, though this was not statistically significant.

LS411N cells are not compatible with the clonogenic survival assay due to their growth characteristics. To assess cell viability in this cell line, and to confirm the results using the clonogenic survival assay in the other cell lines, cell viability was assessed using the alamarBlue assay. As before, cells were plated out and treated with siRNA targeting USP50 and WRN for 48 hours before cells were plated at a low density and incubated for 7-14 days. Cell viability was measured by incubating cells with alamarBlue and measuring fluorescence as a readout

of cell viability. As before, USP50 depletion did not lead to loss of viability in MSI cells compared to MSS cells (figure 4.2b). WRN depletion led to a significant reduction in cell viability in the MSI cell lines HCT116 and RKO as seen before, but LS411N (MSI) cells did not appear to be sensitive to WRN depletion, in contrast with DepMap data and previous findings (Hao *et al.*, 2022).

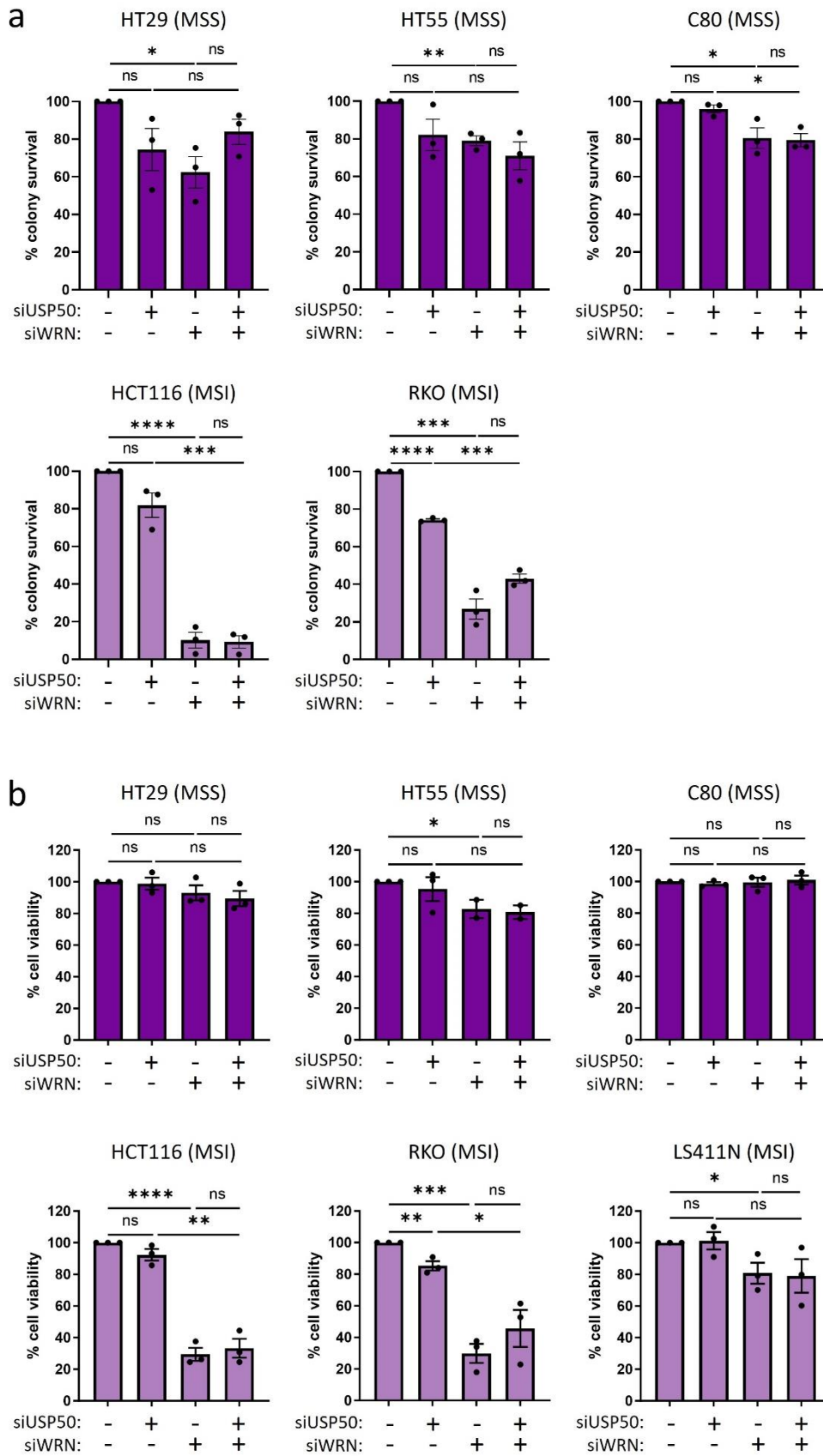


Figure 4.2

a) Cell survival was measured using the clonogenic survival assay and crystal violet staining. Colorectal cancer cells were treated for 72 hours with siRNA targeting USP50 and WRN. Transfection control was with siRNA targeting Luciferase. Results are from 3 independent repeats. Bars indicate the mean, error bars are SEM. Statistical analysis done with unpaired two-tailed t-test; ns= not significant, *= $p \leq 0.05$, ** = $p \leq 0.01$, *** = $p \leq 0.001$, **** = $p \leq 0.0001$.

b) Cell viability was measured using the alamarBlue viability assay. Colorectal cancer cells were treated for 72 hours with siRNA targeting USP50 and WRN. Transfection control was with siRNA targeting Luciferase. Results are from 3 independent repeats. Bars indicate the mean, error bars are SEM. Statistical analysis done with unpaired two-tailed t-test; ns= not significant, *= $p \leq 0.05$, ** = $p \leq 0.01$, *** = $p \leq 0.001$, **** = $p \leq 0.0001$.

4.4 Co-depletion of USP50 and WRN does not rescue fork stalling in MSI cells

Previous data from HeLa cells, which are MSS, suggested that co-depletion of USP50 and WRN led to a decrease in stalled forks compared to either depletion alone (figure 3.5c). We were curious to see whether USP50 and WRN would affect fork stalling differently in MSS vs MSI cells. The DNA fibre assay was used to assess fork stalling in MSS and MSI cells treated with siRNA targeting USP50 and WRN for 72 hours before incubation with CldU and IdU for 20 minutes each (figure 4.3a). In all six cell lines tested, USP50 depletion led to an increase in 1st label terminations, as did WRN depletion (figure 4.3b). We expected to see a higher level of fork stalling in WRN-depleted MSI cells compared to MSS cells, due to the hypothesis that WRN depletion leads to fork stalling and DSBs at (TA)_n repeats. Surprisingly, WRN depletion in the MSI cells led to a comparable increase in the level of stalled forks (65.2 – 89.3% increase) to MSS cells (49.2 – 114% increase). In the three MSS cell lines, co-depletion of USP50 and WRN led to a reduction in stalled forks comparable to levels in untreated cells, similar to the results seen in HeLa cells. In contrast, in the three MSI cell lines, co-depletion of USP50 and WRN did not reduce stalled fork numbers. This suggests that the USP50-WRN axis is different in MSS vs MSI cells.

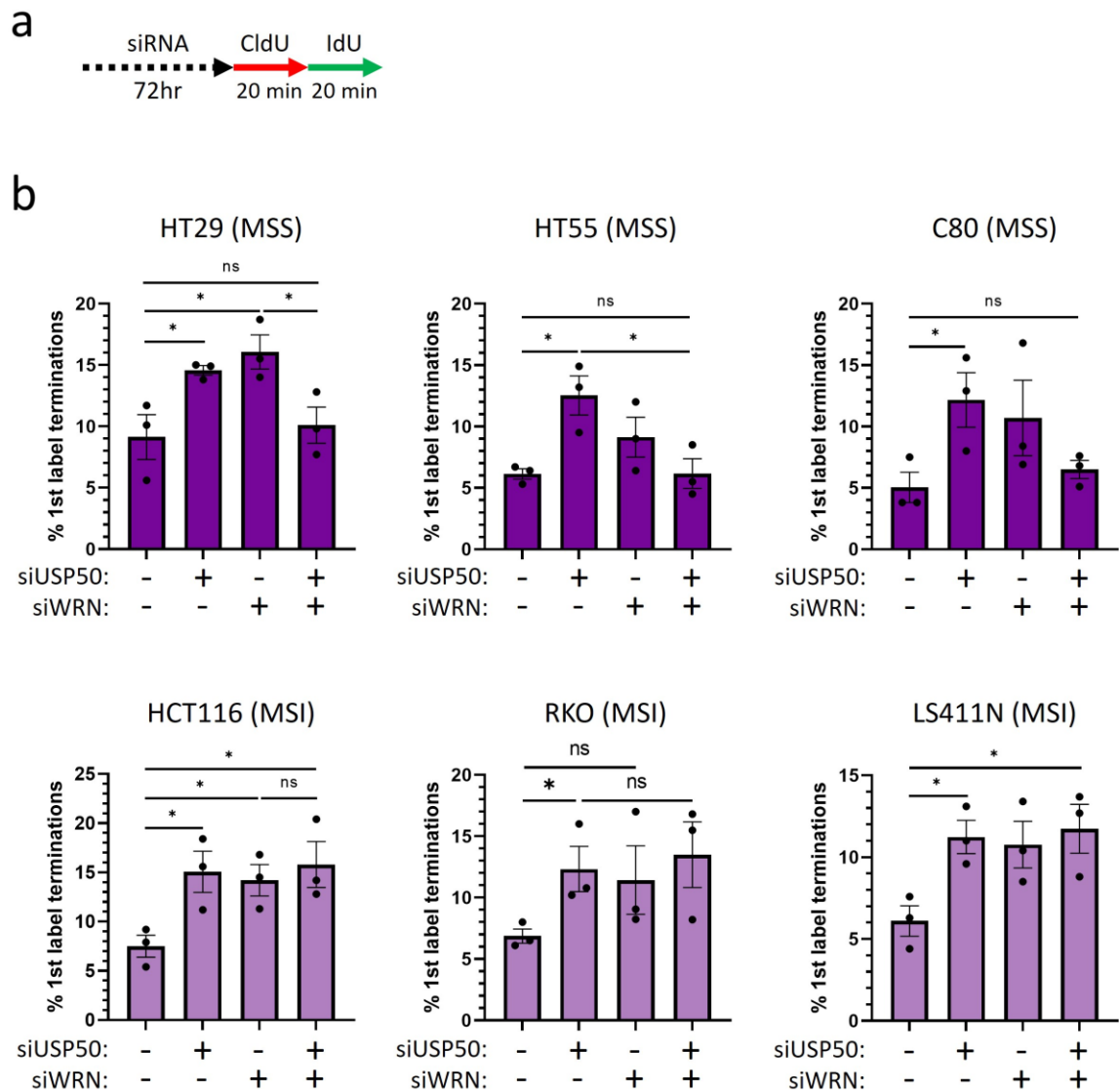


Figure 4.3

a) Schematic of the DNA fibre assay. Colorectal cancer cells were treated with siRNA targeting USP50 and WRN for 72 hours before incubation with CldU and IdU for 20 minutes each.

b) 1st label terminations were examined using the DNA fibre assay in colorectal cancer cells treated with siRNA targeting USP50 and WRN. Transfection control was with siRNA targeting Luciferase. Results are from 3 independent repeats, with n >200 fibres per condition, per repeat. Bars indicate the mean,

error bars are SEM. Statistical analysis done with unpaired two-tailed *t*-test; ns= not significant, *=
 $p \leq 0.05$.

4.5 Depletion of USP50 combined with WRN helicase inhibition does not rescue fork stalling in MSI cells

MSI cells are dependent on the helicase function of WRN specifically, as complementing WRN-depleted MSI cells with helicase-dead WRN fails to rescue cell death (Chan *et al.*, 2019; Kategaya *et al.*, 2019; Lieb *et al.*, 2019). We were curious to see whether the microsatellite status of the cells would influence fork stalling after WRN helicase inhibition. HT29 (MSS) cells and HCT116 (MSI) cells were plated out and treated with siRNA targeting USP50 and 250 nM WRNi for 72 hours, then incubated with CldU and IdU for 20 minutes each (figure 4.4a). Analysis of stalled forks revealed that WRNi treatment alone led to an increase in stalled forks in both cell lines to a similar degree (figure 4.4b). In the MSS cell line HT29, the combination of USP50 depletion and WRNi led to a trend towards a reduction in stalled forks compared to either condition alone, though was not statistically significant. In the MSI cell line HCT116, the combination of USP50 depletion and WRNi treatment did not reduce the levels of stalled forks, suggesting that the microsatellite status of the cell influences fork stalling in response to disruption of the USP50-WRN axis through WRN inhibition.

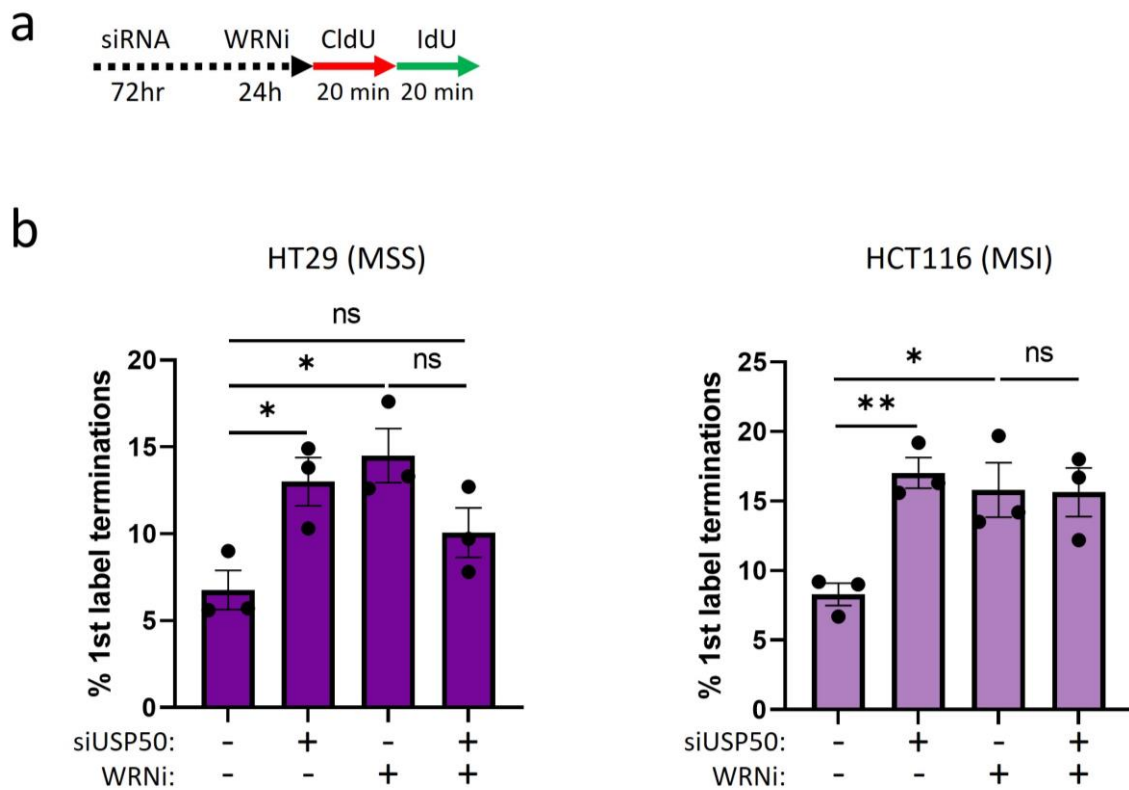


Figure 4.4

a) Schematic of the DNA fibre assay. Colorectal cancer cells were treated with siRNA targeting USP50 and 250 nM WRNi before incubation with CldU and IdU for 20 minutes each.

b) 1st label terminations were examined using the DNA fibre assay in colorectal cancer cells treated with siRNA targeting USP50 and 250 nM WRNi. Transfection control was with siRNA targeting Luciferase. Control cells were treated with vehicle (DMSO). Results are from 3 independent repeats, with $n > 200$ fibres per condition, per repeat. Bars indicate the mean, error bars are SEM. Statistical analysis done with unpaired two-tailed t-test; ns= not significant, *= $p \leq 0.05$, **= $p \leq 0.01$.

4.6 WRN depletion inhibits fork restart more severely in MSI vs MSS cells

WRN has known roles in restarting stalled forks, as previously described. We saw before that USP50 and WRN were epistatic in promoting fork restart in HeLa cells (figure 3.10b). Given the surprising observation that WRN depletion or inhibition led to comparable levels of fork stalling in MSS vs MSI cells, we wondered whether WRN depletion may instead lead to a pronounced fork restart defect in MSI cells. HT29 (MSS) and HCT116 (MSI) cells were treated with siRNA targeting USP50 and WRN for 72 hours, then incubated with CldU for 30 minutes, 5 mM HU for 3 hours, and IdU for one hour to allow time for stalled forks to restart (figure 4.5a). Analysis of restarted and stalled forks indicated that USP50 depletion led to an increase in stalled forks in both cell lines (55.1% in HT29, 31.5% in HCT116) (figure 4.5b). When WRN was depleted, both cell lines showed an increase in stalled forks, but the increase was higher in the HCT116 MSI cell line (52.0% in HT29 vs 67.3% in HCT116). In both cell lines, the combination of USP50 and WRN depletion did not lead to a further increase in stalled forks, suggesting that USP50 and WRN are epistatic in fork restart in both cell lines.

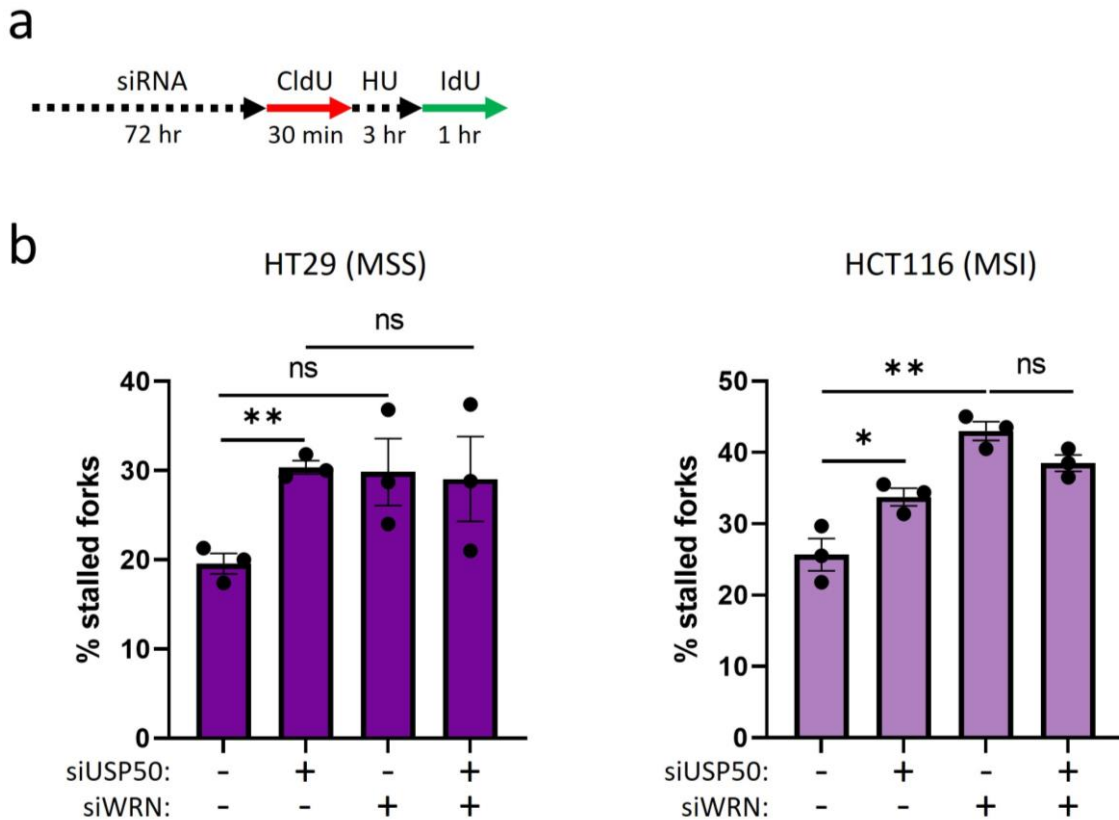


Figure 4.5

a) Schematic of the DNA fibre assay. Colorectal cancer cells were treated with siRNA targeting USP50 and WRN for 72 hours before incubation with CldU, HU and IdU.

b) Stalled forks were examined using the DNA fibre assay in colorectal cancer cells treated with siRNA targeting USP50 and WRN. Transfection control was with siRNA targeting Luciferase. Results are from 3 independent repeats, with $n > 200$ fibres per condition, per repeat. Bars indicate the mean, error bars are SEM. Statistical analysis done with unpaired two-tailed t-test; ns= not significant, $*$ = $p \leq 0.05$, $**$ = $p \leq 0.01$.

4.7 Co-depletion of USP50 and WRN affects fork progression during HU treatment differently in MSS vs MSI cells

Fork reversal is critical in protecting replication forks and allowing them to restart. Given the fork restart defect in HCT116 (MSI) cells when depleted of WRN, we wondered how USP50 and WRN might affect fork progression during HU incubation. We used a modified version of the DNA fibre assay, where HT29 (MSS) and HCT116 (MSI) cells were plated and treated with siRNA targeting USP50 and WRN for 72 hours. Cells were then incubated with CldU for 30 minutes, then 5 mM HU and IdU together for 3 hours (figure 4.6a). The length of the IdU tract was compared to the CldU tract to control for any effects on fork speed. SMARCAL1 knockdown was used as a positive control. We saw that depletion of SMARCAL1, which catalyses fork reversal, led to an increase in IdU: CldU ratio in both cell lines, indicating that forks were travelling further during HU block, possibly due to fork reversal being inhibited (figure 4.6b). When USP50 was depleted, the IdU: CldU ratio increased in HT29 (MSS) cells (0.21 to 0.24), but did not change in HCT116 (MSI) cells (figure 4.6c). WRN depletion led to an increase in the IdU: CldU ratio in HT29 (MSS) cells (0.21 to 0.25), but did affect HCT116 (MSI) cells. When USP50 and WRN were co-depleted, the IdU: CldU ratio was comparable to that of untreated cells in HT29 (MSS) cells, but led to an increase in HCT116 (MSI) cells (0.24 to 0.29). This indicates that USP50 and WRN affect the ability of replication forks to progress differently in the two cell lines, when depleted alone and together.

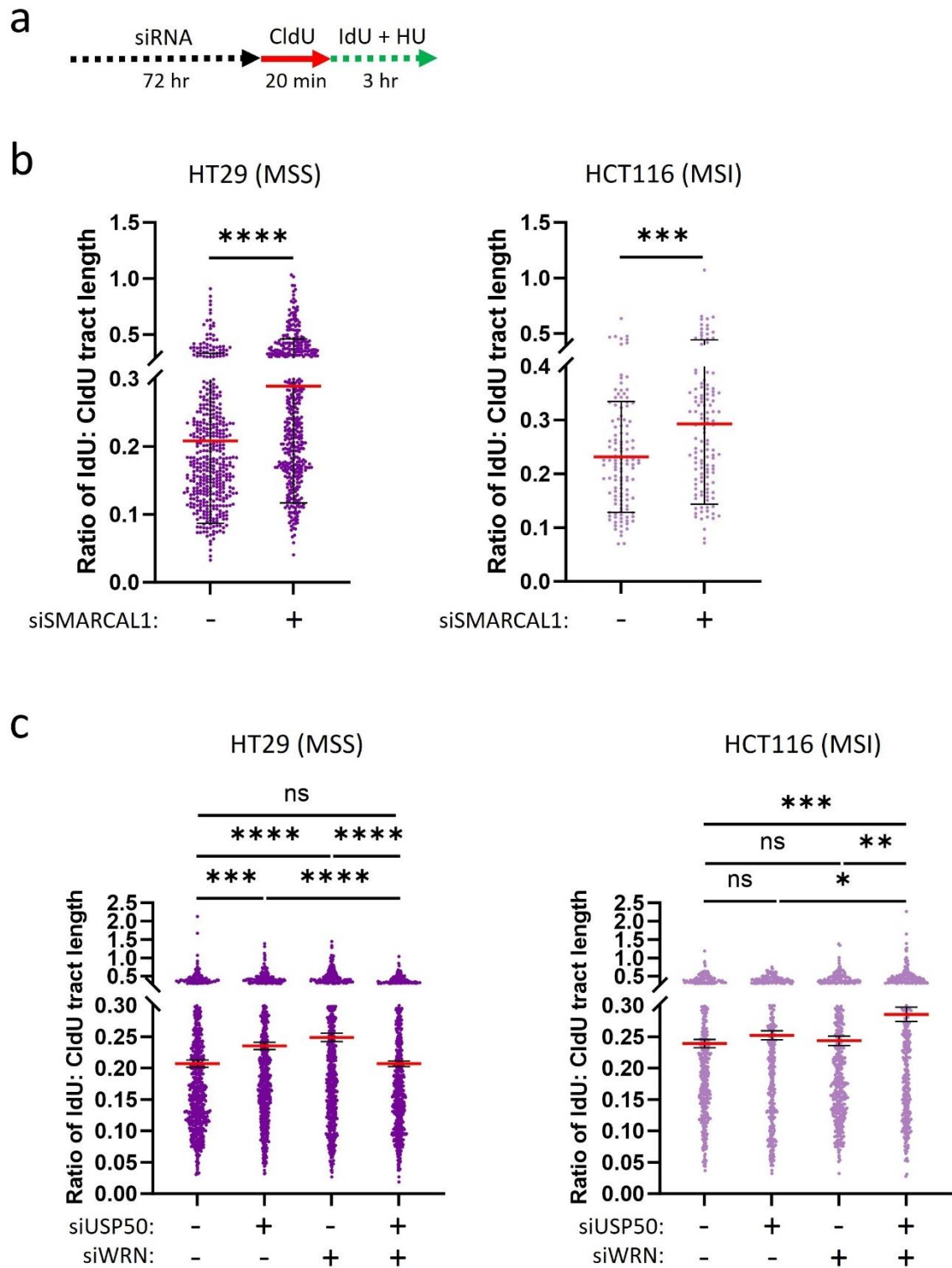


Figure 4.6

a) Schematic of the DNA fibre assay. Colorectal cancer cells were treated with siRNA targeting USP50 and WRN for 72 hours before incubation with CldU, IdU and HU.

b) IdU: CldU lengths were examined using the DNA fibre assay in colorectal cancer cells treated with siRNA targeting SMARCA1. Transfection control was with siRNA targeting Luciferase. Results are from 2 independent repeats, with $n > 100$ fibres per condition, per repeat. Red lines indicate the mean, error bars are SEM. Statistical analysis done with unpaired two-tailed t-test; ns= not significant, *= $p \leq 0.05$, **= $p \leq 0.01$, ***= $p \leq 0.001$, ****= $p \leq 0.0001$.

c) IdU: CldU lengths were examined using the DNA fibre assay in colorectal cancer cells treated with siRNA targeting USP50 and WRN, and 250 nM WRNi. Transfection control was with siRNA targeting Luciferase. Control cells were treated with vehicle (DMSO). Results are from 3 independent repeats, with $n > 100$ fibres per condition, per repeat. Red lines indicate the mean, error bars are SEM. Statistical analysis done with unpaired two-tailed t-test; ns= not significant, *= $p \leq 0.05$, **= $p \leq 0.01$, ***= $p \leq 0.001$, ****= $p \leq 0.0001$.

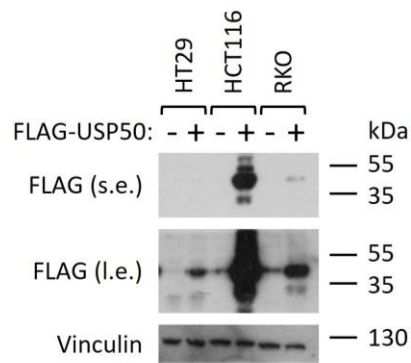
4.8 MSI cells are sensitive to USP50 overexpression

We previously saw that USP50 and WRN co-depletion affected cell survival/ viability differently across the colorectal cancer cell line panel, independent of microsatellite status (figure 4.3a, b). In HT29 (MSS) and RKO (MSI) cells, we saw that depleting USP50 improved cell survival slightly in WRN-depleted cells. Analysis of immunohistochemistry data on proteomicsatlas.org suggests that in liver, testicular, renal and urothelial cancers, medium to high expression of USP50 is observed, though the data is considered unreliable due to poor correlation with RNA transcript data. We wondered how overexpression of USP50 would affect cell survival in a panel of colorectal cancer cells and whether it would reverse the phenotype seen. To test this, cells were plated and treated with siRNA targeting WRN, and transfected with a plasmid encoding FLAG-USP50 (wild-type) to induce transient expression of USP50. After 48 hours, cells were plated out at a low density and incubated for 7-12 days to grow into colonies from single cells. Western blotting was performed from samples harvested 72 hours after transfection to assess protein levels, and showed detectable expression of FLAG-USP50 in each cell line, with HCT116 displaying a relatively higher level of overexpression (figure 4.7a). Overexpression of USP50 led to 13% cell death (though not statistically significant) in HT29 (MSS) cells, 22% cell death in HCT116 (MSI) cells, and 46% cell death in RKO (MSI) cells (figure 4.7b). As seen before, WRN depletion led to considerable cell death in the MSI cell lines (>90%) compared to MSS cells. Depletion of WRN and overexpression of USP50 did not affect cell survival in HT29 (MSS) cells.

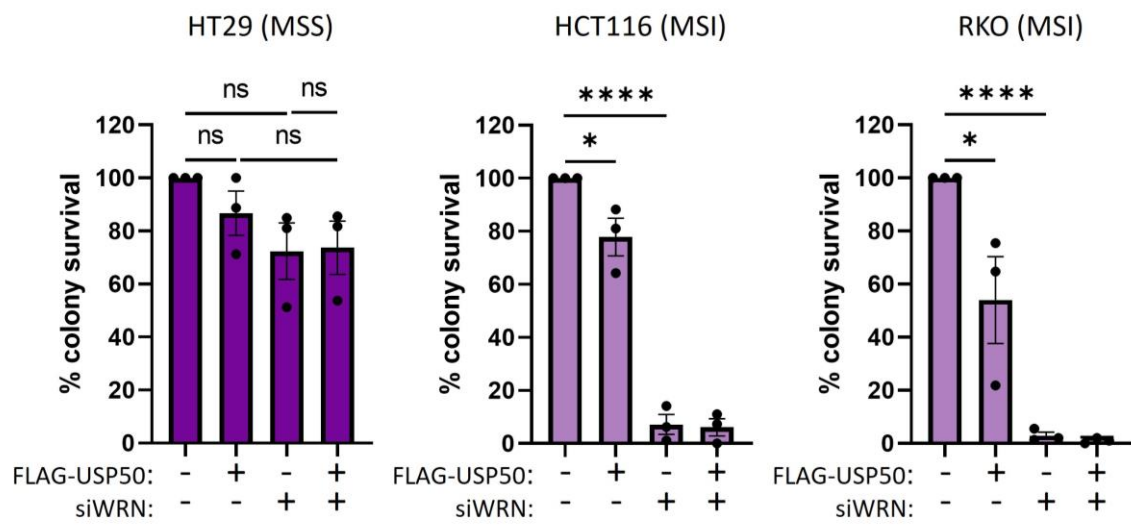
Due to the high level of cell death in WRN-depleted MSI cells, it was difficult to discern subtle differences in cell survival with USP50 overexpression, so a higher number of cells were plated

out to assess impact on cell survival (figure 4.7c). In HCT116 (MSI) cells, the combination of USP50 overexpression and WRN depletion did not cause a further increase in cell death compared to WRN depletion alone. In contrast, in RKO (MSI) cells the overexpression of USP50 led to further cell death in WRN-depleted cells. Together, these results indicate that USP50 overexpression leads to cell death in all three cell lines tested, highlighting the need for this lowly-expressed protein to be regulated at the protein level to avoid toxic effects. The two MSI cell lines, particularly RKO cells, exhibited increased cell death after USP50 overexpression compared to the MSS HT29 cells, perhaps suggesting that higher USP50 protein expression is especially toxic in MSI cells. RKO cells experienced increased cell death with USP50 overexpression than with depletion, suggesting that excessive USP50 activity or presence causes worse outcomes than loss of the protein. Having previously seen a mild rescue in cell survival in HT29 (MSS) and RKO (MSI) cells, we saw that this effect was reversed upon overexpression of USP50, strengthening the previous findings.

a



b



c

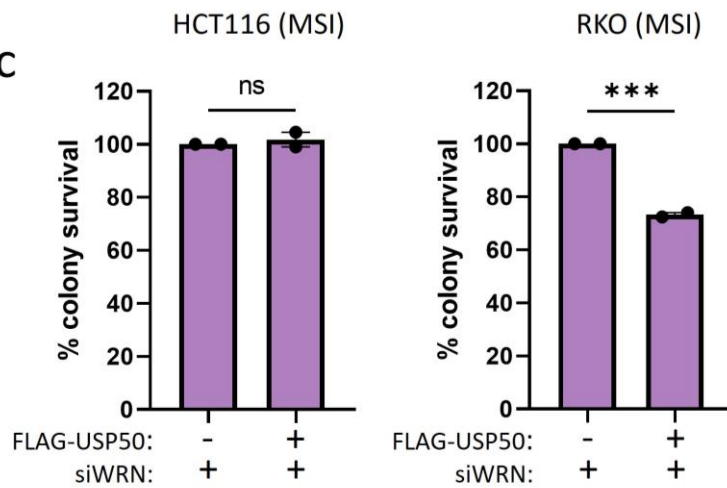


Figure 4.7

a) Western blot showing FLAG-USP50 protein levels 72 hours after transfection with FLAG-USP50 plasmid in colorectal cancer cells. USP50 expression was induced by plasmid transfection; control cells were transfected with empty plasmid. s.e.= short exposure, l.e.= long exposure.

b) Cell survival was measured using the clonogenic survival assay. Colorectal cancer cells were transfected with FLAG-USP50 plasmid and treated with siRNA targeting WRN for 72 hours. USP50 expression was induced by plasmid transfection; control cells were transfected with empty plasmid. Transfection control was with siRNA targeting Luciferase. Results are from 3 independent repeats. Bars indicate the mean, error bars are SEM. Statistical analysis done with unpaired two-tailed t-test; ns= not significant, *= $p \leq 0.05$, ***= $p \leq 0.001$, ****= $p \leq 0.0001$.

c) Cell survival was measured using the clonogenic survival assay. Colorectal cancer cells were transfected with FLAG-USP50 plasmid and treated with siRNA targeting WRN for 72 hours. USP50 expression was induced by plasmid transfection; control cells were transfected with empty plasmid. Transfection control was with siRNA targeting Luciferase. Results are from 3 independent repeats. Bars indicate the mean, error bars are SEM. Statistical analysis done with unpaired two-tailed t-test; ns= not significant, ***= $p \leq 0.001$.

4.9 MSI cells are not hypersensitive to WRN helicase inhibition compared to MSS cells

It has previously been shown that losing the helicase function of WRN led to induction of DSBs, chromosome shattering and cell death in MSI cell lines (Chan *et al.*, 2019; Kategaya *et al.*, 2019; Lieb *et al.*, 2019). Targeting WRN helicase activity in MSI cancers could therefore be of therapeutic interest. Given the availability of a WRN helicase inhibitor, we wondered whether our panel of MSI cells were hypersensitive to WRNi treatment, and whether this could be a potential therapeutic for the treatment of MSI cancers. To test this, MSS and MSI cells were plated out and treated with increasing doses of WRNi for 72 hours, then left to grow until untreated cells were near confluency (figure 4.8a). Cell viability was measured using the alamarBlue assay. Surprisingly, there was no discernible difference in cell viability between MSS and MSI cells at the doses of WRNi tested.

We thought it possible that a 72-hour treatment with the WRNi was not long enough to see hypersensitivity in the MSI cell lines. WRN knockdown led to significant cell death in HCT116 and RKO (both MSI) cell lines, but it is unclear how long the depletion of WRN persists in these cells. It is possible that WRN loss/ inhibition needs several cell cycles to start inducing irreversible cell death in MSI cells. To test this hypothesis, cells were plated and treated with increasing doses of WRNi for 7 days, and cell viability was measured through the alamarBlue assay or staining with crystal violet. HeLa and Capan-1 cells were included to allow comparison between cell of non-colorectal origin. To our surprise, we again saw no hypersensitivity in the MSI cells to WRNi treatment compared to MSS cells (figure 4.8b). Together, these results show that while WRN depletion or genetic loss of helicase function leads to increased cell death in MSI vs MSS cells, inhibition of helicase function with NSC 617145 does not.

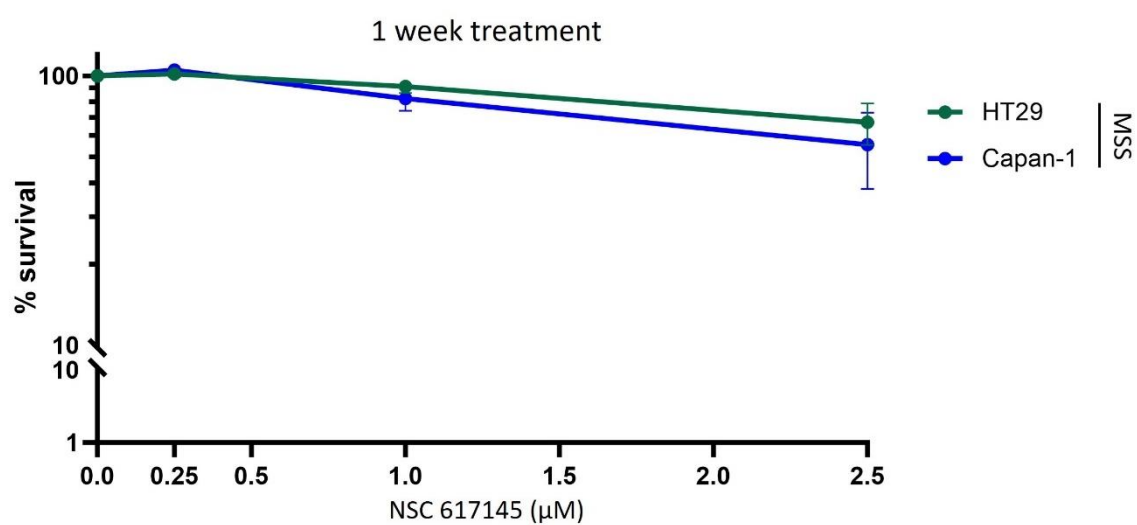
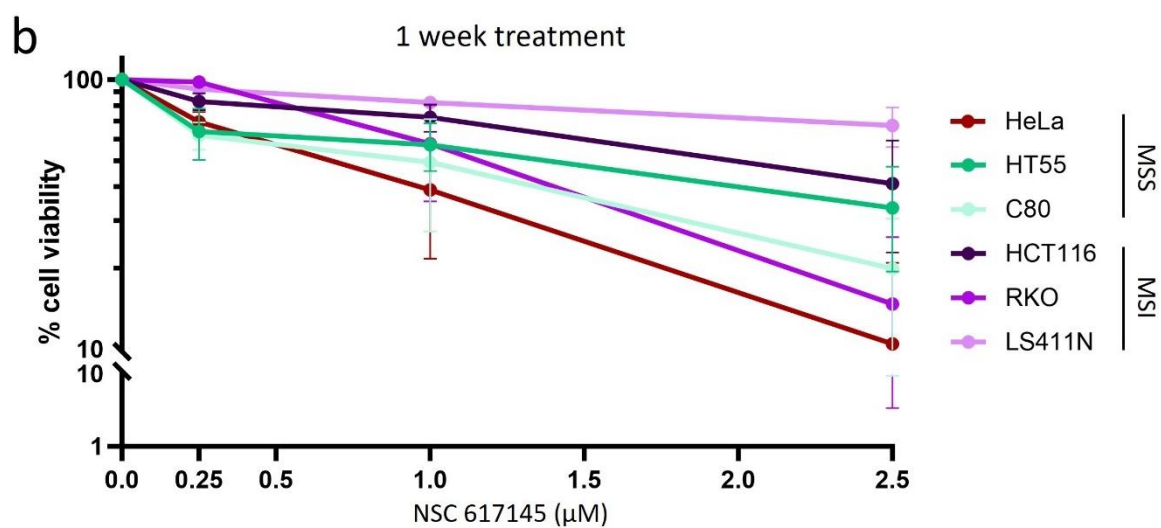
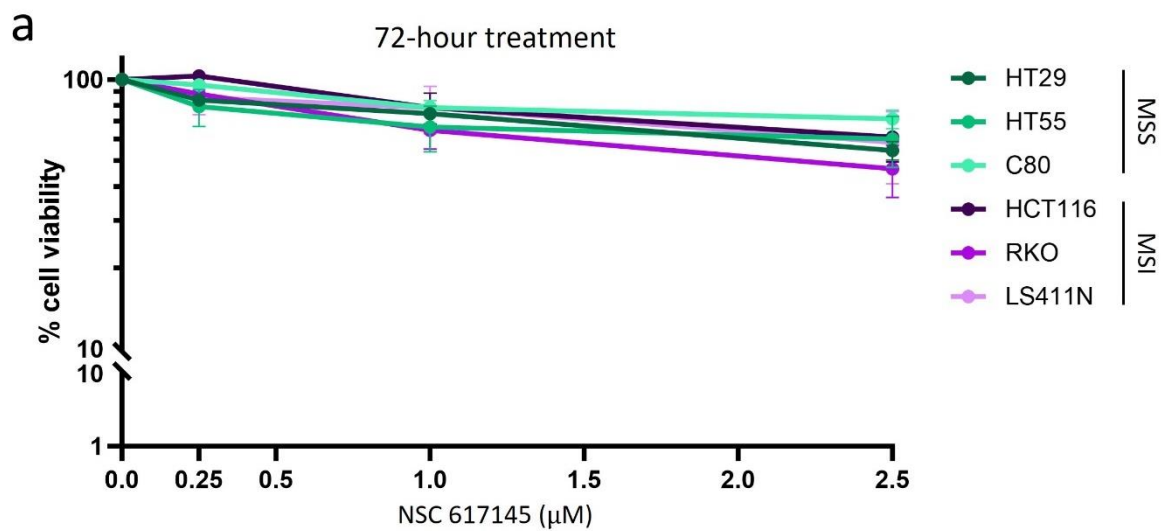


Figure 4.8

a) Cell viability was measured using alamarBlue. Colorectal cancer cells were treated with increasing concentrations of NSC 617145 for 72 hours. Control cells were treated with vehicle (DMSO). Results are from 3 independent repeats. Dots indicate the mean, error bars are SEM.

b) Cell viability was measured using alamarBlue (top graph), and cell survival was measured using crystal violet staining (bottom graph). Colorectal cancer cells, HeLa and Capan-1 cells were treated with increasing concentrations of NSC 617145 for 7 days. Control cells were treated with vehicle (DMSO). Results are from 3 independent repeats. Dots indicate the mean, error bars are SEM.

4.10 WRN depletion, but not inhibition, leads to loss of DNA repair proteins in MSI cells

WRN has known roles in gene regulation, and the helicase function of WRN is thought to be involved in this process. Hundreds of proteins show altered expression when WRN is depleted or knocked out (Tian *et al.*, 2022). Given that WRN depletion seems to show different phenotypes in MSS vs MSI cells, we wondered whether WRN depletion or inhibition may affect gene expression differently between the two cell groups. We focused on DNA replication and repair proteins, as a key step in cell death of WRN-depleted MSI cells is the induction of DSBs and subsequent chromothripsis. Cells were plated out and treated with siRNA targeting WRN and a low or high dose of WRNi for 72 hours, then harvested and analysed by Western blotting. Protein signal was quantified and normalised to both GAPDH loading and protein levels in untreated cells. WRN depletion was effective in all cell lines (figure 4.9a, e). WRN depletion led to a significant reduction in many DNA damage-related proteins in HCT116 and RKO (MSI) cells, including BARD1, RAD51, MUS81, RPA32, FEN1, HUS1, PIN1, EXO1 and RNF168 (to varying degrees between cell lines) compared to HT29 and HT55 (MSS) cells. PCNA levels were not reduced after WRN depletion, and RFW3 levels remained constant or increased across the cell lines. ATM levels were reduced in HT29 (MSS) cells but increased in RKO (MSI) cells.

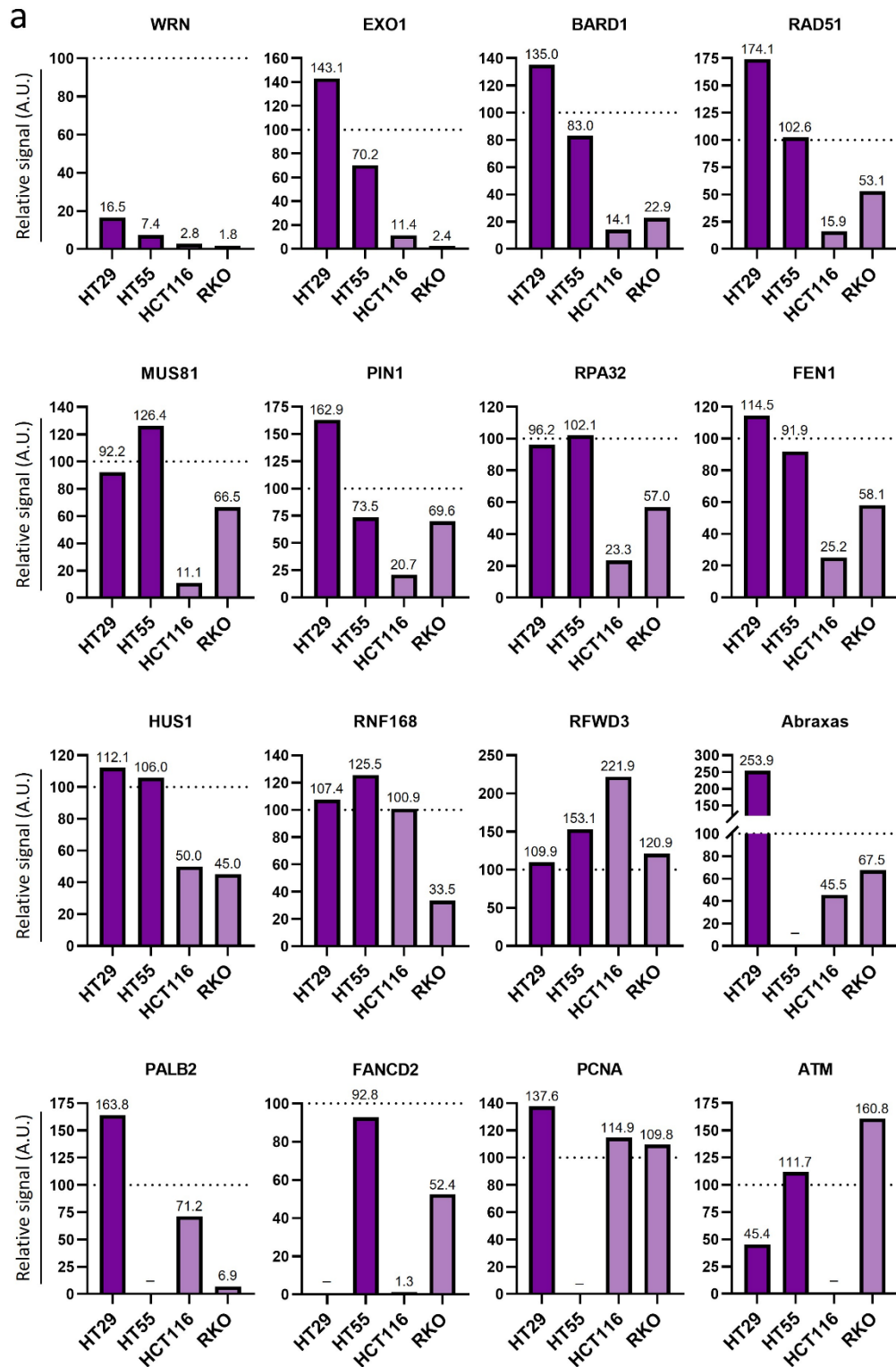
Interestingly, 72-hour WRN helicase inhibitor treatment at 250 nM did not affect protein levels in the same way as WRN depletion (figure 4.9b, e). WRNi treatment did not broadly affect WRN protein levels in the cells, except in RKO (MSI) cells, where a reduction in WRN signal was observed. EXO1 and PALB2 levels were also slightly reduced in RKO (MSI) cells. In HT29 (MSS) cells, BARD1, RAD51, PIN1, HUS1, RFW3, Abraxas, PALB2 and PCNA levels were increased. In HT55 (MSS) cells, PIN1 levels were reduced. In HCT116 (MSI) cells, BARD1, MUS81, RNF168,

PALB2 and FANCD2 levels were increased. ATM levels were reduced in HT29 (MSS) cells, as seen with WRN depletion.

In cells treated with a higher dose of NSC 617145 (1 μ M for 72 hours), WRN protein levels were reduced in HT29 (MSS) and RKO (MSI) cells (figure 4.9c, e). In HT29 (MSS) cells, BARD1, RAD51, PIN1, HUS1, RFW3, Abraxas and PCNA levels were increased, and ATM levels were lower, similar to the lower dose of WRNi tested. In HT55 (MSS) cells, BARD1 and RFW3 levels were increased. In HCT116 (MSI) cells, BARD1, MUS81, RNF168 and FANCD2 levels were increased, and RFW3 levels were decreased. In RKO (MSI) cells, EXO1, PALB2 and RNF168 levels were lower, and ATM levels were increased.

We previously saw that of the MSI cell lines tested, HCT116 and RKO cells exhibited high levels of cell death after WRN depletion, whereas only 19.3% of LS411N cells died. While possible that this is due to lower efficiency of siRNA transfection and reduced WRN depletion in these cells, we theorised that LS411N (MSI) cells may be less sensitive to WRN depletion due to intact expression of DNA repair and replication genes. To test this, we treated LS411N (MSI) cells to siRNA targeting WRN for 72 hours, then collected lysates and analysed protein levels via Western blotting as before (figure 4.10d, e). WRN depletion was effective, and we saw that in the panel of genes tested, none were reduced in cells depleted of WRN, unlike in HCT116 and RKO (MSI) cells. We collated the relative signal for each protein in each cell line, and plotted the data in order of sensitivity to WRN depletion as measured by alamarBlue reduction (figure 4.9f). HT29 and HT55 (MSS) were the least sensitive cell lines, with 93.1% and 82.8% average viability respectively. Of the MSI cells, 80.7% of LS411N cells were viable after WRN depletion, and RKO and HCT116 cells were the most sensitive to WRN depletion, with 29.9% and 29.5%

average viability respectively. In WRN-depleted HT29 (MSS), HT55 (MSS) and LS411N (MSI) cells, the average relative protein signal for all proteins was 124.4%, 99.9% and 130.9% respectively. In the WRN-sensitive MSI cells RKO and HCT116, the average relative protein signal for all proteins was 57.1% and 48.5%. Together this indicates that loss of DNA repair proteins is associated with cell death in WRN-depleted MSI cells.





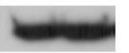

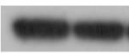



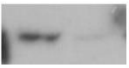


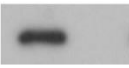


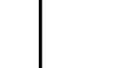





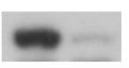
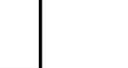




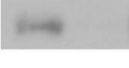

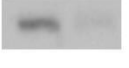
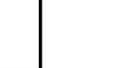
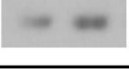

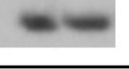
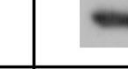
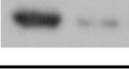

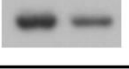
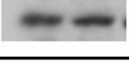

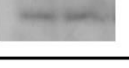



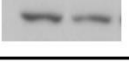
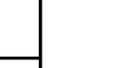
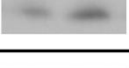
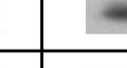
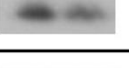

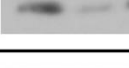

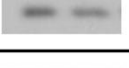
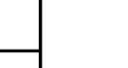
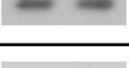

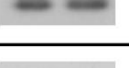

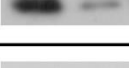

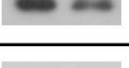
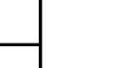






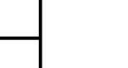
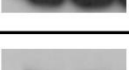

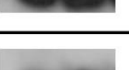

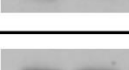


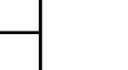
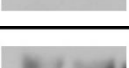
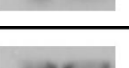

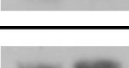

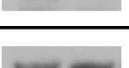
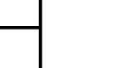

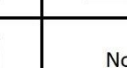




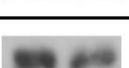
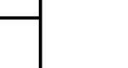

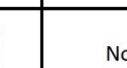
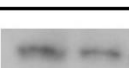

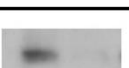

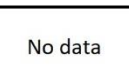


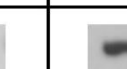
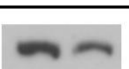



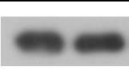

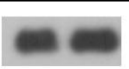



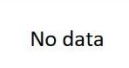


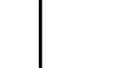





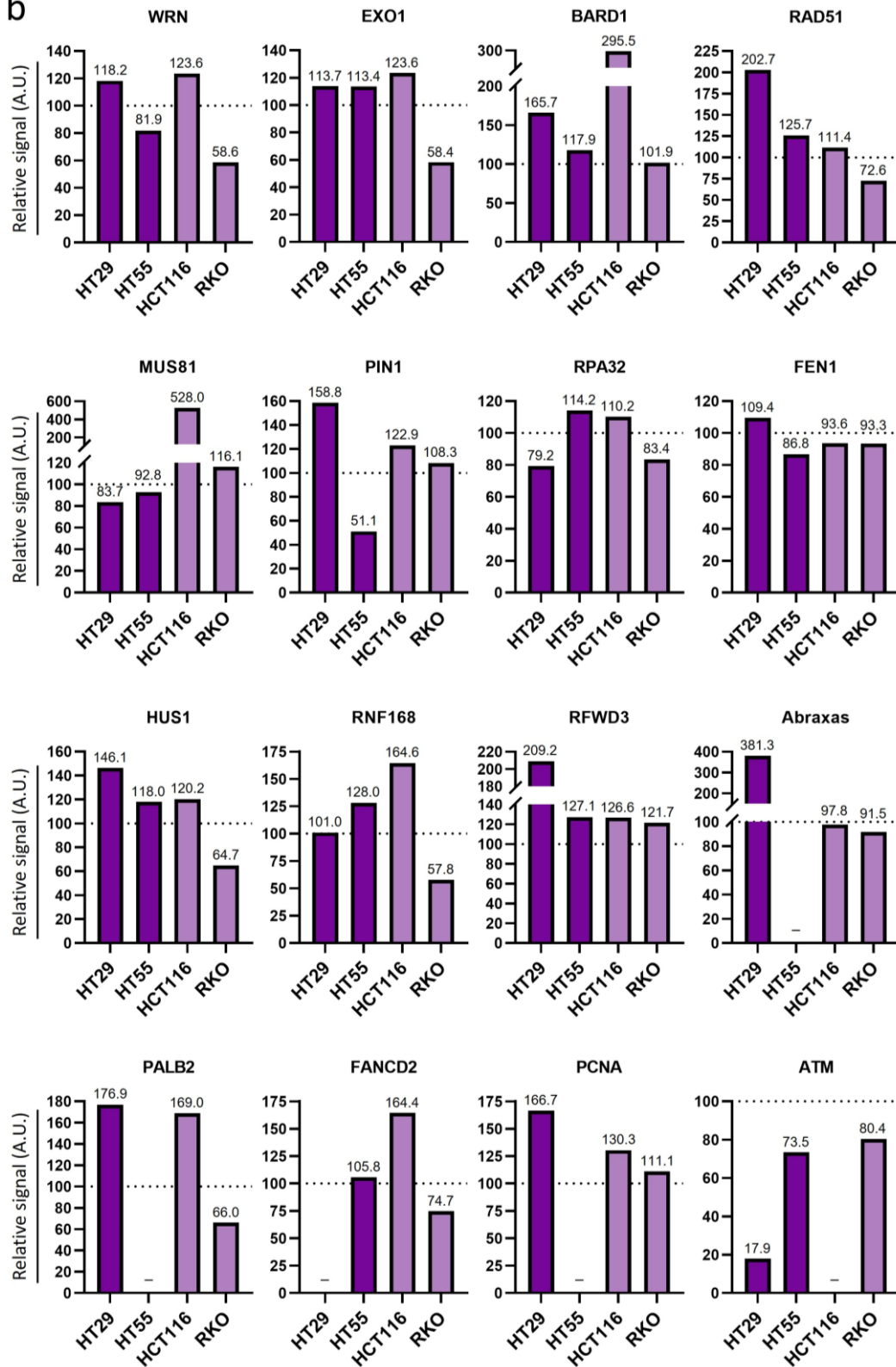
	HT29 (MSS)		HT55 (MSS)		HCT116 (MSI)		RKO (MSI)		1= siNTC 2= siWRN
	1	2	1	2	1	2	1	2	
GAPDH									
WRN									
EXO1									
BARD1									
RAD51									
MUS81									
PIN1									
RPA32									
FEN1									
HUS1									
RNF168									
RFWD3									
Abraxas			No data						
PALB2			No data						
FANCD2	No data								
PCNA			No data						
ATM					No data				

Figure 4.9

a) Western blotting for DNA repair and replication-associated proteins was performed and quantified in colorectal cancer cells treated with siRNA targeting WRN for 72 hours, normalised to a loading control and the signal in cells treated with siRNA targeting NTC. Transfection control was with siRNA targeting Luciferase. The dotted line represents the quantified protein signal in untreated cells (100%). Numbers above bars refer to the quantity measured. A.U.= arbitrary units. Dark purple= MSS, light purple= MSI cell lines.

b

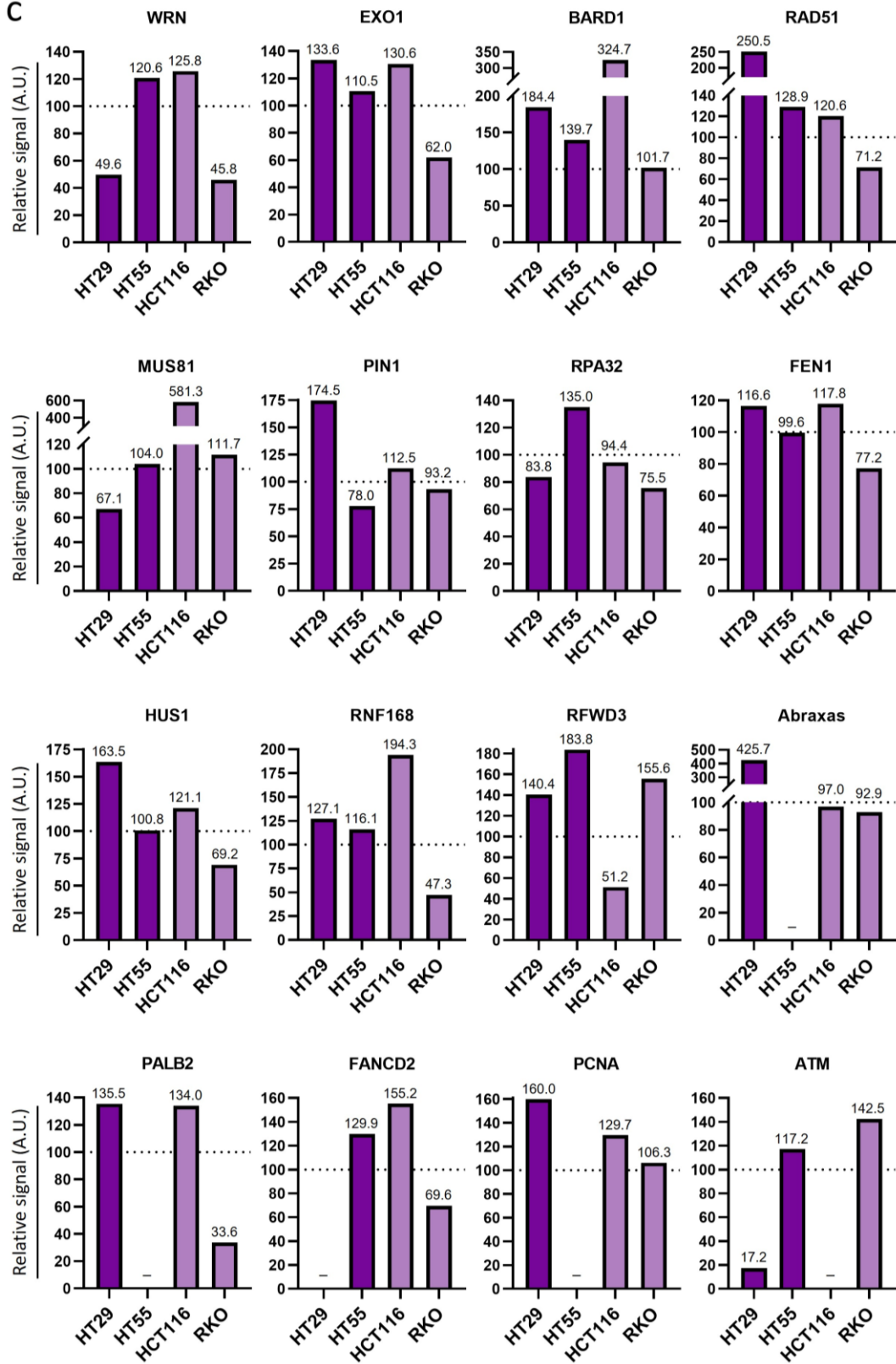


	HT29 (MSS)		HT55 (MSS)		HCT116 (MSI)		RKO (MSI)		1= siNTC 2= 250nM WRNi
	1	2	1	2	1	2	1	2	
GAPDH									
WRN									
EXO1									
BARD1									
RAD51									
MUS81									
PIN1									
RPA32									
FEN1									
HUS1									
RNF168									
RFWD3									
Abraxas			No data						
PALB2			No data						
FANCD2	No data								
PCNA			No data						
ATM					No data				

b) Western blotting for DNA repair and replication-associated proteins was performed and quantified in colorectal cancer cells treated with 250 nM NSC 617145 for 72 hours, normalised to a loading control and the signal in vehicle-treated cells. Control cells were treated with vehicle (DMSO). The dotted line

represents the quantified protein signal in untreated cells (100%). Numbers above bars refer to the quantity measured. A.U.= arbitrary units. Dark purple= MSS, light purple= MSI cell lines.

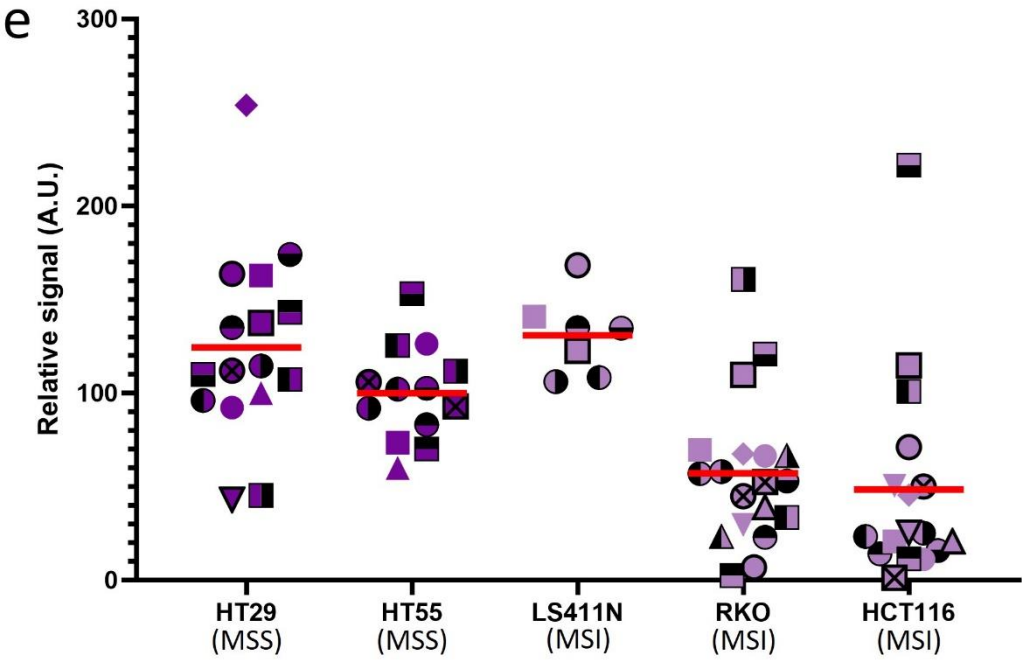
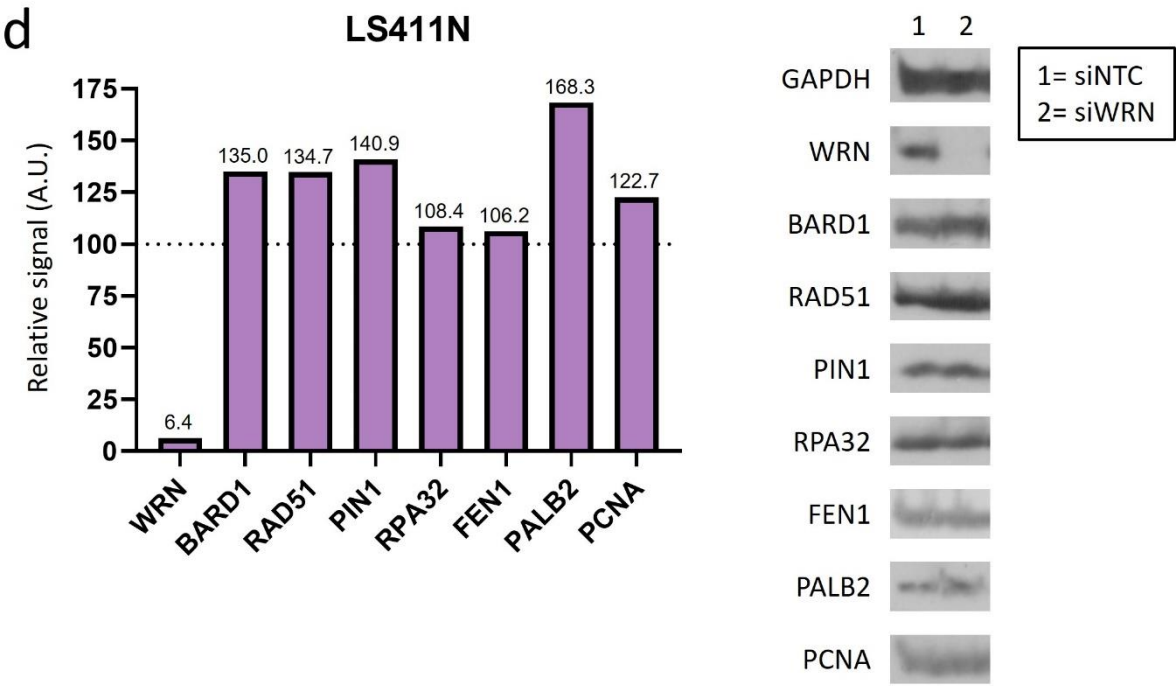
C



	HT29 (MSS)		HT55 (MSS)		HCT116 (MSI)		RKO (MSI)		1= siNTC 2= 1µM WRNi
	1	2	1	2	1	2	1	2	
GAPDH									
WRN									
EXO1									
BARD1									
RAD51									
MUS81									
PIN1									
RPA32									
FEN1									
HUS1									
RNF168									
RFWD3									
Abraxas			No data						
PALB2			No data						
FANCD2	No data								
PCNA			No data						
ATM					No data				

c) Western blotting for DNA repair and replication-associated proteins was performed and quantified in colorectal cancer cells treated with 1 µM NSC 617145 for 72 hours, normalised to a loading control and the signal in vehicle-treated cells. Control cells were treated with vehicle (DMSO). The dotted line

represents the quantified protein signal in untreated cells (100%). Numbers above bars refer to the quantity measured. A.U.= arbitrary units. Dark purple= MSS, light purple= MSI cell lines.



d) Western blotting for DNA repair and replication-associated proteins was performed and quantified in LS411N (MSI) cells treated with siRNA targeting WRN for 72 hours, normalised to a loading control and the signal in cells treated with siRNA targeting NTC. Transfection control was with siRNA targeting Luciferase. The dotted line represents the quantified protein signal in untreated cells (100%). Numbers above bars refer to the quantity measured. A.U.= arbitrary units.

e) Western blot data for each cell line was plotted in order of sensitivity to WRN depletion, with HT29 (MSS) cells being the least sensitive and HCT116 (MSI) cells being the most sensitive. Transfection control was with siRNA targeting Luciferase. Each protein shown is represented by a unique symbol. Red lines represent the average relative signal of all proteins tested. Dark purple= MSS, light purple= MSI cell lines.

4.11 DNA damage response inhibition does not sensitise MSI cells to WRN helicase inhibition compared to MSS cells

Combination therapy, where more than one drug is given at the same time, is a popular and effective strategy in cancer treatment. Combining multiple agents together can enhance efficacy of single agents, and can reduce the ability of the cell to use back-up pathways if multiple pathways are targeted at once (Mokhtari *et al.*, 2017).

Given previous data suggesting that WRN depletion is associated with loss of several other DNA damage response proteins in MSI cells specifically, we wondered whether loss of DDR proteins was a facet of the synthetic lethal relationship between WRN loss and MSI-high cell death. We also wondered whether the lack of hypersensitivity in MSI cells to WRNi treatment was due to intact DDR protein levels, and whether inhibiting WRN helicase activity and the DDR simultaneously could sensitise MSI cells to WRNi treatment. To test this, HT29 (MSS) and HCT116 (MSI) cells were plated at a low density in 6 well plates and treated with B02 (RAD51 inhibitor), KU-55933 (ATM inhibitor) and VE-821 (ATR inhibitor), then incubated for 7-12 days. HT29 and HCT116 had broadly similar sensitivities to each single agent (figure 4.10a). A dose was chosen for each cell line and individual inhibitor that gave 20-30% cell death (figure 4.10b), and this inhibitor concentration was combined with increasing doses of WRNi to assess whether combined treatment led to increased sensitivity to WRNi in the cell lines tested. To our surprise, treatment with ATM, ATR or RAD51 inhibitors did not sensitise either of the cell lines to WRNi, indicating a lack of synergy and cytotoxicity with these drug combinations and at the treatment conditions tested (figure 4.10c). Co-treatment of B02 (RAD51 inhibitor) and 10 μ M WRNi improved survival in HT29 (MSS) cells compared to WRNi treatment alone.

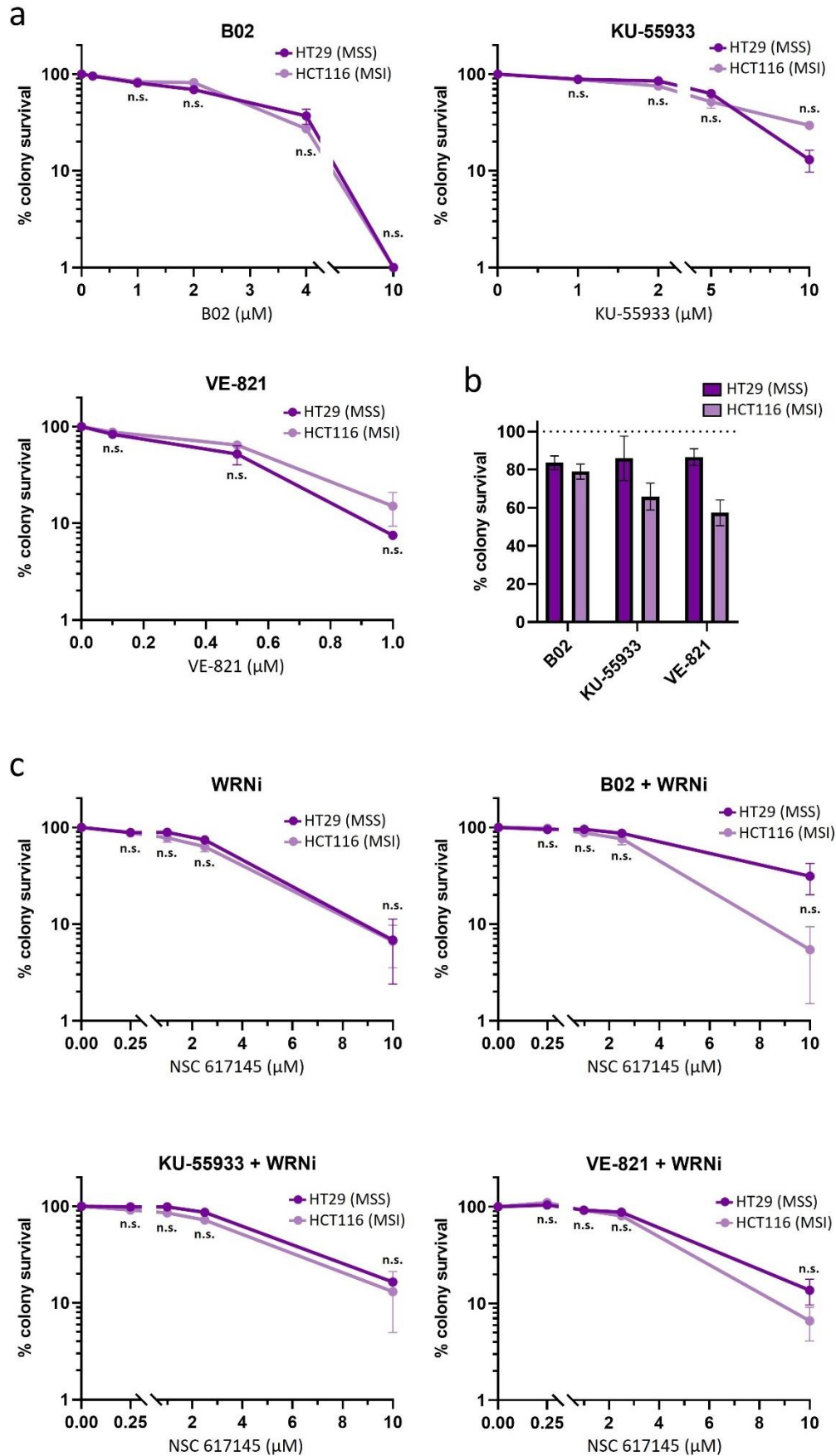


Figure 4.10

a) Cell survival was measured using the clonogenic survival assay with crystal violet staining. HT29 and HCT116 cells were treated with increasing concentrations of B02, KU-55933 and VE-821. Control cells were treated with vehicle (DMSO). Results are from at least 3 independent repeats. Dots indicate the mean, error bars are SEM. Statistical analysis done with two-way ANOVA; ns= not significant.

b) Cell survival was measured using the clonogenic survival assay with crystal violet staining. HT29 and HCT116 were treated with a single dose of B02 (1 μ M in both cell lines), KU-55933 (2.5 and 1.5 μ M respectively) and VE-821 (125 and 200 nM respectively). Control cells were treated with vehicle (DMSO). Results are from at least 3 independent repeats. Bars indicate the mean, error bars are SEM. The dotted line represents survival in untreated cells (100%).

c) Cell survival was measured using the clonogenic survival assay with crystal violet staining. HT29 and HCT116 cells were treated with a fixed dose of B02 (1 μ M in both cell lines), KU-55933 (2.5 and 1.5 μ M respectively) and VE-821 (125 and 200 nM respectively) and increasing concentrations of NSC 617145 (WRNi). Results are from at least 3 independent repeats. Control cells were treated with vehicle (DMSO). Dots indicate the mean, error bars are SEM. Statistical analysis done with two-way ANOVA; ns= not significant.

4.12 Discussion

We previously saw that USP50 and WRN were epistatic in various aspects of replication in HeLa cells, including fork stalling and restart, fork progression during HU treatment, and DSB prevention. WRN loss was recently discovered to be a synthetic lethal target in a subset of MMR-deficient, MSI-high cancer cells, leading us to wonder whether a background of WRN dependency would affect the relationship between USP50 and WRN. A panel of six colorectal cancer cell lines, three with WRN dependency and three without, were used to assess how USP50 and WRN influence replication fork dynamics in MSI-high cells, and to explore the synthetic lethal mechanism further. It is worth noting that the MSI cell line HCT116 carries the KRAS G13D mutation (Shirasawa *et al.*, 1993), which is associated with upregulated autophagy and tumour survival (Guo *et al.*, 2011).

Having optimised siRNA transfection in the cell line panel to ensure effective and comparable protein depletion, we first established that USP50 loss does not lead to a high level of cell death in MSI cells compared to MSS cells, unlike WRN depletion. This result implies that USP50 is not a synthetic lethal target in MSI-high cancers, and that the role of WRN in preventing cell death in MSI-high cells is independent of its shared roles with USP50. We were surprised that while the MSI cell lines HCT116 and RKO exhibited high cell death after WRN depletion, LS411N cells did not, in contrast with DepMap data and its designation as an MSI-high cell line. MSI-high cancer cells are highly mutagenic, and previous reports suggest that WRN dependency develops in MSI-high cells over an extended period of time and many cell divisions (van Wietmarschen *et al.*, 2020). It is possible that the strain of LS411N cells used in our experiments has been in culture for less time than other strains, and thus has not developed

WRN dependency yet. MSI cell death after WRN depletion is mediated by p53, and p53 mutation may rescue cell death (Hao *et al.*, 2022). LS411N cells have a documented p53 mutation (Y126*), which paradoxically has been reported to produce near-full length protein due to alternative splicing, with intact ability to induce apoptosis (Makarov *et al.*, 2017). It is possible that our strain of LS411N has developed another p53 mutation that inactivates pro-apoptotic activity, leading to resistance to WRN depletion. However, another report noted that combined depletion of WRN and p53 did not rescue cell death in MSI cells (Zong *et al.*, 2023), so this hypothesis warrants further study.

Despite differences in response to WRN loss amongst the three MSI cell lines tested, analysis of fork stalling revealed that USP50 and WRN co-depletion did not rescue the proportion of stalled forks in all three MSI cell lines, unlike in MSS cells. This suggests that despite not being sensitive to loss of WRN, LS411N cells behave similarly to HCT116 and RKO (MSI) cells in the context of fork stalling when USP50 and WRN are co-depleted. This could imply that the failure to rescue stalled forks is not related to WRN dependency, but rather another factor which the three MSI cell lines have in common, for example MMR deficiency or other MSI-related mutations. Previous reports suggested that WRN helicase activity was indispensable for allowing the replication machinery to traverse cruciform structures at (TA)_n repeats, so we were surprised that WRN depletion or inhibition did not affect fork stalling to a greater extent in MSI cells compared to MSS cells. It is possible that the number of cruciform-forming (TA)_n repeats in the genomes of MSI cells is too low to have a substantial impact on overall levels of fork stalling, whilst being sufficient in number to cause chromothripsis and cell death after DSB formation. It is also possible that the role of WRN during replication of cruciform DNA structures is not the prevention of fork stalling at (TA)_n repeats.

In our search for replication problems arising in MSI cells after WRN loss, we used the DNA fibre assay to assess fork restart in MSS and MSI cells after HU treatment. We saw that while HCT116 (MSI) cells had a slightly higher basal level of un restarted forks, WRN depletion led to a greater increase in stalled forks compared to HT29 cells. This could indicate that rather than having a primary role in preventing fork stalling at (TA)_n repeats in MSI cells, WRN could be acting to ensure fork restart at these sites to prevent the formation of toxic DSBs. USP50 depletion led to a fork restart defect in both cell lines, and co-depletion of USP50 and WRN did not rescue or exacerbate the proportion of stalled forks, indicating that in both MSS and MSI cells, USP50 and WRN are epistatic in fork restart. USP50 depletion did not increase fork stalling levels to the same extent as WRN depletion in MSI cells however, suggesting that WRN operates in USP50-dependent and -independent fork restart pathways in MSI cells. Examination of IdU incorporation during HU treatment revealed that WRN or USP50 depletion led to longer tract lengths in HT29 (MSS) cells, indicating that replication forks travelled further during HU treatment when either protein was depleted. In contrast, USP50 or WRN depletion in HCT116 (MSI) cells did not have any effect on IdU: CldU ratio, suggesting that either depletion alone does not affect the ability of replication forks to continue progressing during HU treatment. Co-depletion of USP50 and WRN in HT29 (MSS) cells reduced the IdU: CldU to an intermediate level, whereas in HCT116 (MSI) cells, this treatment led to an increase in IdU: CldU ratio, highlighting another difference in phenotypes between MSS and MSI cells.

WRN has the potential to be a good drug target: it has enzymatic function that can be targeted, and patients with WS typically take several decades to display the ageing phenotypes and cancer incidence related to loss of WRN activity (Koshizaka *et al.*, 2020). We were therefore curious to see how the WRN helicase inhibitor NSC 617145 would affect MSI cell viability. We

were surprised to observe that treatment with increasing doses of NSC 617145 for 72 hours or seven days did not result in increased cell death in MSI cells compared to MSS cells. HCT116 and RKO (MSI) cells are both hypersensitive to WRN depletion, but not to WRN helicase inhibition, which raises the question of why WRN helicase inhibition with NSC 617145 fails to phenocopy expression of helicase-dead WRN (Chan *et al.*, 2019; Kategaya *et al.*, 2019; Lieb *et al.*, 2019). The highest dose of WRNi used resulted in significant cell death in each cell line studied, suggesting that the inhibitor concentration was high enough to cause loss of viability in cells. The K577M mutation in WRN targets the ATPase activity of WRN, and WRN helicase activity relies on ATP hydrolysis. It could theoretically be possible that a separate role of WRN ATP hydrolysis exists outside of driving helicase activity, and that this role is responsible for preventing DSBs at (TA)_n repeats and subsequent cell death. It is also possible that NSC 617145 mimics WRN helicase inhibition in *in vitro* helicase assays without directly inhibiting helicase activity, and therefore does not recapitulate helicase-dead WRN expression in MSI cells. Regardless of the reason, NSC 617145 does not appear to be a small molecule capable of selectively killing WRN-dependent MSI cancer cells, and other candidates or approaches are needed to address this as-yet unmet clinical need.

WRN-depleted HCT116 (MSI) cells exhibited a pronounced fork restart defect but no change in fork progression during HU, which is potentially indicative of a lack of effect on fork reversal. Given the known roles of WRN in gene expression regulation, we wondered whether WRN loss was affecting protein levels of DNA damage and replication-associated proteins in MSI cells. Western blotting revealed reductions of various protein levels in MSI but not MSS cells when WRN was depleted. These changes in protein levels correlated with cell death in WRN-depleted MSI cells, with HCT116 and RKO being highly sensitive to WRN loss and exhibiting

loss or reduction of several DNA damage/ replication proteins. In contrast, HT29 and HT55 (MSS) cells and LS411N (MSI but not WRN-dependent) cells did not show overall changes in protein levels after WRN depletion. WRN inhibition with either a low or high dose of NSC 617145 did not affect protein levels in the same way as WRN depletion, indicating a divergence in cellular effects between WRN depletion and inhibition. A limitation of using Western blotting as a readout of protein levels is that the reason for changes in protein levels is not delineated: the loss of DDR proteins in WRN-depleted MSI cells could be due to changes in gene expression or increased protein degradation. Further study is therefore needed to assess whether loss of WRN affects protein levels at the mRNA level, and whether this depends on WRN ATPase/ helicase activity.

MSI cells are highly mutagenic by nature, and genes containing or located near repetitive regions can be affected by the contraction or expansion of microsatellites. It is thought that these secondary gene mutations are the drivers of carcinogenesis in MMR-deficient cells (Gaymes *et al.*, 2013). Genes commonly affected by microsatellite length alteration include BLM, CHK1, RAD50 and MRE11 (Duval *et al.*, 2002). MRE11 intron 4 contains an extended tract of thymines that encourages correct splicing. In MSI cells, shortening of the polyT tract can lead to incorrect splicing and expression of a mutant or truncated MRE11 protein, affecting protein expression, nuclease activity and binding to NBS1 and RAD50 (Giannini *et al.*, 2004). A mutant allele of MRE11 found in HCT116 (MSI) cells was reported to act in a dominant-negative manner through retaining DNA binding ability but lacking nuclease activity, thus impeding replication fork restart (Wen *et al.*, 2008). HCT116 was also reported to carry a RAD50 mutation, and RKO and LS411N (MSI) cells have also been reported to harbour MRE11 and RAD50 mutations (Li *et al.*, 2004; Vilar *et al.*, 2008). Loss of MRE11 reduces HR efficiency

in cells, and loss of the MRN complex impedes fork restart (Bruhn *et al.*, 2014; Shimizu *et al.*, 2020; Syed & Tainer, 2018). Loss or impairment of MRE11 and RAD50, and subsequent reduced recruitment of NBS1, sensitises MSI cells to PARP inhibitor treatment, presumably through the exploitation of incompetent HR (Gaymes *et al.*, 2013; Vilar *et al.*, 2011). MUS81 and EXO1 nucleases co-operate to produce 3' ssDNA overhangs to produce substrates suitable for HR repair (Liu & Kong, 2020). Loss or impairment of MRE11 combined with EXO1 loss after WRN depletion in MSI cells could therefore further impede the ability of these cells to perform HR to repair DSBs. MRE11 protein levels were not examined in MSS and MSI cells in this thesis as Western blots obtained with our MRE11 antibody were of poor quality, so further study is needed to test these hypotheses.

WRN depletion in MSI cells also led to reductions in the levels of BARD1, RAD51, MUS81 and RPA. BARD1 forms an obligate heterodimer with BRCA1 that is essential for BRCA1 E3 ubiquitin ligase activity. Loss of BARD1 in MSI cells after WRN depletion could therefore lead to concurrent loss of BRCA1 protein, impaired HR repair, and defective fork restart. RPA binds ssDNA at stalled replication forks and protects it from nucleolytic degradation. RAD51 displaces RPA to initiate strand invasion in fork restart, so loss of these proteins could abrogate replication restart, lead to exposed ssDNA, and lead to replication fork collapse and replication-associated DSBs in MSI cells. It was previously shown that DSB formation in WRN-depleted MSI cells was dependent on the action of MUS81 (Wietmarschen *et al.*, 2020), yet we observed loss of MUS81 expression in MSI cells after 72 hours of WRN depletion (figure 4.9f). Zong *et al.* observed DSB formation within two hours of WRN depletion (Zong *et al.*, 2023), so it is possible that MUS81-dependent DSB formation occurs only in a short window after WRN depletion in MSI cells, before MUS81 expression is lost. Loss of MUS81 could also affect the

ability of persistently stalled forks to restart via HR. The concurrent losses of WRN, the MRN complex, EXO1, BARD1/ BRCA1, RPA, RAD51 and MUS81 could therefore result in stalled replication forks at (TA)_n repeats that cannot be restarted or repaired by HR, leading to persistent DSBs, chromothripsis and cell death. This model could explain why WRN helicase inhibition does not induce cell death specifically in MSI cells compared to WRN depletion, as RAD51, BARD1, RPA and EXO1 protein levels were not affected to the same degree after 72-hour treatment with NSC 617145 at 1 μ M. It is therefore possible that WRN depletion leads to cell death only when combined with loss of HR-mediated fork restart/ repair, and that restoration of HR competency in these cells could reverse cell death. This could also explain why LS411N (MSI) cells are not hypersensitive to WRN depletion, as WRN depletion did not lead to a reduction in BARD1, RAD51, RPA or PALB2 protein levels. Interestingly, the only protein tested that increased after WRN depletion in HCT116 (MSI) cells was RFWD3, an E3 ubiquitin ligase that promotes ICL repair and TLS. The increase in RFWD3 protein levels in WRN-depleted MSI cells could represent an (unsuccessful) attempt to use a back-up pathway to rescue replication and prevent cell death. Further repeats and experiments are needed to verify these findings.

To test the hypothesis that both WRN helicase activity and HR competency need to be lost to induce cell death in p53-competent MSI cells, we tested the effect of combining WRNi treatment with DDR inhibition in MSS and MSI cells. Both HT29 (MSS) and HCT116 (MSI) cell lines showed similar sensitivities to increasing concentrations of RAD51, ATM or ATR inhibitors. This finding was surprising given that HCT116 cells reportedly lack functional MRE11 activity and therefore may be defective in HR repair. Treatment with a fixed dose of DDR inhibitor to induce mild cell death (20-40%) did not sensitise HCT116 (MSI) cells to increasing

concentrations of WRNi compared to HT29 (MSS) cells. This result contrasts with a previous report demonstrating additive effects on cell survival of targeting WRN and ATR together, though a key difference is that WRN was depleted by use of PROTAC in this study (Zong *et al.*, 2023). This result suggests that the loss of one component of the DDR is not sufficient to sensitise MSI cells to WRNi treatment, and that a combination of DDR inhibitors may be needed. In HT29 (MSS) cells, combining RAD51 inhibition with high-dose WRN inhibition improved cell survival compared to WRNi treatment alone, suggesting that inappropriate RAD51 activity contributes to cell death when WRN is inhibited in these cells. Western blotting revealed that WRN depletion and inhibition led to an increase in RAD51 protein levels in HT29 cells, which may contribute to RAD51-mediated toxicity.

There are still many questions to be answered regarding WRN synthetic lethality in MSI-high cells. It is currently not known why some MSI cell lines exhibit expansion of (TA)_n repeats specifically, and whether the expansion and contraction of distinct microsatellites is affected by type or severity of MMR mutation or other background genetic factors. An intriguing aspect of WRN synthetic lethality is the observation that WS patients are predisposed to developing cancer, but that theoretically an MMR-deficient, MSI cancer in WS patients would not be able to develop significantly expanded (TA)_n tracts, as the lack of functional WRN in these cells would lead to cell death. Another interesting observation is that germline MMR deficiency, known as Lynch syndrome, is caused by mutation or loss of canonical MMR proteins. Lynch-like syndrome phenocopies Lynch syndrome, but is caused by a non-MMR mutation that subsequently affects the MMR pathway. A patient presenting with synchronous endometrial and ovarian cancer was recently found to have Lynch-like syndrome linked to WRN mutation that led to undetectable MLH1 and PMS2 protein expression (Kamburova *et al.*, 2023). Lynch-

like syndrome with WRN mutation would theoretically not be able to develop extended (TA)_n tracts and cruciform DNA due to lack of functional WRN and subsequent cell death.

4.13 Future experiments

Several questions remain regarding the roles of USP50 and WRN in MSS and MSI cells.

1) Is loss of DDR proteins in MSI cells dependent on loss of WRN helicase activity?

We observed that in WRN-sensitive MSI cells, WRN depletion led to loss of several proteins involved in the DDR (figure 4.9a). We did not observe this effect when MSI cells were treated with WRNi. Given that the helicase function of WRN is critical for MSI cell survival, we wonder whether WRN helicase activity is also needed to maintain DDR protein expression. To test this, we would deplete WRN in the colorectal cancer cell lines and transfect cells with siRNA-resistant wild-type, helicase-dead and exonuclease-dead WRN constructs. We would perform Western blotting as before to examine how expression of the WRN constructs affects DDR protein expression in the MSS and MSI cell lines.

2) What is the mechanism of loss of DDR proteins in WRN-depleted MSI cells?

In this chapter we saw that depletion of WRN led to loss of several key DDR proteins in MSI cells exclusively (figure 4.9a). However, we do not know how this occurs. Protein levels are affected by many factors, such as transcriptional regulation, protein translation, and

proteasomal degradation. Elucidating the mechanism behind the loss of DDR proteins in WRN-depleted MSI cells would allow us to study why this process does not happen in MSS cells. It could also inform us of potential resistance mechanisms that could emerge after WRN inhibition or degradation in MSI cancers. It would be interesting to deplete WRN and treat cells with an inhibitor of the ubiquitin-mediated proteasomal pathway, such as the VCP/ p97 inhibitor CB-5083 (Le Moigne *et al.*, 2017), and observe whether DDR protein levels are restored. Alternatively, reverse transcription qPCR could be employed to look for changes in gene expression in MSI cells after WRN depletion.

3) Does restoration of DDR proteins rescue cell survival in WRN-depleted MSI cells?

We observed an association between sensitivity to WRN depletion and reduction in DDR protein levels (figure 4.9f). We wonder whether restoring the levels of certain DDR proteins would rescue or improve survival of WRN-depleted MSI cells. We would test this by depleting WRN in MSI cells and transfecting with constructs expressing DDR proteins. We would then perform clonogenic survival assays and Western blotting to link survival to DDR protein restoration. If DDR protein loss in WRN-depleted MSI cells is mediated by ubiquitination and proteasomal degradation, this approach may not result in restoration of DDR protein levels.

4) Are RECQL4 and RECQL5 responsible for rescue of replication progression in USP50- and WRN-depleted MSS cells?

In chapter 3 we saw that RECQL4 or RECQL5 depletion reverses the restoration of replication progression in USP50- and WRN-depleted HeLa cells (figure 3.12e, f). We observed that USP50 and WRN co-depletion rescues fork stalling levels in MSS cells, but not MSI cells (figure 4.3b). We wonder whether the USP50-WRN-RECQL4-RECQL5 axis is active in MSS colorectal cancer cells. To test this, we would repeat the DNA fibre assay to look at fork stalling with USP50, WRN and RECQL4/ 5 depletion.

5. USP50 suppresses or promotes DSB formation depending on genomic location

5.1 Introduction

Genome stability is constantly threatened by DNA lesions from endogenous and exogenous sources (Wang & Lindahl, 2016). The DDR protects DNA from alteration and loss in order to preserve genetic information and prevent mutation and disease (Ekundayo & Bleichert, 2019; Wang & Lindahl, 2016). DSBs are the most dangerous lesion, and several pathways exist to repair these and prevent alteration or loss of the genetic code, or cell death (Scully *et al.*, 2019). However, in limited circumstances DSBs are induced by cells and serve an important physiological role, for example in V(D)J recombination and fork restart (Kondratick *et al.*, 2021; Libri *et al.*, 2022).

Knowing the location and number of DSBs occurring in cells can give useful information on hotspots of genomic instability, effects of DNA-damaging agents, and roles of proteins in DSB formation. Several techniques exist to map DSBs in cells. INDUCE-seq is a method of determining the number and genomic location of DSBs in cells, without using a PCR amplification step (Dobbs *et al.*, 2022). This avoids biases arising from sequences with variable ability to be amplified by PCR (Dobbs *et al.*, 2022). Each sequencing read generated by INDUCE-seq represents one DSB.

We previously observed that depletion of USP50 in HeLa cells leads to an increase in replication-associated DSBs, as measured by IF for 53BP1 (figure 3.7d). An increase in γ -H2AX foci was also observed upon USP50 depletion, which indicates replication stress and DSBs (figure 3.7b). However, this approach does not give any information on where or how these

DSBs occur. We used INDUCE-seq to map DSBs in HeLa cells with and without USP50 depletion to examine how USP50 functions to prevent the formation of DSBs.

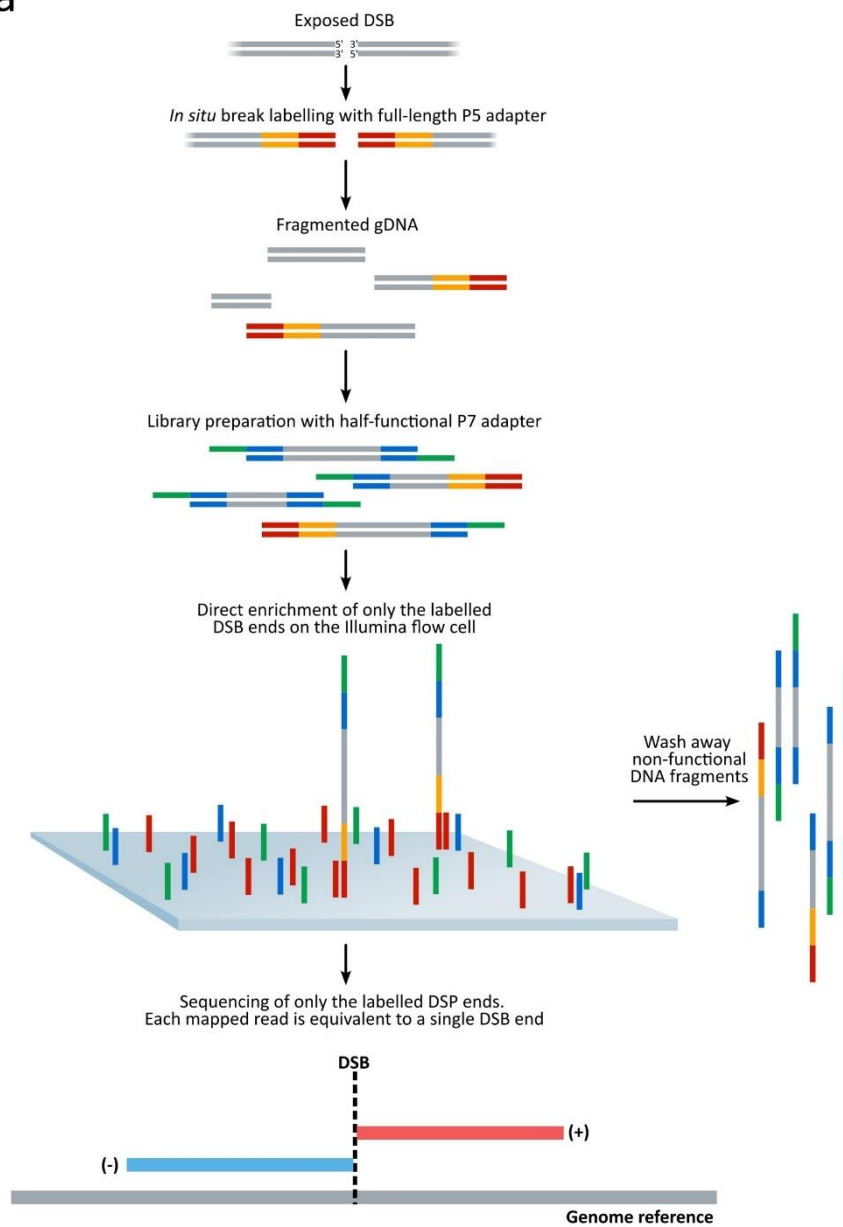
5.2 USP50 depletion leads to an overall increase in INDUCE-seq reads

INDUCE-seq detects the number and genomic position of DSBs in a sample of fixed cells (Dobbs *et al.*, 2022). We used INDUCE-seq to examine DSBs in HeLa cells with or without USP50 depletion. Cells were plated and treated with siRNA targeting USP50 or NTC for 72 hours. 120,000 cells were fixed onto poly-L-lysine-coated wells of a 24 well plate. The fixed cell samples were processed by Broken String Biosciences for DNA library preparation and sequencing (figure 5.1a). Sequencing reads generated by the INDUCE-seq protocol were processed and returned as BAM, SAM and BED files for analysis. The reads generated by INDUCE-seq are around 70-80 nucleotides long, meaning that DSBs are mapped precisely to the genome.

Analysis of sequencing reads in Galaxy (usegalaxy.org; Afgan *et al.*, 2022) revealed that in NTC-depleted cells there were a total of 567,594 reads, and in USP50-depleted cells there were 781,481 reads (excluding reads mapped to the mitochondrial genome; figure 5.1b). This represents an increase of 37.7% in the number of DSBs when USP50 is depleted, assuming that equal numbers of cells were processed in both conditions. We previously saw that depleting USP50 led to a 19% increase in γ -H2AX foci in non-replicating cells, and an 84% increase in S phase cells (figure 3.7a, b). The cells submitted for INDUCE-seq analysis were not synchronised or enriched for any phase of the cell cycle, and therefore represent a mixed population of cell phases. Combining the IF data from non-S phase and S phase cells revealed that USP50 depletion leads to an increase in γ -H2AX foci from 2.9 to 4.1 average foci per cell (figure 5.1c), representing an increase of 41.4%. The increase in INDUCE-seq reads upon USP50 depletion

correlates with the IF data. Taken together, these data strengthen our theory that USP50 suppresses the formation of DSBs.

a



b

siNTC	siUSP50
567,594	781,481

c

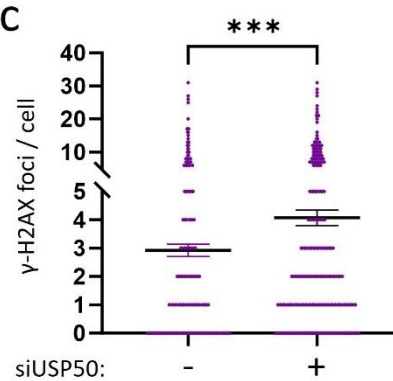


Figure 5.1

a) Schematic of the INDUCE-seq workflow. Cells are treated, fixed and permeabilised. Exposed DSBs are labelled via ligation to a P5 sequencing adapter. The genomic DNA is then extracted and fragmented, and the DNA ends are end-prepared and labelled through ligation to a half-functional P7 adapter. The DNA fragments are applied to an Illumina flow cell. Only DNA fragments labelled with the P5 adapter bind to the flow cell, and the non-functional DNA fragments are washed away. The P5- and P7-ligated DNA fragments are sequenced. Adapted from (Dobbs *et al.*, 2022).

b) Number of INDUCE-seq reads in HeLa cells with or without USP50 depletion.

c) γ -H2AX foci were examined using IF in HeLa cells with USP50 depletion. Transfection control was with siRNA targeting Luciferase. Results are from 3 independent repeats, with $n > 100$ cells per condition, per repeat. Red lines indicate the mean, error bars are SEM. Statistical analysis done with unpaired two-tailed t-test; ***= $p \leq 0.001$.

5.3 Recurrent INDUCE-seq reads are enriched or lost upon USP50 depletion in a locus-dependent manner

We previously observed that USP50 depletion led to an increase in INDUCE-seq reads in HeLa cells (figure 5.1b). We wanted to ascertain whether the increase in INDUCE-seq reads after USP50 depletion was specific to certain areas of the genome or was distributed generally. INDUCE-seq reads for NTC- and USP50-depleted cells were aligned to the human genome (chm13 2.0; Nurk *et al.*, 2022) using the 'BowTie2' feature in Galaxy (Langmead & Salzberg, 2012). The positions and number of reads across the whole human genome were visualised in Integrative Genome Viewer (igv.org; Thorvaldsdóttir *et al.*, 2013) (figure 5.2a). The locations of sequencing reads across the genome are broadly similar. For example, a large peak of DSBs was observed at chromosome 5 in NTC- and USP50-depleted cells, spanning the entire length of the short arm of the chromosome.

We were curious to see how many INDUCE-seq reads were unique to USP50-depleted cells, in order to eliminate "shared" DSBs occurring in both samples and focus on breaks specifically caused by USP50 depletion. To this end, we ran the 'Subtract' tool in Galaxy to subtract shared reads, and the Intersect Intervals tool to subtract overlapping reads between the two samples. These tools returned 760,000+ INDUCE-seq reads that were unique to the USP50-depleted cells (out of a total of 781,481 reads), indicating that the vast majority of breaks in the samples are not overlapping or identical, but are stochastic. This implies that while USP50 depletion leads to an overall increase in breaks, most of the breaks occurring in the cells are randomly distributed. However, upon closer inspection of identical or overlapping INDUCE-seq reads, which represent recurrent DSBs, differences are observed between cells treated with siRNA

targeting NTC and USP50. We observed that at the ASTN1 gene on chromosome 1, 30 near-identical reads/ breaks were detected in untreated cells compared to one read in USP50-depleted cells (figure 5.2b). Conversely, an intergenic region at chromosome 3p11.2 showed 0 breaks in untreated cells, and 9 identical breaks in USP50-depleted cells (figure 5.2c). This suggests that while the majority of “extra” DSBs caused by USP50 depletion are stochastic, individual loci in the genome are susceptible to enrichment or loss of DSBs.

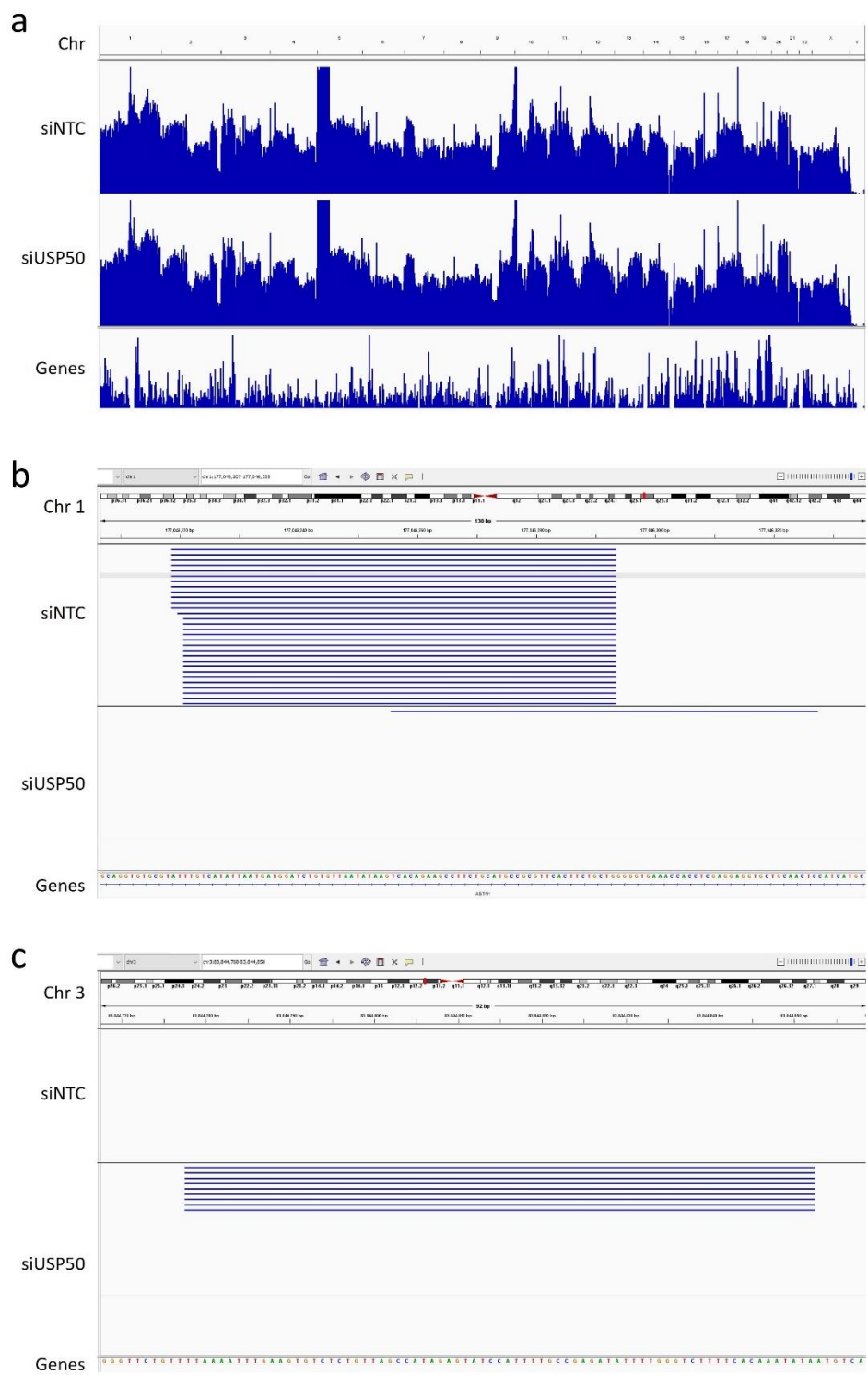


Figure 5.2

a) INDUCE-seq reads from untreated and USP50-depleted cells were aligned to the human genome and visualised in Integrative Genome Viewer. Blue lines represent INDUCE-seq reads.

b) Visualisation of INDUCE-seq reads in HeLa cells with USP50 depletion at ASTN1 gene on chromosome 1. Blue lines represent individual INDUCE-seq reads.

c) Visualisation of INDUCE-seq reads in HeLa cells with USP50 depletion at an intergenic region of chromosome 3p11.2. Blue lines represent individual INDUCE-seq reads.

5.4 USP50 loss has mixed effects on numbers of breaks at common fragile sites

CFSs are large genomics regions that are prone to fork stalling, DSB formation and deletion in conditions of RS and DNA damage (LeTallec *et al.*, 2013; Li & Wu, 2020). We were curious to see whether USP50 depletion affects the numbers of breaks occurring at CFSs. We used the 'Intersect Intervals' tool in Galaxy to align INDUCE-seq reads from cells treated with siRNA targeting NTC and USP50 with CFSs, to analyse the numbers of DSBs at each CFS in the human genome. Human CFS locations were identified from the HumCFS database (webs.iitd.edu.in/raghava/humcfs/chrom.html; (Kumar *et al.*, 2019)). In NTC-depleted cells we identified 204,689 reads that overlapped with CFSs, compared to 279,252 in USP50-depleted cells. This represents an increase of 36.4% when USP50 is depleted, similar to the overall increase in DSBs at all genomic regions (37.7%; figure 5.1b). We then examined each individual CFS to determine whether some were more susceptible to breakage than others when USP50 is depleted (figure 5.3a). The fold change in breaks between USP50-depleted and untreated cells was calculated and plotted from lowest to highest, excluding CFSs with fewer than 100 reads. We saw that 20 CFSs had fold changes lower than one standard deviation (SD) (0.0732) from the overall fold change (1.364), and 18 had a higher fold change than one SD above the overall fold change. The fold changes ranged from 1.18 for FRA1C to 1.57 for FRA12A. FRA1C therefore saw a relative reduction in DSBs, and FRA12A saw a relative increase in DSBs when compared to overall breaks. This suggests that USP50 has mixed and unique effects on different CFSs in the human genome.

a

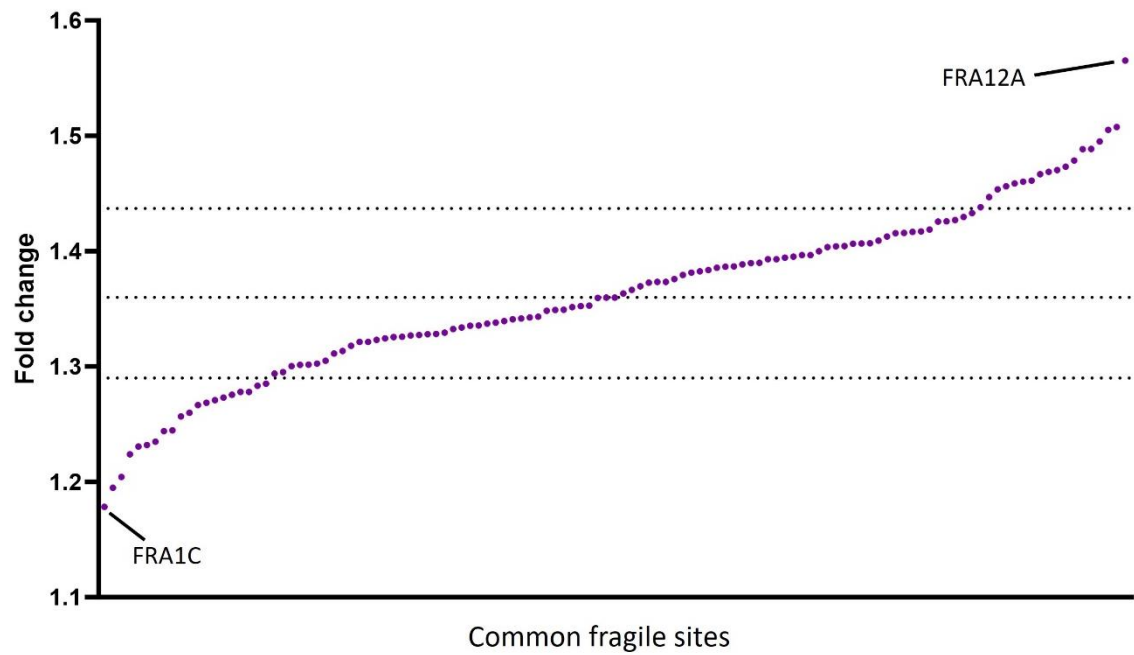


Figure 5.3

a) INDUCE-seq reads from untreated and USP50-depleted cells were mapped against CFSs. The fold change of reads from USP50-depleted: NTC-depleted samples was calculated and plotted from lowest to highest. CFSs with <100 reads were excluded for confidence. Dotted lines represent overall fold change \pm one SD.

5.5 USP50 loss has mixed effects on numbers of breaks at very large genes

Very large genes (VLGs) represent a challenge to the replication machinery due to an increased chance of TRCs (LeTallec *et al.*, 2013). Indeed, many VLGs are found within CFSs, and may contribute to the likelihood of these regions to break (LeTallec *et al.*, 2013). We examined how USP50 depletion affects DSB formation at VLGs. We compiled a list of the top 49 VLGs in the human genome as reported by Guide to the Human Genome (cshlp.org/) (where a VLG is defined as containing an annotated untranslated region and encoding a transcript), and identified their genomic locations using Integrative Genome Viewer. We then used the 'Intersect Intervals' tool on Galaxy to determine number of breaks at these genes in USP50-depleted and untreated cells. We identified 11,871 and 16,303 INDUCE-seq reads in untreated and USP50-depleted cells respectively, representing an increase of 37.3% when USP50 is depleted. Looking at the fold change in DSBs at individual VLGs, we saw that 6 genes had lower fold changes, and 10 had higher fold changes, than the overall fold change \pm one SD (0.12) (figure 5.4a). The lowest fold change was 1.05 seen in the IL1RAPL2 gene, and the highest fold change was 1.59 for the AGBL4 gene. This suggests that USP50 has varying effects on individual VLGs, but is unlikely to contribute to DSB formation at these regions overall.

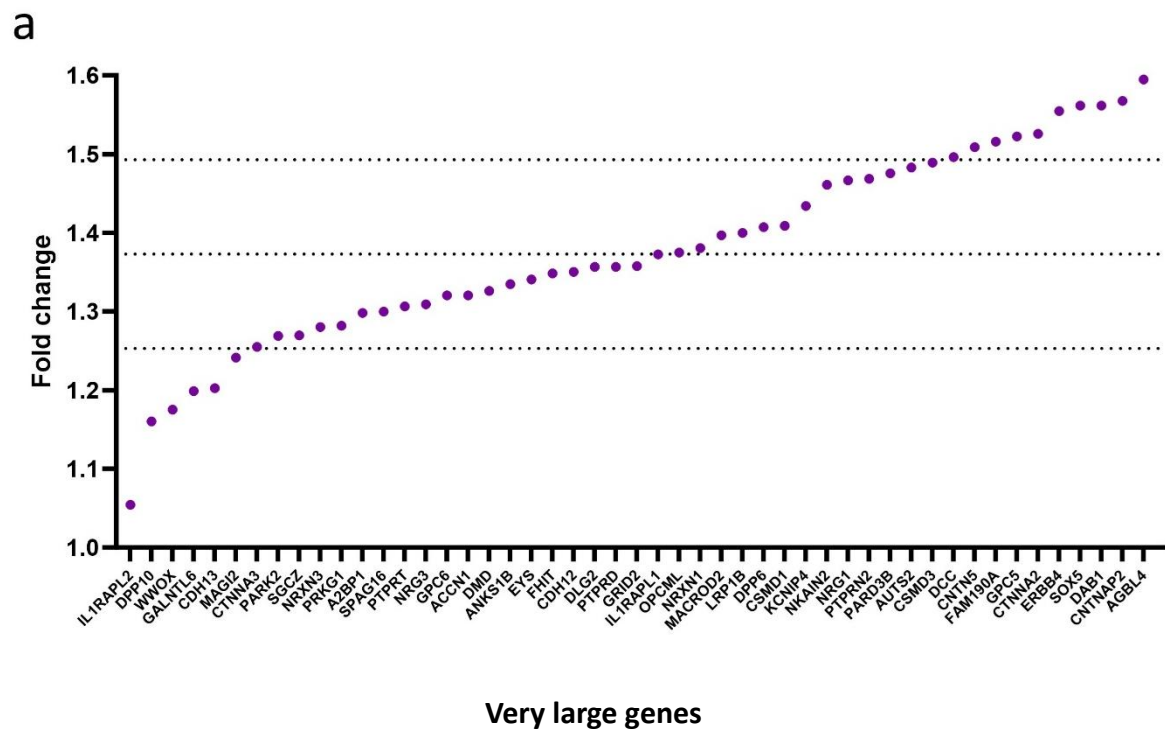


Figure 5.4

a) INDUCE-seq reads from untreated and USP50-depleted cells were mapped against VLGs. The fold change of reads from siUSP50: siNTC samples was calculated and plotted from lowest to highest. All VLGs analysed had >100 reads in both conditions. Dotted lines represent overall fold change \pm one SD.

5.6 USP50 affects proximity of breaks to transcription start sites

We previously saw that USP50 and WRN are epistatic in fork stalling and restart (figure 3.5c, 3.10b). WRN also has known roles in transcription (Balajee *et al.*, 1999; Mizutani *et al.*, 2015; Shiratori *et al.*, 2002). TRCs are a known source of RS, leading to fork stalling and DSBs (García-Muse & Aguilera, 2016). We were interested to see whether USP50 affects DSB formation at transcription start sites (TSS). We identified TSSs and examined windows of 1kb up- and downstream of the TSS to capture breaks occurring near these sites (Yamashita *et al.*, 2011). We used the 'ClosestBED' tool in Galaxy to examine the distances between INDUCE-seq reads and TSS windows. Of the 39,616 TSSs analysed, we identified 42,809 and 45,045 close or overlapping reads in untreated and USP50-depleted cells respectively, representing an increase of 5.2% when USP50 is depleted. This suggests that USP50 depletion leads to a modest increase in DSBs at TSSs compared to the rest of the genome. We analysed the distances of each proximal read from the TSS windows, and saw that the distances were reduced in USP50-depleted cells (figure 5.5a). This implies that when USP50 is depleted, DSBs occur nearer TSS windows and are suppressed at further distances.

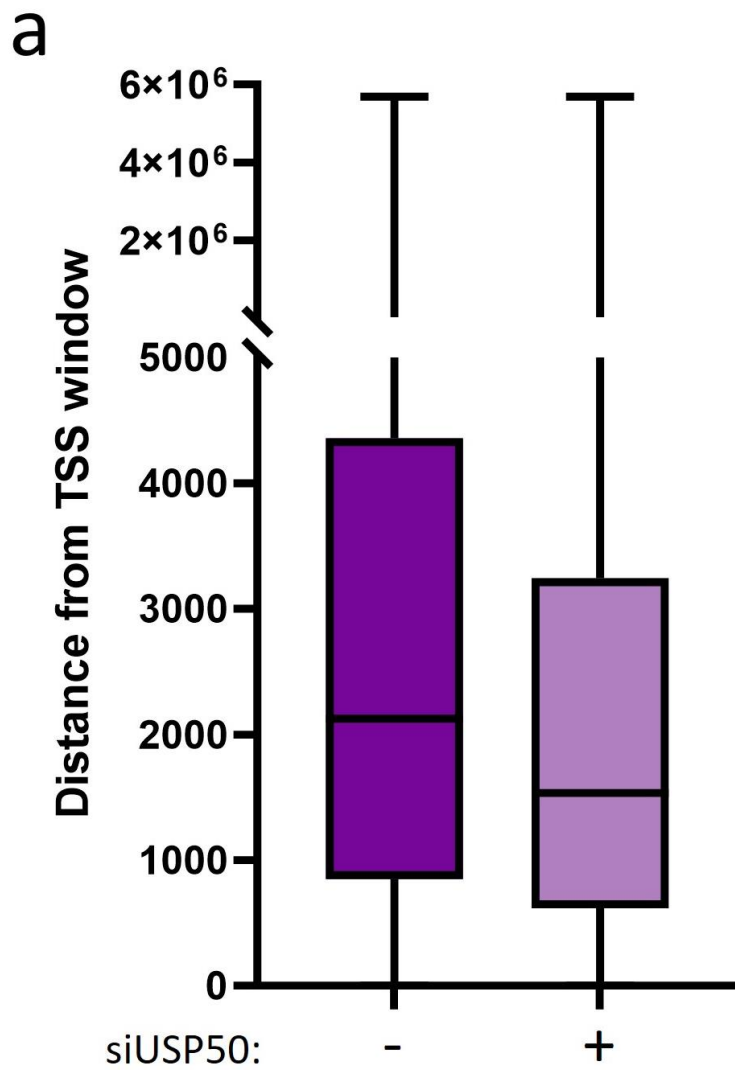


Figure 5.5

a) Distances of INDUCE-seq reads in HeLa cells depleted of USP50 from TSS windows were plotted. 27,626 reads in siNTC-treated cells were compared to 24,369 reads from siUSP50-treated cells. The box represents median, 25th and 75th percentiles. Whiskers represent minimum and maximum values.

5.7 Discussion

DSBs are highly toxic lesions that threaten cell viability and long-term health of organisms. Several repair pathways have evolved to repair DSBs, highlighting the importance of eliminating this type of damage. We had previously seen that USP50 depletion leads to an increase in DSBs, especially in S phase cells, and that these breaks were the result of MUS81 cleavage (figure 3.1b, c). In this chapter we utilised a new method of analysing location and number of DSBs called INDUCE-seq. INDUCE-seq was performed on NTC- and USP50-depleted HeLa cells to examine how USP50 contributes to DSB formation and whether specific genomic features are susceptible to breakage. This could enable us to better understand how USP50 suppresses DSB formation and inform future experiments.

INDUCE-seq processing of cell samples results in sequencing reads of 70-80 nucleotides in length, with one read reported to represent one DSB. The technique can therefore be used to analyse DSBs that occur at the same site in the same sample. This allows the examination of sites prone to breakage, as well as stochastic DSBs. We saw that USP50 depletion led to a 37.7% increase in INDUCE-seq reads in HeLa cells (figure 5.1b), in good agreement with γ -H2AX IF data (figure 5.1c). This result affirms the finding that USP50 depletion leads to a small but significant increase in DSBs. Of the 781,481 breaks detected in USP50-depleted cells, 760,000+ did not overlap with reads from the untreated cells, suggesting that the majority of breaks occurring in both samples are stochastic and sequence-independent. Given the short length of the sequencing reads, it is possible that larger, break-prone genomic features could produce several non-overlapping INDUCE-seq reads. It is therefore not surprising that the vast majority of reads in the samples do not overlap.

Visualisation of the DSBs over the whole genome in Integrative Genome Viewer revealed that the landscape of reads is broadly similar in untreated and USP50-depleted cells. Several peaks of reads are seen across the genome in both samples, for example in chromosome 1, 10 and 18. However, closer examination reveals that these peaks are located at regions of the genome with unknown sequence, often near centromeres or telomeres. It is likely that the INDUCE-seq reads are artificially grouped together at these genomic locations of repetitive DNA sequences, thus hindering further analysis of these sites. Interestingly, we noted a broad peak of DSBs spanning the entire length of the short arm of chromosome 5 in both untreated and USP50-depleted cells at regions with defined sequence, indicating a propensity for breaks to form in this region in HeLa cells. Partial loss of chromosome 5p in gametogenesis leads to Cri-du-chat syndrome, one of the most common chromosomal abnormalities found in newborns (Rodríguez-Caballero *et al.*, 2010). The large number of breaks mapped to chromosome 5p could indicate that this chromosome arm is particularly prone to DSB formation, which could result in chromosomal rearrangements or loss of segments.

Whilst the majority of breaks in both samples appear stochastic in nature, we identified several areas of recurrent breaks that showed loss or enrichment when USP50 was depleted. We identified 30 almost identical, overlapping breaks at the ASTN1 gene on chromosome 1 in untreated cells. In USP50-depleted cells, the same region produced only one read, suggesting that USP50 promotes breakage at this site in untreated cells. Alternatively, an intergenic region of chromosome 3 exhibited 0 breaks in untreated cells and 9 breaks upon USP50 depletion, implying that USP50 suppresses break formation at this site in untreated cells. This could suggest that USP50 promotes DSB formation at certain sites while protecting others, through

an unknown mechanism. Deeper analysis of the sequence and features of these two regions could reveal reasons for the difference in DSB formation at these sites with USP50 depletion.

We were curious to see whether USP50 is involved in protecting CFSs from breakage. CFSs are prone to replication fork stalling and formation of DSBs for several reasons, including high AT content, secondary structure formation, TRCs at VLGs, lack of replication origins, and late replication (Li & Wu, 2020). CFSs were identified and mapped from HumCFS, and the number of INDUCE-seq reads that overlapped with these regions was calculated using Galaxy. We found that the number of breaks at CFSs increased by 36.4% upon USP50 depletion, which closely matches the overall increase in breaks (37.7%). This suggests that USP50 depletion does not cause a change in DSB formation at CFSs in general. Upon examination of individual CFSs, we observed that each CFS exhibited an increase in DSBs in USP50-depleted cells. Interestingly, 38 sites showed a fold change in DSBs lower or higher than one SD away from the overall fold change between untreated and USP50-depleted cells. This suggests that these sites exhibit significantly fewer or greater DSBs than expected upon USP50 depletion, though the reason for this remains unclear. Particular genomic features that are present in some CFSs but not others may contribute to their likelihood to form DSBs when USP50 is depleted, thus warranting further analysis.

VLGs are hotspots for replication fork stalling and DSB formation due to the increased likelihood of TRCs (García-Muse & Aguilera, 2016). We wanted to examine whether USP50 is involved in DSB formation at VLGs, which could point towards a role in preventing TRCs. To this end, we identified the genomic locations of 49 VLGs and analysed the numbers of reads at each gene in untreated and USP50-depleted cells. The number of breaks at all VLGs increased

by 37.3% upon USP50 depletion, closely resembling the overall increase in INDUCE-seq reads in USP50-depleted cells. This implies that VLGs are not particularly prone to forming DSBs compared to the rest of the genome when USP50 is depleted. Examination of individual VLGs revealed that 16 VLGs showed a DSB fold change lower or higher than one SD from the overall fold change with USP50 depletion. These sites therefore exhibited fewer or more breaks than would be expected based on the overall increase in breaks at VLGs and across the whole genome. The reason for this however remains unknown.

Finally, we examined DSBs at TSSs in untreated and USP50-depleted cells. We looked at genomic windows 1kb upstream and downstream of the TSS to capture breaks appearing near these sites. We then asked how many breaks were occurring in or near this window. We found that upon USP50 depletion, the number of DSBs at or near TSSs increased by 5.2%, which is lower than the overall increase in breaks of 37.7%. Examination of the distances between DSBs and TSS windows revealed that DSBs in USP50-depleted cells were closer to the TSS windows than in cells treated with siRNA targeted to NTC. This suggests that in untreated cells, USP50 acts to promote DSB formation outside TSS windows. We wonder whether this could imply a role for USP50 in promoting transcription, thus generating TRCs and DSBs.

5.8 Future experiments

In this chapter we used a bioinformatics approach to examine DSB formation in HeLa cells depleted of USP50. Little is known about how USP50 prevents the formation of replication-associated DSBs, so we used INDUCE-seq to assess the association of genomic features with DSB formation in USP50-depleted cells. It would be of interest to experimentally validate these

findings and explore the mechanisms of USP50-mediated prevention of replication-associated DSBs in further detail.

1) Are other genomic features associated with DSB formation after USP50 depletion?

In this chapter we probed the number of DSBs occurring in USP50-depleted cells at chosen genomic features, such as CFSSs, VLGs and TSSs. It would be interesting to expand the list of genomic features tested, and include features such as G-quadruplex-forming DNA sequences, transcription termination sites, and chromatin marks.

2) Does USP50 promote transcription?

In this chapter we observed that DSBs occurring proximal to TSS windows are under-represented in USP50-depleted cells (figure 5.5a), suggesting that USP50 may have a role in transcription. It would therefore be interesting to experimentally confirm this novel role for USP50 in transcription using a single-molecule optical tweezers assay to measure RNA polymerase II movement along DNA with and without USP50.

3) Does WRN affect USP50-dependent DSBs at TSSs?

We saw in chapter 3 that depletion of USP50 or WRN leads to an increase in DSBs, which is rescued upon co-depletion of both (figure 3.1d, 3.7d). It would be interesting to repeat

INDUCE-seq with cells treated with siRNA targeting USP50 and WRN to investigate whether WRN regulates the formation of these TSS window-proximal breaks.

6. General discussion

Previous work in the laboratory had identified USP50 as an inactive DUB with roles in promoting replication fork progression and preventing replication-associated, MUS81-dependent DSBs (figure 1.11b-d). Analysis of DSB markers in S phase cells showed that USP50 and WRN co-depletion rescued DSB formation, suggesting a relationship between these two proteins in replication (figure 1.11h). WRN has many known roles in replication, including preventing fork stalling, restarting reversed forks, and telomere replication (Rodríguez-López *et al.*, 2002; Saharia *et al.*, 2010; Sidorova *et al.*, 2008; Thangavel *et al.*, 2015). WRN has also recently emerged as a synthetic lethal target in MSI cancers (Chan *et al.*, 2019; Kategaya *et al.*, 2019; Lieb *et al.*, 2019), so learning more about the roles and regulation of WRN are of scientific and clinical interest. We were interested to further investigate the relationship between USP50 and WRN, and elucidate the mechanisms behind the rescue in replication fork progression seen when both are depleted. The aims of this thesis were to further examine the relationship between USP50 and WRN in replication and RS, learn more about WRN as a synthetic lethal target, and elucidate possible mechanisms of action for USP50.

Knowing that DSB formation in USP50-depleted cells is dependent on MUS81, we looked at replication fork stalling and saw that MUS81 depletion does not affect fork stalling in USP50-depleted cells, suggesting that USP50 acts before MUS81 cleavage to prevent replication fork stalling (figure 3.4d). We then depleted WRN and observed an increase in fork stalling, which was reversed upon co-depletion with USP50 (figure 3.5c). A similar effect was seen when combining USP50 with inhibition of WRN helicase with the small molecule NSC 617145 (figure 3.5h). This effect was specific to WRN helicase inhibition, as the combination of WRN depletion

and WRN inhibition did not cause levels of stalled forks to change (figure 3.5f). This suggested to us that when USP50 was depleted, WRN helicase activity caused an increase in stalled forks. We used stable HeLa cell lines expressing doxycycline-inducible, GFP-tagged WRN constructs, and found that only wild-type WRN rescued fork stalling in USP50-depleted cells, pointing towards a role for both enzymatic activities of WRN in restoring replication progression. Previous literature has pinpointed the helicase function of WRN as being involved in replication fork restart, so the identification of exonuclease function in this process contradicts current and established ideas in our understanding of the roles of WRN.

Using chromatin fractionation, we observed that USP50 depletion leads to a 50.3% reduction in WRN at chromatin in HU-treated cells, suggesting that USP50 helps localise WRN to stalled forks. Combined with the DNA fibre data, we hypothesise that WRN levels at the replication fork are critical for determining fork progression and success. Fork stalling in USP50-depleted cells could result from a loss of WRN at replication forks, which is rescued upon restoration of WRN at forks through inducible overexpression. The observation that knockdown of WRN also rescues fork progression suggested to us the existence of a back-up pathway of replication progression that was suppressed when WRN was fully or partially localised to stalled forks, but activated when WRN was removed. Indeed, RECQL4 and RECQL5 were identified as critical for restoring replication fork progression in the absence of USP50 and WRN, suggesting that RECQL4 and RECQL5 co-operate to provide a back-up pathway for WRN in replication (figure 6.1a). This finding is novel as there are no previous reports showing that RECQ helicases can act as a substitute when one is absent, or a method for co-ordinating the recruitment or activity of the RECQ helicases on DNA. We showed that USP50 influences WRN localisation to chromatin after HU-induced replication stress, suggesting that USP50 may act as a regulator

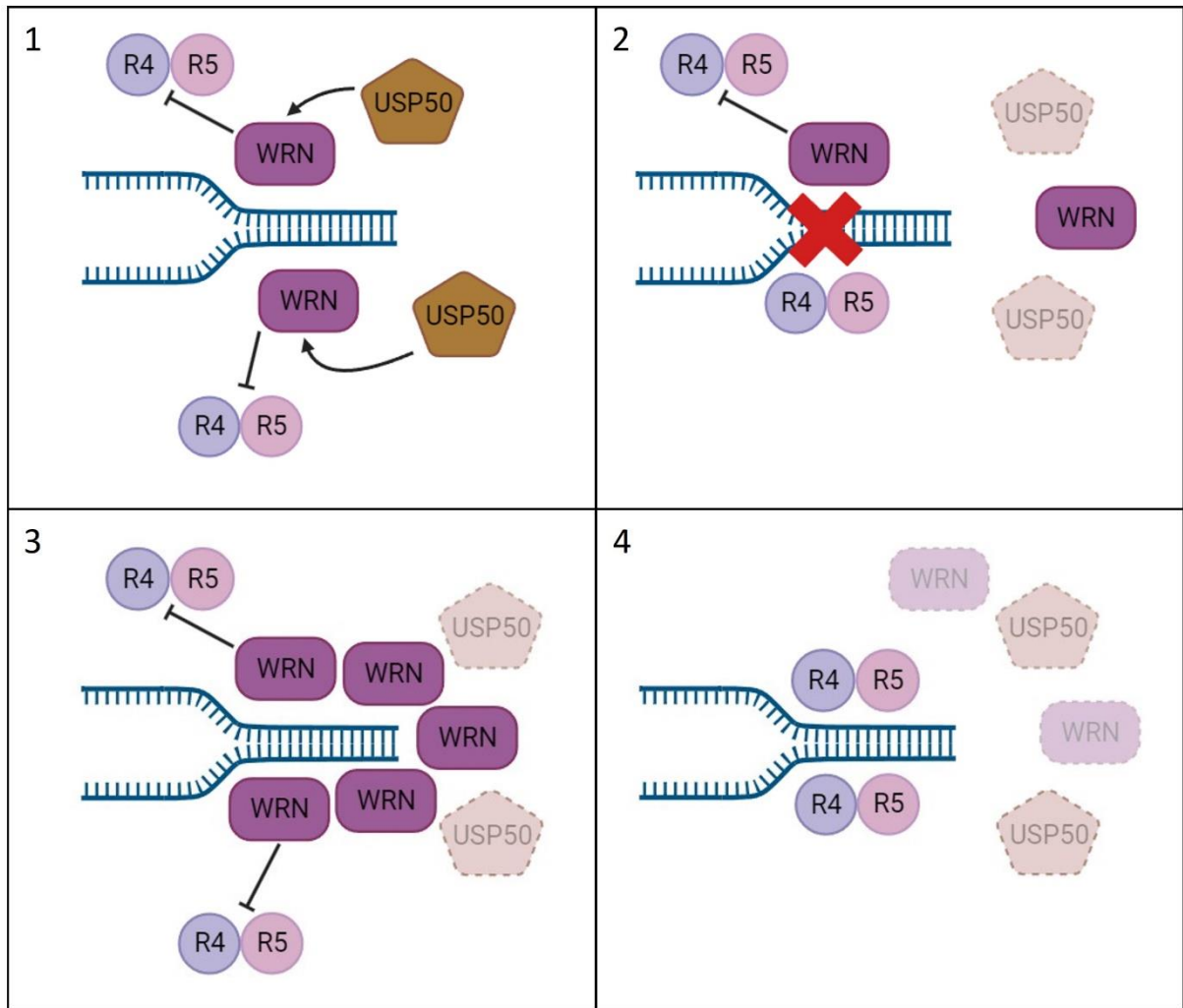


Figure 6.1a

An illustration of the hypothesised mechanism behind the USP50-WRN-RECQL4-RECQL5 axis. 1) In normal cells, USP50 recruits WRN to stalled forks to aid replication progression. WRN inhibits inappropriate use of RECQL4 and RECQL5. 2) USP50 depletion results in a reduction in WRN at stalled forks, leading to inappropriate use of RECQL4 and RECQL5 and replication fork stalling. 3) Wild-type WRN overexpression rescues fork stalling in USP50-depleted cells through increased presence at replication forks and inhibition of inappropriate use of RECQL4 and RECQL5. 4) In the absence of USP50 and WRN, RECQL4 and RECQL5 co-operate to restore replication progression. Created with BioRender.com.

and co-ordinator of multiple RECQ helicases at stalled replication forks. It is possible that the defects in replication-associated processes such as fork stalling and collapse into DSBs seen in cells isolated from Werner syndrome patients would be worsened if RECQL4 or RECQL5 were unavailable, as we showed that RECQL4-RECQL5 may be able to act as a back-up pathway to rescue ongoing replication in the absence of WRN. Indeed, RECQL5 has been found to be enriched at sites of DNA damage in WS cells and promotes cell survival (Popuri *et al.*, 2013). It would be interesting to investigate whether there are any WS patients with concurrent RECQL4 or RECQL5 mutations, or whether tumours in WS patients are competent for RECQL4 and RECQL5.

Moving into colorectal cancer cell lines, we observed a similar effect on fork stalling upon USP50 and WRN co-depletion in MSS cells, but not MSI cells. This result suggested to us that WRN-dependent MSI cells are wired differently to MSS cells. This could be due to faulty MMR-induced mutations in microsatellite-containing genes of MSI cells. HCT116 (MSI) cells have a reported RECQL1 frameshift mutation, and RKO (MSI) cells have a reported RECQL5 point mutation (depmap.org). None of the MSS cells used in this thesis contain known mutations in RECQ helicases, including HeLa cells. It is therefore also possible that mutations in the other RECQ helicases prevent rescue of replication progression in the absence of USP50 and WRN. Western blotting in the colorectal cancer cell lines showed that WRN depletion led to the loss of several DDR proteins in WRN-sensitive MSI cells only. This could also help explain the differences seen between WRN-depleted MSS and MSI cells, as the effects seen may not be a direct effect of WRN loss, but could be due to loss of EXO1, RAD51, BARD1 or any of the other proteins affected by WRN depletion. We found no differences in cell survival or viability between MSS and MSI cells after treatment with the WRNi NSC 617145, which could indicate

that this small molecule inhibitor may not be an effective treatment for patients with an MSI-high tumour in the clinic, and that alternative WRN-targeting therapies are needed to better treat patient with MSI-high tumours.

In chapter 5 we examined locations and numbers of DSBs occurring in siNTC- and siUSP50-treated cells and observed a loss of DSBs proximal to TSSs when USP50 was depleted. This provides an exciting opportunity to investigate a potential, unexpected role for USP50 in transcription, which could help us to understand the roles of USP50 better. We hypothesise that USP50 promotes TRCs through encouraging transcription progression, and that loss of USP50 leads to a reduction in transcription, TRCs and subsequent DSBs near TSSs.

Together these data point towards a primary role for USP50 and WRN in promoting ongoing replication in MSS cells, with RECQL4 and RECQL5 providing a back-up pathway to rescue fork stalling.

7. References

- Adelfalk, C., Scherthan, H., Hirsch-Kauffmann, M., & Schweiger, M. (2005). Nuclear deformation characterizes Werner syndrome cells. *Cell Biology International*, 29(12), 1032–1037.
- Afgan, E., Nekrutenko, A., Grünig, B. A., Blankenberg, D., Goecks, J., Schatz, M. C., Ostrovsky, A. E., Mahmoud, A., Lonie, A. J., Syme, A., Fouilloux, A., Bretaudeau, A., Nekrutenko, A., Kumar, A., Eschenlauer, A. C., Desanto, A. D., Guerler, A., Serrano-Solano, B., Batut, B., ... Briggs, P. J. (2022). The Galaxy platform for accessible, reproducible and collaborative biomedical analyses: 2022 update. *Nucleic Acids Research*, 50(W1), W345–W351.
- Aggarwal, M., Banerjee, T., Sommers, J. A., Iannascoli, C., Pichierri, P., Shoemaker, R. H., & Brosh, R. M. (2013). Werner syndrome helicase has a critical role in DNA damage responses in the absence of a functional Fanconi anemia pathway. *Cancer Research*, 73(17), 5497–5507.
- Aggarwal, M., Sommers, J. A., Morris, C., & Brosh, R. M. (2010). Delineation of WRN Helicase Function with EXO1 in the Replicational Stress Response. *DNA Repair*, 9(7), 765.
- Ammazzalorso, F., Pirzio, L. M., Bignami, M., Franchitto, A., & Pichierri, P. (2010). ATR and ATM differently regulate WRN to prevent DSBs at stalled replication forks and promote replication fork recovery. *The EMBO Journal*, 29(18), 3156.
- Anand, R. P., Lovett, S. T., & Haber, J. E. (2013). Break-Induced DNA Replication. *Cold Spring Harbor Perspectives in Biology*, 5(12).
- André, T., Shiu, K.-K., Kim, T. W., Jensen, B. V., Jensen, L. H., Punt, C., Smith, D., Garcia-Carbonero, R., Benavides, M., Gibbs, P., de la Fouchardiere, C., Rivera, F., Elez, E., Bendell, J.,

Le, D. T., Yoshino, T., Van Cutsem, E., Yang, P., Farooqui, M. Z. H., ... Diaz, L. A. (2020). Pembrolizumab in Microsatellite-Instability–High Advanced Colorectal Cancer. *New England Journal of Medicine*, 383(23), 2207–2218.

Aparicio, T., Guillo, E., Coloma, J., Montoya, G., & Méndez, J. (2009). The human GINS complex associates with Cdc45 and MCM and is essential for DNA replication. *Nucleic Acids Research*, 37(7), 2087.

Arora, A., Agarwal, D., Abdel-Fatah, T. M. A., Lu, H., Croteau, D. L., Moseley, P., Aleskandarany, M. A., Green, A. R., Ball, G., Rakha, E. A., Chan, S. Y. T., Ellis, I. O., Wang, L. L., Zhao, Y., Balajee, A. S., Bohr, V. A., & Madhusudan, S. (2016). RECQL4 helicase has oncogenic potential in sporadic breast cancers. *The Journal of Pathology*, 238(4), 495.

Awasthi, P., Foiani, M., & Kumar, A. (2015). ATM and ATR signaling at a glance. *Journal of Cell Science*, 128(23), 4255–4262.

Bai, G., Kermi, C., Stoy, H., Schiltz, C. J., Bacal, J., Zaino, A. M., Hadden, M. K., Eichman, B. F., Lopes, M., & Cimprich, K. A. (2020). HLF Promotes Fork Reversal, Limiting Replication Stress Resistance and Preventing Multiple Mechanisms of Unrestrained DNA Synthesis. *Molecular Cell*, 78(6), 1237-1251.e7.

Bainbridge, L. J., Teague, R., & Doherty, A. J. (2021). Repriming DNA synthesis: an intrinsic restart pathway that maintains efficient genome replication. *Nucleic Acids Research*, 49(9), 4831–4847.

Balajee, A. S., Machwe, A., May, A., Gray, M. D., Oshima, J., Martin, G. M., Nehlin, J. O., Brosh, R., Orren, D. K., & Bohr, V. A. (1999). The Werner syndrome protein is involved in RNA polymerase II transcription. *Molecular Biology of the Cell*, 10(8), 2655–2668.

Banerjee, T., Aggarwal, M., Sommers, J. A., & Brosh, R. M. (2016). Biochemical and cell biological assays to identify and characterize DNA helicase inhibitors. *Methods (San Diego, Calif.)*, 108, 130–141.

Baranovskiy, A. G., Babayeva, N. D., Suwa, Y., Gu, J., Pavlov, Y. I., & Tahirov, T. H. (2014). Structural basis for inhibition of DNA replication by aphidicolin. *Nucleic Acids Research*, 42(22), 14013.

Bass, T. E., Luzwick, J. W., Kavanaugh, G., Carroll, C., Dungrawala, H., Glick, G. G., Feldkamp, M. D., Putney, R., Chazin, W. J., & Cortez, D. (2016). ETAA1 acts at stalled replication forks to maintain genome integrity. *Nature Cell Biology*, 18(11), 1185–1195.

Baynton, K., Otterlei, M., Bjørås, M., Von Kobbe, C., Bohr, V. A., & Seeberg, E. (2003). WRN Interacts Physically and Functionally with the Recombination Mediator Protein RAD52. *Journal of Biological Chemistry*, 278(38), 36476–36486.

Bębenek, A., & Ziuzia-Graczyk, I. (2018). Fidelity of DNA replication—a matter of proofreading. *Current Genetics*, 64(5), 985.

Berezney, R., Dubey, D. D., & Huberman, J. A. (2000). Heterogeneity of eukaryotic replicons, replicon clusters, and replication foci. *Chromosoma*, 108(8), 471–484.

Berti, M., Chaudhuri, A. R., Thangavel, S., Gomathinayagam, S., Kenig, S., Vujanovic, M., Odreman, F., Glatter, T., Graziano, S., Mendoza-Maldonado, R., Marino, F., Lucic, B., Biasin, V.,

- Gstaiger, M., Aebersold, R., Sidorova, J. M., Monnat, R. J., Lopes, M., & Vindigni, A. (2013). Human RECQ1 promotes restart of replication forks reversed by DNA topoisomerase I inhibition. *Nature Structural & Molecular Biology*, 20(3), 347.
- Bétous, R., Couch, F. B., Mason, A. C., Eichman, B. F., Manosas, M., & Cortez, D. (2013). Substrate-selective repair and restart of replication forks by DNA translocases. *Cell Reports*, 3(6), 1958–1969.
- Bhat, K. P., & Cortez, D. (2018). RPA and RAD51: Fork reversal, fork protection, and genome stability. *Nature Structural & Molecular Biology*, 25(6), 446.
- Bhatia, V., Barroso, S. I., García-Rubio, M. L., Tumini, E., Herrera-Moyano, E., & Aguilera, A. (2014). BRCA2 prevents R-loop accumulation and associates with TREX-2 mRNA export factor PCID2. *Nature*, 511(7509), 362–365.
- Bhowmick, R., Hickson, I. D., & Liu, Y. (2023). Completing genome replication outside of S phase. *Molecular Cell*, 83(20), 3596–3607.
- Billing, D., Horiguchi, M., Wu-Baer, F., Taglialatela, A., Leuzzi, G., Nanez, S. A., Jiang, W., Zha, S., Szabolcs, M., Lin, C. S., Ciccio, A., & Baer, R. (2018). The BRCT Domains of the BRCA1 and BARD1 Tumor Suppressors Differentially Regulate Homology-Directed Repair and Stalled Fork Protection. *Molecular Cell*, 72(1), 127-139.e8.
- Blander, G., Kipnis, J., Leal, J. F. M., Yu, C. E., Schellenberg, G. D., & Oren, M. (1999). Physical and functional interaction between p53 and the Werner's syndrome protein. *The Journal of Biological Chemistry*, 274(41), 29463–29469.

- Blandert, G., Zalle, N., Daniely, Y., Taplick, J., Gray, M. D., & Oren, M. (2002). DNA Damage-induced Translocation of the Werner Helicase Is Regulated by Acetylation. *Journal of Biological Chemistry*, 277(52), 50934–50940.
- Boland, C. R., Thibodeau, S. N., Hamilton, S. R., Sidransky, D., Eshleman, J. R., Burt, R. W., Meltzer, S. J., Rodriguez-Bigas, M. A., Fodde, R., Ranzani, G. N., & Srivastava, S. (1998). A National Cancer Institute Workshop on Microsatellite Instability for Cancer Detection and Familial Predisposition: Development of International Criteria for the Determination of Microsatellite Instability in Colorectal Cancer. *Cancer Res.* 1998 Nov 15;58(22):5248-57.
- Bonnell, E., Pasquier, E., & Wellinger, R. J. (2021). Telomere Replication: Solving Multiple End Replication Problems. *Frontiers in Cell and Developmental Biology*, 9, 668171.
- Boos, D., & Ferreira, P. (2019). Origin Firing Regulations to Control Genome Replication Timing. *Genes*, 10(3).
- Bowater, R. P., Bohálová, N., & Brázda, V. (2022). Interaction of Proteins with Inverted Repeats and Cruciform Structures in Nucleic Acids. *International Journal of Molecular Sciences*, 23(11).
- Brosh, R. M., Orren, D. K., Nehlin, J. O., Ravn, P. H., Kenny, M. K., Machwe, A., & Bohr, V. A. (1999). Functional and physical interaction between WRN helicase and human replication protein A. *The Journal of Biological Chemistry*, 274(26), 18341–18350.
- Brown, M. W., Kim, Y., Williams, G. M., Huck, J. D., Surtees, J. A., & Finkelstein, I. J. (2016). Dynamic DNA binding licenses a repair factor to bypass roadblocks in search of DNA lesions. *Nature Communications* 2016 7:1, 7(1), 1–12.

- Bruhn, C., Zhou, Z. W., Ai, H., & Wang, Z. Q. (2014). The Essential Function of the MRN Complex in the Resolution of Endogenous Replication Intermediates. *Cell Reports*, 6(1), 182–195.
- Bryant, J. A., & Aves, S. J. (2011). Initiation of DNA replication: functional and evolutionary aspects. *Annals of Botany*, 107(7), 1119.
- Budd, M. E., & Campbell, J. L. (1997). A Yeast Replicative Helicase, Dna2 Helicase, Interacts with Yeast FEN-1 Nuclease in Carrying Out Its Essential Function. *Molecular and Cellular Biology*, 17(4), 2136–2142.
- Bugreev, D. V., Rossi, M. J., & Mazin, A. V. (2011). Cooperation of RAD51 and RAD54 in regression of a model replication fork. *Nucleic Acids Research*, 39(6), 2153.
- Bullock, C. R., Xing, X., & Shcherbakova, P. V. (2020). DNA polymerase δ proofreads errors made by DNA polymerase ϵ . *Proceedings of the National Academy of Sciences of the United States of America*, 117(11), 6035–6041.
- Burgers, P. M. J., & Kunkel, T. A. (2017). Eukaryotic DNA Replication Fork. *Annual Review of Biochemistry*, 86, 417.
- Butler, L. R., Densham, R. M., Jia, J., Garvin, A. J., Stone, H. R., Shah, V., Weekes, D., Festy, F., Beesley, J., & Morris, J. R. (2012). The proteasomal de-ubiquitinating enzyme POH1 promotes the double-strand DNA break response. *The EMBO Journal*, 31(19), 3918.
- Byun, T. S., Pacek, M., Yee, M. C., Walter, J. C., & Cimprich, K. A. (2005). Functional uncoupling of MCM helicase and DNA polymerase activities activates the ATR-dependent checkpoint. *Genes & Development*, 19(9), 1040.

- Cannan, W. J., & Pederson, D. S. (2016). Mechanisms and Consequences of Double-strand DNA Break Formation in Chromatin. *Journal of Cellular Physiology*, 231(1), 3.
- Carroll, C., Bansbach, C. E., Zhao, R., Jung, S. Y., Qin, J., & Cortez, D. (2014). Phosphorylation of a C-terminal auto-inhibitory domain increases SMARCAL1 activity. *Nucleic Acids Research*, 42(2), 918.
- Cayrou, C., Coulombe, P., Puy, A., Rialle, S., Kaplan, N., Segal, E., & Méchali, M. (2012). New insights into replication origin characteristics in metazoans. *Cell Cycle*, 11(4), 658.
- Cayrou, C., Coulombe, P., Vigneron, A., Stanojcic, S., Ganier, O., Peiffer, I., Rivals, E., Puy, A., Laurent-Chabalier, S., Desprat, R., & Méchali, M. (2011). Genome-scale analysis of metazoan replication origins reveals their organization in specific but flexible sites defined by conserved features. *Genome Research*, 21(9), 1438–1449.
- Chan, E. M., Shibue, T., McFarland, J. M., Gaeta, B., Ghandi, M., Dumont, N., Gonzalez, A., McPartlan, J. S., Li, T., Zhang, Y., Bin Liu, J., Lazaro, J. B., Gu, P., Piett, C. G., Apffel, A., Ali, S. O., Deasy, R., Keskula, P., Ng, R. W. S., ... Bass, A. J. (2019). WRN Helicase is a Synthetic Lethal Target in Microsatellite Unstable Cancers. *Nature*, 568(7753), 551.
- Chan, K. L., North, P. S., & Hickson, I. D. (2007). BLM is required for faithful chromosome segregation and its localization defines a class of ultrafine anaphase bridges. *The EMBO Journal*, 26(14), 3397.
- Charbin, A., Bouchoux, C., & Uhlmann, F. (2014). Condensin aids sister chromatid decatenation by topoisomerase II. *Nucleic Acids Research*, 42(1), 340.

Chen, L., Huang, S., Lee, L., Davalos, A., Schiestl, R. H., Campisi, J., & Oshima, J. (2003). WRN, the protein deficient in Werner syndrome, plays a critical structural role in optimizing DNA repair. *Aging Cell*, 2(4), 191–199.

Cheng, W. H., Kusumoto, R., Opresko, P. L., Sui, X. F., Huang, S., Nicolette, M. L., Paull, T. T., Campisi, J., Seidman, M., & Bohr, V. A. (2006). Collaboration of Werner syndrome protein and BRCA1 in cellular responses to DNA interstrand cross-links. *Nucleic Acids Research*, 34(9), 2751.

Cheng, W. H., Von Kobbe, C., Opresko, P. L., Arthur, L. M., Komatsu, K., Seidman, M. M., Carney, J. P., & Bohr, V. A. (2004). Linkage between Werner Syndrome Protein and the Mre11 Complex via Nbs1. *Journal of Biological Chemistry*, 279(20), 21169–21176.

Cheng, W. H., Von Kobbe, C., Opresko, P. L., Fields, K. M., Ren, J., Kufe, D., & Bohr, V. A. (2003). Werner Syndrome Protein Phosphorylation by Abl Tyrosine Kinase Regulates Its Activity and Distribution. *Molecular and Cellular Biology*, 23(18), 6385.

Chilkova, O., Stenlund, P., Isoz, I., Stith, C. M., Grabowski, P., Lundström, E. B., Burgers, P. M., & Johansson, E. (2007). The eukaryotic leading and lagging strand DNA polymerases are loaded onto primer-ends via separate mechanisms but have comparable processivity in the presence of PCNA. *Nucleic Acids Research*, 35(19), 6588–6597.

Choucair, K., Radford, M., Bansal, A., Park, R., & Saeed, A. (2021). Advances in immune therapies for the treatment of microsatellite instability-high/deficient mismatch repair metastatic colorectal cancer (Review). *International Journal of Oncology*, 59(3).

Chung, L., Onyango, D., Guo, Z., Jia, P., Dai, H., Liu, S., Zhou, M., Lin, W., Pang, I., Li, H., Yuan, Y. C., Huang, Q., Zheng, L., Lopes, J., Nicolas, A., Chai, W., Raz, D., Reckamp, K. L., & Shen, B. (2015). The FEN1 E359K germline mutation disrupts the FEN1-WRN interaction and FEN1 GEN activity, causing aneuploidy-associated cancers. *Oncogene*, 34(7), 902.

Cimprich, K. A., & Cortez, D. (2008). ATR: An Essential Regulator of Genome Integrity. *Nature Reviews. Molecular Cell Biology*, 9(8), 616.

Clarke, T. L., & Mostoslavsky, R. (2022). DNA repair as a shared hallmark in cancer and ageing. *Molecular Oncology*, 16(18), 3352.

Cooper, M. P., Machwe, A., Orren, D. K., Brosh, R. M., Ramsden, D., & Bohr, V. A. (2000). Ku complex interacts with and stimulates the Werner protein. *Genes & Development*, 14(8), 907–912.

Cortez, D. (2015). Preventing Replication Fork Collapse to Maintain Genome Integrity. *DNA Repair*, 32, 149.

Cortez, D., Guntuku, S., Qin, J., & Elledge, S. J. (2001). ATR and ATRIP: Partners in checkpoint signaling. *Science*, 294(5547), 1713–1716.

Costa, A., & Diffley, J. F. X. (2022). The Initiation of Eukaryotic DNA Replication. *Annu Rev Biochem*. 2022 Jun 21:91:107-131.

Costa, A., Ilves, I., Tamberg, N., Petojevic, T., Nogales, E., Botchan, M. R., & Berger, J. M. (2011). The structural basis for MCM2–7 helicase activation by GINS and Cdc45. *Nature Structural & Molecular Biology* 2011 18:4, 18(4), 471–477.

- Couch, F. B., Bansbach, C. E., Driscoll, R., Luzwick, J. W., Glick, G. G., Bétous, R., Carroll, C. M., Jung, S. Y., Qin, J., Cimprich, K. A., & Cortez, D. (2013). ATR phosphorylates SMARCA1 to prevent replication fork collapse. *Genes & Development*, 27(14), 1610.
- Croteau, D. L., Popuri, V., Opresko, P. L., & Bohr, V. A. (2014). Human RecQ helicases in DNA repair, recombination, and replication. *Annual Review of Biochemistry*, 83, 519–552.
- Cruz, L., Soares, P., & Correia, M. (2021). Ubiquitin-Specific Proteases: Players in Cancer Cellular Processes. *Pharmaceuticals* 2021, Vol. 14, Page 848, 14(9), 848.
- Daigaku, Y., Keszthelyi, A., Müller, C. A., Miyabe, I., Brooks, T., Retkute, R., Hubank, M., Nieduszynski, C. A., & Carr, A. M. (2015). A global profile of replicative polymerase usage. *Nature Structural & Molecular Biology*, 22(3), 192.
- de Renty, C., Pond, K. W., Yagle, M. K., & Ellis, N. A. (2022). BLM Sumoylation Is Required for Replication Stability and Normal Fork Velocity During DNA Replication. *Frontiers in Molecular Biosciences*, 9, 875102.
- Deem, A., Keszthelyi, A., Blackgrove, T., Vayl, A., Coffey, B., Mathur, R., Chabes, A., & Malkova, A. (2011). Break-Induced Replication Is Highly Inaccurate. *PLoS Biology*, 9(2), 1000594.
- Delacroix, S., Wagner, J. M., Kobayashi, M., Yamamoto, K. I., & Karnitz, L. M. (2007). The Rad9–Hus1–Rad1 (9–1–1) clamp activates checkpoint signaling via TopBP1. *Genes & Development*, 21(12), 1472.
- Deshmukh, A. L., Kumar, C., Singh, D. K., Maurya, P., & Banerjee, D. (2016). Dynamics of replication proteins during lagging strand synthesis: A crossroads for genomic instability and cancer. *DNA Repair*, 42, 72–81.

Dewar, J. M., & Walter, J. C. (2017). Mechanisms of DNA replication termination. *Nature Reviews. Molecular Cell Biology*, 18(8), 507.

Dewar, J. M., Budzowska, M., & Walter, J. C. (2015). The mechanism of DNA replication termination in vertebrates. *Nature*, 525(7569), 345.

Di Marco, S., Hasanova, Z., Kanagaraj, R., Chappidi, N., Altmannova, V., Menon, S., Sedlackova, H., Langhoff, J., Surendranath, K., Hühn, D., Bhowmick, R., Marini, V., Ferrari, S., Hickson, I. D., Krejci, L., & Janscak, P. (2017). RECQ5 Helicase Cooperates with MUS81 Endonuclease in Processing Stalled Replication Forks at Common Fragile Sites during Mitosis. *Molecular Cell*, 66(5), 658-671.e8.

Di Micco, R., Fumagalli, M., Cicalese, A., Piccinin, S., Gasparini, P., Luise, C., Schurra, C., Garré, M., Giovanni Nuciforo, P., Bensimon, A., Maestro, R., Giuseppe Pelicci, P., & D'Adda Di Fagagna, F. (2006). Oncogene-induced senescence is a DNA damage response triggered by DNA hyper-replication. *Nature*, 444(7119), 638–642.

Díaz-Talavera, A., Montero-Conde, C., Leandro-García, L. J., & Robledo, M. (2022). PrimPol: A Breakthrough among DNA Replication Enzymes and a Potential New Target for Cancer Therapy. *Biomolecules*, 12(2).

Ding, Q., & Koren, A. (2020). Positive and Negative Regulation of DNA Replication Initiation. *Trends in Genetics*, 36(11), 868–879.

Dmowski, M., Jedrychowska, M., Makiela-Dzbenska, K., Denkiewicz-Kruk, M., Sharma, S., Chabes, A., Araki, H., & Fijalkowska, I. J. (2022). Increased contribution of DNA polymerase

delta to the leading strand replication in yeast with an impaired CMG helicase complex. *DNA Repair*, 110, 103272.

Dobbs, F. M., van Eijk, P., Fellows, M. D., Loiacono, L., Nitsch, R., & Reed, S. H. (2022). Precision digital mapping of endogenous and induced genomic DNA breaks by INDUCE-seq. *Nature Communications*, 13(1).

Dominguez-Valentin, M., Sampson, J. R., Seppälä, T. T., ten Broeke, S. W., Plazzer, J. P., Nakken, S., Engel, C., Aretz, S., Jenkins, M. A., Sunde, L., Bernstein, I., Capella, G., Balaguer, F., Thomas, H., Evans, D. G., Burn, J., Greenblatt, M., Hovig, E., de Vos tot Nederveen Cappel, W. H., ... Møller, P. (2020). Cancer risks by gene, age, and gender in 6350 carriers of pathogenic mismatch repair variants: findings from the Prospective Lynch Syndrome Database. *Genetics in Medicine*, 22(1), 15.

Dorn, E. S., & Cook, J. G. (2011). Nucleosomes in the neighborhood: New roles for chromatin modifications in replication origin control. *Epigenetics*, 6(5), 552.

Duursma, A. M., Driscoll, R., Elias, J. E., & Cimprich, K. A. (2013). A role for the MRN complex in ATR activation through TOPBP1 recruitment. *Molecular Cell*, 50(1), 116.

Duval, A., Reperant, M., & Hamelin, R. (2002). Comparative analysis of mutation frequency of coding and non coding short mononucleotide repeats in mismatch repair deficient colorectal cancers. *Oncogene*, 21(52), 8062–8066.

Eckert, K. A., & Hile, S. E. (2009). Every Microsatellite is Different: Intrinsic DNA Features Dictate Mutagenesis of Common Microsatellites Present in the Human Genome. *Molecular Carcinogenesis*, 48(4), 379.

- Ekholm-Reed, S., Méndez, J., Tedesco, D., Zetterberg, A., Stillman, B., & Reed, S. I. (2004). Deregulation of cyclin E in human cells interferes with prereplication complex assembly. *Journal of Cell Biology*, 165(6), 789–800.
- Ekundayo, B., & Bleichert, F. (2019). Origins of DNA replication. *PLoS Genetics*, 15(9).
- Evrin, C., Clarke, P., Zech, J., Lurz, R., Sun, J., Uhle, S., Li, H., Stillman, B., & Speck, C. (2009). A double-hexameric MCM2-7 complex is loaded onto origin DNA during licensing of eukaryotic DNA replication. *Proceedings of the National Academy of Sciences of the United States of America*, 106(48), 20240.
- Fang, Y., Tsao, C. C., Goodman, B. K., Furumai, R., Tirado, C. A., Abraham, R. T., & Wang, X. F. (2004). ATR functions as a gene dosage-dependent tumor suppressor on a mismatch repair-deficient background. *The EMBO Journal*, 23(15), 3164–3174.
- Fasching, C. L., Cejka, P., Kowalczykowski, S. C., & Heyer, W. D. (2015). Top3-Rmi1 dissolve Rad51-mediated D-loops by a topoisomerase-based mechanism. *Molecular Cell*, 57(4), 595.
- Flynn, R. L., & Zou, L. (2011). ATR: a Master Conductor of Cellular Responses to DNA Replication Stress. *Trends in Biochemical Sciences*, 36(3), 133.
- Fragkos, M., Ganier, O., Coulombe, P., & Méchali, M. (2015). DNA replication origin activation in space and time. *Nature Reviews Molecular Cell Biology* 2015 16:6, 16(6), 360–374.
- Franchitto, A., Pirzio, L. M., Prosperi, E., Sapora, O., Bignami, M., & Pichierri, P. (2008). Replication fork stalling in WRN-deficient cells is overcome by prompt activation of a MUS81-dependent pathway. *The Journal of Cell Biology*, 183(2), 241.

Friedrich, K., Lee, L., Leistriz, D. F., Nürnberg, G., Saha, B., Hisama, F. M., Eyman, D. K., Lessel, D., Nürnberg, P., Li, C., Garcia-F-Villalta, M. J., Kets, C. M., Schmidtke, J., Cruz, V. T., Van Den Akker, P. C., Boak, J., Peter, D., Compoginis, G., Cefle, K., ... Oshima, J. (2010). WRN mutations in Werner syndrome patients: genomic rearrangements, unusual intronic mutations and ethnic-specific alterations. *Human Genetics*, 128(1), 103.

Fugger, K., Mistrik, M., Neelsen, K. J., Yao, Q., Zellweger, R., Kousholt, A. N., Haahr, P., Chu, W. K., Bartek, J., Lopes, M., Hickson, I. D., & Sørensen, C. S. (2015). FBH1 Catalyzes Regression of Stalled Replication Forks. *Cell Reports*, 10(10), 1749–1757.

Furnari, B., Rhind, N., & Russell, P. (1997). Cdc25 mitotic inducer targeted by chk1 DNA damage checkpoint kinase. *Science (New York, N.Y.)*, 277(5331), 1495–1497.

Gaillard, H., García-Muse, T., & Aguilera, A. (2015). Replication stress and cancer. *Nature Reviews Cancer* 2015 15:5, 15(5), 276–289.

Garcia, P. L., Liu, Y., Jiricny, J., West, S. C., & Janscak, P. (2004). Human RECQ5 β , a protein with DNA helicase and strand-annealing activities in a single polypeptide. *The EMBO Journal*, 23(14), 2882.

García-Muse, T., & Aguilera, A. (2016). Transcription–replication conflicts: how they occur and how they are resolved. *Nature Reviews Molecular Cell Biology* 2016 17:9, 17(9), 553–563.

Gari, K., Décaillot, C., Delannoy, M., Wu, L., & Constantinou, A. (2008). Remodeling of DNA replication structures by the branch point translocase FANCM. *Proceedings of the National Academy of Sciences of the United States of America*, 105(42), 16107.

Garrido-Ramos, M. A. (2017). Satellite DNA: An Evolving Topic. *Genes* 2017, Vol. 8, Page 230, 8(9), 230.

Gaymes, T. J., Mohamedali, A. M., Patterson, M., Matto, N., Smith, A., Kulasekararaj, A., Chelliah, R., Curtin, N., Farzaneh, F., Shall, S., & Mufti, G. J. (2013). Microsatellite instability induced mutations in DNA repair genes CtIP and MRE11 confer hypersensitivity to poly (ADP-ribose) polymerase inhibitors in myeloid malignancies. *Haematologica*, 98(9), 1397–1406.

Ge, X. Q., & Blow, J. J. (2010). Chk1 inhibits replication factory activation but allows dormant origin firing in existing factories. *The Journal of Cell Biology*, 191(7), 1285–1297.

Ge, X. Q., Jackson, D. A., & Blow, J. J. (2007). Dormant origins licensed by excess Mcm2–7 are required for human cells to survive replicative stress. *Genes & Development*, 21(24), 3331.

Giannini, G., Rinaldi, C., Ristori, E., Ambrosini, M. I., Cerignoli, F., Viel, A., Bidoli, E., Berni, S., D'Amati, G., Scambia, G., Frati, L., Screpanti, I., & Gulino, A. (2004). Mutations of an intronic repeat induce impaired MRE11 expression in primary human cancer with microsatellite instability. *Oncogene*, 23(15), 2640–2647.

Gillespie, P. J., & Blow, J. J. (2022). DDK: The Outsourced Kinase of Chromosome Maintenance. *Biology* 2022, Vol. 11, Page 877, 11(6), 877.

Gilson, E., & Géli, V. (2007). How telomeres are replicated. *Nature Reviews Molecular Cell Biology* 2007 8:10, 8(10), 825–838.

Gonzalez-Huici, V., Szakal, B., Urulangodi, M., Psakhye, I., Castellucci, F., Menolfi, D., Rajakumara, E., Fumasoni, M., Bermejo, R., Jentsch, S., & Branzei, D. (2014). DNA bending

facilitates the error-free DNA damage tolerance pathway and upholds genome integrity. The EMBO Journal, 33(4), 327.

Goto, M., Miller, R. W., Ishikawa, Y., & Sugano, H. (1996). Excess of Rare Cancers in Werner Syndrome (Adult Progeria). 5, 239–246.

Gravel, S., Chapman, J. R., Magill, C., & Jackson, S. P. (2008). DNA helicases Sgs1 and BLM promote DNA double-strand break resection. Genes & Development, 22(20), 2767–2772.

Gray, M. D., Shen, J. C., Kamath-Loeb, A. S., Blank, A., Sopher, B. L., Martin, G. M., Oshima, J., & Loeb, L. A. (1997). The Werner syndrome protein is a DNA helicase. Nature Genetics, 17(1), 100–103.

Gray, M. D., Wang, L., Youssoufian, H., Martin, G. M., & Oshima, J. (1998). Werner helicase is localized to transcriptionally active nucleoli of cycling cells. Experimental Cell Research, 242(2), 487–494.

Gudmundsrud, R., Skjånes, T. H., Gilmour, B. C., Caponio, D., Lautrup, S., & Fang, E. F. (2021). Crosstalk among DNA Damage, Mitochondrial Dysfunction, Impaired Mitophagy, Stem Cell Attrition, and Senescence in the Accelerated Ageing Disorder Werner Syndrome. Cytogenetic and Genome Research, 161(6–7), 297.

Guilliam, T. A., & Doherty, A. J. (2017). PrimPol—Prime Time to Reprime. Genes, 8(1).

Guilliam, T. A., Bailey, L. J., Brissett, N. C., & Doherty, A. J. (2016). PolDIP2 interacts with human PrimPol and enhances its DNA polymerase activities. Nucleic Acids Research, 44(7), 3317.

- Guo, C., Kumagai, A., Schlacher, K., Shevchenko, A., Shevchenko, A., & Dunphy, W. G. (2015). Interaction of Chk1 with Treslin negatively regulates the initiation of chromosomal DNA replication. *Molecular Cell*, 57(3), 492–505.
- Gupta, A., Hunt, C. R., Chakraborty, S., Pandita, R. K., Yordy, J., Ramnarain, D. B., Horikoshi, N., & Pandita, T. K. (2014). Role of 53BP1 in the Regulation of DNA Double-Strand Break Repair Pathway Choice. *Radiation Research*, 181(1), 1.
- Gupta, P., Majumdar, A. G., & Patro, B. S. (2022). Non-enzymatic function of WRN RECQL helicase regulates removal of topoisomerase-I-DNA covalent complexes and triggers NF- κ B signaling in cancer. *Aging Cell*, 21(6).
- Hampel, H., Frankel, W. L., Martin, E., Arnold, M., Khanduja, K., Kuebler, P., Nakagawa, H., Sotamaa, K., Prior, T. W., Westman, J., Panescu, J., Fix, D., Lockman, J., Comeras, I., & de la Chapelle, A. (2005). Screening for the Lynch syndrome (hereditary nonpolyposis colorectal cancer). *The New England Journal of Medicine*, 352(18), 1851–1860.
- Hand, R., & German, J. (1975). A retarded rate of DNA chain growth in Bloom's syndrome. *Proceedings of the National Academy of Sciences of the United States of America*, 72(2), 758.
- Hao, S., Tong, J., Jha, A., Risnik, D., Lizardo, D., Lu, X., Goel, A., Opresko, P. L., Yu, J., & Zhang, L. (2022). Synthetical lethality of Werner helicase and mismatch repair deficiency is mediated by p53 and PUMA in colon cancer. *Proceedings of the National Academy of Sciences of the United States of America*, 119(51).

Hashimoto, Y., Puddu, F., & Costanzo, V. (2012). RAD51 and MRE11 dependent reassembly of uncoupled CMG helicase complex at collapsed replication forks. *Nature Structural & Molecular Biology*, 19(1), 17.

Heintzman, D. R., Campos, L. V., Byl, J. A. W., Osheroff, N., & Dewar, J. M. (2019). Topoisomerase II Is Crucial for Fork Convergence during Vertebrate Replication Termination. *Cell Reports*, 29(2), 422.

Heller, R. C., Kang, S., Lam, W. M., Chen, S., Chan, C. S., & Bell, S. P. (2011). Eukaryotic origin-dependent DNA replication in vitro reveals sequential action of DDK and S-CDK kinases. *Cell*, 146(1), 80–91.

Hertz, E. P. T., Vega, I. A. de, Kruse, T., Wang, Y., Hendriks, I. A., Bizard, A. H., Eugui-Anta, A., Hay, R. T., Nielsen, M. L., Nilsson, J., Hickson, I. D., & Mailand, N. (2023). The SUMO–NIP45 pathway processes toxic DNA catenanes to prevent mitotic failure. *Nature Structural & Molecular Biology* 2023 30:9, 30(9), 1303–1313.

Higgs, M. R., Reynolds, J. J., Winczura, A., Blackford, A. N., Borel, V., Miller, E. S., Zlatanou, A., Niemiuszczy, J., Ryan, E. L., Davies, N. J., Stankovic, T., Boulton, S. J., Niedzwiedz, W., & Stewart, G. S. (2015). BOD1L Is Required to Suppress Deleterious Resection of Stressed Replication Forks. *Molecular Cell*, 59(3), 462–477.

Huang, S., Lee, L., Hanson, N. B., Lenaerts, C., Hoehn, H., Poot, M., Rubin, C. D., Chen, D. F., Yang, C. C., Juch, H., Dorn, T., Spiegel, R., Oral, E. A., Abid, M., Battisti, C., Lucci-Cordisco, E., Neri, G., Steed, E. H., Kidd, A., ... Oshima, J. (2006). The Spectrum of WRN Mutations in Werner Syndrome Patients. *Human Mutation*, 27(6), 558.

- Hughes, C. R., & Queller, D. C. (1993). Detection of highly polymorphic microsatellite loci in a species with little allozyme polymorphism. *Molecular Ecology*, 2(3), 131–137.
- Iannascoli, C., Palermo, V., Murfuni, I., Franchitto, A., & Pichierri, P. (2015). The WRN exonuclease domain protects nascent strands from pathological MRE11/EXO1-dependent degradation. *Nucleic Acids Research*, 43(20), 9788.
- Imamura, O., Fujita, K., Itoh, C., Takeda, S., Furuichi, Y., & Matsumoto, T. (2002). Werner and Bloom helicases are involved in DNA repair in a complementary fashion. *Oncogene* 2002 21:6, 21(6), 954–963.
- Islam, M. N., Fox, D., Guo, R., Enomoto, T., & Wang, W. (2010). RecQL5 promotes genome stabilization through two parallel mechanisms--interacting with RNA polymerase II and acting as a helicase. *Molecular and Cellular Biology*, 30(10), 2460–2472.
- Izumi, M., Yatagai, F., & Hanaoka, F. (2001). Cell Cycle-dependent Proteolysis and Phosphorylation of Human Mcm10. *Journal of Biological Chemistry*, 276(51), 48526–48531.
- Javle, M., & Curtin, N. J. (2011). The role of PARP in DNA repair and its therapeutic exploitation. *British Journal of Cancer*, 105(8), 1114.
- Jones, R. M., Mortusewicz, O., Afzal, I., Lorvellec, M., García, P., Helleday, T., & Petermann, E. (2012). Increased replication initiation and conflicts with transcription underlie Cyclin E-induced replication stress. *Oncogene* 2013 32:32, 32(32), 3744–3753.
- Kadyrov, F. A., Dzantiev, L., Constantin, N., & Modrich, P. (2006). Endonucleolytic function of MutL α in human mismatch repair. *Cell*, 126(2), 297–308.

Kamath-Loeb, A. S., Loeb, L. A., Johansson, E., Burgers, P. M. J., & Fry, M. (2001). Interactions between the Werner Syndrome Helicase and DNA Polymerase δ Specifically Facilitate Copying of Tetraplex and Hairpin Structures of the d(CGG)_n Trinucleotide Repeat Sequence. *Journal of Biological Chemistry*, 276(19), 16439–16446.

Kamath-Loeb, A., Loeb, L. A., & Fry, M. (2012). The Werner Syndrome Protein Is Distinguished from the Bloom Syndrome Protein by Its Capacity to Tightly Bind Diverse DNA Structures. *PLoS ONE*, 7(1), 30189.

Kamburova, Z. B., Dimitrova, P. D., Dimitrova, D. S., Kovacheva, K. S., Popovska, S. L., & Nikolova, S. E. (2023). Lynch-like syndrome with germline WRN mutation in Bulgarian patient with synchronous endometrial and ovarian cancer. *Hereditary Cancer in Clinical Practice*, 21(1), 1–8.

Karanam, K., Kafri, R., Loewer, A., & Lahav, G. (2012). Quantitative live cell imaging reveals a gradual shift between DNA repair mechanisms and a maximal use of HR in mid-S phase. *Molecular Cell*, 47(2), 320.

Karmakar, P., Piotrowski, J., Brosh, R. M., Sommers, J. A., Lees Miller, S. P., Cheng, W. H., Snowden, C. M., Ramsden, D. A., & Bohr, V. A. (2002). Werner Protein Is a Target of DNA-dependent Protein Kinase in Vivo and in Vitro, and Its Catalytic Activities Are Regulated by Phosphorylation. *Journal of Biological Chemistry*, 277(21), 18291–18302.

Karras, G. I., Fumasoni, M., Sienski, G., Vanoli, F., Branzei, D., & Jentsch, S. (2013). Noncanonical role of the 9-1-1 clamp in the error-free DNA damage tolerance pathway. *Molecular Cell*, 49(3), 536–546.

Kategaya, L., Perumal, S. K., Hager, J. H., & Belmont, L. D. (2019). Werner Syndrome Helicase Is Required for the Survival of Cancer Cells with Microsatellite Instability. *IScience*, 13, 488.

Kawabe, Y. ichi, Seki, M., Yoshimura, A., Nishino, K., Hayashi, T., Takeuchi, T., Iguchi, S., Kusa, Y., Ohtsuki, M., Tsuyama, T., Imamura, O., Matsumoto, T., Furuichi, Y., Tada, S., & Enomoto, T. (2006). Analyses of the interaction of WRNIP1 with Werner syndrome protein (WRN) in vitro and in the cell. *DNA Repair*, 5(7), 816–828.

Kitamura, E., Blow, J. J., & Tanaka, T. U. (2006). Live-cell imaging reveals replication of individual replicons in eukaryotic replication factories. *Cell*, 125(7), 1297–1308.

Kolinjivadi, A. M., Sannino, V., De Antoni, A., Zadorozhny, K., Kilkenny, M., Técher, H., Baldi, G., Shen, R., Ciccio, A., Pellegrini, L., Krejci, L., & Costanzo, V. (2017). Smarcal1-Mediated Fork Reversal Triggers Mre11-Dependent Degradation of Nascent DNA in the Absence of Brca2 and Stable Rad51 Nucleofilaments. *Molecular Cell*, 67(5), 867.

Kolodner, R. D., & Marsischky, G. T. (1999). Eukaryotic DNA mismatch repair. *Current Opinion in Genetics & Development*, 9(1), 89–96.

Kondratick, C. M., Washington, M. T., & Spies, M. (2021). Making choices: DNA replication fork recovery mechanisms. *Seminars in Cell & Developmental Biology*, 113, 27–37.

Koshizaka, M., Maezawa, Y., Maeda, Y., Shoji, M., Kato, H., Kaneko, H., Ishikawa, T., Kinoshita, D., Kobayashi, K., Kawashima, J., Sekiguchi, A., Motegi, S. ichiro, Nakagami, H., Yamada, Y., Tsukamoto, S., Taniguchi, A., Sugimoto, K., Shoda, Y., Hashimoto, K., ... Yokote, K. (2020). Time gap between the onset and diagnosis in Werner syndrome: a nationwide survey and the 2020 registry in Japan. *Aging (Albany NY)*, 12(24), 24940.

- Kotsantis, P., Petermann, E., & Boulton, S. J. (2018). Mechanisms of oncogene-induced replication stress: Jigsaw falling into place. In *Cancer Discovery* (Vol. 8, Issue 5, pp. 537–555).
- Kotsantis, P., Silva, L. M., Irmischer, S., Jones, R. M., Folkes, L., Gromak, N., & Petermann, E. (2016). Increased global transcription activity as a mechanism of replication stress in cancer. *Nature Communications*, 7.
- Koundrioukoff, S., Carignon, S., Técher, H., Letessier, A., Brison, O., & Debatisse, M. (2013). Stepwise Activation of the ATR Signaling Pathway upon Increasing Replication Stress Impacts Fragile Site Integrity. *PLoS Genetics*, 9(7).
- Kramara, J., Osia, B., Malkova, A. (2018). Break-Induced Replication: The Where, The Why, and The How. *Trends in Genetics*, 34(7), 518–531.
- Kumagai, A., Lee, J., Yoo, H. Y., & Dunphy, W. G. (2006). TopBP1 activates the ATR-ATRIP complex. *Cell*, 124(5), 943–955.
- Kumar, R., Nagpal, G., Kumar, V., Usmani, S. S., Agrawal, P., & Raghava, G. P. S. (2019). HumCFS: A database of fragile sites in human chromosomes. *BMC Genomics*, 19(9), 1–8.
- Kunkel, T. A., & Burgers, P. M. J. (2017). Arranging eukaryotic nuclear DNA polymerases for replication: Specific interactions with accessory proteins arrange Pols α , δ , and ϵ in the replisome for leading-strand and lagging-strand DNA replication. *BioEssays : News and Reviews in Molecular, Cellular and Developmental Biology*, 39(8).
- Kunkel, T. A., & Erie, D. A. (2015). Eukaryotic Mismatch Repair in Relation to DNA Replication. *Annual Review of Genetics*, 49, 291.

- Kuo, L. J., & Yang, L. X. (2008). γ -H2AX - A Novel Biomarker for DNA Double-strand Breaks. In *Vivo*, 22(3), 305–309.
- Kusumoto, R., Dawut, L., Marchetti, C., Jae, W. L., Vindigni, A., Ramsden, D., & Bohr, V. A. (2008). Werner protein cooperates with the XRCC4-DNA ligase IV complex in end-processing. *Biochemistry*, 47(28), 7548–7556.
- Kusumoto-Matsuo, R., Ghosh, D., Karmakar, P., May, A., Ramsden, D., & Bohr, V. A. (2014). Serines 440 and 467 in the Werner syndrome protein are phosphorylated by DNA-PK and affects its dynamics in response to DNA double strand breaks. *Aging*, 6(1), 70–81.
- Kusumoto-Matsuo, R., Opresko, P. L., Ramsden, D., Tahara, H., & Bohr, V. A. (2010). Cooperation of DNA-PKcs and WRN helicase in the maintenance of telomeric D-loops. *Aging*, 2(5), 274–284.
- Kuzminov, A. (2001). Single-strand interruptions in replicating chromosomes cause double-strand breaks. *Proceedings of the National Academy of Sciences of the United States of America*, 98(15), 8241–8246.
- Labib, K., & de Piccoli, G. (2011). Surviving chromosome replication: the many roles of the S-phase checkpoint pathway. *Philosophical Transactions of the Royal Society B: Biological Sciences*, 366(1584), 3554.
- Lachapelle, S., Gagné, J. P., Garand, C., Desbiens, M., Coulombe, Y., Bohr, V. A., Hendzel, M. J., Masson, J. Y., Poirier, G. G., & Lebel, M. (2011). Proteome-wide Identification of WRN-Interacting Proteins in Untreated and Nuclease-Treated Samples. *Journal of Proteome Research*, 10(3), 1216.

- Lachaud, C., Moreno, A., Marchesi, F., Toth, R., Blow, J. J., & Rouse, J. (2016). Ubiquitinated Fancd2 recruits Fan1 to stalled replication forks to prevent genome instability. *Science (New York, N.Y.)*, 351(6275), 846.
- Langmead, B., & Salzberg, S. L. (2012). Fast gapped-read alignment with Bowtie 2. *Nature Methods* 2012 9:4, 9(4), 357–359.
- Laud, P. R., Multani, A. S., Bailey, S. M., Wu, L., Ma, J., Kingsley, C., Lebel, M., Pathak, S., DePinho, R. A., & Chang, S. (2005). Elevated telomere-telomere recombination in WRN-deficient, telomere dysfunctional cells promotes escape from senescence and engagement of the ALT pathway. *Genes & Development*, 19(21), 2560.
- Lauper, J. M., Krause, A., Vaughan, T. L., & Monnat, R. J. (2013). Spectrum and Risk of Neoplasia in Werner Syndrome: A Systematic Review. *PLoS ONE*, 8(4).
- Le Moigne, R., Aftab, B. T., Djakovic, S., Dhimolea, E., Valle, E., Murnane, M., King, E. M., Soriano, F., Menon, M. K., Wu, Z. Y., Wong, S. T., Lee, G. J., Yao, B., Wiita, A. P., Lam, C., Rice, J., Wang, J., Chesi, M., Bergsagel, P. L., ... Rolfe, M. (2017). The p97 Inhibitor CB-5083 Is a Unique Disrupter of Protein Homeostasis in Models of Multiple Myeloma. *Molecular Cancer Therapeutics*, 16(11), 2375–2386.
- Le, D. T., Durham, J. N., Smith, K. N., Wang, H., Bartlett, B. R., Aulakh, L. K., Lu, S., Kemberling, H., Wilt, C., Lubner, B. S., Wong, F., Azad, N. S., Rucki, A. A., Laheru, D., Donehower, R., Zaheer, A., Fisher, G. A., Crocenzi, T. S., Lee, J. J., ... Diaz, L. A. (2017). Mismatch-repair deficiency predicts response of solid tumors to PD-1 blockade. *Science (New York, N.Y.)*, 357(6349), 409.

Lebel, M., & Leder, P. (1998). A deletion within the murine Werner syndrome helicase induces sensitivity to inhibitors of topoisomerase and loss of cellular proliferative capacity. *Proceedings of the National Academy of Sciences of the United States of America*, 95(22), 13097.

Lee, M., Shin, S., Uhm, H., Hong, H., Kirk, J., Hyun, K., Kulikowicz, T., Kim, J., Ahn, B., Bohr, V. A., & Hohng, S. (2018). Multiple RPAs make WRN syndrome protein a superhelicase. *Nucleic Acids Research*, 46(9), 4689.

Lee, S. Y., Lee, H., Kim, E. S., Park, S., Lee, J., & Ahn, B. (2015). WRN translocation from nucleolus to nucleoplasm is regulated by SIRT1 and required for DNA repair and the development of chemoresistance. *Mutation Research*, 774, 40–48.

Lehmann, A. R., Niimi, A., Ogi, T., Brown, S., Sabbioneda, S., Wing, J. F., Kannouche, P. L., & Green, C. M. (2007). Translesion synthesis: Y-family polymerases and the polymerase switch. *DNA Repair*, 6(7), 891–899.

Lehmann, C. P., Jiménez-Martín, A., Branzei, D., & Tercero, J. A. (2020). Prevention of unwanted recombination at damaged replication forks. *Current Genetics*, 66(6), 1045.

Lemaçon, D., Jackson, J., Quinet, A., Brickner, J. R., Li, S., Yazinski, S., You, Z., Ira, G., Zou, L., Mosammaparast, N., & Vindigni, A. (2017). MRE11 and EXO1 nucleases degrade reversed forks and elicit MUS81-dependent fork rescue in BRCA2-deficient cells. *Nature Communications*, 8(1).

LeTallec, B., Millot, G. A., Blin, M. E., Brison, O., Dutrillaux, B., & Debatisse, M. (2013). Common fragile site profiling in epithelial and erythroid cells reveals that most recurrent cancer deletions lie in fragile sites hosting large genes. *Cell Reports*, 4(3), 420–428.

- Leuzzi, G., Marabitti, V., Pichierri, P., & Franchitto, A. (2016). WRNIP1 protects stalled forks from degradation and promotes fork restart after replication stress. *The EMBO Journal*, 35(13), 1437–1451.
- Li, G. M. (2007). Mechanisms and functions of DNA mismatch repair. *Cell Research* 2008 18:1, 18(1), 85–98.
- Li, H., & Stillman, B. (2012). The origin recognition complex: a biochemical and structural view. *Sub-Cellular Biochemistry*, 62, 37.
- Li, K., Casta, A., Wang, R., Lozada, E., Fan, W., Kane, S., Ge, Q., Gu, W., Orren, D., & Luo, J. (2008). Regulation of WRN Protein Cellular Localization and Enzymatic Activities by SIRT1-mediated Deacetylation. *Journal of Biological Chemistry*, 283(12), 7590–7598.
- Li, K., Wang, R., Lozada, E., Fan, W., Orren, D. K., & Luo, J. (2010). Acetylation of WRN protein regulates its stability by inhibiting ubiquitination. *PloS One*, 5(4).
- Li, M., Liu, B., Yi, J., Yang, Y., Wang, J., Zhu, W. G., & Luo, J. (2020). MIB1-mediated degradation of WRN promotes cellular senescence in response to camptothecin treatment. *The FASEB Journal*, 34(9), 11488–11497.
- Li, N., Gao, N., & Zhai, Y. (2023). DDK promotes DNA replication initiation: Mechanistic and structural insights. *Current Opinion in Structural Biology*, 78, 102504.
- Li, S., & Wu, X. (2020). Common fragile sites: protection and repair. *Cell & Bioscience* 2020 10:1, 10(1), 1–9.

Liao, H., Ji, F., Helleday, T., & Ying, S. (2018). Mechanisms for stalled replication fork stabilization: new targets for synthetic lethality strategies in cancer treatments. *EMBO Reports*, 19(9).

Libri, A., Marton, T., & Deriano, L. (2022). The (Lack of) DNA Double-Strand Break Repair Pathway Choice During V(D)J Recombination. *Frontiers in Genetics*, 12, 823943.

Lieb, S., Blaha-Ostermann, S., Kamper, E., Rippka, J., Schwarz, C., Ehrenhöfer-Wölfer, K., Schlattl, A., Wernitznig, A., Lipp, J. J., Nagasaka, K., Van Der Lelij, P., Bader, G., Koi, M., Goel, A., Neumüller, R. A., Peters, J. M., Kraut, N., Pearson, M. A., Petronczki, M., & Wöhrle, S. (2019). Werner syndrome helicase is a selective vulnerability of microsatellite instability-high tumor cells. *ELife*, 8.

Lindström, M. S., Jurada, D., Bursac, S., Orsolic, I., Bartek, J., & Volarevic, S. (2018). Nucleolus as an emerging hub in maintenance of genome stability and cancer pathogenesis. *Oncogene* 2018 37:18, 37(18), 2351–2366.

Liu, B., Yi, J., Yang, X., Liu, L., Lou, X., Zhang, Z., Qi, H., Wang, Z., Zou, J., Zhu, W. G., Gu, W., & Luo, J. (2019). MDM2-mediated degradation of WRN promotes cellular senescence in a p53-independent manner. *Oncogene*, 38(14), 2501–2515.

Liu, S., & Kong, D. (2020). End resection: a key step in homologous recombination and DNA double-strand break repair. *Genome Instability & Disease* 2020 2:1, 2(1), 39–50.

Llosa, N. J., Cruise, M., Tam, A., Wicks, E. C., Hechenbleikner, E. M., Taube, J. M., Blosser, R. L., Fan, H., Wang, H., Lubber, B. S., Zhang, M., Papadopoulos, N., Kinzler, K. W., Vogelstein, B., Sears, C. L., Anders, R. A., Pardoll, D. M., & Housseau, F. (2015). The vigorous immune

microenvironment of microsatellite instable colon cancer is balanced by multiple counter-inhibitory checkpoints. *Cancer Discovery*, 5(1), 43.

Loeb, L. A., & Monnat, R. J. (2008). DNA polymerases and human disease. *Nature Reviews Genetics* 2008 9:8, 9(8), 594–604.

Lord, C. J., & Ashworth, A. (2017). PARP Inhibitors: The First Synthetic Lethal Targeted Therapy. *Science (New York, N.Y.)*, 355(6330), 1152.

Lowe, J., Sheerin, A., Jennert-Burston, K., Burton, D., Ostler, E. L., Bird, J., Green, M. H. L., & Faragher, R. G. A. (2004). Camptothecin Sensitivity in Werner Syndrome Fibroblasts as Assessed by the COMET Technique. *Annals of the New York Academy of Sciences*, 1019(1), 256–259.

Lozada, E., Yi, J., Luo, J., & Orren, D. K. (2014). Acetylation of Werner syndrome protein (WRN): relationships with DNA damage, DNA replication and DNA metabolic activities. *Biogerontology*, 15(4), 347.

Lugli, N., Sotiriou, S. K., & Halazonetis, T. D. (2017). The role of SMARCA1 in replication fork stability and telomere maintenance. *DNA Repair*, 56, 129–134.

Luo, J. (2010). WRN protein and Werner syndrome. *North American Journal of Medicine & Science*, 3(4), 205.

Luong, T. T., & Bernstein, K. A. (2021). Role and Regulation of the RECQL4 Family during Genomic Integrity Maintenance. *Genes*, 12(12).

Macheret, M., & Halazonetis, T. D. (2015). DNA Replication Stress as a Hallmark of Cancer. *Annu Rev Pathol.* 2015:10:425-48.

Machwe, A., Xiao, L., Groden, J., & Orren, D. K. (2006). The Werner and Bloom syndrome proteins catalyze regression of a model replication fork. *Biochemistry*, 45(47), 13939–13946.

Machwe, A., Xiao, L., Lloyd, R. G., Bolt, E., & Orren, D. K. (2007). Replication fork regression in vitro by the Werner syndrome protein (WRN): Holliday junction formation, the effect of leading arm structure and a potential role for WRN exonuclease activity. *Nucleic Acids Research*, 35(17), 5729.

Maestroni, L., Matmati, S., & Coulon, S. (2017). Solving the Telomere Replication Problem. *Genes*, 8(2).

Makarov, E. M., Shtam, T. A., Kovalev, R. A., Pantina, R. A., Varfolomeeva, E. Y., & Filatov, M. V. (2017). The rare nonsense mutation in p53 triggers alternative splicing to produce a protein capable of inducing apoptosis. *PLoS ONE*, 12(9).

Malacaria, E., Pugliese, G. M., Honda, M., Marabitti, V., Aiello, F. A., Spies, M., Franchitto, A., & Pichierri, P. (2019). Rad52 prevents excessive replication fork reversal and protects from nascent strand degradation. *Nature Communications* 2019 10:1, 10(1), 1–19.

Malkova, A., & Ira, G. (2013). Break-induced replication: functions and molecular mechanism. *Current Opinion in Genetics & Development*, 23(3), 271.

Malkova, A., Naylor, M. L., Yamaguchi, M., Ira, G., & Haber, J. E. (2005). RAD51-Dependent Break-Induced Replication Differs in Kinetics and Checkpoint Responses from RAD51-Mediated Gene Conversion. *Molecular and Cellular Biology*, 25(3), 933.

- Mannava, S., Grachtchouk, V., Wheeler, L. J., Im, M., Zhuang, D., Slavina, E. G., Mathews, C. K., Shewach, D. S., & Nikiforov, M. A. (2008). Direct role of nucleotide metabolism in C-MYC-dependent proliferation of melanoma cells. *Cell Cycle*, 7(15), 2392–2400.
- Marciniak, R. A., Lombard, D. B., Johnson, F. B., & Guarente, L. (1998). Nucleolar localization of the Werner syndrome protein in human cells. *Proceedings of the National Academy of Sciences of the United States of America*, 95(12), 6887.
- Marco, S. Di, Hasanova, Z., Kanagaraj, R., Hickson, I. D., Krejci, L., & Correspondence, P. J. (2017). RECQ5 Helicase Cooperates with MUS81 Endonuclease in Processing Stalled Replication Forks at Common Fragile Sites during Mitosis. *Molecular Cell*, 66, 658-671.e8.
- Marian, A. J. (2013). Errors in DNA replication and genetic diseases. *Current Opinion in Cardiology*, 28(3), 269–271.
- Martin, S. K., & Wood, R. D. (2019). DNA polymerase ζ in DNA replication and repair. *Nucleic Acids Research*, 47(16), 8348–8361.
- Martín-López, J. V., & Fishel, R. (2013). The mechanism of mismatch repair and the functional analysis of mismatch repair defects in Lynch syndrome. *Familial Cancer*, 12(2), 159.
- Masai, H. (2011). RecQL4: a helicase linking formation and maintenance of a replication fork. *The Journal of Biochemistry*, 149(6), 629–631.
- Masai, H., Matsumoto, S., You, Z., Yoshizawa-Sugata, N., & Oda, M. (2010). Eukaryotic Chromosome DNA Replication: Where, When, and How? *Annu Rev Biochem*. 2010:79:89-130.
- Masuda-Sasa, T., Imamura, O., & Campbell, J. L. (2006). Biochemical analysis of human Dna2. *Nucleic Acids Research*, 34(6), 1865–1875.

Mazouzi, A., Velimezi, G., & Loizou, J. I. (2014). DNA replication stress: Causes, resolution and disease. *Experimental Cell Research*, 329(1), 85–93.

McClendon, A. K., Rodriguez, A. C., & Osheroff, N. (2005). Human Topoisomerase II α Rapidly Relaxes Positively Supercoiled DNA: IMPLICATIONS FOR ENZYME ACTION AHEAD OF REPLICATION FORKS. *Journal of Biological Chemistry*, 280(47), 39337–39345.

McDonald, E. R., de Weck, A., Schlabach, M. R., Billy, E., Mavrakis, K. J., Hoffman, G. R., Belur, D., Castelletti, D., Frias, E., Gampa, K., Golji, J., Kao, I., Li, L., Megel, P., Perkins, T. A., Ramadan, N., Ruddy, D. A., Silver, S. J., Sovath, S., ... Sellers, W. R. (2017). Project DRIVE: A Compendium of Cancer Dependencies and Synthetic Lethal Relationships Uncovered by Large-Scale, Deep RNAi Screening. *Cell*, 170(3), 577-592.e10.

Méchali, M. (2010). Eukaryotic DNA replication origins: many choices for appropriate answers. *Nature Reviews. Molecular Cell Biology*, 11(10), 728–738.

Mei, L., Zhang, J., He, K., & Zhang, J. (2019). Ataxia telangiectasia and Rad3-related inhibitors and cancer therapy: where we stand. *Journal of Hematology & Oncology*, 12(1).

Mengoli, V., Ceppi, I., Sanchez, A., Cannavo, E., Halder, S., Scaglione, S., Gaillard, P., McHugh, P. J., Riesen, N., Pettazzoni, P., & Cejka, P. (2023). WRN helicase and mismatch repair complexes independently and synergistically disrupt cruciform DNA structures. *The EMBO Journal*, 42(3).

Meselson, M., & Stahl, F. W. (1958). The replication of DNA in *Escherichia coli*. *Proceedings of the National Academy of Sciences of the United States of America*, 44(7), 671.

Meyers, R. M., Bryan, J. G., McFarland, J. M., Weir, B. A., Sizemore, A. E., Xu, H., Dharia, N. V., Montgomery, P. G., Cowley, G. S., Pantel, S., Goodale, A., Lee, Y., Ali, L. D., Jiang, G., Lubonja,

R., Harrington, W. F., Strickland, M., Wu, T., Hawes, D. C., ... Tsherniak, A. (2017). Computational correction of copy-number effect improves specificity of CRISPR-Cas9 essentiality screens in cancer cells. *Nature Genetics*, 49(12), 1779.

Mimitou, E. P., & Symington, L. S. (2008). Sae2, Exo1 and Sgs1 collaborate in DNA double-strand break processing. *Nature*, 455(7214), 770–774.

Minocherhomji, S., Ying, S., Bjerregaard, V. A., Bursomanno, S., Aleliunaite, A., Wu, W., Mankouri, H. W., Shen, H., Liu, Y., & Hickson, I. D. (2015). Replication stress activates DNA repair synthesis in mitosis. *Nature*, 528(7581), 286–290.

Mizutani, T., Ishizaka, A., & Furuichi, Y. (2015). The Werner Protein Acts as a Coactivator of Nuclear Factor κ B (NF- κ B) on HIV-1 and Interleukin-8 (IL-8) Promoters. *Journal of Biological Chemistry*, 290(30), 18391–18399.

Mokhtari, R. B., Homayouni, T. S., Baluch, N., Morgatskaya, E., Kumar, S., Das, B., & Yeger, H. (2017). Combination therapy in combating cancer. *Oncotarget*, 8(23), 38022.

Moreno, S. P., & Gambus, A. (2020). Mechanisms of eukaryotic replisome disassembly. *Biochemical Society Transactions*, 48(3), 823.

Motegi, A., Liaw, H. J., Lee, K. Y., Roest, H. P., Maas, A., Wu, X., Moinova, H., Markowitz, S. D., Ding, H., Hoeijmakers, J. H. J., & Myung, K. (2008). Polyubiquitination of proliferating cell nuclear antigen by HLTF and SHPRH prevents genomic instability from stalled replication forks. *Proceedings of the National Academy of Sciences of the United States of America*, 105(34), 12411.

- Mourón, S., Rodríguez-Acebes, S., Martínez-Jiménez, M. I., García-Gómez, S., Chocrón, S., Blanco, L., & Méndez, J. (2013). Repriming of DNA synthesis at stalled replication forks by human PrimPol. *Nature Structural & Molecular Biology* 20:12, 20(12), 1383–1389.
- Mukherjee, S., Wright, W. D., Ehmsen, K. T., & Heyer, W. D. (2014). The Mus81-Mms4 structure-selective endonuclease requires nicked DNA junctions to undergo conformational changes and bend its DNA substrates for cleavage. *Nucleic Acids Research*, 42(10), 6511.
- Multani, A. S., & Chang, S. (2007). WRN at telomeres: implications for aging and cancer. *Journal of Cell Science*, 120(5), 713–721.
- Murfuni, I., De Santis, A., Federico, M., Bignami, M., Pichierri, P., & Franchitto, A. (2012). Perturbed replication induced genome wide or at common fragile sites is differently managed in the absence of WRN. *Carcinogenesis*, 33(9), 1655–1663.
- Musiałek, M. W., & Rybaczek, D. (2021). Hydroxyurea—The Good, the Bad and the Ugly. *Genes*, 12(7), 1096.
- Nayak, S., Calvo, J. A., Cong, K., Peng, M., Berthiaume, E., Jackson, J., Zaino, A. M., Vindigni, A., Hadden, M. K., & Cantor, S. B. (2020). Inhibition of the translesion synthesis polymerase REV1 exploits replication gaps as a cancer vulnerability. *Science Advances*, 6(24).
- Neelsen, K. J., & Lopes, M. (2015). Replication fork reversal in eukaryotes: from dead end to dynamic response. *Nature Reviews Molecular Cell Biology* 2015 16:4, 16(4), 207–220.
- Negrini, S., Gorgoulis, V. G., & Halazonetis, T. D. (2010). Genomic instability — an evolving hallmark of cancer. *Nature Reviews Molecular Cell Biology* 2010 11:3, 11(3), 220–228.

Newman, J. A., Gavard, A. E., Lieb, S., Ravichandran, M. C., Hauer, K., Werni, P., Geist, L., Böttcher, J., Engen, J. R., Rumpel, K., Samwer, M., Petronczki, M., & Gileadi, O. (2021). Structure of the helicase core of Werner helicase, a key target in microsatellite instability cancers. *Life Science Alliance*, 4(1).

Nickoloff, J. A., Sharma, N., Taylor, L., Allen, S. J., & Hromas, R. (2021). The Safe Path at the Fork: Ensuring Replication-Associated DNA Double-Strand Breaks are Repaired by Homologous Recombination. *Frontiers in Genetics*, 12, 748033.

Nishitani, H., & Lygerou, Z. (2004). DNA replication licensing. *Frontiers in Bioscience : A Journal and Virtual Library*, 9, 2115–2132.

Niv, Y. (2007). Microsatellite instability and MLH1 promoter hypermethylation in colorectal cancer. *World Journal of Gastroenterology : WJG*, 13(12), 1767.

Nurk, S., Koren, S., Rhie, A., Rautiainen, M., Bzikadze, A. V., Mikheenko, A., Vollger, M. R., Altemose, N., Uralsky, L., Gershman, A., Aganezov, S., Hoyt, S. J., Diekhans, M., Logsdon, G. A., Alonge, M., Antonarakis, S. E., Borchers, M., Bouffard, G. G., Brooks, S. Y., ... Phillippy, A. M. (2022). The complete sequence of a human genome. *Science*, 376(6588), 44–53.

Ockey, C. H., & Saffhill, R. (1986). Delayed DNA maturation, a possible cause of the elevated sister-chromatid exchange in Bloom's syndrome. *Carcinogenesis*, 7(1), 53–57.

Ogburn, C. E., Oshima, J., Poot, M., Chen, R., Hunt, K. E., Gollahon, K. A., Rabinovitch, P. S., & Martin, G. M. (1997). An apoptosis-inducing genotoxin differentiates heterozygotic carriers for Werner helicase mutations from wild-type and homozygous mutants. *Human Genetics*, 101(2), 121–125.

- Opresko, P. L., Otterlei, M., Graakjær, J., Bruheim, P., Dawut, L., Kølvrå, S., May, A., Seidman, M. M., & Bohr, V. A. (2004). The Werner syndrome helicase and exonuclease cooperate to resolve telomeric D loops in a manner regulated by TRF1 and TRF2. *Molecular Cell*, 14(6), 763–774.
- Orren, D. K., Machwe, A., Karmakar, P., Piotrowski, J., Cooper, M. P., & Bohr, V. A. (2001). A functional interaction of Ku with Werner exonuclease facilitates digestion of damaged DNA. *Nucleic Acids Research*, 29(9), 1926.
- Ortiz-Bazán, M. Á., Gallo-Fernández, M., Saugar, I., Jiménez-Martín, A., Vázquez, M. V., & Tercero, J. A. (2014). Rad5 plays a major role in the cellular response to DNA damage during chromosome replication. *Cell Reports*, 9(2), 460–468.
- Otterlei, M., Bruheim, P., Ahn, B., Bussen, W., Karmakar, P., Baynton, K., & Bohr, V. A. (2006). Werner syndrome protein participates in a complex with RAD51, RAD54, RAD54B and ATR in response to ICL-induced replication arrest. *Journal of Cell Science*, 119(Pt 24), 5137–5146.
- Overman, M. J., McDermott, R., Leach, J. L., Lonardi, S., Lenz, H. J., Morse, M. A., Desai, J., Hill, A., Axelson, M., Moss, R. A., Goldberg, M. V., Cao, Z. A., Ledezine, J. M., Maglinte, G. A., Kopetz, S., & André, T. (2017). Nivolumab in patients with metastatic DNA mismatch repair deficient/microsatellite instability–high colorectal cancer (CheckMate 142): results of an open-label, multicentre, phase 2 study. *The Lancet. Oncology*, 18(9), 1182.
- Palermo, V., Rinalducci, S., Sanchez, M., Grillini, F., Sommers, J. A., Brosh, R. M., Zolla, L., Franchitto, A., & Pichierri, P. (2016). CDK1 phosphorylates WRN at collapsed replication forks. *Nature Communications*, 7.

- Pardo, B., Moriel-Carretero, M., Vicat, T., Aguilera, A., & Pasero, P. (2020). Homologous recombination and Mus81 promote replication completion in response to replication fork blockage. *EMBO Reports*, 21(7).
- Parker, M. W., Botchan, M. R., & Berger, J. M. (2017). Mechanisms and regulation of DNA replication initiation in eukaryotes. *Critical Reviews in Biochemistry and Molecular Biology*, 52(2), 107–144.
- Pećina-Šlaus, N., Kafka, A., Salamon, I., & Bukovac, A. (2020). Mismatch Repair Pathway, Genome Stability and Cancer. *Frontiers in Molecular Biosciences*, 7, 535672.
- Pellegrini, L. (2023). The CMG DNA helicase and the core replisome. *Current Opinion in Structural Biology*, 81, 102612.
- Peng, C. Y., Graves, P. R., Thoma, R. S., Wu, Z., Shaw, A. S., & Piwnicka-Worms, H. (1997). Mitotic and G2 checkpoint control: regulation of 14-3-3 protein binding by phosphorylation of Cdc25C on serine-216. *Science (New York, N.Y.)*, 277(5331), 1501–1505.
- Peng, M., Cong, K., Panzarino, N. J., Nayak, S., Calvo, J., Deng, B., Zhu, L. J., Morocz, M., Hegedus, L., Haracska, L., & Cantor, S. B. (2018). Opposing Roles of FANCD1 and HLF1 Protect Forks and Restrain Replication during Stress. *Cell Reports*, 24(12), 3251–3261.
- Petermann, E., & Helleday, T. (2010). Pathways of mammalian replication fork restart. *Nature Reviews Molecular Cell Biology* 2010 11:10, 11(10), 683–687.
- Pfeiffer, V., & Lingner, J. (2013). Replication of Telomeres and the Regulation of Telomerase. *Cold Spring Harbor Perspectives in Biology*, 5(5), 10405–10406.

Philip, K. T., Dutta, K., Chakraborty, S., & Patro, B. S. (2023). Functional inhibition of RECQL5 helicase elicits non-homologous end joining response and sensitivity of breast cancers to PARP inhibitor. *The International Journal of Biochemistry & Cell Biology*, 161, 106443.

Piberger, A. L., Bowry, A., Kelly, R. D. W., Walker, A. K., González-Acosta, D., Bailey, L. J., Doherty, A. J., Méndez, J., Morris, J. R., Bryant, H. E., & Petermann, E. (2020). PrimPol-dependent single-stranded gap formation mediates homologous recombination at bulky DNA adducts. *Nature Communications*, 11(1).

Picco, G., Cattaneo, C. M., van Vliet, E. J., Crisafulli, G., Rospo, G., Consonni, S., Vieira, S. F., Rodríguez, I. S., Cancelliere, C., Banerjee, R., Schipper, L. J., Oddo, D., Dijkstra, K. K., Cinatl, J., Michaelis, M., Yang, F., Di Nicolantonio, F., Sartore-Bianchi, A., Siena, S., ... Garnett, M. J. (2021). Werner helicase is a synthetic-lethal vulnerability in mismatch repair– deficient colorectal cancer refractory to targeted therapies, chemotherapy, and immunotherapy. *Cancer Discovery*, 11(8), 1923–1937.

Pichierri, P., Franchitto, A., Mosesso, P., & Palitti, F. (2000). Werner's syndrome cell lines are hypersensitive to camptothecin-induced chromosomal damage. *Mutation Research/Fundamental and Molecular Mechanisms of Mutagenesis*, 456(1–2), 45–57.

Pichierri, P., Franchitto, A., Mosesso, P., & Palitti, F. (2001). Werner's Syndrome Protein Is Required for Correct Recovery after Replication Arrest and DNA Damage Induced in S-Phase of Cell Cycle. *Molecular Biology of the Cell*, 12, 2412–2421.

Pirzio, L. M., Pichierri, P., Bignami, M., & Franchitto, A. (2008). Werner syndrome helicase activity is essential in maintaining fragile site stability. *The Journal of Cell Biology*, 180(2), 305.

Poli, J., Tsaponina, O., Crabbé, L., Keszthelyi, A., Pantesco, V., Chabes, A., Lengronne, A., & Pasero, P. (2012). dNTP pools determine fork progression and origin usage under replication stress. *The EMBO Journal*, 31(4), 883.

Pommier, Y., Nussenzweig, A., Takeda, S., & Austin, C. (2022). Human topoisomerases and their roles in genome stability and organization. *Nature Reviews Molecular Cell Biology* 2022 23:6, 23(6), 407–427.

Poole, L. A., & Cortez, D. (2017). Functions of SMARCAL1, ZRANB3, and HLTF in maintaining genome stability. *Critical Reviews in Biochemistry and Molecular Biology*, 52(6), 696.

PooT, M., Hoehn, H., Rünger, T. M., & Martin, G. M. (1992). Impaired S-phase transit of Werner syndrome cells expressed in lymphoblastoid cell lines. *Experimental Cell Research*, 202(2), 267–273.

Poot, M., Yom, J. S., Whang, S. H., Kato, J. T., Gollahon, K. A., & Rabinovitch, P. S. (2001). Werner syndrome cells are sensitive to DNA cross-linking drugs. *The FASEB Journal*, 15(7), 1224–1226.

Popuri, V., Huang, J., Ramamoorthy, M., Tadokoro, T., Croteau, D. L., & Bohr, V. A. (2013). RECQL5 plays co-operative and complementary roles with WRN syndrome helicase. *Nucleic Acids Research*, 41(2), 881–899.

Popuri, V., Tadokoro, T., Croteau, D. L., & Bohr, V. A. (2013). Human RECQL5: Guarding the crossroads of DNA replication and transcription and providing backup capability. *Critical Reviews in Biochemistry and Molecular Biology*, 48(3), 289–299.

Prindle, M. J., & Loeb, L. A. (2012). DNA polymerase delta in DNA replication and genome maintenance. *Environmental and Molecular Mutagenesis*, 53(9), 666.

- Prioleau, M. N., & MacAlpine, D. M. (2016). DNA replication origins—where do we begin? *Genes & Development*, 30(15), 1683.
- Qiu, S., Jiang, G., Cao, L., & Huang, J. (2021). Replication Fork Reversal and Protection. *Frontiers in Cell and Developmental Biology*, 9.
- Quesada, V., Díaz-Perales, A., Gutiérrez-Fernández, A., Garabaya, C., Cal, S., & López-Otín, C. (2004). Cloning and enzymatic analysis of 22 novel human ubiquitin-specific proteases. *Biochemical and Biophysical Research Communications*, 314(1), 54–62.
- Ralf, C., Hickson, I. D., & Wu, L. (2006). The Bloom's syndrome helicase can promote the regression of a model replication fork. *The Journal of Biological Chemistry*, 281(32), 22839–22846.
- Ray Chaudhuri, A., Hashimoto, Y., Herrador, R., Neelsen, K. J., Fachinetti, D., Bermejo, R., Cocito, A., Costanzo, V., & Lopes, M. (2012). Topoisomerase I poisoning results in PARP-mediated replication fork reversal. *Nature Structural & Molecular Biology*, 19(4), 417–423.
- Remus, D., Beuron, F., Tolun, G., Griffith, J. D., Morris, E. P., & Diffley, J. F. X. (2009). Concerted Loading of Mcm2-7 Double Hexamers Around DNA during DNA Replication Origin Licensing. *Cell*, 139(4), 719.
- Reuswig, K. U., & Pfander, B. (2019). Control of Eukaryotic DNA Replication Initiation—Mechanisms to Ensure Smooth Transitions. *Genes*, 10(2).
- Rickman, K., & Smogorzewska, A. (2019). Advances in understanding DNA processing and protection at stalled replication forks. *Journal of Cell Biology*, 218(4), 1096–1107.

Ripley, B. M., Gildenberg, M. S., & Todd Washington, M. (2020). Control of DNA Damage Bypass by Ubiquitylation of PCNA. *Genes*, 11(2).

Rodríguez-Caballero, Á., Torres-Lagares, D., Rodríguez-Pérez, A., Serrera-Figallo, M. Á., Hernández-Guisado, J. M., & Machuca-Portillo, G. (2010). Cri du chat syndrome: a critical review. *Medicina Oral, Patología Oral y Cirugía Bucal*, 15(3).

Rodríguez-López, A. M., Jackson, D. A., Iborra, F., & Cox, L. S. (2002). Asymmetry of DNA replication fork progression in Werner's syndrome. *Aging Cell*, 1(1), 30–39.

Rodríguez-López, A. M., Jackson, D. A., Nehlin, J. O., Iborra, F., Warren, A. V., & Cox, L. S. (2003). Characterisation of the interaction between WRN, the helicase/exonuclease defective in progeroid Werner's syndrome, and an essential replication factor, PCNA. *Mechanisms of Ageing and Development*, 124(2), 167–174.

Rohilla, K. J., & Gagnon, K. T. (2017). RNA biology of disease-associated microsatellite repeat expansions. *Acta Neuropathologica Communications* 2017 5:1, 5(1), 1–22.

Rossi, M. L., Ghosh, A. K., Kulikowicz, T., Croteau, D. L., & Bohr, V. A. (2010). Conserved helicase domain of human RECQ4 is required for strand annealing-independent DNA unwinding. *DNA Repair*, 9(7), 796.

Saharia, A., Teasley, D. C., Duxin, J. P., Dao, B., Chiappinelli, K. B., & Stewart, S. A. (2010). FEN1 Ensures Telomere Stability by Facilitating Replication Fork Re-initiation. *Journal of Biological Chemistry*, 285(35), 27057–27066.

Saintigny, Y., Makienko, K., Swanson, C., Emond, M. J., & Jr., R. J. M. (2002). Homologous Recombination Resolution Defect in Werner Syndrome. *Molecular and Cellular Biology*, 22(20), 6971–6978.

Sakofsky, C. J., & Malkova, A. (2017). Break Induced Replication in eukaryotes: mechanisms, functions, and consequences. *Critical Reviews in Biochemistry and Molecular Biology*, 52(4), 395.

Saldivar, J. C., Cortez, D., & Cimprich, K. A. (2017). The essential kinase ATR: ensuring faithful duplication of a challenging genome. *Nature Reviews Molecular Cell Biology* 2017 18:10, 18(10), 622–636.

Saldivar, J. C., Hamperl, S., Bocek, M. J., Chung, M., Bass, T. E., Cisneros-Soberanis, F., Samejima, K., Xie, L., Paulson, J. R., Earnshaw, W. C., Cortez, D., Meyer, T., & Cimprich, K. A. (2018). An intrinsic S/G2 checkpoint enforced by ATR. *Science (New York, N.Y.)*, 361(6404), 806.

Samanta, S., & Karmakar, P. (2012). Recruitment of HRDC domain of WRN and BLM to the sites of DNA damage induced by mitomycin C and methyl methanesulfonate. *Cell Biology International*, 36(10), 873–881.

Sanchez, Y., Wong, C., Thoma, R. S., Richman, R., Wu, Z., Piwnica-Worms, H., & Elledge, S. J. (1997). Conservation of the Chk1 checkpoint pathway in mammals: linkage of DNA damage to Cdk regulation through Cdc25. *Science (New York, N.Y.)*, 277(5331), 1497–1501.

Sangrithi, M. N., Bernal, J. A., Madine, M., Philpott, A., Lee, J., Dunphy, W. G., & Venkitaraman, A. R. (2005). Initiation of DNA Replication Requires the RECQL4 Protein Mutated in Rothmund-Thomson Syndrome. *Cell*, 121(6), 887–898.

Santa Maria, S. (2014). Homologous Recombination in Lesion Bypass. *Molecular Life Sciences*, 1–8.

Saponaro, M., Kantidakis, T., Mitter, R., Kelly, G. P., Heron, M., Williams, H., Söding, J., Stewart, A., & Svejstrup, J. Q. (2014). RECQL5 controls transcript elongation and suppresses genome instability associated with transcription stress. *Cell*, 157(5), 1037–1049.

Sartori, A. A., Lukas, C., Coates, J., Mistrik, M., Fu, S., Bartek, J., Baer, R., Lukas, J., & Jackson, S. P. (2007). Human CtIP promotes DNA end resection. *Nature*, 450(7169), 509–514.

Saxena, S., & Zou, L. (2022). Hallmarks of DNA replication stress. *Molecular Cell*, 82(12), 2298–2314.

Scaramuzza, S., Jones, R. M., Sadurni, M. M., Reynolds-Winczura, A., Poovathumkadavil, D., Farrell, A., Natsume, T., Rojas, P., Cuesta, C. F., Kanemaki, M. T., Saponaro, M., & Gambus, A. (2023). TRAIP resolves DNA replication-transcription conflicts during the S-phase of unperturbed cells. *Nature Communications* 2023 14:1, 14(1), 1–20.

Schlacher, K., Wu, H., & Jasin, M. (2012). A distinct replication fork protection pathway connects Fanconi anemia tumor suppressors to RAD51-BRCA1/2. *Cancer Cell*, 22(1), 106–116.

Schmidt, M. H. M., & Pearson, C. E. (2016). Disease-associated repeat instability and mismatch repair. *DNA Repair*, 38, 117–126.

Scully, R., Panday, A., Elango, R., & Willis, N. A. (2019). DNA double-strand break repair-pathway choice in somatic mammalian cells. *Nature Reviews Molecular Cell Biology* 2019 20:11, 20(11), 698–714.

Shah, S. N., Opresko, P. L., Meng, X., Lee, M. Y. W. T., & Eckert, K. A. (2010). DNA structure and the Werner protein modulate human DNA polymerase delta-dependent replication dynamics within the common fragile site FRA16D. *Nucleic Acids Research*, 38(4), 1149–1162.

Shamanna, R. A., Lu, H., De Freitas, J. K., Tian, J., Croteau, D. L., & Bohr, V. A. (2016). WRN regulates pathway choice between classical and alternative non-homologous end joining. *Nature Communications* 2016 7:1, 7(1), 1–12.

Sharma, S., Otterlei, M., Sommers, J. A., Driscoll, H. C., Dianov, G. L., Kao, H. I., Bambara, R. A., & Brosh, R. M. (2004). WRN Helicase and FEN-1 Form a Complex upon Replication Arrest and Together Process Branch-migrating DNA Structures Associated with the Replication Fork. *Molecular Biology of the Cell*, 15(2), 734–750.

Sharma, S., Sommers, J. A., Driscoll, H. C., Uzdilla, L., Wilson, T. M., & Brosh, R. M. (2003). The exonucleolytic and endonucleolytic cleavage activities of human exonuclease 1 are stimulated by an interaction with the carboxyl-terminal region of the Werner syndrome protein. *The Journal of Biological Chemistry*, 278(26), 23487–23496.

Shcherbakova, P. V., & Pavlov, Y. I. (1996). 3' -> 5' Exonucleases of DNA Polymerases ϵ and δ Correct Base Analog Induced DNA Replication Errors on opposite DNA Strands in *Saccharomyces Cerevisiae*. *Genetics*, 142(3), 717.

Shen, J. C., & Loeb, L. A. (2000). Werner syndrome exonuclease catalyzes structure-dependent degradation of DNA. *Nucleic Acids Research*, 28(17), 3260.

Shimizu, N., Akagawa, R., Shunichi Takeda, ·, & Sasanuma, · Hiroyuki. (2020). The MRE11 nuclease promotes homologous recombination not only in DNA double-strand break resection

but also in post-resection in human TK6 cells. *Genome Instability & Disease* 2020 1:4, 1(4), 184–196.

Shiratori, M., Suzuki, T., Itoh, C., Goto, M., Furuichi, Y., & Matsumoto, T. (2002). WRN helicase accelerates the transcription of ribosomal RNA as a component of an RNA polymerase I-associated complex. *Oncogene*, 21(16), 2447–2454.

Shorrocks, A. M. K., Jones, S. E., Tsukada, K., Morrow, C. A., Belblidia, Z., Shen, J., Vendrell, I., Fischer, R., Kessler, B. M., & Blackford, A. N. (2021). The Bloom syndrome complex senses RPA-coated single-stranded DNA to restart stalled replication forks. *Nature Communications* 2021 12:1, 12(1), 1–15.

Sidorova, J. M., Li, N., Folch, A., & Monnat, R. J. (2008). The RecQ helicase WRN is required for normal replication fork progression after DNA damage or replication fork arrest. *Cell Cycle (Georgetown, Tex.)*, 7(6), 796.

Siitonen, A. H., Sotkasiira, J., Biervliet, M., Benmansour, A., Capri, Y., Cormier-Daire, V., Crandall, B., Hannula-Jouppi, K., Hennekam, R., Herzog, D., Keymolen, K., Lipsanen-Nyman, M., Miny, P., Plon, S. E., Riedl, S., Sarkar, A., Vargas, F. R., Verloes, A., Wang, L. L., ... Kestilä, M. (2009). The mutation spectrum in RECQL4 diseases. *European Journal of Human Genetics*, 17(2), 151.

Singhal, G., Leo, E., Setty, S. K. G., Pommier, Y., & Thimmapaya, B. (2013). Adenovirus E1A Oncogene Induces Rereplication of Cellular DNA and Alters DNA Replication Dynamics. *Journal of Virology*, 87(15), 8767–8778.

- Smeets, M. F., Deluca, E., Wall, M., Quach, J. M., Chalk, A. M., Deans, A. J., Heierhorst, J., Purton, L. E., Izon, D. J., & Walkley, C. R. (2014). The Rothmund-Thomson syndrome helicase RECQL4 is essential for hematopoiesis. *The Journal of Clinical Investigation*, 124(8), 3551.
- Sogo, J. M., Lopes, M., & Foiani, M. (2002). Fork reversal and ssDNA accumulation at stalled replication forks owing to checkpoint defects. *Science (New York, N.Y.)*, 297(5581), 599–602.
- Somyajit, K., Saxena, S., Babu, S., Mishra, A., & Nagaraju, G. (2015). Mammalian RAD51 paralogs protect nascent DNA at stalled forks and mediate replication restart. *Nucleic Acids Research*, 43(20), 9835–9855.
- Sonneville, R., Bhowmick, R., Hoffmann, S., Mailand, N., Hickson, I. D., & Labib, K. (2019). TRAP drives replisome disassembly and mitotic DNA repair synthesis at sites of incomplete DNA replication. *ELife*, 8.
- Sparks, M. A., Burgers, P. M., & Galletto, R. (2020). Pif1, RPA, and FEN1 modulate the ability of DNA polymerase δ to overcome protein barriers during DNA synthesis. *Journal of Biological Chemistry*, 295(47), 15883–15891.
- Stead, E. R., & Bjedov, I. (2021). Balancing DNA repair to prevent ageing and cancer. *Experimental Cell Research*, 405(2).
- Stillman, B. (2008). DNA polymerases at the replication fork in eukaryotes. *Molecular Cell*, 30(3), 259.
- Stinson, B. M., & Loparo, J. J. (2021). Repair of DNA Double-Strand Breaks by the Non-homologous End Joining Pathway. *Annual Review of Biochemistry*, 90, 137.

Stroik, S., & Hendrickson, E. A. (2020). Telomere replication—When the going gets tough. *DNA Repair*, 94, 102875.

Sturzenegger, A., Burdova, K., Kanagaraj, R., Levikova, M., Pinto, C., Cejka, P., & Janscak, P. (2014). DNA2 Cooperates with the WRN and BLM RecQ Helicases to Mediate Long-range DNA End Resection in Human Cells. *The Journal of Biological Chemistry*, 289(39), 27314.

Su, F., Mukherjee, S., Yang, Y., Mori, E., Bhattacharya, S., Kobayashi, J., Yannone, S. M., Chen, D. J., & Asaithamby, A. (2014). Non-enzymatic Role for WRN in Preserving Nascent DNA Strands after Replication Stress. *Cell Reports*, 9(4), 1387.

Sun, H., Ma, L., Tsai, Y. F., Abeywardana, T., Shen, B., & Zheng, L. (2023). Okazaki fragment maturation: DNA flap dynamics for cell proliferation and survival. *Trends in Cell Biology*, 33(3), 221–234.

Sun, L., Nakajima, S., Teng, Y., Chen, H., Yang, L., Chen, X., Gao, B., Levine, A. S., & Lan, L. (2017). WRN is recruited to damaged telomeres via its RQC domain and tankyrase1-mediated poly-ADP-ribosylation of TRF1. *Nucleic Acids Research*, 45(7), 3844–3859.

Syed, A., & Tainer, J. A. (2018). The MRE11–RAD50–NBS1 Complex Conducts the Orchestration of Damage Signaling and Outcomes to Stress in DNA Replication and Repair. *Annual Review of Biochemistry*, 87, 263.

Symington, L. S. (2014). End resection at double-strand breaks: mechanism and regulation. *Cold Spring Harbor Perspectives in Biology*, 6(8).

Tadokoro, T., Kulikowicz, T., Dawut, L., Croteau, D. L., & Bohr, V. A. (2012). DNA binding residues in the RQC domain of Werner protein are critical for its catalytic activities. *Aging*, 4(6), 417–429.

Taglialatela, A., Alvarez, S., Leuzzi, G., Sannino, V., Ranjha, L., Huang, J. W., Madubata, C., Anand, R., Levy, B., Rabadan, R., Cejka, P., Costanzo, V., & Ciccia, A. (2017). Restoration of replication fork stability in BRCA1- and BRCA2-deficient cells by inactivation of SNF2-family fork remodelers. *Molecular Cell*, 68(2), 414.

Takami, Y., Ono, T., Fukagawa, T., Shibahara, K. I., & Nakayama, T. (2007). Essential Role of Chromatin Assembly Factor-1–mediated Rapid Nucleosome Assembly for DNA Replication and Cell Division in Vertebrate Cells. *Molecular Biology of the Cell*, 18(1), 129.

Takeuchi, F., Hanaoka, F., Goto, M., Yamada, M. A., & Miyamoto, T. (1982). Prolongation of S phase and whole cell cycle in Werner's syndrome fibroblasts. *Experimental Gerontology*, 17(6), 473–480.

Tanaka, S., Tak, Y. S., & Araki, H. (2007). The role of CDK in the initiation step of DNA replication in eukaryotes. *Cell Division*, 2(1), 1–6.

Thandapani, P., Couturier, A. M., Yu, Z., Li, X., Couture, J. F., Li, S., Masson, J. Y., & Richard, S. (2017). Lysine methylation of FEN1 by SET7 is essential for its cellular response to replicative stress. *Oncotarget*, 8(39), 64918.

Thangavel, S., Berti, M., Levikova, M., Pinto, C., Gomathinayagam, S., Vujanovic, M., Zellweger, R., Moore, H., Lee, E. H., Hendrickson, E. A., Cejka, P., Stewart, S., Lopes, M., & Vindigni, A.

(2015). DNA2 drives processing and restart of reversed replication forks in human cells. *The Journal of Cell Biology*, 208(5), 545.

Thangavel, S., Mendoza-Maldonado, R., Tissino, E., Sidorova, J. M., Yin, J., Wang, W., Raymond J. Monnat, J., Falaschi, A., & Vindigni, A. (2010). Human RECQ1 and RECQ4 Helicases Play Distinct Roles in DNA Replication Initiation. *Molecular and Cellular Biology*, 30(6), 1382.

Thorvaldsdóttir, H., Robinson, J. T., & Mesirov, J. P. (2013). Integrative Genomics Viewer (IGV): high-performance genomics data visualization and exploration. *Briefings in Bioinformatics*, 14(2), 178–192.

Tian, Y., Wang, W., Lautrup, S., Zhao, H., Li, X., Law, P. W. N., Dinh, N. D., Fang, E. F., Cheung, H. H., & Chan, W. Y. (2022). WRN promotes bone development and growth by unwinding SHOX-G-quadruplexes via its helicase activity in Werner Syndrome. *Nature Communications* 2022 13:1, 13(1), 1–20.

Toledo, L. I., Altmeyer, M., Rask, M. B., Lukas, C., Larsen, D. H., Povlsen, L. K., Bekker-Jensen, S., Mailand, N., Bartek, J., & Lukas, J. (2013). ATR prohibits replication catastrophe by preventing global exhaustion of RPA. *Cell*, 155(5), 1088.

Topatana, W., Juengpanich, S., Li, S., Cao, J., Hu, J., Lee, J., Suliyanto, K., Ma, D., Zhang, B., Chen, M., & Cai, X. (2020). Advances in synthetic lethality for cancer therapy: cellular mechanism and clinical translation. *Journal of Hematology & Oncology* 2020 13:1, 13(1), 1–22.

Traven, A., & Heierhorst, J. (2005). SQ/TQ cluster domains: concentrated ATM/ATR kinase phosphorylation site regions in DNA-damage-response proteins. *BioEssays : News and Reviews in Molecular, Cellular and Developmental Biology*, 27(4), 397–407.

- Tsegay, P. S., Lai, Y., & Liu, Y. (2019). Replication Stress and Consequential Instability of the Genome and Epigenome. *Molecules*, 24(21).
- Tubbs, A., & Nussenzweig, A. (2017). Endogenous DNA Damage as a Source of Genomic Instability in Cancer. *Cell*, 168(4), 644.
- Tye, S., Ronson, G. E., & Morris, J. R. (2021). A fork in the road: Where homologous recombination and stalled replication fork protection part ways. *Seminars in Cell & Developmental Biology*, 113, 14–26.
- Ubhi, T., & Brown, G. W. (2019). Exploiting DNA replication stress for cancer treatment. *Cancer Research*, 79(8), 1730–1739.
- Udroiu, I., Marinaccio, J., & Sgura, A. (2022). Many Functions of Telomerase Components: Certainties, Doubts, and Inconsistencies. *International Journal of Molecular Sciences*, 23(23), 15189.
- Umar, A., Risinger, J. I., Glaab, W. E., Tindall, K. R., Barrett, J. C., & Kunkel, T. A. (1998). Functional Overlap in Mismatch Repair by Human MSH3 and MSH6. *Genetics*, 148(4), 1637–1646.
- Ünsal-Kaçmaz, K., & Sancar, A. (2004). Quaternary Structure of ATR and Effects of ATRIP and Replication Protein A on Its DNA Binding and Kinase Activities. *Molecular and Cellular Biology*, 24(3), 1292–1300.
- Urban, V., Dobrovolna, J., Hühn, D., Fryzelkova, J., Bartek, J., & Janscak, P. (2016). RECQ5 helicase promotes resolution of conflicts between replication and transcription in human cells. *The Journal of Cell Biology*, 214(4), 401–415.

Valton, A. L., Hassan-Zadeh, V., Lema, I., Boggetto, N., Alberti, P., Saintomé, C., Riou, J. F., & Prioleau, M. N. (2014). G4 motifs affect origin positioning and efficiency in two vertebrate replicators. *The EMBO Journal*, 33(7), 732.

van Wietmarschen, N., Sridharan, S., Nathan, W. J., Tubbs, A., Chan, E. M., Callen, E., Wu, W., Belinky, F., Tripathi, V., Wong, N., Foster, K., Noorbakhsh, J., Garimella, K., Cruz-Migoni, A., Sommers, J. A., Huang, Y., Borah, A. A., Smith, J. T., Kalfon, J., ... Nussenzweig, A. (2020). Repeat expansions confer WRN dependence in microsatellite-unstable cancers. *Nature*, 586(7828), 292.

Vashee, S., Cvetic, C., Lu, W., Simancek, P., Kelly, T. J., & Walter, J. C. (2003). Sequence-independent DNA binding and replication initiation by the human origin recognition complex. *Genes & Development*, 17(15), 1894.

Vesela, E., Chroma, K., Turi, Z., & Mistrik, M. (2017). Common Chemical Inductors of Replication Stress: Focus on Cell-Based Studies. *Biomolecules*, 7(1).

Vieira, M. L. C., Santini, L., Diniz, A. L., & Munhoz, C. de F. (2016). Microsatellite markers: what they mean and why they are so useful. *Genetics and Molecular Biology*, 39(3), 312.

Vilar, E., Bartnik, C. M., Stenzel, S. L., Raskin, L., Ahn, J., Moreno, V., Mukherjee, B., Iniesta, M. D., Morgan, M. A., Rennert, G., & Gruber, S. B. (2011). MRE11 deficiency increases sensitivity to poly(ADP-ribose) polymerase inhibition in microsatellite unstable colorectal cancers. *Cancer Research*, 71(7), 2632.

Vilar, E., Scaltriti, M., Balmãa, J., Saura, C., Guzman, M., Arribas, J., Baselga, J., & Tabernero, J. (2008). Microsatellite instability due to hMLH1 deficiency is associated with increased

cytotoxicity to irinotecan in human colorectal cancer cell lines. *British Journal of Cancer*, 99(10), 1607.

Vujanovic, M., Krietsch, J., Raso, M. C., Terraneo, N., Zellweger, R., Schmid, J. A., Taglialatela, A., Huang, J. W., Holland, C. L., Zwicky, K., Herrador, R., Jacobs, H., Cortez, D., Ciccio, A., Penengo, L., & Lopes, M. (2017). Replication Fork Slowing and Reversal upon DNA Damage Require PCNA Polyubiquitination and ZRANB3 DNA Translocase Activity. *Molecular Cell*, 67(5), 882.

Wang, A. T., Kim, T., Wagner, J. E., Conti, B. A., Lach, F. P., Huang, A. L., Molina, H., Sanborn, E. M., Zierhut, H., Cornes, B. K., Abhyankar, A., Sougnez, C., Gabriel, S. B., Auerbach, A. D., Kowalczykowski, S. C., & Smogorzewska, A. (2015). A dominant mutation in human RAD51 reveals its function in DNA interstrand crosslink repair independent of homologous recombination. *Molecular Cell*, 59(3), 478.

Wang, J., & Lindahl, T. (2016). Maintenance of Genome Stability. *Genomics, Proteomics & Bioinformatics*, 14(3), 119–121.

Wei, X., Samarabandu, J., Devdhar, R. S., Siegel, A. J., Acharya, R., & Berezney, R. (1998). Segregation of transcription and replication sites into higher order domains. *Science*, 281(5382), 1502–1505.

Wen, Q., Scora, J., Phear, G., Rodgers, G., Rodgers, S., & Meuth, M. (2008). A Mutant Allele of MRE11 Found in Mismatch Repair-deficient Tumor Cells Suppresses the Cellular Response to DNA Replication Fork Stress in a Dominant Negative Manner. *Molecular Biology of the Cell*, 19(4), 1693.

- Willaume, S., Rass, E., Paulafontanilla-Ramirez, P., Moussa, A., Wanschoor, P., & Bertrand, P. (2021). A Link between Replicative Stress, Lamin Proteins, and Inflammation. *Genes*, 12(4).
- Woods, Y. L., Xirodimas, D. P., Prescott, A. R., Sparks, A., Lane, D. P., & Saville, M. K. (2004). p14 Arf Promotes Small Ubiquitin-like Modifier Conjugation of Werners Helicase. *Journal of Biological Chemistry*, 279(48), 50157–50166.
- Wu, R. A., Pellman, D. S., & Walter, J. C. (2021). The ubiquitin ligase TRAP: double-edged sword at the replisome. *Trends in Cell Biology*, 31(2), 75.
- Xia, Y. (2021). The Fate of Two Unstoppable Trains After Arriving Destination: Replisome Disassembly During DNA Replication Termination. *Frontiers in Cell and Developmental Biology*, 9, 658003.
- Xie, M., Yen, Y., Owonikoko, T. K., Ramalingam, S. S., Khuri, F. R., Curran, W. J., Doetsch, P. W., & Deng, X. (2014). Bcl2 induces DNA replication stress by inhibiting ribonucleotide reductase. *Cancer Research*, 74(1), 212–223.
- Xu, S., Wu, X., Wu, L., Castillo, A., Liu, J., Atkinson, E., Paul, A., Su, D., Schlacher, K., Komatsu, Y., You, M. J., & Wang, B. (2017). Abro1 maintains genome stability and limits replication stress by protecting replication fork stability. *Genes and Development*, 31(14), 1469–1482.
- Xu, X., Chang, C. W., Li, M., Omabe, K., Le, N., Chen, Y. H., Liang, F., & Liu, Y. (2023). DNA replication initiation factor RECQ4 possesses a role in antagonizing DNA replication initiation. *Nature Communications* 2023 14:1, 14(1), 1–16.
- Xu, Y., Ning, S., Wei, Z., Xu, R., Xu, X., Xing, M., Guo, R., & Xu, D. (2017). 53BP1 and BRCA1 control pathway choice for stalled replication restart. *ELife*, 6.

- Yamashita, R., Sathira, N. P., Kanai, A., Tanimoto, K., Arauchi, T., Tanaka, Y., Hashimoto, S. I., Sugano, S., Nakai, K., & Suzuki, Y. (2011). Genome-wide characterization of transcriptional start sites in humans by integrative transcriptome analysis. *Genome Research*, 21(5), 775.
- Yan, S., Sorrell, M., & Berman, Z. (2014). Functional interplay between ATM/ATR-mediated DNA damage response and DNA repair pathways in oxidative stress. *Cellular and Molecular Life Sciences : CMLS*, 71(20), 3951.
- Yan, Y., Xu, Z., Huang, J., Guo, G., Gao, M., Kim, W., Zeng, X., Kloeber, J. A., Zhu, Q., Zhao, F., Luo, K., & Lou, Z. (2020). The deubiquitinase USP36 Regulates DNA replication stress and confers therapeutic resistance through PrimPol stabilization. *Nucleic Acids Research*, 48(22), 12711–12726.
- Yang, W. (2011). Surviving the sun: Repair and bypass of DNA UV lesions. *Protein Science: A Publication of the Protein Society*, 20(11),
- Yang, W., & Woodgate, R. (2007). What a difference a decade makes: Insights into translesion DNA synthesis. *Proceedings of the National Academy of Sciences of the United States of America*, 104(40), 15591.
- Yankiwski, V., Marciniak, R. A., Guarente, L., & Neff, N. F. (2000). Nuclear structure in normal and Bloom syndrome cells. *Proceedings of the National Academy of Sciences of the United States of America*, 97(10), 5214.
- Yannone, S. M., Roy, S., Chan, D. W., Murphy, M. B., Huang, S., Campisi, J., & Chen, D. J. (2001). Werner Syndrome Protein Is Regulated and Phosphorylated by DNA-dependent Protein Kinase. *Journal of Biological Chemistry*, 276(41), 38242–38248.

- Yoon, J. H., Prakash, S., & Prakash, L. (2012). Requirement of Rad18 protein for replication through DNA lesions in mouse and human cells. *Proceedings of the National Academy of Sciences of the United States of America*, 109(20), 7799–7804.
- Yoshimura, A., Seki, M., & Enomoto, T. (2017). The role of WRNIP1 in genome maintenance. *Cell Cycle*, 16(6), 515.
- Yu, C. E., Oshima, J., Fu, Y. H., Wijsman, E. M., Hisama, F., Alisch, R., Matthews, S., Nakura, J., Miki, T., Ouais, S., Martin, G. M., Mulligan, J., & Schellenberg, G. D. (1996). Positional cloning of the Werner's syndrome gene. *Science (New York, N.Y.)*, 272(5259), 258–262.
- Yuan, J., Luo, K., Deng, M., Li, Y., Yin, P., Gao, B., Fang, Y., Wu, P., Liu, T., & Lou, Z. (2014). HERC2-USP20 axis regulates DNA damage checkpoint through Claspin. *Nucleic Acids Research*, 42(21), 13110.
- Zecevic, A., Menard, H., Gurel, V., Hagan, E., DeCaro, R., & Zhitkovich, A. (2009). WRN helicase promotes repair of DNA double-strand breaks caused by aberrant mismatch repair of chromium-DNA adducts. *Cell Cycle (Georgetown, Tex.)*, 8(17), 2769–2778.
- Zellweger, R., Dalcher, D., Mutreja, K., Berti, M., Schmid, J. A., Herrador, R., Vindigni, A., & Lopes, M. (2015). Rad51-mediated replication fork reversal is a global response to genotoxic treatments in human cells. *The Journal of Cell Biology*, 208(5), 563.
- Zeman, M. K., & Cimprich, K. A. (2014). Causes and Consequences of Replication Stress. *Nature Cell Biology*, 16(1), 2.
- Zhang, J. M., & Zou, L. (2020). Alternative lengthening of telomeres: from molecular mechanisms to therapeutic outlooks. *Cell & Bioscience* 2020 10:1, 10(1), 1–9.

Zhang, J., Chen, M., Pang, Y., Cheng, M., Huang, B., Xu, S., Liu, M., Lian, H., & Zhong, C. (2022). Flap endonuclease 1 and DNA-PKcs synergistically participate in stabilizing replication fork to encounter replication stress in glioma cells. *Journal of Experimental & Clinical Cancer Research: CR*, 41(1), 140.

Zhang, T., Rawal, Y., Jiang, H., Kwon, Y., Sung, P., & Greenberg, R. A. (2023). Break-induced replication orchestrates resection-dependent template switching. *Nature* 2023 619:7968, 619(7968), 201–208.

Zhang, W., Feng, J., & Li, Q. (2020). The replisome guides nucleosome assembly during DNA replication. *Cell & Bioscience* 2020 10:1, 10(1), 1–14.

Zhao, H., Rybak, P., Dobrucki, J., Traganos, F., & Darzynkiewicz, Z. (2012). Relationship of DNA Damage Signaling to DNA Replication Following Treatment with DNA Topoisomerase Inhibitors Camptothecin/Topotecan, Mitoxantrone, or Etoposide. *Cytometry. Part A : The Journal of the International Society for Analytical Cytology*, 81(1), 45.

Zheng, L., & Shen, B. (2011). Okazaki fragment maturation: nucleases take centre stage. *Journal of Molecular Cell Biology*, 3(1), 23.

Zheng, L., Zhou, M., Chai, Q., Parrish, J., Xue, D., Patrick, S. M., Turchi, J. J., Yannone, S. M., Chen, D., & Shen, B. (2005). Novel function of the flap endonuclease 1 complex in processing stalled DNA replication forks. *EMBO Reports*, 6(1), 83–89.

Zhou, Z. X., & Kunkel, T. A. (2022). Extrinsic proofreading. *DNA Repair*, 117, 103369.

Zhu, Z., Chung, W. H., Shim, E. Y., Lee, S. E., & Ira, G. (2008). Sgs1 helicase and two nucleases Dna2 and Exo1 resect DNA double-strand break ends. *Cell*, 134(6), 981–994.

Zonderland, G., Vanzo, R., Gadi, S. A., Martín-Doncel, E., Coscia, F., Mund, A., Lerdrup, M., Benada, J., Boos, D., & Toledo, L. (2022). The TRESLIN-MTBP complex couples completion of DNA replication with S/G2 transition. *Molecular Cell*, 82(18), 3350-3365.e7.

Zong, D., Koussa, N. C., Cornwell, J. A., Pankajam, A. V., Kruhlak, M. J., Wong, N., Chari, R., Cappell, S. D., & Nussenzweig, A. (2023). Comprehensive mapping of cell fates in microsatellite unstable cancer cells supports dual targeting of WRN and ATR. *Genes & Development*, 37(19–20), 913–928.

Zvereva, M. I., Shcherbakova, D. M., & Dontsova, O. A. (2010). Telomerase: structure, functions, and activity regulation. *Biochemistry. Biokhimiia*, 75(13), 1563–1583.